Haptic Recognition for Reproduction of Human Motion

February 2011

A thesis submitted in partial fulfilment of the requirements for the degree of
Doctor of Philosophy in Engineering

Keio University

Graduate School of Science and Technology
School of Integrated Design Engineering

YOKOKURA, Yuki

Acknowledgments

Research on this dissertation was carried out at Katsura Laboratory, Department of System Design Engineering and School of Integrated Design Engineering, Keio University. First of all, I would like to express my gratitude to my supervisor Professor Dr. Seiichiro Katsura, Department of System Design Engineering, Keio University. I appreciate Professor Dr. Kiyoshi Ohishi, Department of Electrical Engineering, Nagaoka University of Technology.

I would like particularly to thank sincerely the members of my Ph. D. Dissertation Committee, Professor Dr. Kouhei Ohnishi, Keio University, Professor Dr. Hiroshi Yabuno, Keio University, Professor Dr. Kenji Oguni, Keio University.

Moreover, I appreciate the members of Ohishi Laboratory and of Power Laboratory, Nagaoka University of Technology. I would like to thank the members of Katsura Laboratory and of the SUM group.

In addition, this research was supported by the Ministry of Education, Science, Sports and Culture, Grant-in-Aid for JSPS Fellows. This work was supported in part by Global COE Program "High-Level Global Cooperation for Leading-Edge Platform on Access Spaces (C12)." I appreciate also Industrial Technology Research Grant Program from Strategic Information and Communications R and D Promotion Programme (SCOPE) of Japan, and New Energy and Industrial Technology Development Organization (NEDO) of Japan.

Yuki Yokokura
Keio University
February 2011

Contents

Acknowledgments **i**

1 Introduction **1**

1.1 Background 1

1.2 Motivation 2

1.3 Outline of the thesis 3

2 Haptic Recognition Based on Passive Motion **5**

2.1 Haptic Representation using Haptograph 5

2.1.1 Introduction 5

2.1.2 Modeling of Mobile Robot 7

2.1.2.1 Dynamic Relationship in Joint Space 8

2.1.3 Motion Control for Mobile Robot 9

2.1.3.1 Sensor-less Recognition of Road Surface 9

2.1.3.2 Velocity Control System using a Quarry Matrix 10

2.1.3.3 Modal Decomposition of Haptic Information from Road Surface 12

2.1.4 Haptic Representation using Haptograph 12

2.1.4.1 Definition of Haptograph 12

2.1.4.2 Generation of Haptograph 13

2.1.5 Experiment 13

2.1.5.1 Experimental setup 13

2.1.5.2 Experimental Results 15
2.1.6 Conclusions 17
2.2 Recognition of Driving Road Environment 19
2.2.1 Introduction 19
2.2.2 Motion Control of Mobile Robot 19
2.2.3 Trajectory Planning for Obstacle Avoidance 20
2.2.4 Experiment of Obstacle Avoidance 23
2.2.5 Trajectory Planning using Haptograph 23
2.2.6 Experiment 26
2.2.7 Examination 27
2.2.8 Conclusion 28

3 Haptic Recognition Based on Human Motion 29
3.1 Motion-Copying System 30
3.1.1 Motion-Copying System Based on Real-World Haptics 30
3.1.1.1 Introduction 30
3.1.1.2 Concepts of Motion-Copying System 32
3.1.1.3 Motion-Saving System using a Bilateral Controller 33
3.1.1.4 Motion-Loading System using a Master-Slave Controller 36
3.1.1.5 Experiment 37
3.1.1.6 Conclusion 39
3.1.2 Reproduction of Multi Degree-of-Freedom Motion by Motion-Copying System 43
3.1.2.1 Introduction 43
3.1.2.2 Motion-Copying System 44
3.1.2.3 Motion-Saving System 45
3.1.2.4 Motion-Loading System 49
3.1.2.5 Experiment 50

3.1.2.6 Conclusion 54
3.1.3 Motion-Copying System Based on Real-World Haptics in Variable Speed . 55
3.1.3.1 Introduction 55
3.1.3.2 Concept of Motion-Copying System in Variable Speed 57
3.1.3.3 Motion-Saving System using Bilateral Controller 59
3.1.3.4 Motion-Loading System considering Variable Reproduction Velocity 62
3.1.3.5 Experiment 63
3.1.3.6 Conclusions 65
3.1.4 Realization of Motion-Copying System Based on Multilateral Control . . 70
3.1.4.1 Introduction 70
3.1.4.2 Multilateral Control considering Identity Ratio 71
3.1.4.3 Motion-Copying System Based on Multilateral Control 73
3.1.4.4 Experiment 74
3.1.4.5 Conclusion 75
3.1.5 Stability Analysis and Experimental Validation of Motion-Copying System 79
3.1.5.1 Introduction 79
3.1.5.2 Motion-Copying System 80
3.1.5.3 Stability of Motion-Copying System 85
3.1.5.4 Experiment 89
3.1.5.5 Conclusion 91
3.1.6 Improvement of Force Reproducibility for Motion-Copying System 98
3.1.6.1 Introduction 98
3.1.6.2 Conventional Motion-Copying System 99
3.1.6.3 Acceleration Observer 102
3.1.6.4 Force Controller with Acceleration Observer 105

3.1.6.5 Proposed Motion-Copying System . . . 107
3.1.6.6 Evaluation of Force Reproducibility . . . 110
3.1.6.7 Conclusion . . . 114
3.1.7 Construction of Motion Database using Motion-Copying System . . . 116
3.1.7.1 Introduction . . . 116
3.1.7.2 Concept of Motion Database System . . . 116
3.1.7.3 Motion Control . . . 117
3.1.7.4 Experiment . . . 117
3.1.7.5 Conclusion . . . 118
3.1.8 Motion-Copying System in Work Space . . . 121
3.1.8.1 Motion-Saving System . . . 121
3.1.8.2 Motion-Loading System . . . 124
3.1.8.3 Experiment . . . 125
3.1.8.4 Conclusion . . . 126
3.2 Environmental Copying System . . . 128
3.2.1 Introduction . . . 128
3.2.2 Concept of Environmental Copying System . . . 130
3.2.3 Environmental Saving System . . . 131
3.2.3.1 Concept . . . 131
3.2.3.2 Motion Control . . . 132
3.2.4 Environmental Loading System . . . 134
3.2.4.1 Concept . . . 134
3.2.4.2 Motion Control . . . 135
3.2.5 Experiment . . . 137
3.2.5.1 Experimental Setup . . . 137
3.2.5.2 Experimental Results . . . 139
3.2.6 Conclusion . . . 140

4 Haptic Recognition on Remote Environment 143

4.1 Bilateral Control over Network 144

4.1.1 Bilateral Control with Communication Time Delay by Using Motion-Copying System 144

4.1.1.1 Introduction 144

4.1.1.2 Bilateral Control with Time Delay 146

4.1.1.3 Motion-Copying System 147

4.1.1.4 Communication Delay Compensation Based on Motion-Copying System 148

4.1.1.5 Experiment 155

4.1.1.6 Conclusion 156

4.1.2 Bilateral Teleoperation over Network Based on Environmental Data Memory 157

4.1.2.1 Introduction 157

4.1.2.2 Concept of Bilateral Control using Environmental Data Memory 159

4.1.2.3 Motion Control 160

4.1.2.4 Environmental Data Memory 164

4.1.2.5 Experiment 165

4.1.2.6 Conclusions 169

4.1.3 Bilateral Control using Compressor/Decompressor under Low-Rate Communication Network 170

4.1.3.1 Introduction 170

4.1.3.2 Motion-Copying System 172

4.1.3.3 Motion-Copying System based Bilateral Control 173

4.1.3.4 Bilateral Control using Compressor/Decompressor 176

4.1.3.5 Experiment 178

4.1.3.6 Conclusion 179

4.1.4 Bilateral Control Using Master/Slave Simulator for Haptic Communication 185

4.1.4.1 Introduction . . . 185
4.1.4.2 Concept of Proposed Method . . . 186
4.1.4.3 Motion Control . . . 187
4.1.4.4 Bilateral Control using Environmental Data Memory . . . 188
4.1.4.5 Experiment . . . 190
4.1.4.6 Conclusion . . . 191
4.2 Multilateral Control over Network . . . 198
4.2.1 Introduction . . . 198
4.2.2 Multilateral Control with Time Delay . . . 199
4.2.3 Multilateral Control using Motion-Copying System . . . 201
4.2.4 Experiment . . . 203
4.2.4.1 Experimental Setup . . . 203
4.2.4.2 Experimental Results . . . 203
4.2.5 Conclusion . . . 204

5 Reproduction of Human Motion 211
5.1 Search of Haptic Sensation . . . 212
5.1.1 Motion Index/Search System Based on Real-World Haptics . . . 212
5.1.1.1 Introduction . . . 212
5.1.1.2 Bilateral Control System . . . 214
5.1.1.3 Motion Index System . . . 216
5.1.1.4 Motion search system . . . 218
5.1.1.5 Experiment . . . 220
5.1.1.6 Conclusion . . . 222
5.1.2 Searching System of Haptic Environment . . . 227
5.1.2.1 Introduction . . . 227
5.1.2.2 Environment-Copying System . . . 229
5.1.2.3 Searching System . . . 236

5.1.2.4 Experiment 239
5.1.2.5 Conclusion 240
5.1.3 Identification of Stiffness in Differential Mode 242
5.1.3.1 Introduction 242
5.1.3.2 Identification Method 242
5.1.3.3 Experiment 244
5.1.3.4 Conclusion 246
5.2 Selective Motion-Copying System 248
5.2.1 Introduction 248
5.2.2 Motion-Copying System 249
5.2.3 Storage of Environmental Haptic Information 250
5.2.3.1 Concept 250
5.2.3.2 Motion Control 251
5.2.3.3 Storage Method 251
5.2.3.4 Decomposition Method of Reaction Force 252
5.2.4 Selective Motion-Copying System 254
5.2.4.1 Concept 254
5.2.4.2 Motion-Saving System 256
5.2.4.3 Selective Motion-Loading System 256
5.2.4.4 Environmental Search Algorithm 257
5.2.5 Experiment 259
5.2.5.1 Normal Motion-Copying System 259
5.2.5.2 Storage of Environmental Haptic Information 259
5.2.5.3 Proposed Method 262
5.2.6 Conclusion 262

6 Conclusions **265**

References **269**

List of Achievements **283**

List of Figures

1.1 Contents of the thesis. 4

2.1 The driving road environment in the real-world. 7
2.2 Modeling of the mobile robot. 7
2.3 Block diagram of disturbance observer. 9
2.4 Velocity control system of the mobile robot with the quarry matrix and disturbance observer. 10
2.5 Picture of road environments. (a) Non-slip steel plate floor. (b) Concrete floor. 13
2.6 Road environment which is configured in the experiment. 14
2.7 Appearance of the mobile robot which is used in the experiment. 14
2.8 Control system of the mobile robot using a real time Linux kernel. 15
2.9 Experimental results of translational mode. (a) Waveform of disturbance force F^{dis}. (b) Translational mode haptograph. 16
2.10 Experimental results of rotational mode. (a) Waveform of disturbance force T^{dis}. (b) Rotational mode haptograph. 17
2.11 Translational mode force and rotational mode position control system using quarry matrix. 20
2.12 Potential field of simple obstacle. 21
2.13 Potential field. 22
2.14 Contour map of potential field and trajectory of mobile robot (Experiment). . . . 23
2.15 Experimental results. (a) Disturbance force. (b) Haptograph. 24

2.16 Weighting function 25
2.17 Processed experimental results. (a) Weighted haptograph. (b) Result for integration. 25
2.18 Haptic map which is considered by haptic information of driving road environment. 26
2.19 Contour map of potential field and trajectory of mobile robot (Proposed method). 27
2.20 Experimental results. (a) Disturbance force. (b) Haptograph. (Velocity = 0.24 m/s) 28
2.21 Experimental results. (a) Disturbance force. (b) Haptograph. (Velocity = 0.16 m/s) 28
2.22 Potential field. (Velocity = 0.24 m/s) 28
2.23 Potential field. (Velocity = 0.16 m/s) 28

3.1 Storage and reproduction of acoustic, visual, and haptic information. 30
3.2 Conceptual diagram of motion-copying system. 32
3.3 Block diagram of motion-saving system using bilateral control system. 34
3.4 Block diagram of motion-loading system using virtual master system. 37
3.5 Experimental device of motion-saving system. 38
3.6 Experimental device of motion-loading system. 39
3.7 Free motion. (a) Saved Position. (b) Saved Force. (c) Loaded Position. (d) Loaded Force. 40
3.8 Push motion. (a) Saved Position. (b) Saved Force. (c) Loaded Position. (d) Loaded Force. 41
3.9 Contact motion. (a) Saved Position. (b) Saved Force. (c) Loaded Position. (d) Loaded Force. 42
3.10 Conceptual diagram of motion-copying system. 44
3.11 Block diagram of the master system and the slave system. 45
3.12 Block diagram of motion-saving system. 47
3.13 Block diagram of motion-loading system. 49

3.14 Experimental devices. (In the case of motion-loading system, the master system is not used.) 51

3.15 Experimental results of the motion-saving system.
(a) Force of X-axis. (b) Position of X-axis.
(c) Force of Y-axis. (d) Position of Y-axis. 52

3.16 Experimental results of the motion-loading system.
(a) Force of X-axis. (b) Position of X-axis.
(c) Force of Y-axis. (d) Position of Y-axis. 53

3.17 Motion-copying system considering variable reproduction velocity. 56

3.18 Conceptual diagram of motion-copying system in variable reproduction velocity. . 57

3.19 Processing of force and position information in a motion data memory. 59

3.20 Block diagram of motion-saving system using bilateral control system. 60

3.21 Block diagram of motion-loading system considering variable reproduction velocity. 62

3.22 Experimental device of motion-saving system. 63

3.23 Experimental device of motion-loading system in variable speed. 64

3.24 Saved motion data using motion-saving system.
(a) Saved position (b) Saved force 65

3.25 Loaded motion data using motion-loading system.
(Reproduction velocity is normal) (a) Loaded position (b) Loaded force 66

3.26 Loaded motion data using motion-loading system.
(Reproduction velocity is twice) (a) Loaded position (b) Loaded force 67

3.27 Loaded motion data using motion-loading system.
(Reproduction velocity is third-time) (a) Loaded position (b) Loaded force . . . 68

3.28 Loaded motion data using motion-loading system.
(Reproduction velocity is one-half) (a) Loaded position (b) Loaded force 69

3.29 Conceptual diagram of motion-copying system using multilateral controller. . . . 71

3.30 Block diagram of multilateral control system with identity ratio. 72

3.31 Block diagram of motion-saving system based on multilateral control and identity ratio. 74
3.32 Block diagram of motion-loading system using multilateral controller. 75
3.33 Experimental setup of motion-saving system 76
3.34 Experimental setup of motion-loading system 76
3.35 Saved motion data using motion-saving system (a) Position (b) Force (c) Identity ratio 77
3.36 Loaded motion data using motion-loading system (a) Position (b) Force (c) Identity ratio 78
3.37 Conceptual diagram of motion-copying system. 81
3.38 Block diagram of motion-saving system using bilateral control system. 82
3.39 Block diagram of motion-loading system using virtual master system. 85
3.40 Block diagram of motion-loading system considering the environmental impedance. 86
3.41 Equivalent conversion block diagram of Fig. 3.41. 86
3.42 Experimental device of motion-saving system. 88
3.43 Experimental device of motion-loading system. 88
3.44 Displacement of the poles with the transition of environmental stiffness K_ℓ. . . . 92
3.45 Displacement of the poles with the transition of environmental damper D_ℓ. . . . 92
3.46 Displacement of the poles with the transition of environmental stiffness K_ℓ. . . . 93
3.47 Displacement of the poles with the transition of environmental damper D_ℓ. . . . 93
3.48 Block diagram of environments reproduction system. (Impedance control) 94
3.49 Experimental result of motion-saving system. (a) position (b) force (Environmental stiffness K_s is 300, damper D_s is 50) 94
3.50 Experimental result of motion-loading system. (a) position (b) force (Environmental stiffness K_ℓ is 100 to 700, damper D_ℓ is 50) 95

3.51 Experimental result of motion-loading system. (a) position (b) force (Environmental stiffness K_ℓ is 300, damper D_ℓ is 20 to 200) 96
3.52 The actual pole placement in the experiment. (a) Transition of the stiffness K_ℓ (The experiment of Fig. 3.50) (b) Transition of the damper D_ℓ (The experiment of Fig. 3.51) 97
3.53 Conventional Motion-Copying System 99
3.54 Block diagram of force controller. 101
3.55 Block diagram of acceleration observer. 103
3.56 Experimental results of acceleration observer. 105
3.57 Block diagram of improved force controller. 106
3.58 Experimental results of force controller. 107
3.59 Experimental results of improved force controller. 108
3.60 Motion-copying system proposed in this thesis. 109
3.61 Experimental results of conventional motion-loading system. 111
3.62 Experimental results of improved motion-loading system. 112
3.63 Power spectrum density (conventional). 113
3.64 Power spectrum density (proposed). 113
3.65 Histogram of force error. 114
3.66 Magnified figure of Fig. 3.65. 115
3.67 Conceptual diagram of motion database system and control system. 116
3.68 Structure of motion database. 117
3.69 Block diagram of motion insertion. 118
3.70 Block diagram of motion retrieval. 119
3.71 Insertion of “Motion A.” 119
3.72 Insertion of “Motion B.” 119
3.73 Insertion of “Motion C.” 120
3.74 Insertion of “Motion D.” 120

3.75 Motion retrieval. (a) Motion request. (b) Force responses. (c) Position responses. 120
3.76 Block diagram of motion-saving system. 121
3.77 Block diagram of motion-loading system. 124
3.78 Model of parallel link robot. 125
3.79 Experimental setup. 125
3.80 Trajectory of storage phase and trajectory of reproduction phase. 126
3.81 Experimental results of motion-saving system and motion-loading system. (a) Force (X-axis). (b) Force (Y-axis). (c) Position (X-axis). (d) Position (Y-axis). 127
3.82 Preservation and reproduction system of acoustic, visual and haptic information. 128
3.83 Conceptual diagram of the environmental saving system. 131
3.84 Block diagram of the master system and the slave system. 132
3.85 Block diagram of the environmental saving system. 133
3.86 Conceptual diagram of the environmental loading system. 135
3.87 Block diagram of the environmental loading system. 135
3.88 Force information in the environment data memory. (a) In case of stiffness. (b) In case of damper. (c) In case of stiffness and damper. 137
3.89 Experimental setup (In case of environmental loading system, the slave system is unused). 138
3.90 Experimental results of the environmental saving system. (a) Force responses. (b) Position responses. (c) Velocity responses. 139
3.91 The force information in the environment data memory. 140
3.92 Experimental results of the environmental loading system. (a) Force responses. (b) Position responses. (c) Velocity responses. 141
3.93 Experimental results of the environmental loading system. 142

4.1 Transmission of acoustic and visual, haptic information. 145
4.2 Bilateral control system with communication time delay. 146
4.3 Conceptual diagram of motion-saving system. 148

4.4 Conceptual diagram of motion-loading system. 148
4.5 Conceptual diagram of bilateral control with time delay compensation based on motion-copying system. 149
4.6 Block diagram of master and slave system. 150
4.7 Block diagram of bilateral control system using time delay compensation based on motion-copying system. 151
4.8 Experimental devices. 153
4.9 Position response without time delay compensation (Communication delay time $T_d = 3$ ms). 153
4.10 Force response without time delay compensation (Communication delay time $T_d = 3$ ms). 153
4.11 Position response using motion-copying system (Communication delay time $T_d = 3$ ms). 154
4.12 Force response using motion-copying system (Communication delay time $T_d = 3$ ms). 154
4.13 Force response using motion-copying system (Communication delay time $T_d = 30$ ms). 154
4.14 Force response using motion-copying system (Communication delay time $T_d = 30$ ms). 154
4.15 Transmission of acoustic, visual and haptic information. 158
4.16 Conceptual diagram of the proposed method. 159
4.17 Block diagram of master system, slave system simulator and slave system. 161
4.18 Block diagram of bilateral control system over network based on environmental data memory. 162
4.19 Experimental setup 163
4.20 Experimental results (**Time delay = 0 s**). (a) Force. (b) Position. 163
4.21 Magnified figure of Fig. 4.20. (a) Shifted force. (b) Shifted position. 163

4.22 Experimental results (**Time delay = 1 s**). (a) Force. (b) Position. 165
4.23 Magnified figure of Fig. 4.22. (a) Shifted force. (b) Shifted position. 165
4.24 Experimental results (**Time delay = 3 s**). (a) Force. (b) Position. 166
4.25 Magnified figure of Fig. 4.24. (a) Shifted force. (b) Shifted position. 166
4.26 Experimental results (**Time delay = 5 s**). (a) Force. (b) Position. 166
4.27 Magnified figure of Fig. 4.26. (a) Shifted force. (b) Shifted position. 166
4.28 Experimental results (**Time delay = 10 s**). (a) Force. (b) Position. 167
4.29 Magnified figure of Fig. 4.28. (a) Shifted force. (b) Shifted position. 167
4.30 Force information in the environmental data memory. 168
4.31 Transfer of the visual, acoustic and haptic information. 171
4.32 Conceptual diagram of motion-copying system. 172
4.33 Conceptual diagram of bilateral controller based on motion-copying system. . . . 173
4.34 Block diagram of bilateral controller based on motion-copying system considering effect of communication network. 180
4.35 Detailed block diagram of master and slave system. 181
4.36 Block diagram of bilateral control based on motion-copying system using compressors and decompressors. 181
4.37 Experimental devices. 182
4.38 Block diagram of force control system. 182
4.39 Experimental results without proposed method. ($T_t = 100\mu$s) 183
4.40 Experimental results using proposed method. ($T_t = 100\mu$s) 183
4.41 Experimental results without proposed method. ($T_t = 1$ms) 183
4.42 Experimental results using proposed method. ($T_t = 1$ms) 183
4.43 Experimental results without proposed method. ($T_t = 2$ms) 184
4.44 Experimental results using proposed method. ($T_t = 2$ms) 184
4.45 Data transfer period T_t vs. S/N ratio of force signal. 184
4.46 Conceptual diagram of the proposed method 185

4.47 Bilateral control through communication network. 186
4.48 Block diagram of master and slave systems. 187
4.49 Block diagram of bilateral control system by using master/slave simulator. 193
4.50 Experimental setup. 194
4.51 Experimental results of sinusoidal waveform inputs. (a) Force responses $\hat{F}_M^{ext}$, $\hat{F}_S^{ext}$. (b) Position responses x_M^{res}, x_S^{res}. (c) Switching coefficients S_R, S_L. 195
4.52 Experimental results of frequency modulated signal inputs. (a) Force responses $\hat{F}_M^{ext}$, $\hat{F}_S^{ext}$. (b) Position responses x_M^{res}, x_S^{res}. (c) Switching coefficients S_R, S_L. . 196
4.53 Force information preserved in the environmental data memory. 197
4.54 Conceptual diagram of multilateral control with communication time delay by using motion-copying system 198
4.55 Block diagram of multilateral control with communication time delay 200
4.56 Block diagram of multilateral control with communication time delay by using motion-copying system 205
4.57 Experimental setup. 206
4.58 Experimental results without proposed method (a) Position response (b) Force response ($T_d = 800$ μs) 207
4.59 Experimental results using motion-copying system (a) Position response (b) Force response ($T_d = 800$ μs) 208
4.60 Experimental results using motion-copying system (a) Position response (b) Force response ($T_d = 50$ ms) 209
4.61 Experimental results using motion-copying system (a) Position response (b) Force response ($T_d = 100$ ms) 210

5.1 Recognition, analysis and database of information. 213
5.2 Block diagram of bilateral control system. 214
5.3 Conceptual diagram of motion indexing system. 217
5.4 Conceptual diagram of motion search system. 218

5.5 Experimental Setup 220

5.6 Indexed Motion (Grasping Motion). (a) Forces ${}^{1}_{1}\Phi$ and ${}^{2}_{1}\Phi$. (b) Positions ${}^{1}_{1}\Xi$ and ${}^{2}_{1}\Xi$. 221

5.7 Indexed Motion (Release Motion). (a) Forces ${}^{1}_{2}\Phi$ and ${}^{2}_{2}\Phi$. (b) Positions ${}^{1}_{2}\Xi$ and ${}^{2}_{2}\Xi$. 222

5.8 Grasping motion. (a) Force ${}^{M1}F^{ext}$ and ${}^{M2}F^{ext}$. (b) Position ${}^{M1}X^{res}$ and ${}^{M2}X^{res}$. (c) searching result of grasping motion ${}_{1}R$. (d) searching result of release motion ${}_{2}R$. 223

5.9 Fast grasping motion. (a) Force ${}^{M1}F^{ext}$ and ${}^{M2}F^{ext}$. (b) Position ${}^{M1}X^{res}$ and ${}^{M2}X^{res}$. (c) searching result of grasping motion ${}_{1}R$. (d) searching result of release motion ${}_{2}R$. 224

5.10 Kneading motion. (a) Force ${}^{M1}F^{ext}$ and ${}^{M2}F^{ext}$. (b) Position ${}^{M1}X^{res}$ and ${}^{M2}X^{res}$. (c) searching result of grasping motion ${}_{1}R$. (d) searching result of release motion ${}_{2}R$. 225

5.11 Fast kneading motion. (a) Force ${}^{M1}F^{ext}$ and ${}^{M2}F^{ext}$. (b) Position ${}^{M1}X^{res}$ and ${}^{M2}X^{res}$. (c) searching result of grasping motion ${}_{1}R$. (d) searching result of release motion ${}_{2}R$. 226

5.12 Relation of power electronics, motion control, and real-world haptics. 227

5.13 Conceptual diagram of the environment-saving system. 229

5.14 Block diagram of the environment-saving system. 229

5.15 Force information in the environment data memory. (a) In case of stiffness. (b) In case of damper. (c) In case of stiffness and damper. 230

5.16 Conceptual diagram of the environment-loading system. 232

5.17 Block diagram of the environment-loading system. 232

5.18 Storage of environmental haptic information. 233

5.19 Conceptual diagram of environmental search system. 234

5.20 Block diagram of search system for haptic environment. 235

5.21 Experimental setup. 237

5.22 Environments used in the experiment. (a) Sponge. (N=1) (b) Aluminum block. (N=2) 237

5.23 Stored force information to environmental data memory. (Environment is sponge. N=1) 238

5.24 Stored force information to environmental data memory. (Environment is aluminum block. N=2) 239

5.25 Experimental results. (a) Force response F^{ext}. (b) Reproduced Force in the case of sponge ${}^1F^{mem}$. (c) Reproduced force in the case of aluminum alloy ${}^2F^{mem}$. (d) Search results ${}^1R$, ${}^2R$. 240

5.26 Model of target object. 242

5.27 Position control system in modal space. 243

5.28 Model of experimental devices. 244

5.29 Experimental setup. 245

5.30 Experimental results. (a) Force responses $\hat{F}_1^{dis}$, $\hat{F}_2^{dis}$. (b) Position responses X_1^{res}, X_2^{res}. 246

5.31 Experimental results. (a) Force responses in the differential mode $\hat{F}_D^{dis}$. (b) Position responses in the differential mode X_D^{res}. (c) Identified stiffness between node 1 and node 2 $\hat{K}_{12}$. 247

5.32 Conceptual diagram of motion-copying system. 249

5.33 Storage of environmental haptic information. 250

5.34 Storage of environmental haptic information. 251

5.35 Conceptual diagram of motion-saving systems. 254

5.36 Conceptual diagram of selective motion-loading system. (Proposed method) . . . 255

5.37 Block diagram of motion-saving system. 256

5.38 Block diagram of selective motion-loading system. (Proposed method) 257

5.39 Experimental results of normal motion-loading system. (Rubber block) (a) Force $\hat{F}_M^{ext}$, $\hat{F}_S^{ext}$. (b) Position X_M^{res}, X_S^{res}. 259

5.40 Experimental results of normal motion-loading system. (Rubber ball) (a) Force $\hat{F}_M^{ext}$, $\hat{F}_S^{ext}$. (b) Position X_M^{res}, X_S^{res}. 260

5.41 Environments used in the experiment. (a) Rubber ball. (b) Rubber block. 260

5.42 Experimental setup of selective motion-loading system. 261

5.43 Experimental results of haptic storage. (Rubber ball) (a) Force $\hat{F}_F^{ext}$. (b) Position X_F^{res}. 261

5.44 Experimental results of haptic storage. (Rubber block) (a) Force $\hat{F}_F^{ext}$. (b) Position X_F^{res}. 262

5.45 Environmental data memory. (Rubber Ball) (a) Force f_K. (b) Momentum p_D. . 263

5.46 Environmental data memory. (Rubber Block) (a) Force f_K. (b) Momentum p_D. 263

5.47 Experimental results of selective motion-loading system. (a) Force $\hat{F}_M^{ext}$, $\hat{F}_S^{ext}$. (b) Position X_M^{res}, X_S^{res}. (c) Reproduced force by environmental data memory F_R. (d) Moving correlation C. (e) Search results. 264

List of Tables

2.1 Setup Parameters 15

3.1 Setup Parameters. 38
3.2 Setup Parameters 51
3.3 Setup Parameters 90
3.4 Setup Parameters 138

4.1 Setup Parameters 155
4.2 Setup Parameters 167
4.3 Correlation coefficients 168
4.4 Setup Parameters 178
4.5 Setup parameters. 191
4.6 Correlation coefficient. 191
4.7 Setup parameters 203

Chapter 1

Introduction

1.1 Background

"Information" which represents aspect and content of various circumstance, is necessary for human society. In ancient times, record and transfer of "Information" were conducted by using characters, graphic symbols, and pictorial arts. For example, the history in ancient Egypt was recorded by the distinctive characters, called Egyptian hieroglyph. In cathedrals, mosques, and temples, many pictures of sacred subject speak for various aspects. In recent times, a phonograph which is capable of storing and reproducing auditory information has been invented. By using the phonograph, an expression method of "Information" using sound was established. In 18 and 19 century, wired and wireless telegraph was also proposed [1, 2]. It is some sort of a communication system for transmission of text information. Since the wired and wireless communication system was in practical use, transmission as well as storage and reproduction of "Information" became possible. Additionally, transmission of auditory information was realized by telephone [3, 4] and sound radio. These techniques are able to convey sound information, voice, and music. In addition, photography which represents a visual image was invented in 19 century [5]. Televisions developed by some researchers and developers became possible to transmit and to receive motion pictures [6]–[8]. Therefore, storage, record, and transmission of visual information were realized. In 1960s, an origin of Internet, called ARPANET [9]–[11], was developed by DARPA(Defense Advanced Research Project Agency) of United States. It is

capable of sharing “Information” in entire world. In short, these technologies are able to treat “Information” which consists of text information, auditory information, and visual information.

On the other hand, a human body has five organs including acoustic organs, visual organs, olfactory organs, gustatory organ, and haptic organs. However, the practical techniques cannot treat sensation other than acoustic and visual sensation. “Information” used in modern society contains only the auditory information and the visual information. In other words, the “Information” is incomplete.

1.2 Motivation

Since a human recognizes objective world using the five organs, the “Information” should include the residual information. In terms of the acoustic information and the visual information, great many researchers conduct research and development. On the other hand, compared with the research for the acoustic and visual information, a technique for the haptic information has not adequately researched yet. In concrete terms, storage, reproduction, recognition, and transmission method for the haptic information is not in practical use.

Realization of a treatment method for the haptic information brings various benefit. For example, a future television using the haptic technologies is able to provide not only the sound and th visual image but also the haptic sensation of an object. The audiences can grasp the target object in the television. Therefore, the current stalemated advertising market will be dramatically changed by the real-world haptics. By using the haptic information, artistic expressions including the haptic sensation might be also changed. If the haptic technologies will be established completely, an amount of available “Information” will dramatically increase. Additionally, a novel telephone with a haptic transmission system become possible to convey a realistic environment located at distant place. The users of the novel telephone can feel interaction force between a human and human, or a human and a target object. In short, a worker located at manufactory repairs products in a home without movement, by using the novel telephone. An on-demand distribution system for the haptic sensation of a target object will be

able to be constructed. Moreover, the haptic devices store and reproduce sensitive motion of an industrial expert technician, cook, medical operator, and so on. The haptic devices reproduces motion of the cook, so that the users can eat the dinner cooked by the professional chef.

By this means, the robot which utilizes the haptic information exponentially changes feature of life in human society, when the haptic information will be under control. Consequently, this thesis studies about treatment and utilization of the haptic information, in order to help to build the much further convenient society.

1.3 Outline of the thesis

The outline of this thesis is illustrated in Fig. 1.1.

In terms of acoustic information and visual information, great many researchers conduct research and development. On the other hand, the technique for haptic information has not adequately researched yet. In concrete terms, storage, reproduction, recognition, and transmission method for the haptic information is not in practical use. Moreover, the current systems for human-support do not consider the haptic information. Consequently, this thesis studies about haptic recognition for reproduction of human motion.

Firstly, Chapter 1 describes the background of this research. Chapter 2 describes the recognition method for the haptic sensation. The mobile robot obtains haptic information of road surface from haptograph that is generated by haptic recognition algorithm. Gabor continuance wavelet transform realizes the haptic recognition algorithm. It is possible to make a haptic map that visualizes the driving environment of road. By using this method, the mobile robot is able to avoid rough road taking ride ability into account. In Chapter 3, a motion-copying system which is capable of storing and reproducing human motion is proposed. The motion-copying system reproduces the force as well as the position. In other words, the proposed system is able to reproduce the human motion beyond time and space. This thesis also proposes a novel motion-copying system considering variable reproduction velocity, and improvement method for force reproducibility. In Chapter 4, the haptic recognition from the remote environment using

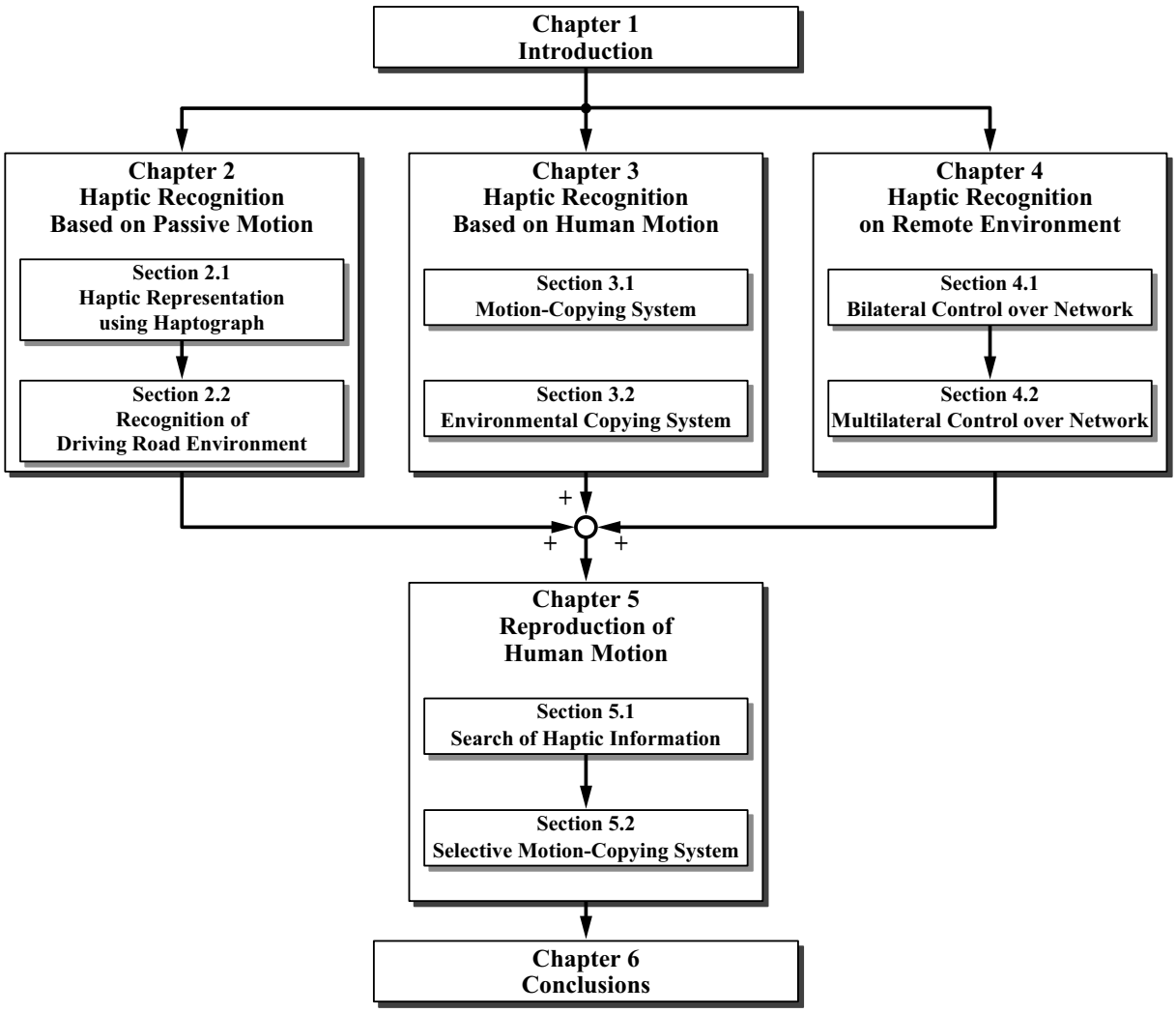

Fig. 1.1. Contents of the thesis.

communication network is explained. The proposed system is able to reconstruct the environment to suppress the effects of time delay and communication loss. In Chapter 5, a selective motion-copying system is realized. The motion-copying system proposed in Chapter 2 cannot reproduce precise force and position, when the environment is changed in reproduction phase. Hence, the environmental search algorithm detects the contact environment and provides the environmental information to the motion-copying system, in order to reproduce the force and the position accurately. Finally, Chapter 6 concludes this thesis.

Chapter 2

Haptic Recognition Based on Passive Motion

Abstract

Recently, human cooperative robots are desired in an aging society. In particular, recognition performance of environment is the most important. Visual and/or auditory sensors are used to recognize the environment; however, they are not able to recognize contact information. Tactile and/or haptic information is very important for action in unknown environment. The thesis gives the haptic sensation to a robot. Furthermore, the obtained haptic information is visualized by haptograph. The haptograph is useful for haptic mapping of environment and trajectory planning for a mobile robot. The experimental results show the viability of the proposed method.

2.1 Haptic Representation using Haptograph

2.1.1 Introduction

In the real world, robots are required to recognize environment in order to support human. That requirements particularly comes from field of welfare and medical services, and that demand is increasing, A adaptive ability to the environment should be advanced to prepare for an aging society. For that purpose, it is very important to install not only visual recognition but also haptic recognition. There is much research about [12]–[14]. Also, various techniques for

adaptation to environment [15],[16] are developing. The researches on tactile sensation are also presented [17],[18]. However, a research of motion control from the viewpoint of haptic recognition is not enough. The research for installing tactile organ to a robot which acts autonomously should be developed. Thus, this thesis proposes to add tactile organ to an autonomous robot. After the robot feels advanced haptic information, the robot make a decision for could actions.

A video camera and a laser ranger are devices that recognize environment. GPS provides position of a mobile robot, and help to calculate trajectory [19],[20]. Such devices are used to avoid collision with obstacles [21]–[23]. Also, the mobile robot has to grasp condition of road surface to select optimal corridor. (When the mobile robot selected beeline, which established course is not necessarily optimal.) Since, dirt and roughness roads exist on the actual roads; however, visualized and auditory devices are unable to recognize tactile information of road surface. Future human assist robot should have haptic ability. Haptic camera has been proposed to obtain the impedance parameter of the contact environment [92].

In this thesis, we propose a haptic recognition of road surface by using a disturbance observer [66]. The road surface is recognized by result of frequency analysis of output signals from the observer. In other words that is named as haptograph [24]–[27]. This haptograph represent information of environmental characteristics in discretional place. Fig. 2.1 shows complex driving road situation in the real-world. Once such sensation is installed, safety and friendly functions are generated in an autonomous robot. If haptic map of driving road in the real-world is generated, the mobile robot may grasp the situation, and consider riding ability. Also, a haptic map provides making a search for similar driving road environment.

This research is organized as follows. Subsection 2.1.2 shows dynamics, and model of a mobile robot. In 2.1.3, motion control of the mobile robot is shown. The velocity control system is designed. Also, subsection 2.1.3 describes that the disturbance observer is able to recognize road surface without force sensor. Haptograph which represents tactile information is described in 2.1.4. The experimental results are shown in 2.1.5. The last subsection summarizes this research.

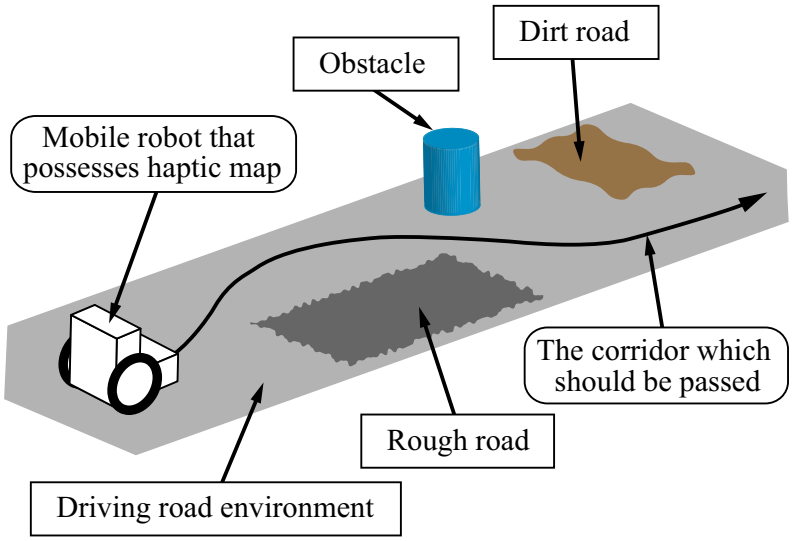

Fig. 2.1. The driving road environment in the real-world.

2.1.2 Modeling of Mobile Robot

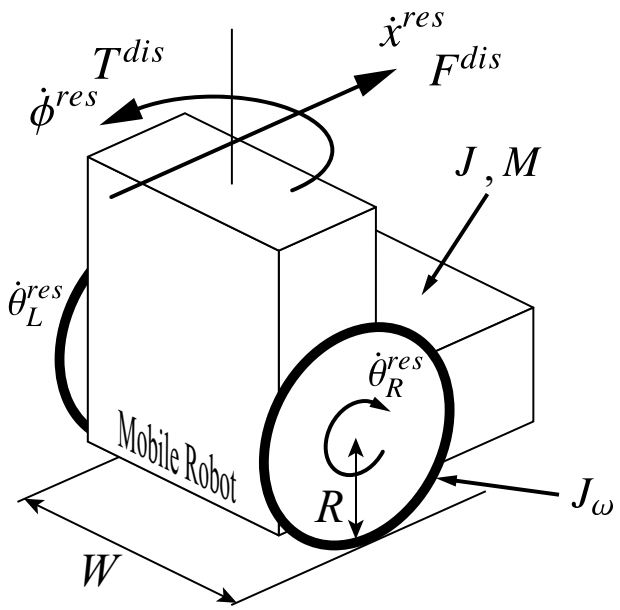

Fig. 2.2. Modeling of the mobile robot.

The model of the mobile robot used in this thesis is shown Fig. 2.2 [28]. This mobile robot is driven by two motors, and it has translational and/or rotational motions. The model parameters

are described as follows,

$\dot{x}$	:	translational velocity of the mobile robot;
$\dot{\phi}$	:	rotational velocity of the mobile robot;
F^{dis}	:	disturbance force of translational mode;
T^{dis}	:	disturbance torque of rotational mode;
$\dot{\theta}_R$	:	velocity of right wheel;
$\dot{\theta}_L$	:	velocity of left wheel;
J	:	inertia of the mobile robot with respect to a vertical axis;
J_ω	:	inertia of driving motor and wheel;
R	:	radius of driving wheel;
W	:	tread of the mobile robot;
M	:	mass of the mobile robot.

2.1.2.1 Dynamic Relationship in Joint Space

This section shows an equivalent inertia matrix to construct the mobile robot control system. When the parameters that are shown in Fig. 2.2 are fixed; movement energy function is defined by (2.1)

$$\begin{aligned} K = & \frac{1}{2}M\left(\frac{R}{2}(\dot{\theta}_R+\dot{\theta}_L)\right)^2 \\ + & \frac{1}{2}J\left(\frac{R}{W}(\dot{\theta}_R-\dot{\theta}_L)\right)^2 \\ + & \frac{1}{2}J_\omega(\dot{\theta}_R^2+\dot{\theta}_L^2) \end{aligned} \tag{2.1}$$

In equation (2.1), the first term of right side is the translational movement energy, the second term is the rotational energy of the mobile robot, and third term of right side is the rotation energy of the right and left wheels. The dynamics of the mobile robot should be defined by solving the Lagrange equation from (2.1), yields and it represent in equation (2.2)

$$\begin{bmatrix} \tau_R \\ \tau_L \end{bmatrix} = \boldsymbol{M}_\theta \begin{bmatrix} \ddot{\theta}_R \\ \ddot{\theta}_L \end{bmatrix}. \tag{2.2}$$

where τ_R and τ_L is torque of right and left driving motor, respectively. In regard to $\boldsymbol{M}_\theta$, it is called the equivalent inertia matrix. The equivalent inertia matrix $\boldsymbol{M}_\theta$ is expressed as (2.3)

$$\boldsymbol{M}_\theta = R^2\begin{bmatrix} \frac{M}{4}+\frac{J}{W^2}+\frac{J_\omega}{R^2} & \frac{M}{4}-\frac{J}{W^2} \\ \frac{M}{4}-\frac{J}{W^2} & \frac{M}{4}+\frac{J}{W^2}+\frac{J_\omega}{R^2} \end{bmatrix}. \tag{2.3}$$

The control system of the mobile robot composes using equations (2.2) and (2.3).

2.1.3 Motion Control for Mobile Robot

The thesis uses a disturbance observer to obtain information of road surface.

2.1.3.1 Sensor-less Recognition of Road Surface

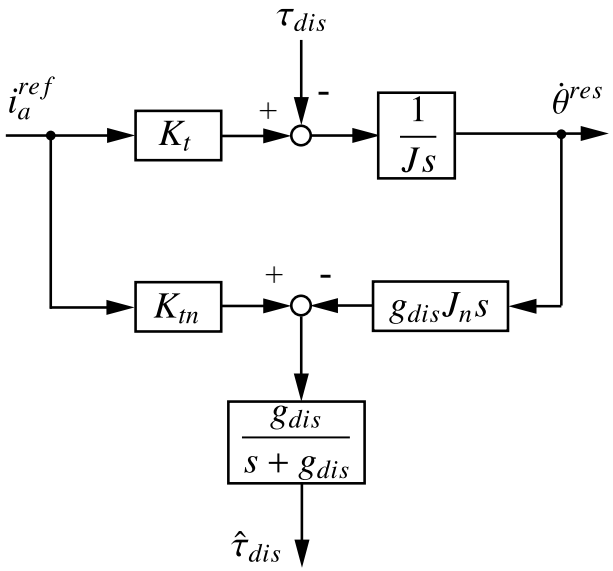

Fig. 2.3. Block diagram of disturbance observer.

A block diagram of a disturbance observer is shown in Fig. 2.3. The disturbance observer estimates disturbance torque from environment. The disturbance torque $\hat{\tau}_{dis}$ is calculated by input current i_a^{ref} and velocity of the motor $\dot{\theta}^{res}$. If this observer is constructed, the mobile robot is able to detect disturbance torque $\hat{\tau}^{dis}$ without sensors. The disturbance torque $\hat{\tau}^{dis}$ that is estimated through the first-order low-pass filter is shown by (2.4)

$$\hat{\tau}^{dis} = \frac{g_{dis}}{s + g_{dis}} \tau^{dis} \tag{2.4}$$

where g_{dis} is pole of the disturbance observer, and determine frequency bandwidth. The disturbance torque $\hat{\tau}^{dis}$ which is estimated is used to compensate disturbance. The estimated disturbance torque $\hat{\tau}^{dis}$ is used for making a haptograph. That observer obtains the disturbance torque $\hat{\tau}^{dis}$ in order to analyze frequency component of the force signal from road surface. It is

possible to obtain data of haptograph on any roads. The detail of the haptograph is explained in section 4.

2.1.3.2 Velocity Control System using a Quarry Matrix

The mobile robot which is used in this thesis is controlled by velocity control system. Fig.

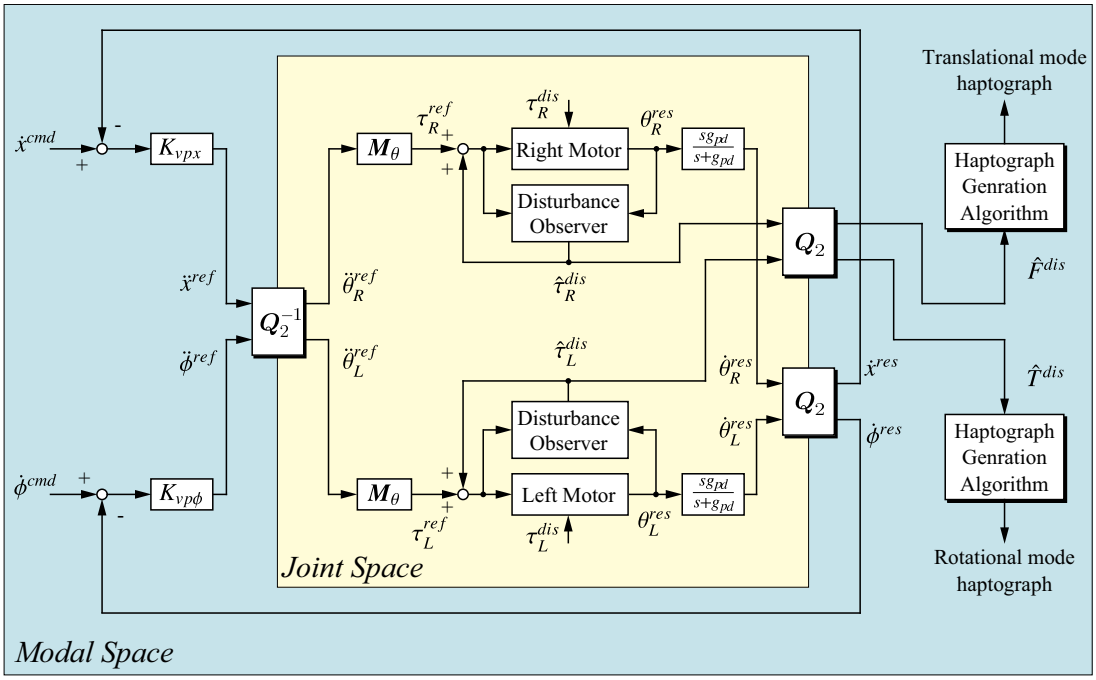

Fig. 2.4. Velocity control system of the mobile robot with the quarry matrix and disturbance observer.

2.4 shows block diagram of the velocity control system. The each parameter is described as follows,

K_{vpx} : proportional gain of translational mode; velocity control;

$K_{vp\phi}$: proportional gain of rotational mode; velocity control;

g_{pd} : pole of pseudo-derivative.

The conversion from real-world joint space to virtual-world modal space achieve using a quarry matrix [65]. The second-order quarry matrix $\boldsymbol{Q}_2$ is defined by (2.5) [63]

$$\boldsymbol{Q}_2 = \frac{1}{2}\begin{bmatrix} 1 & 1 \\ 1 & -1 \end{bmatrix}. \tag{2.5}$$

Equation (2.6) shows the velocity response of right and left driving motor $\dot{\theta}_R^{res}$, $\dot{\theta}_L^{res}$ is transformed to translational mode velocity response $\dot{x}^{res}$, rotational mode velocity response $\dot{\phi}^{res}$ by the second order quarry matrix $\boldsymbol{Q}_2$

$$\begin{aligned} \begin{bmatrix} \dot{x}^{res} \\ \dot{\phi}^{res} \end{bmatrix} &= \boldsymbol{Q}_2 \begin{bmatrix} \dot{\theta}_R^{res} \\ \dot{\theta}_L^{res} \end{bmatrix} \\ &= \frac{1}{2} \begin{bmatrix} 1 & 1 \\ 1 & -1 \end{bmatrix} \begin{bmatrix} \dot{\theta}_R^{res} \\ \dot{\theta}_L^{res} \end{bmatrix}. \end{aligned} \tag{2.6}$$

This system controls translational mode velocity $\dot{x}^{res}$ and rotational mode velocity $\dot{\phi}^{res}$, respectively. The acceleration reference of each mode $\ddot{x}^{ref}$, $\ddot{\phi}^{ref}$ is denoted by (2.7), (2.8)

$$\ddot{x}^{ref} = K_{vpx} \left(\dot{x}^{cmd} - \dot{x}^{res}\right) \tag{2.7}$$

$$\ddot{\phi}^{ref} = K_{vp\phi} \left(\dot{\phi}^{cmd} - \dot{\phi}^{res}\right) \tag{2.8}$$

where the translational mode velocity response $\dot{x}^{res}$ and rotational mode response $\dot{\phi}^{res}$ follows translational mode velocity command $\dot{x}^{cmd}$ and rotational mode velocity command $\dot{\phi}^{cmd}$.

On the other hand, the transformation from virtual-world modal space to real-world joint space is realized by equation (2.9)

$$\begin{aligned} \begin{bmatrix} \ddot{\theta}_R^{ref} \\ \ddot{\theta}_L^{ref} \end{bmatrix} &= \boldsymbol{Q}_2^{-1} \begin{bmatrix} \ddot{x}^{ref} \\ \ddot{\phi}^{ref} \end{bmatrix} \\ &= \begin{bmatrix} 1 & 1 \\ 1 & -1 \end{bmatrix} \begin{bmatrix} \ddot{x}^{ref} \\ \ddot{\phi}^{ref} \end{bmatrix}. \end{aligned} \tag{2.9}$$

where $\boldsymbol{Q}_2^{-1}$ is inverse matrix of the quarry matrix $\boldsymbol{Q}_2$. More specifically, the translational and rotational mode acceleration reference $\ddot{x}^{ref}$, $\ddot{\phi}^{ref}$ that are calculated by (2.7), (2.8) can be converted to acceleration reference of right and left driving motors $\ddot{\theta}_R^{ref}$, $\ddot{\theta}_L^{ref}$. The acceleration references are attained by robust acceleration control.

By this means, the velocity control system of the mobile robot using the quarry matrix achieve independently translational mode velocity and rotational mode velocity.

2.1.3.3 Modal Decomposition of Haptic Information from Road Surface

The quarry matrix $\boldsymbol{Q}_2$ is able to apply for conversion of disturbance force. It is represented as (2.10)

$$\begin{aligned} \begin{bmatrix} \hat{F}^{dis} \\ \hat{T}^{dis} \end{bmatrix} &= \boldsymbol{Q}_2 \begin{bmatrix} \hat{\tau}_R^{dis} \\ \hat{\tau}_L^{dis} \end{bmatrix} \\ &= \frac{1}{2} \begin{bmatrix} 1 & 1 \\ 1 & -1 \end{bmatrix} \begin{bmatrix} \hat{\tau}_R^{dis} \\ \hat{\tau}_L^{dis} \end{bmatrix}. \end{aligned} \tag{2.10}$$

Each disturbance torque of right and left wheels $\hat{\tau}_R^{dis}$, $\hat{\tau}_L^{dis}$ which is estimated by disturbance observer is transformed into modal space by the quarry matrix $\boldsymbol{Q}_2$. The translational mode disturbance force $\hat{F}^{dis}$ and rotational mode disturbance torque $\hat{T}^{dis}$ are obtained. Then, these estimated disturbance force and torque $\hat{F}^{dis}$, $\hat{T}^{dis}$ are calculated in order to acquire haptograph in each mode.

2.1.4 Haptic Representation using Haptograph

This section expresses that haptograph is available for haptic representation. Also, this thesis explains how to generate haptograph.

2.1.4.1 Definition of Haptograph

The visual and auditory recognitions have been researched in the world. This visual or auditory information easily can be saved, replayed and transmitted. On the other hand, it is difficult to store and/or evaluate tactile information. A visual organ and auditory organ have been installed to several robots, but haptic organ that is prepared for robots is hardly adequate.

Haptograph helps representing haptic information of environment. Haptograph is able to visually express tactile information of environmental surface [24]. The estimated disturbance force comprises stiffness, viscosity, friction, shape of environment surface and so on. Therefore, haptograph that is obtained by disturbance force includes characteristics of environment. If haptograph adapt to the mobile robot, the mobile robot acquire tactile organ respect to driving road. It is like that we feel road condition by bottom of one's foot. Haptograph uses to visualize

tactile information of the driving road environment.

2.1.4.2 Generation of Haptograph

The estimated disturbance force contains environment characteristics. A frequency analysis realizes generating haptograph, and come out that characteristic. The frequency analysis is carried out by using Fourier transformation or wavelet transformation. This thesis employ latter, and use Gabor continuous wavelet transform(GCWT). GCWT provides haptograph every position of the mobile robot. Hence, the mobile robot achieves making haptic map. The haptic map that is generated by GCWT fills in tactile information to real-world space. The GCWT composes haptograph generation algorithm which is shown in Fig. 2.4.

2.1.5 Experiment

2.1.5.1 Experimental setup

This experiment carries out both on concrete floor and on non-slip steel plate floor. Fig. 2.5

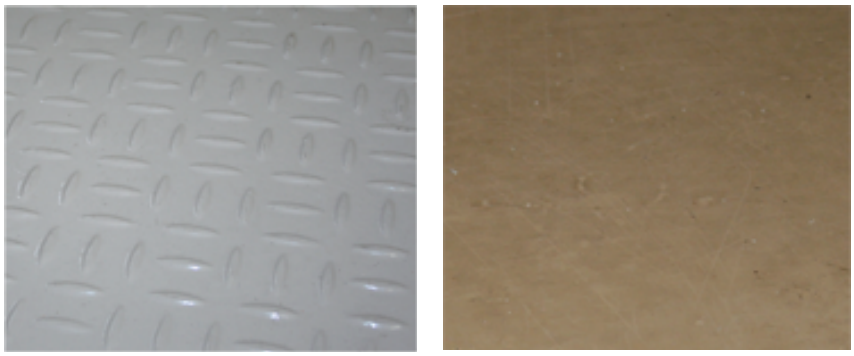

Fig. 2.5. Picture of road environments. (a) Non-slip steel plate floor. (b) Concrete floor.

shows pictures of concrete floor and non-slip steel plate floor that are used in this experiment. The concrete floor is approximately flat; on the other hand the non-slip steel plate is rough. These materials are deployed as Fig. 2.6. The mobile robot which is on concrete floor moves to non-slip steel plate. At the same time the mobile robot generates haptograph of the configured driving road environment. This method realizes making haptic map that includes tactile

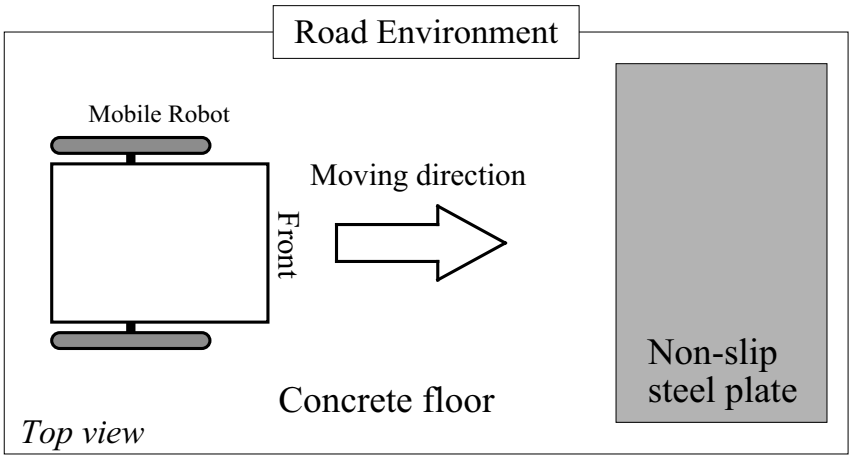

Fig. 2.6. Road environment which is configured in the experiment.

information of road.

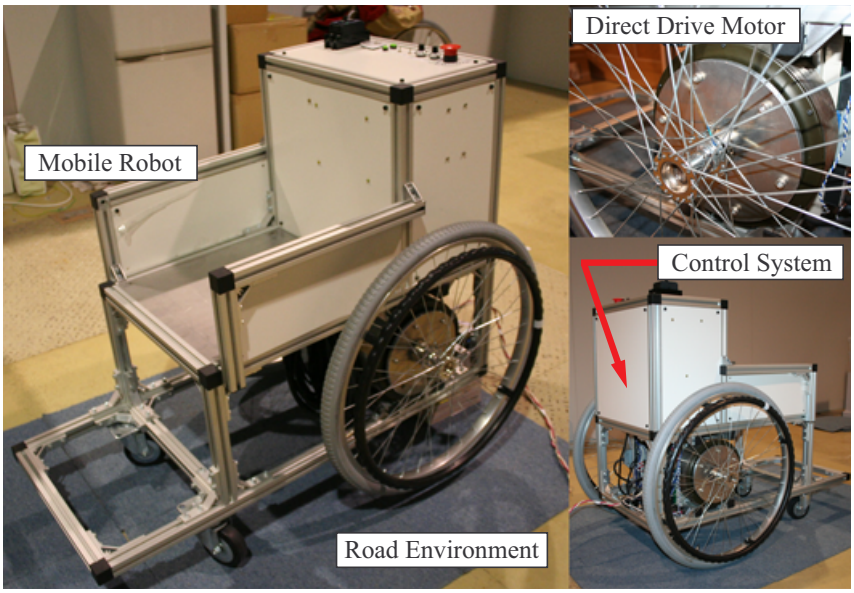

Fig. 2.7. Appearance of the mobile robot which is used in the experiment.

The mobile robot is shown in Fig. 2.7. The mobile robot mounts two direct drive motors. Fig. 2.8 represents the mobile robot control system. The controlling equipment which is composed by RT-Linux 3.2, realizes the speed control system with the disturbance observer and quarry matrix. In this experiment, the sampling time of the control system is set to 100 μs. Table 2.1

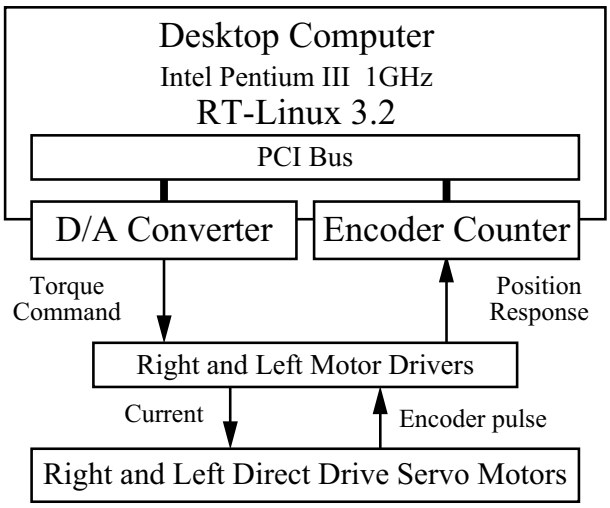

Fig. 2.8. Control system of the mobile robot using a real time Linux kernel.

shows the values of each parameter in this experiment. The length overall of the mobile robot

Table 2.1. Setup Parameters

K_{vpx}	Proportional gain of translational mode	5.0	
$K_{vp\phi}$	Proportional gain of rotational mode	5.0	
M	Mass of the mobile robot	50	kg
W	Tread of the mobile robot	0.580	m
R	Radius of wheel	0.306	m
K_t	Torque constant of the motor	4.46	Nm/A
J_ω	Inertia of wheel and motor	0.14	kgm^2
J_n	Inertia of body of the mobile robot	5.7	kgm^2
g_{dis}	Pole of the disturbance observer	300	rad/s
g_{pd}	Pole of the pseudo-derivative	600	rad/s

is 1000 mm, and the tread is 580 mm.

2.1.5.2 Experimental Results

Fig. 2.9 and Fig. 2.10 show the experimental results of translational mode haptograph and rotational mode haptograph, respectively. A waveform of disturbance force and torque F^{dis}, T^{dis} are shown in (a) of each figure. The haptograph representation which is generated by GCWT is shown in (b). In regard to configured road environment, concrete floor is 0 to 0.9 m;

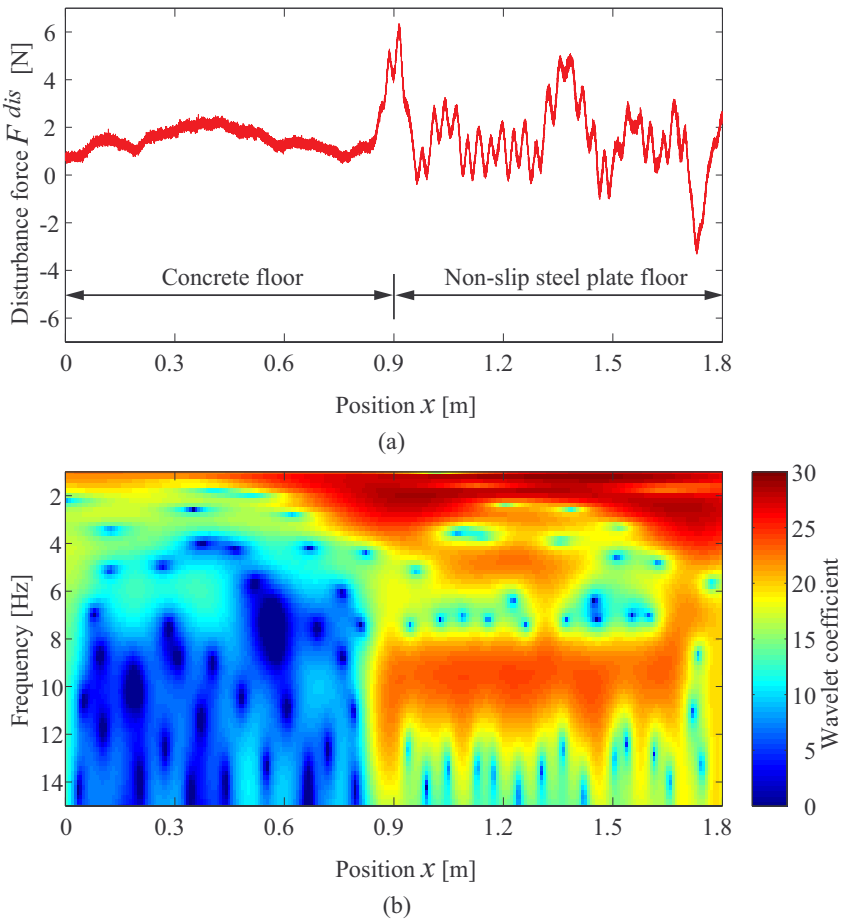

Fig. 2.9. Experimental results of translational mode. (a) Waveform of disturbance force F^{dis}. (b) Translational mode haptograph.

non-slip steel plate floor is 0.9 to 1.8 m. Translational mode velocity command $\dot{x}^{cmd}$ is set to 0.3 m/s, Rotational mode velocity command $\dot{\phi}^{cmd}$ is set to 0 rad/s.

A section of 0 to 0.9 m in the haptograph representation is approximately blue color. On the contrary, a section of 0.9 to 1.8 m of haptograph includes several components. These results show that the haptograph represents the driving road environment. Furthermore it is possible to grasps the tactile information of road with respect to the position response. The frequency components at arbitrary position are important.

The experimental haptograph represents characteristic frequency components of 10 Hz. In other words, the environment surface of rough road has 10 Hz component, when the mobile

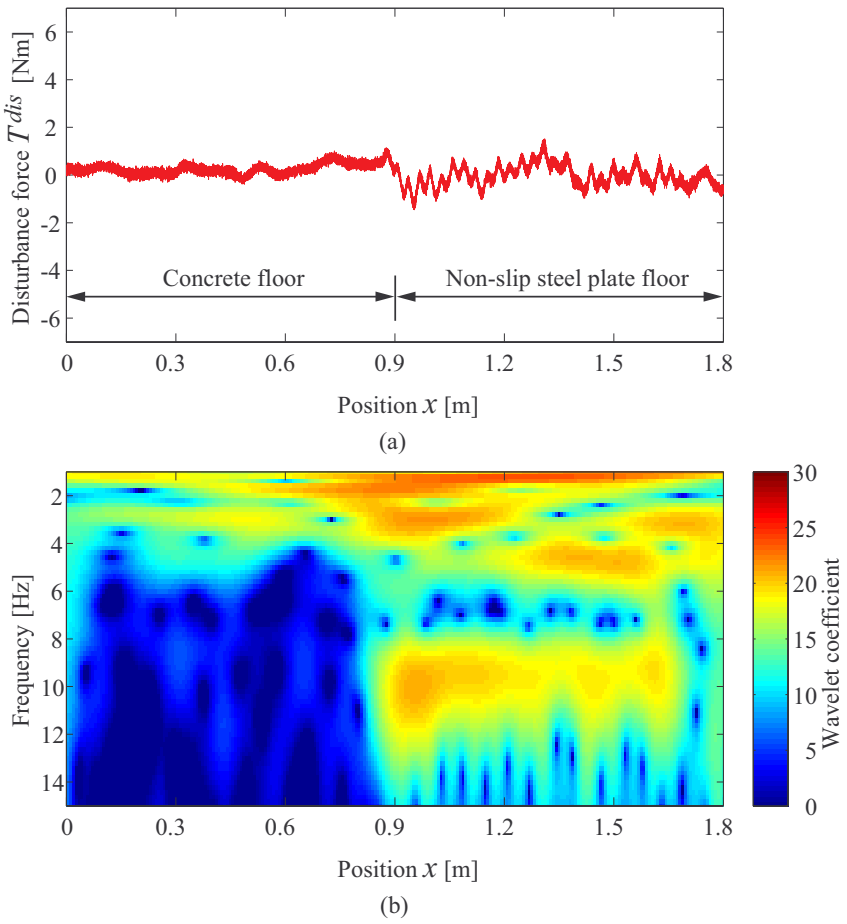

Fig. 2.10. Experimental results of rotational mode. (a) Waveform of disturbance force T^{dis}. (b) Rotational mode haptograph.

robot drives at speed of 0.3 m/s. Therefore, this place of road should be avoided for achieving better ride quality.

As a result, the mobile robot recognizes tactile information of road using the haptograph.

2.1.6 Conclusions

The thesis proposes a novel haptic recognition. The velocity control system using a quarry matrix and disturbance observer is mounted on the mobile robot in order to represent tactile information of road surface. Such velocity control system achieves controlling translational and rotational speed, independently. The mobile robot obtains haptic information of road surface

from haptograph that is generated by haptic recognition algorithm. Gabor continuance wavelet transformation realizes the haptic recognition algorithm. The calculated haptograph images vary according to material and/or condition of road surface. It is possible to make a haptic map that visualizes the driving environment of road. An availability of haptograph for haptic recognition is confirmed in this thesis. This thesis exhibits enhancing tactile recognition ability of a mobile robot respect to driving road environment. In the future, the mobile robot is able to avoid rough road taking ride ability into account. It will be useful for welfare human assistance.

2.2 Recognition of Driving Road Environment

2.2.1 Introduction

Recent motion systems begin to spread in the society and they are required to have ability to recognize unknown and/or unstructured environments. Especially, the future robots should have haptic ability. In the thesis, a haptic sensation is installed into a mobile robot.

A control system of the mobile robot using a quarry matrix respectively controls translational force and rotational angle of the mobile robot. Therefore, the control system carries out flexible motion in order to enhance the safety for human and obstacle. Additionally, established potential field realizes avoidance of obstacles and arriving in destination. A haptograph generation algorithm employing Gabor continuous wavelet transform generates haptograph using estimated disturbance torque by a disturbance observer. The haptic information in the real-world is visualized by haptograph. The weighting function can be arbitrarily configured, which processes haptograph in order to consider ride quality and/or week point of mounted device on the mobile robot. The weighted haptograph is useful for making haptic map of driving road environment and trajectory planning for a mobile robot. Finally, the mobile robot achieves arriving in destination, and avoidance of not only obstacle but also punishing road. The experimental results show viability of the proposed method.

2.2.2 Motion Control of Mobile Robot

Fig. 2.11 shows control system of the mobile robot. Fundamentally, control method used in this research is almost same as the control system mentioned in the previous section. However, controllers in the modal space is different. In concrete terms, translational acceleration reference $\ddot{x}^{ref}$ is calculated as

$$\ddot{x}^{ref} = C_f \ (F^{cmd} - F^{ext}) \tag{2.11}$$

where C_f and F^{cmd} denote gain of force controller and force command, respectively. On the other hand, rotational acceleration reference $\ddot{\phi}^{ref}$ is given by

$$\ddot{\phi}^{ref} = (K_P + sK_D) \ (\phi^{cmd} - \phi^{res}) \tag{2.12}$$

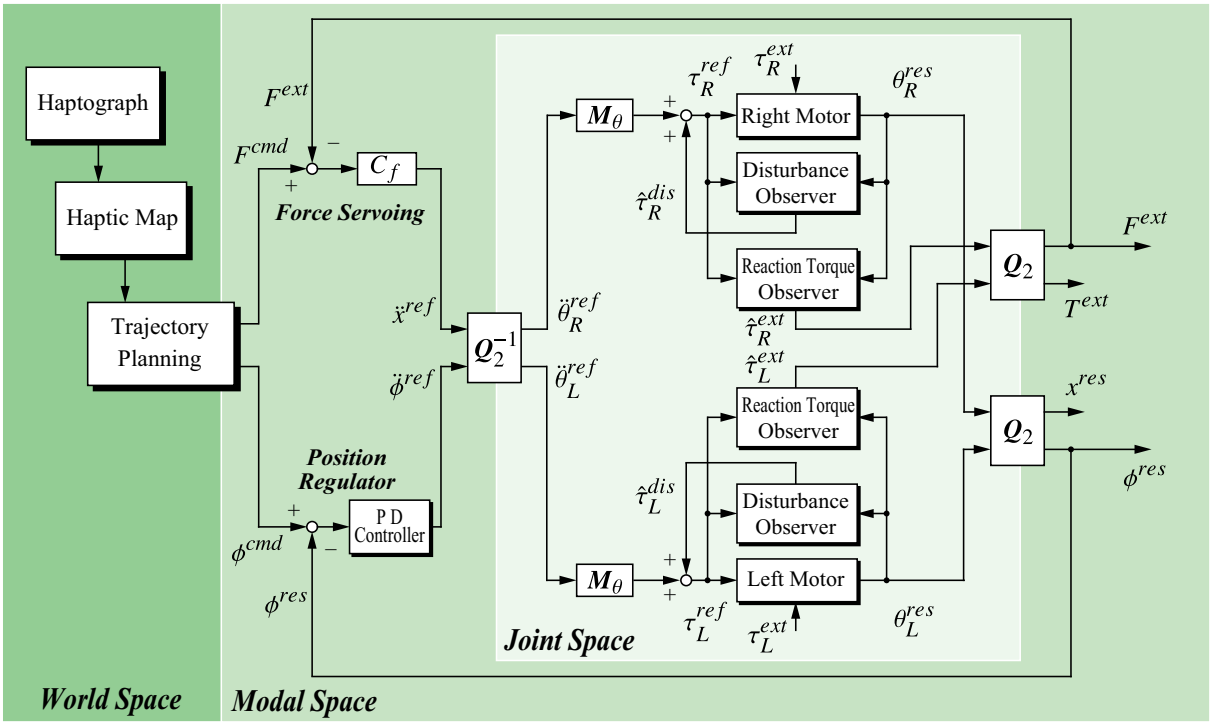

Fig. 2.11. Translational mode force and rotational mode position control system using quarry matrix.

where K_P represents proportional gain, K_D means differential gain of position controller. ϕ^{cmd} and ϕ^{res} are position command and position response. In other words, the force controller and the position controller are implemented in the translational mode and the rotational mode, respectively.

2.2.3 Trajectory Planning for Obstacle Avoidance

In this thesis, trajectory generation for the mobile robot shown in the previous section is conducted by using the potential field. The force command in the translational mode and the yaw angle control in the rotational mode are obtained by the potential field, so that the mobile robot is able to arrive at destination without contact to obstacles. The Gaussian surface shown in Fig. 2.12 represents potential field of the obstacle. The potential field of the obstacle P_{obs} is

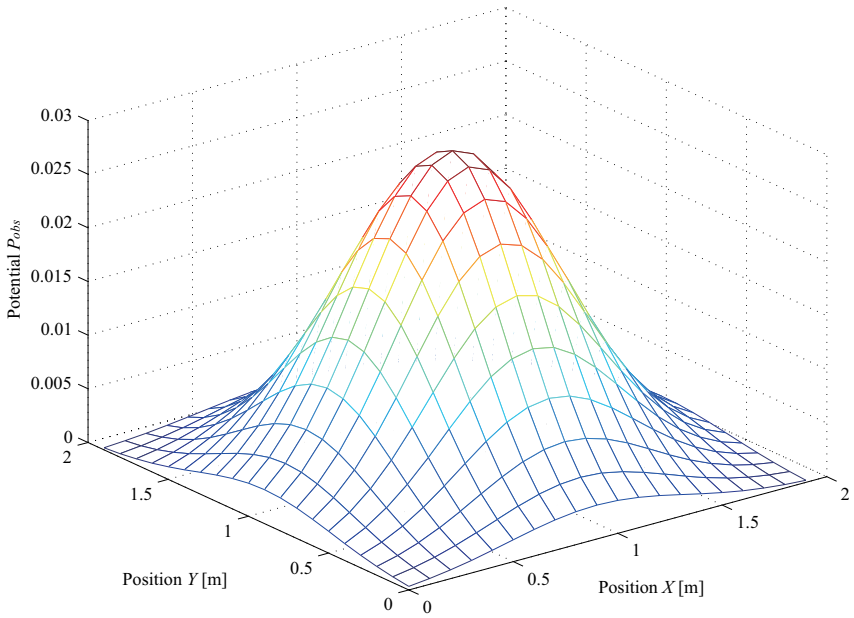

Fig. 2.12. Potential field of simple obstacle.

calculated as

$$P_{obs} = A \exp\left(-\frac{(X - X_{obs})^2 + (Y - Y_{obs})^2}{\sigma^2}\right) \tag{2.13}$$

where A denotes height of the Gaussian surface, σ is spread of the Gaussian surface. X_{obs} andY_{obs} mean position of the obstacle.

On the other hand, the potential field considering the destination P_{dest} is given by

$$P_{dest} = (X - X_{dest})^2 + (Y - Y_{dest})^2 \tag{2.14}$$

where X_{dest} and Y_{dest} denote position of the destination. Additionally, the potential field shown in Fig. 2.13 considering the obstacle and the destination P is calculated as

$$P = P_{dest} + P_{obs}. \tag{2.15}$$

Fig. 2.11 shows force control system for the mobile robot. By using the potential field P shown in Fig. 2.13, the command values for the control system shown in Fig. 2.11 are calculated. In case that the destination is distant, the force command of the translational mode F^{cmd} is set to constant value. On the other hand, when height value of the potential field P is nearly equal to

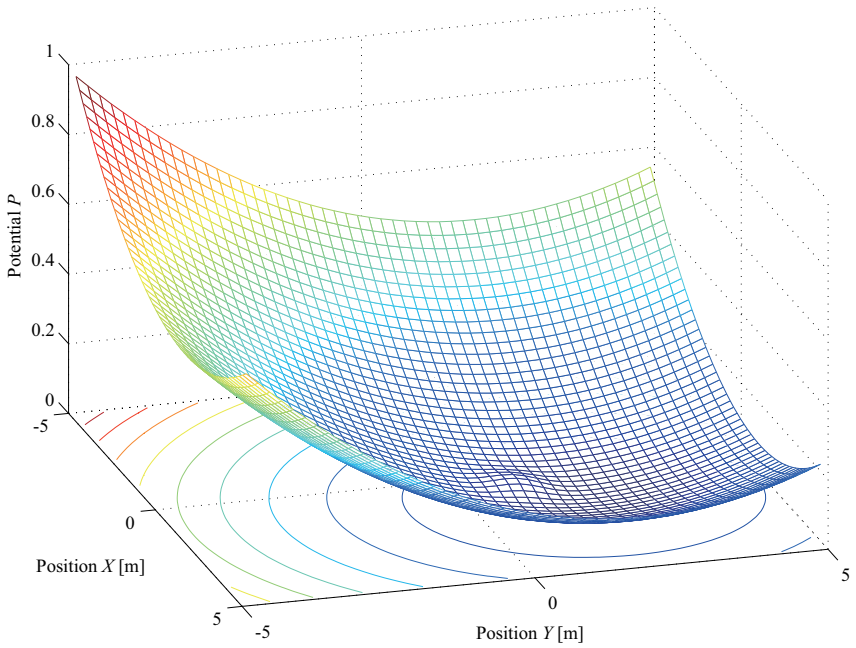

Fig. 2.13. Potential field.

0, the force command of the translational mode F^{cmd} is set to 0.

$$F_{i,j}^{cmd} = \begin{cases} 0 & (P_{i,j} \simeq 0) \\ \text{const} & (P_{i,j} > 0) \end{cases} \tag{2.16}$$

i and j are element number of lattice in the potential field.

In addition, the yaw angle command of the rotational mode ϕ^{cmd} is determined by direction of slope in the potential field P as follows:

$$\frac{\partial P_{i,j}}{\partial X} = \frac{1}{2\ \Delta X}\left(P_{i+1,j} - P_{i-1,j}\right) \tag{2.17}$$

$$\frac{\partial P_{i,j}}{\partial Y} = \frac{1}{2\ \Delta Y}\left(P_{i,j+1} - P_{i,j-1}\right) \tag{2.18}$$

$$\phi_{i,j}^{cmd} = \tan^{-1}\left(-\frac{\partial P_{i,j}}{\partial Y} \Big/ -\frac{\partial P_{i,j}}{\partial X}\right) \tag{2.19}$$

where ΔX and ΔY represent interval of the lattice in the potential field. By this means, the force command in the translational mode F^{cmd} and the command of yaw angle ϕ^{cmd} can be obtained.

2.2.4 Experiment of Obstacle Avoidance

In this experiment, the position of the obstacle is set as $X_{obs} = 1.0$ m, $Y_{obs} = 1.0$ m, the destination position is set as $X_{dest} = 2.0$ m, $Y_{dest} = 1.5$ m. Initial position of the mobile robot is set as $X = 0.0$ m , $Y = 0.0$ m. Moreover, interval of lattice ΔX, ΔY are set to 10 cm. Fig. 2.14 shows contour map of the potential field P and trajectory of the mobili robot. The

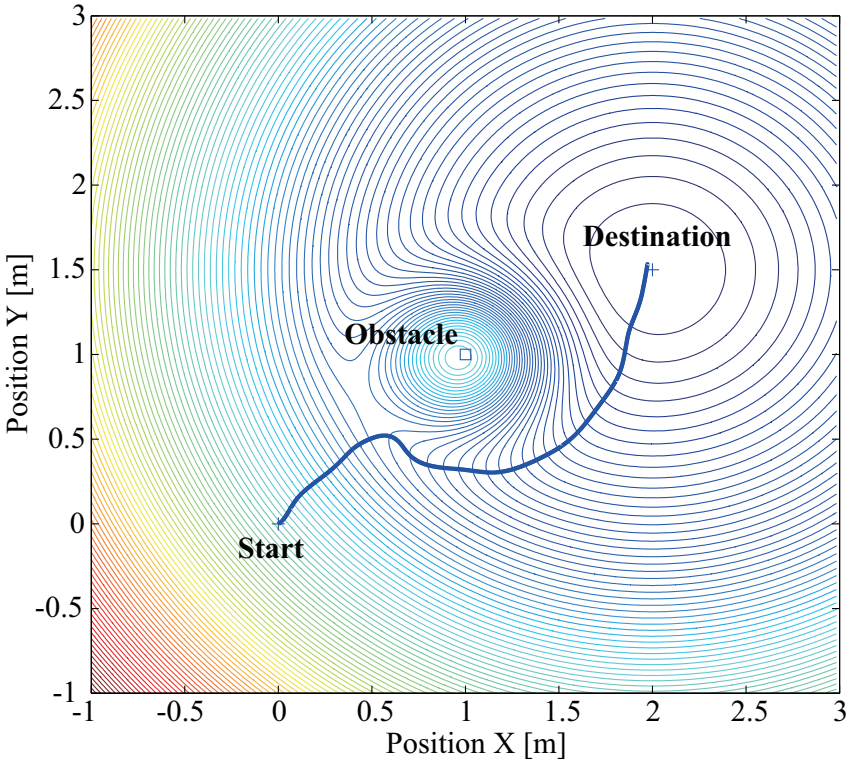

Fig. 2.14. Contour map of potential field and trajectory of mobile robot (Experiment).

feasibility of the method mentined above is verified.

2.2.5 Trajectory Planning using Haptograph

In order to avoid rough road and/or dirt road, the proposed method generate potential field according to the haptograph mentioned in the previous section. This thesis focuses on disturbance force in the translational mode F^{dis}. At first, Gabor continuous wavelet transform

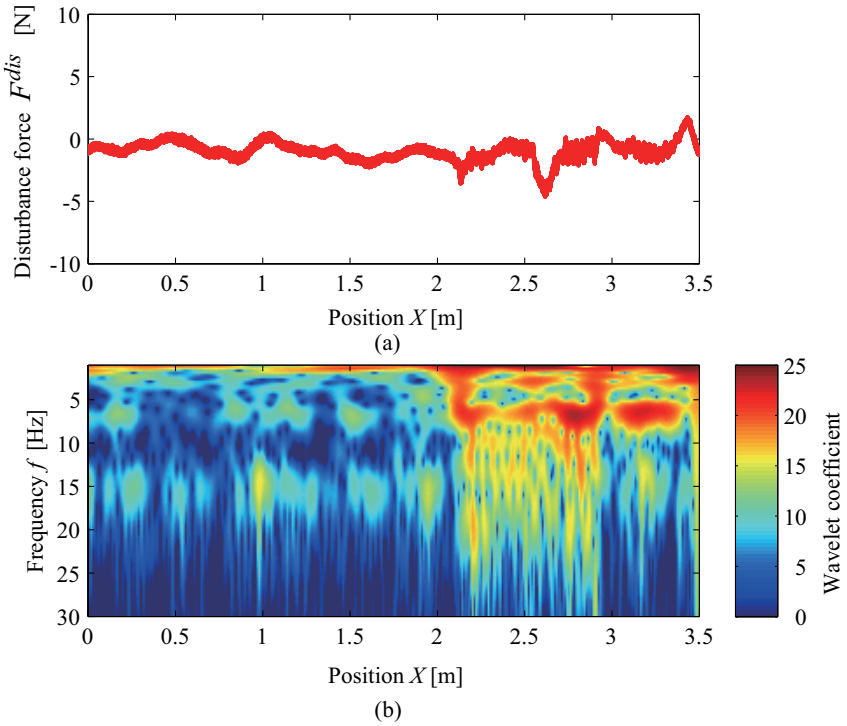

Fig. 2.15. Experimental results. (a) Disturbance force. (b) Haptograph.

generates the haptograph as follows:

$$H = \int \psi^*_{f,X} \; F^{dis} \;\; dx \tag{2.20}$$

where $\psi_{f,X}$, f, and X mean Gabor mother wavelet, frequency, and position of the mobile robot. Figs. 2.15(a) and (b) show experimental results and the calculated haptograph.

This thesis assume that the mobile robot carries human. Therefore, the proposed method is able to calculate trajectory for improvement of ride quality. Fig. 2.16 represents form of weighting function W. The weighting function can be set arbitrarily according to sensitive frequency of human body and/or resonance frequency of installed devices. Thus, the mobile robot is able to avoid road surface, which has the frequency component. At the position X, the haptograph shown in Fig. 2.15 is multiplied by the weighting function W. The calculated haptograph considering the weighting function is shown Fig. 2.17(a).

In the next step, to calculate the ride quality, summation with respect to frequency axis of the

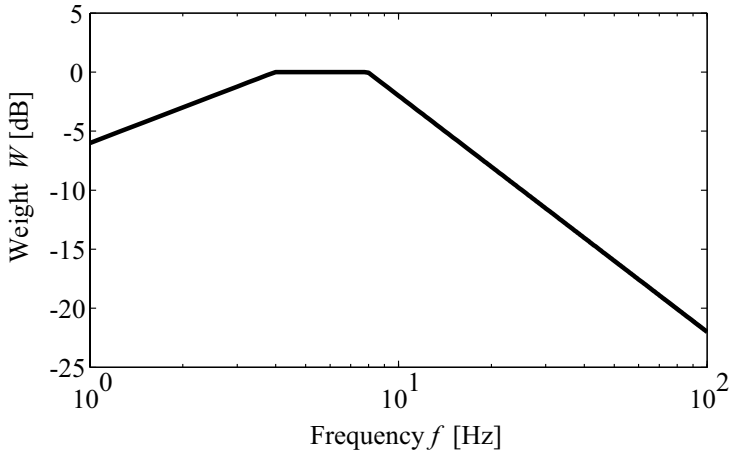

Fig. 2.16. Weighting function

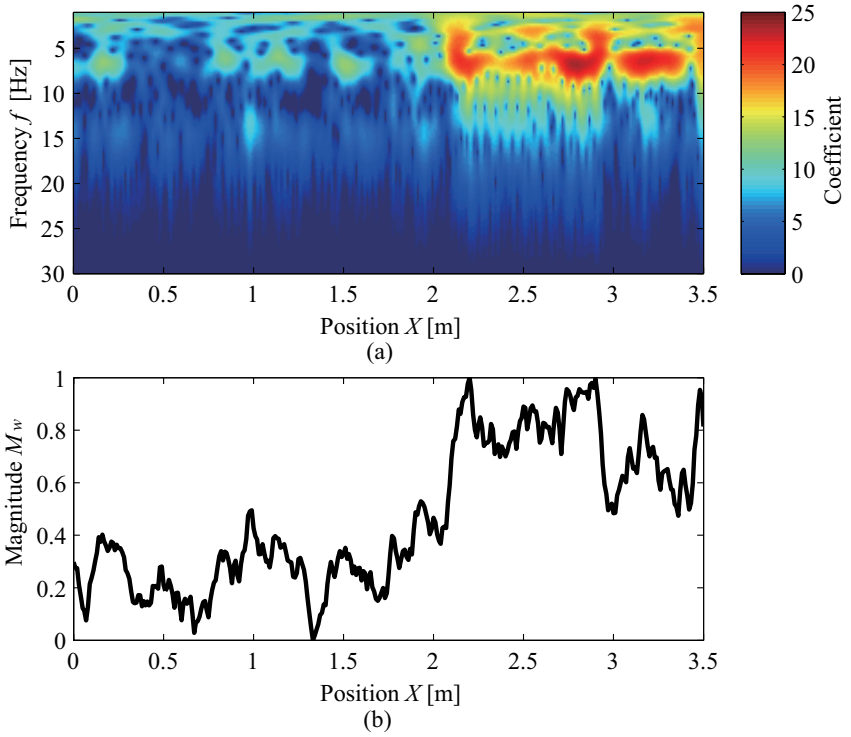

Fig. 2.17. Processed experimental results. (a) Weighted haptograph. (b) Result for integration.

haptograph is calculated. Additionally, value of the summation is standardized by maximum value of the haptograph. Fig. 2.17(b) shows the summation value, which indicates the ride quality. The potential field considering the haptic sensation of the road surface P_{hap} is given

by the ride quality. Fig. 2.18 shows the potential field obtained by the proposed method. In

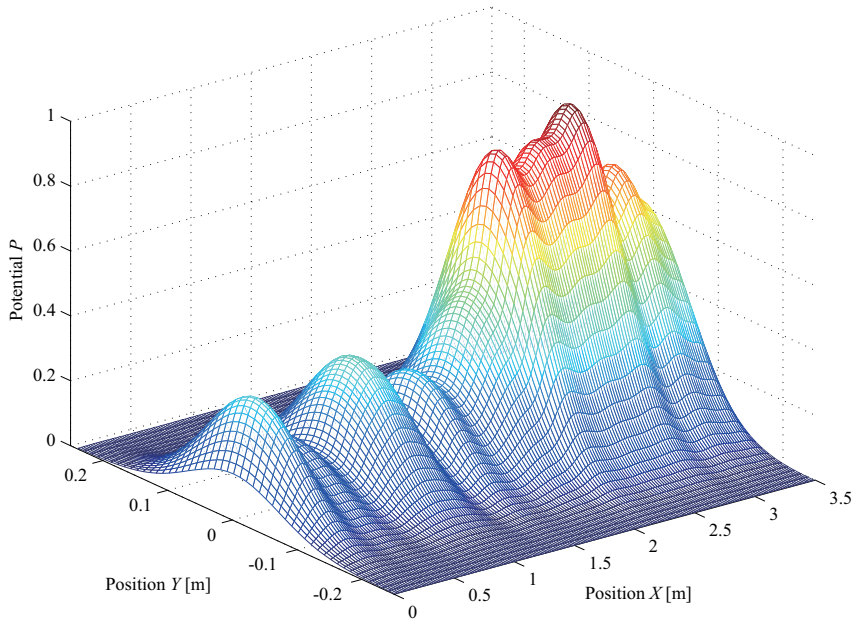

Fig. 2.18. Haptic map which is considered by haptic information of driving road environment.

Fig. 2.18, the low potential value indicates the concrete floor. On the other hand, the high value indicates the rough road. This thesis calls Fig. 2.18 haptic map.

Finally, the potential field including the ride quality as well as the destination and the obstacle is given by

$$P = k_1\ P_{dest}\ +\ k_2\ P_{obs}\ +\ k_3\ P_{hap} \tag{2.21}$$

where k_1, k_2, and k_3 denote coefficients, which can be set arbitrarily. By this means, the mobile robot, which installed the potential field using the haptic map, is capable of avoiding the obstacle and the punishing road.

2.2.6 Experiment

Fig. 2.19 shows experimental results of the proposed method. In this experiment, the mobile robot avoids not only the obstacle but also the rough road, by using the potential field calculated by the haptograph. Hence, validity of the proposed method is verified by the experiment.

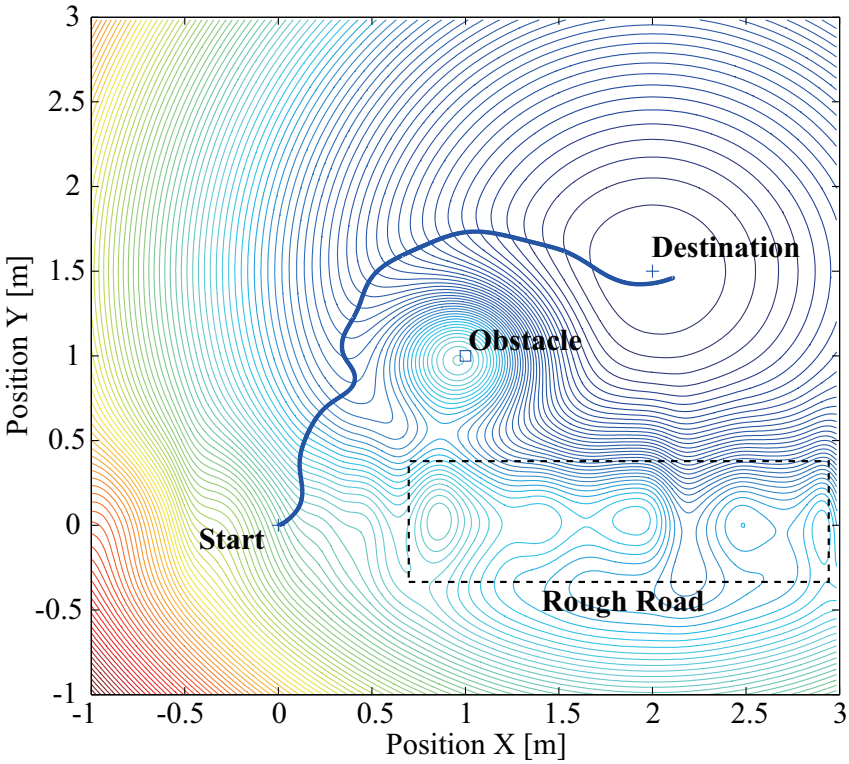

Fig. 2.19. Contour map of potential field and trajectory of mobile robot (Proposed method).

2.2.7 Examination

In this subsection, the effect of velocity variation of the mobile robot is investigated. Fig. 2.20 shows experimental results. The disturbance force and the haptograph are shown in Fig. 2.20(a) and (b), respectively. In the experiment, the velocity of the mobile robot is set to 0.24 m/s. Besides, the disturbance force and the haptograph are shown in Fig. 2.21(a) and (b), when the velocity is set to 0.16 m/s. Compared with Fig. 2.21(b), the high frequency components appear in the haptograph shown in Fig. 2.20(b). This experiment confirms that the frequency components depend on the velocity of the mobile robot. In addition, the potential field generated by the haptograph is shown in Figs 2.20 and 2.23. Though the shape of the potential field is different between 0.24 m/s and 0.16 m/s, the rough road can be represented in each cases. Therefore, the mobile robot is able to recognize the rough road even if the velocity is changed.

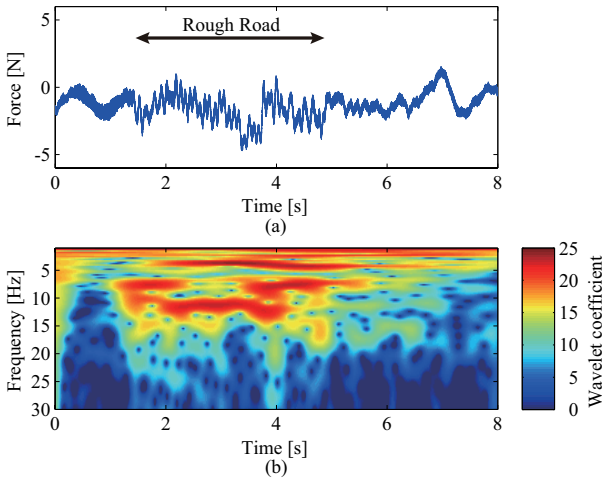

Fig. 2.20. Experimental results. (a) Disturbance force. (b) Haptograph. (Velocity = 0.24 m/s)

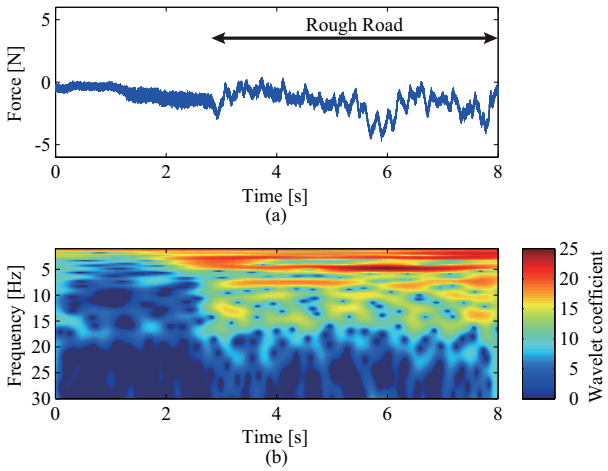

Fig. 2.21. Experimental results. (a) Disturbance force. (b) Haptograph. (Velocity = 0.16 m/s)

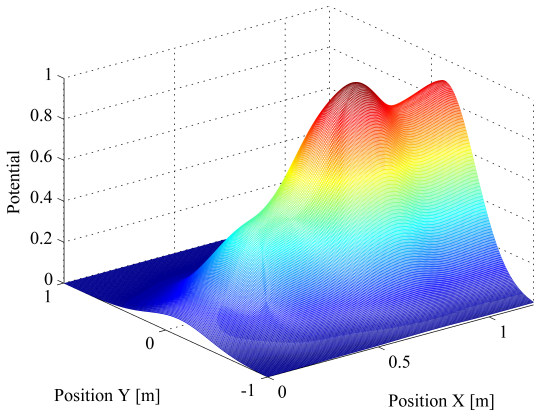

Fig. 2.22. Potential field. (Velocity = 0.24 m/s)

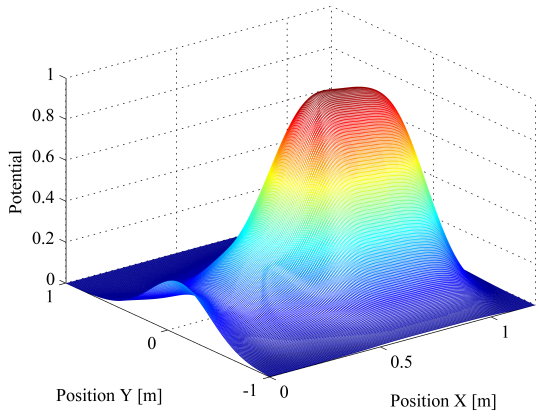

Fig. 2.23. Potential field. (Velocity = 0.16 m/s)

2.2.8 Conclusion

This thesis proposed the avoidance method of the rough road and of the obstacle. Since the method proposed in this thesis utilized the haptic map and the haptograph which represented haptic sensation of the road surface, the ride quality was able to be considered. Therefore, the mobile robot avoided the punishing road. By the experiment, validity of the proposed method is verified.

Chapter 3

Haptic Recognition Based on Human Motion

Abstract

In this chapter, a novel motion-copying system which is able to recognition and reproduce human motion is mentioned. The motion-copying system proposed in this thesis consists of a motion-saving system and a motion-loading system. Using modal decomposition based bilateral controller, the motion-saving system stores motion of the human operator. After that, the motion-loading system is realized by a virtual-world master system and real-world slave systems. The motion-loading system operates according to position and force responses stored by the motion-saving system, so that the human motion is reproduced. By using the proposed method, the reproduced position and the reproduced force correspond to stored ones without mathematical model. The validity of the motion-copying system proposed in this thesis is verified from the view point of theoretical study and experimental results.

In addition, this thesis proposes an environmental copying system, which stores and reproduces the haptic sensation of a target object. The proposed system consists of an environmental saving system and an environmental loading system. The environmental saving system stores the haptic information of the environment to a environmental data memory. On the other hand, the environmental loading system reproduces the environmental haptic sensation using the environmental data memory, and stimulates the human operator. The environmental copying

system proposed in this thesis realizes storage and reproduction of real world haptic information without environmental mathematical model. By the experiments, the validity of the proposed method is confirmed. It will be useful for industrial applications, medical and welfare human support.

3.1 Motion-Copying System

3.1.1 Motion-Copying System Based on Real-World Haptics

3.1.1.1 Introduction

In order to increase the amount and variety of available information in the human society, not only the acoustic and visual, but also haptic informational preservation and/or reproduction technique should be researched and developed, because the human utilizes the information, which is given by the five organs. Fig. 3.1 shows the technique of saving and loading with respect

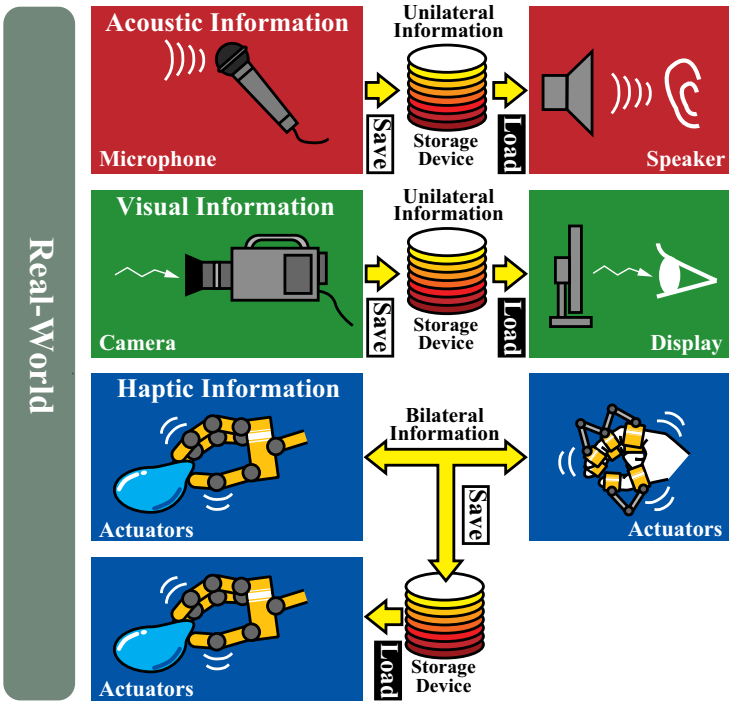

Fig. 3.1. Storage and reproduction of acoustic, visual, and haptic information.

to acoustic, visual and haptic information. The microphone catches air vibration, which comes

from the environment in the real-world. The acoustic information is stored to the memory, and can be reproduced to the real-world by the speaker systems. Additionally, the camera or video camera takes the pictures of the environment. The display system plays the visual information according to the memory. There are much researched and developed, however the research and development in regard to the haptic information is not enough.

The acoustic information and visual information are unilateral information. On the other hand, the haptic informational handling is difficult, because it is bilateral information. The environment is formed by the motion of the human, if the human touches to the environment. Thus, the mutual characteristics are influenced. This situation makes difficult to realize preservation and reproduction of the haptic information. The acquisition methods of the human motion based on visual information are researched [29]–[32]. Also, the method using reaction force between the environment and the human has been proposed [33]. However, these methods consider only either position information or force information. Therefore, it is hard to extract the motion of the human operator. The research considering both the position/velocity and the force has been proposed [34]–[37], though the point of view with respect to saving and loading of the haptic information is not presented.

This thesis proposes a novel motion-copying system [38]–[43], which consists of mainly two parts. The first part is motion-saving system; the other part is motion-loading system. The motion-copying system is constructed by master-slave system using a bilateral control [44]–[62] and quarry matrix [63]. This system observes position and reaction force of master motor by a linear encoder and reaction force observer [64]. The numerical values of observed position and reaction force are stored to the data memories. The stored data represents motion information of a human operator.

On the other hand, the motion-loading system is constructed by virtual master-slave system using the quarry matrix. The motion-loading system reproduces motion of the human operator according to the saved motion data by motion-saving system. At the same time, this system can be operated without the master system in the real-world.

The motion-copying system realizes reproduction of motion. The reproduced position and force by the motion-loading system corresponds to the saved motion data. It is possible to store and reproduce skill of expert engineers by the motion-copying system.

3.1.1.2 Concepts of Motion-Copying System

This section explains concepts of a motion-copying system. Fig. 3.2 shows conceptual diagram of the motion-copying system. The motion-copying system is constructed by two components. The first component is a motion-saving system, and the other component is a motion-loading system.

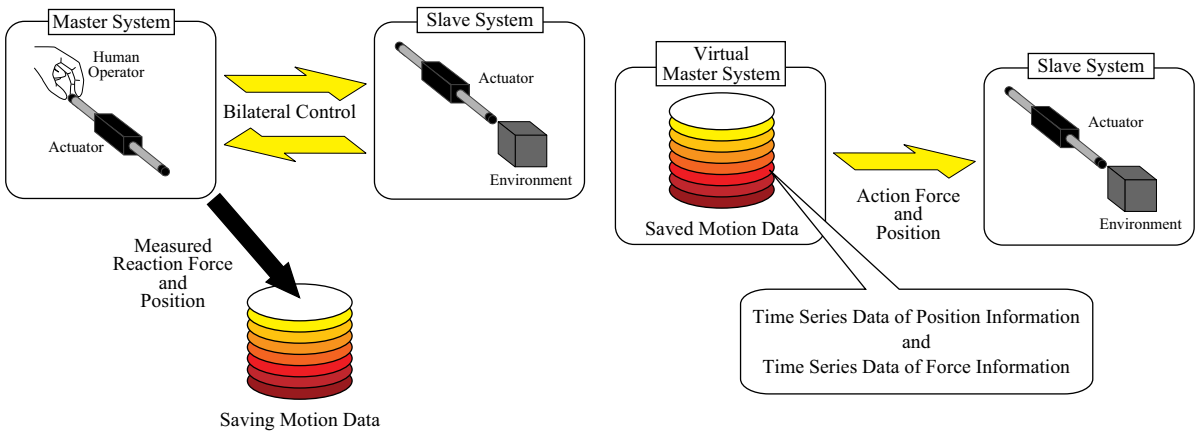

(a) Motion-saving system. (b) Motion-loading system.

Fig. 3.2. Conceptual diagram of motion-copying system.

Concepts of Motion-Saving System The motion-saving system is shown in Fig. 3.2(a). A bilateral control realizes the motion-saving system. A human operator is able to contact to an environment using the bilateral control system. When the human operator impresses action force to a master motor, a slave motor operates according to it. At the same time, the slave motor of the bilateral controller contacts to the environment, and senses reaction force from the environment. The impressed force to each motor is estimated by a reaction force observer. The

estimated force of master motor is saved to a saving motion data memory.

On the other hand, position information of the master motor and slave motor is also considered. The position of the slave motor moves according to the position of the master motor by the bilateral controller. The motion-saving system also saves the position information of the master motor to motion data memory.

In short, the motion-saving system saves the impressed force and position of the master motor to the data memory, and is realized. The motion data in the memory is time series data. Therefore, it is easy to treat the saved motion data.

Concepts of Motion-Loading System Fig. 3.2(b) shows the motion-loading system. In this system, the slave motor is used in the real-world; however, the master motor does not exist in the real-world. The data memory which memorizes motion data composes the master system. The saved motion data in the memory is comprised by the position information and force information. The master system sends the position and force information to the slave system using the saved motion data. The slave motor in the real-world operates according to the sent position and force information. The motion-loading system is constructed based on the bilateral control system. Therefore, the position response and force of the slave motor is able to correspond to the position and force of the master system. Thus, the slave motor reproduces saved motions.

In this way, the motion saving and loading system is realized. Also, the motion-copying system copies motion of human operator.

3.1.1.3 Motion-Saving System using a Bilateral Controller

This section expresses detail of motion-saving system.

Fig. 3.3 shows block diagram of motion-saving system. The motion-saving system consists of the master and slave motors, and controlled by bilateral control system. The block diagram parameters are described as follows,

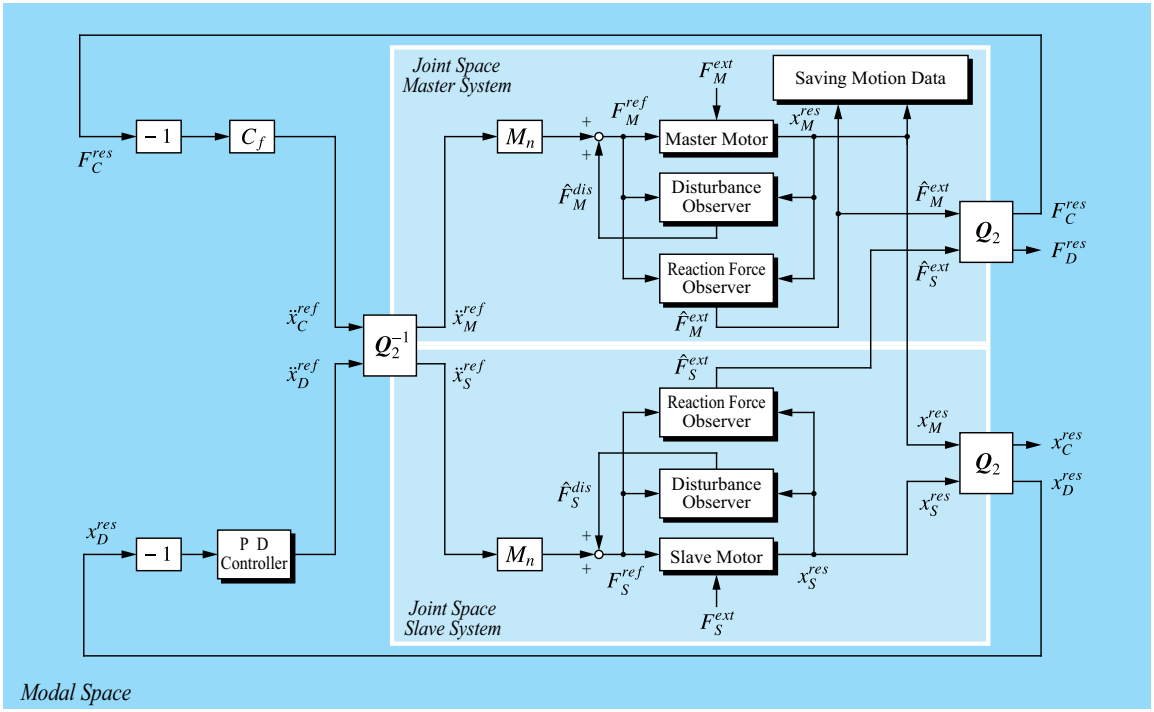

Fig. 3.3. Block diagram of motion-saving system using bilateral control system.

F_C^{res} : Common mode force response ;
F_D^{res} : Differential mode force response ;
x_C^{res} : Common mode position response ;
x_D^{res} : Differential mode position response ;
$\ddot{x}_C^{ref}$: Common mode acceleration reference ;
$\ddot{x}_D^{ref}$: Differential mode acceleration reference ;
$\ddot{x}_M^{ref}$: Acceleration reference of the master motor ;
$\ddot{x}_S^{ref}$: Acceleration reference of the slave motor ;
$\hat{F}_M^{dis}$: Estimated disturbance force of the master motor system ;
$\hat{F}_S^{dis}$: Estimated disturbance force of the slave motor system ;
F_M^{ext} : External force of the master motor ;
F_M^{ext} : External force of the slave motor ;

$\hat{F}_M^{ext}$: Estimated external force of the master motor ;
$\hat{F}_S^{ext}$: Estimated external force of the slave motor ;
x_M^{res} : Position response of the master motor ;
x_S^{res} : Position response of the slave motor ;
F_M^{ref} : Force reference of the master motor ;
F_S^{ref} : Force reference of the slave motor ;
C_f : Assist gain of force feedback control ;
M_n : Mass of actuator component.

The motion-saving system includes three parts. These parts are modal space section, a joint space of the master system section and a joint space of the slave system section. The conversion from real-world joint space to virtual-world modal space achieves using a quarry matrix [65]. The quarry matrix realizes the bilateral controller. The second-order quarry matrix $\boldsymbol{Q}_2$ is defined by (3.1) [63]

$$\boldsymbol{Q}_2 = \frac{1}{2}\begin{bmatrix} 1 & 1 \\ 1 & -1 \end{bmatrix}. \tag{3.1}$$

Equation (3.2) shows the estimated reaction force of the master and slave motor $\hat{F}_M^{ext}$, $\hat{F}_S^{ext}$ by the reaction force observer is transformed to common mode force response F_C^{res} , differential mode force response F_D^{res} by the second order quarry matrix $\boldsymbol{Q}_2$

$$\begin{aligned} \begin{bmatrix} F_C^{res} \\ F_D^{res} \end{bmatrix} &= \boldsymbol{Q}_2 \begin{bmatrix} \hat{F}_M^{ext} \\ \hat{F}_S^{ext} \end{bmatrix} \\ &= \frac{1}{2}\begin{bmatrix} 1 & 1 \\ 1 & -1 \end{bmatrix}\begin{bmatrix} \hat{F}_M^{ext} \\ \hat{F}_S^{ext} \end{bmatrix}. \end{aligned} \tag{3.2}$$

The common mode means sort of overall movement such as bias. On the other hand, the differential mode represents movement between each actuator.

Additionally, the quarry matrix $\boldsymbol{Q}_2$ transforms from the position response of each motor x_M^{res} , x_S^{res} to common mode position response x_C^{res} , differential mode position x_D^{res}.

$$\begin{aligned} \begin{bmatrix} x_C^{res} \\ x_D^{res} \end{bmatrix} &= \boldsymbol{Q}_2 \begin{bmatrix} x_M^{res} \\ x_S^{res} \end{bmatrix} \\ &= \frac{1}{2}\begin{bmatrix} 1 & 1 \\ 1 & -1 \end{bmatrix}\begin{bmatrix} x_M^{res} \\ x_S^{res} \end{bmatrix} \end{aligned} \tag{3.3}$$

This system controls common mode force F_C^{res} and differential mode position x_D^{res}. The acceleration reference of each mode $\ddot{x}_C^{ref}$, $\ddot{x}_D^{ref}$ is denoted by (3.4), (3.5)

$$\ddot{x}_C^{ref} = -C_f\ F_C^{res} \tag{3.4}$$

$$\ddot{x}_D^{ref} = -(K_p + s\ K_d)\ x_D^{res}. \tag{3.5}$$

where, K_p and K_d is proportional gain and differential gain, respectively. The position of differential mode is controlled by PD controller. Also, the disturbance observer operates to cancel the disturbance force as quickly as possible [66]–[71]. The force response of differential mode F_D^{res} and the position response of common mode x_C^{res} is unused to control this system.

On the other hand, the transformation from virtual-world modal space to real-world joint space is realized by equation (3.6)

$$\begin{aligned} \begin{bmatrix} \ddot{x}_M^{ref} \\ \ddot{x}_S^{ref} \end{bmatrix} &= \boldsymbol{Q}_2^{-1} \begin{bmatrix} \ddot{x}_C^{ref} \\ \ddot{x}_D^{ref} \end{bmatrix} \\ &= \begin{bmatrix} 1 & 1 \\ 1 & -1 \end{bmatrix} \begin{bmatrix} \ddot{x}_C^{ref} \\ \ddot{x}_D^{ref} \end{bmatrix}. \end{aligned} \tag{3.6}$$

where $\boldsymbol{Q}_2^{-1}$ is inverse matrix of the quarry matrix $\boldsymbol{Q}_2$. More specifically, the common and differential mode acceleration references $\ddot{x}_C^{ref}$, $\ddot{x}_D^{ref}$ that are calculated by (3.4), (3.5) can be transformed to acceleration reference of the master and slave motors $\ddot{x}_M^{ref}$, $\ddot{x}_S^{ref}$. The acceleration references are attained by robust acceleration control.

The position and force of master motor x_M^{res}, F_M^{res} is varied by the human operator. These two parameters are saved to data memory in order to realize the motion-saving system.

3.1.1.4 Motion-Loading System using a Master-Slave Controller

Fig. 3.4 shows block diagram of the motion-loading system. Fundamentally, a control of the motion-loading system is similar to control of the motion-saving system. The motion-loading system consist of the modal space section, the joint space section of a virtual-world master system and real-world slave system. Each parameter in Fig. 3.4 is calculated, as with case of the motion-saving system. However, the position response x_M^{res} and force response F_M^{res} are set

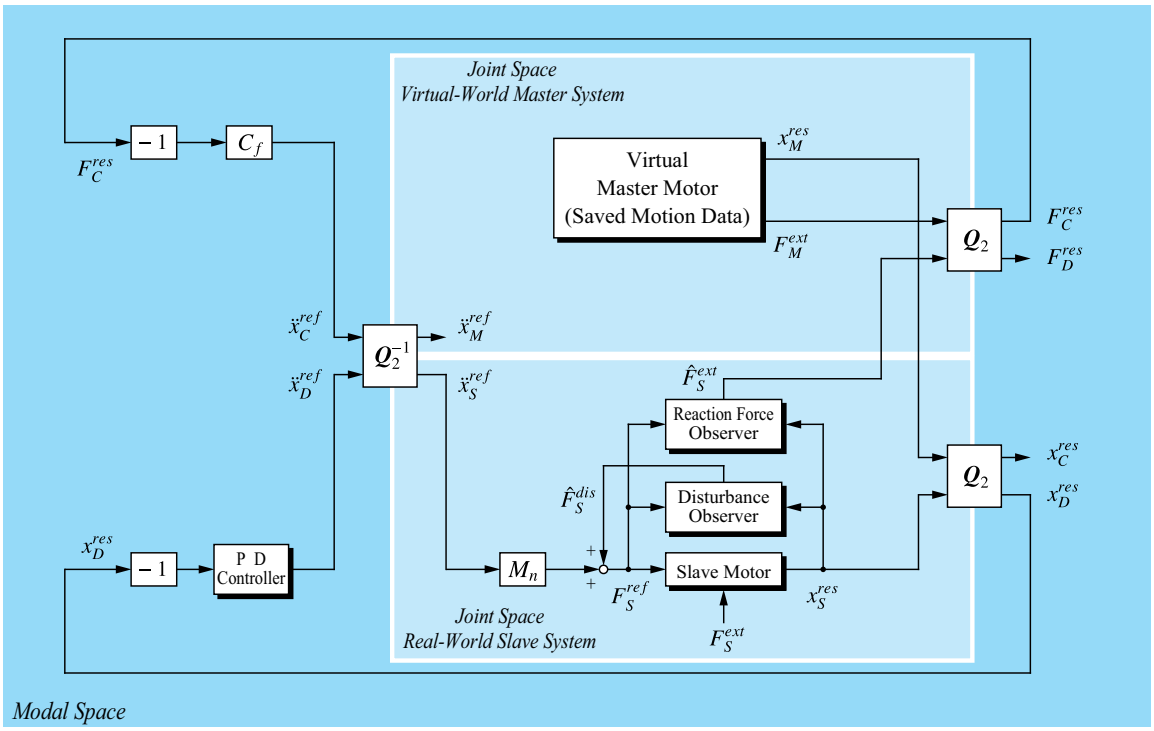

Fig. 3.4. Block diagram of motion-loading system using virtual master system.

to values of the saved motion data. Therefore, the motion-loading system based on master-slave controller reproduces motion according to the saved motion data.

3.1.1.5 Experiment

Experimental Setup Fig. 3.5 and Fig. 3.6 shows the experimental device of the motion-saving system and motion-loading system, respectively. These devices consist of the linear motor and linear encoder. A tip of the slave motor is able to contact to the environment.

The motion-saving system uses two linear motors. On the other hand, the motion-loading system uses one motor. RT-Linux 3.2 controls these motors, and realizes the motion-saving system and motion-loading system. The utilized environment in this experiment is iron block. Table 3.1 shows the values of each parameter in this experiment. In the experiment of each system, the initial positions of the motors are surface of the environment.

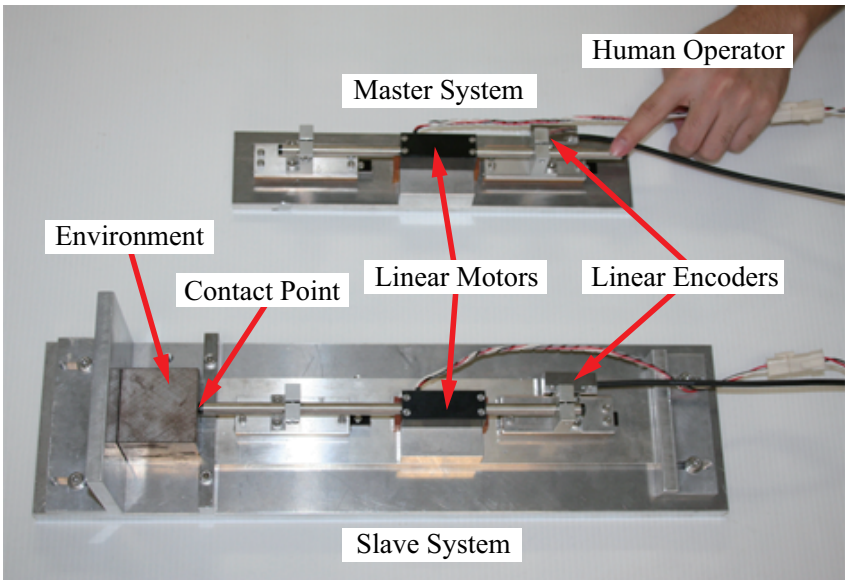

Fig. 3.5. Experimental device of motion-saving system.

Table 3.1. Setup Parameters.

T_s	Period of control system	100	μs
K_{tn}	Force constant	3.33	N/A
M_n	Mass of nominal	0.18	kg
C_f	Assist gain	15	
K_p	Proportional gain of the PD controller	10000	
K_d	Differential gain of PD controller	200	
g_{pd}	Pole of pseudo derivative for the PD controller	10000	rad/s
g_{dis}	Pole of the disturbance observer	1000	rad/s
g_{reac}	Pole of the reaction force observer	1000	rad/s

Experimental Results The experiments of free motion, push motion and contact motion are carried out. Fig. 3.7, Fig. 3.8 and Fig. 3.9 shows free motion, push motion and contact motion, respectively. Fig. 3.7(a),(b), Fig. 3.9(a),(b) and Fig. 3.8(a),(b) shows the experimental results of the motion-saving system. The experimental results of the motion-loading system are shown in Fig. 3.7(c),(d), Fig. 3.9(c),(d) and Fig. 3.8(c),(d). The experiments of free motion, contact motion and push motion are carried out. These experimental results confirm that

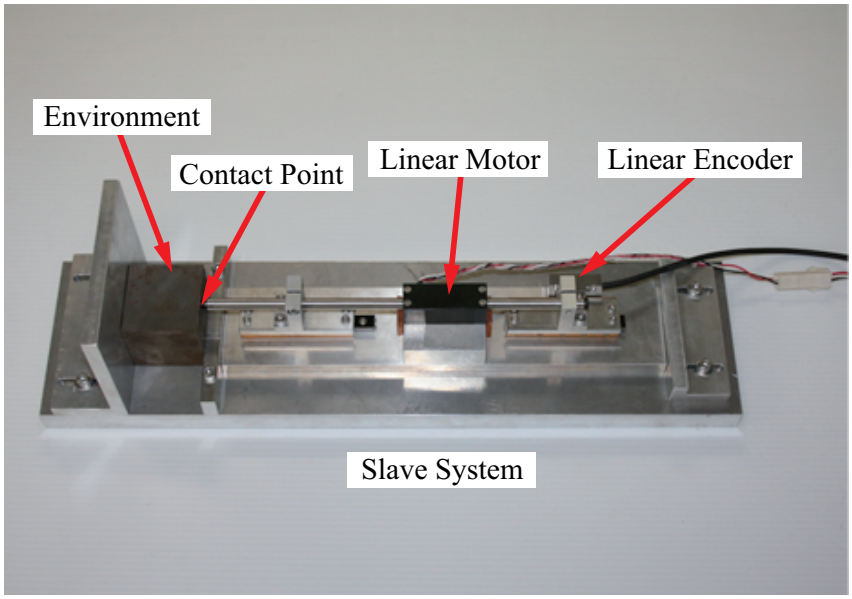

Fig. 3.6. Experimental device of motion-loading system.

reproduced position and force information corresponds to saved position and force information. Therefore, the motion-loading system perfectly reproduces the saved motion using the motion-saving system. Even if the motor operates as free motion, contact motion, or push motion, the reproduced motion corresponds to the stored motion. If absolute position from the environment is considered, the motion-copying system reproduces motion without initial value of position.

3.1.1.6 Conclusion

The thesis proposes a novel motion-copying system. The motion-saving system consists of a bilateral controller. The bilateral controller controls common mode force and differential mode position using a quarry matrix, independently. The experimental results confirm that the motion-saving system saves motion of human operator.

Meanwhile, the motion-loading system is operated by a virtual-world master system and real-world slave system. The virtual-world master system is composed by saved motion data. The reproduced position and force corresponds to the saved position and force information. Therefore, the real-world slave system operates according to saved motion data. In the experiment,

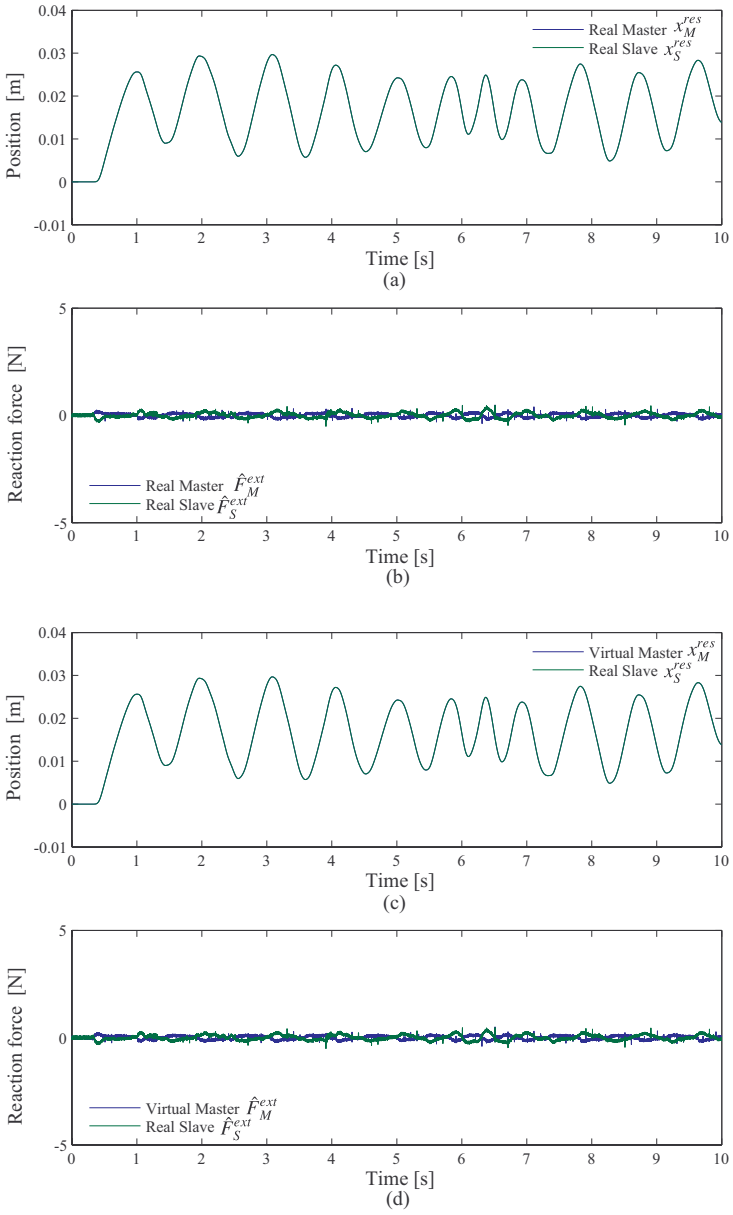

Fig. 3.7. Free motion. (a) Saved Position. (b) Saved Force. (c) Loaded Position. (d) Loaded Force.

the operation of the motion-loading system is confirmed.

By this means, the motion-copying system is realized. In the future, it will be useful for industrial application, medical and welfare human assistance.

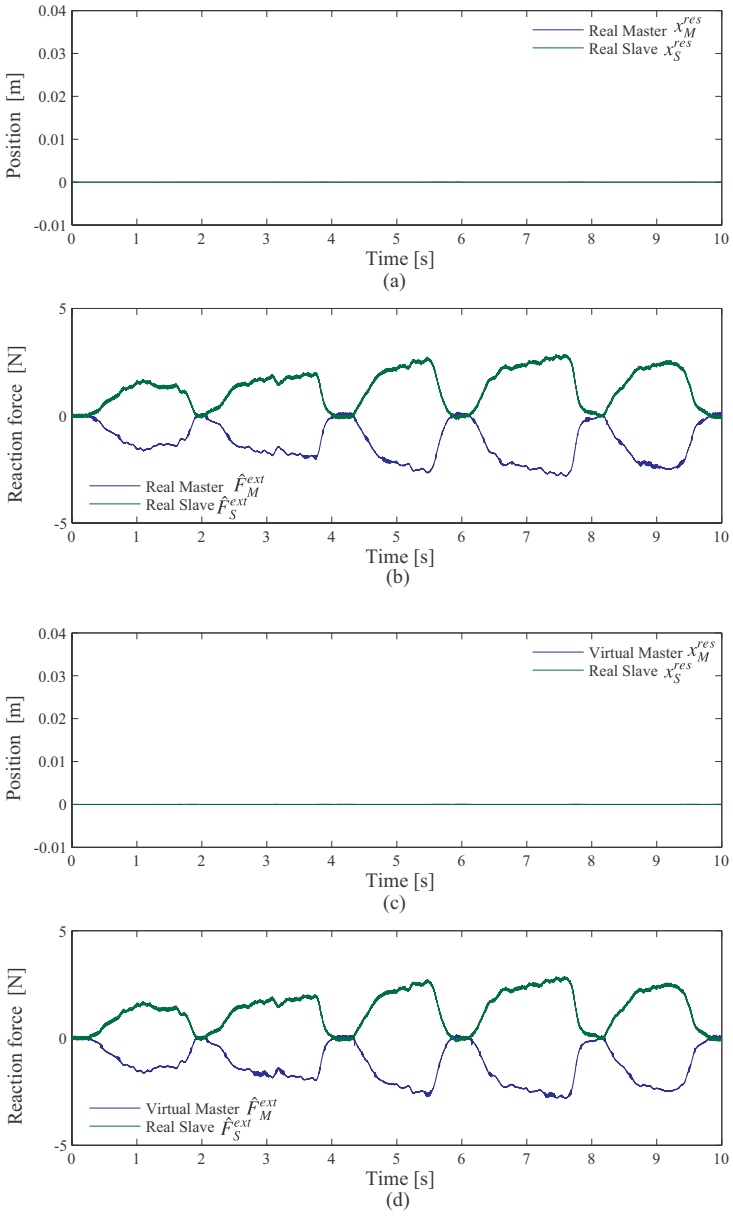

Fig. 3.8. Push motion. (a) Saved Position. (b) Saved Force. (c) Loaded Position. (d) Loaded Force.

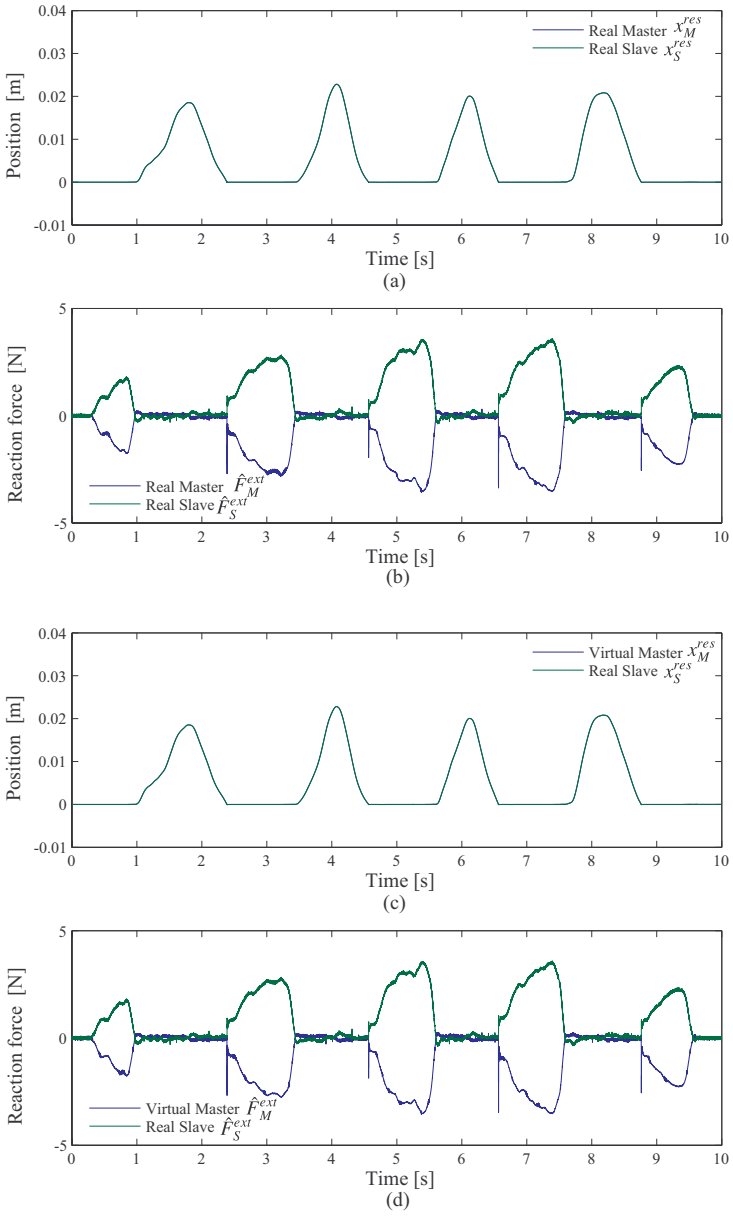

Fig. 3.9. Contact motion. (a) Saved Position. (b) Saved Force. (c) Loaded Position. (d) Loaded Force.

3.1.2 Reproduction of Multi Degree-of-Freedom Motion by Motion-Copying System

3.1.2.1 Introduction

Information and communication technology has been continuously grown. The current information technology treats acoustic information and visual information such as JPEG documents, mp3 sounds and video files and so on. However, the human has five organs, which recognizes acoustic, visual, olfactory, gustatory and haptic information. Therefore, the information technology should treat residual information in order to provide realistic environment in the distant place.

In this thesis, the haptic information is considered. The motion-copying system has been proposed [38]. The motion-copying system stores the motion of the human operator. Moreover, the motion-copying system is able to reproduce not only the position but also the force without mathematical model of the environment. Therefore, the human motion is generated by the motion-copying system.

The thesis proposes the motion-copying system considering multi degree-of-freedom systems. The conventional motion-copying system proposed in [38] cannot be utilized for the multi degree-of-freedom human motion. On the contrary, respective motion-copying systems stores and reproduces independently motion of the respective degrees of freedom, so that the motion-copying system is able to treat multi degree-of-freedom motion. Since the proposed system treats multi degree-of-freedom motion, the motion-copying system in this thesis reproduces complex human motion. By the proposed method, motion of expert engineers and motion of surgical operators can be stored and reproduced.

This research is organized as follows. In 3.1.2.2, fundamental concept of the motion-copying system is explained. The detailed control method of motion-saving system is described in 3.1.2.3. The reproduction method of the human motion using the motion-loading system is mentioned in 3.1.2.4. In 3.1.2.5, the experiments are shown. Finally, the last section concludes this study.

3.1.2.2 Motion-Copying System

In this section, fundamental concept of the motion-copying system is explained. Fig. 3.10 shows conceptual diagram of the motion-copying system. The motion-copying system consists of the motion-saving system and the motion-loading system.

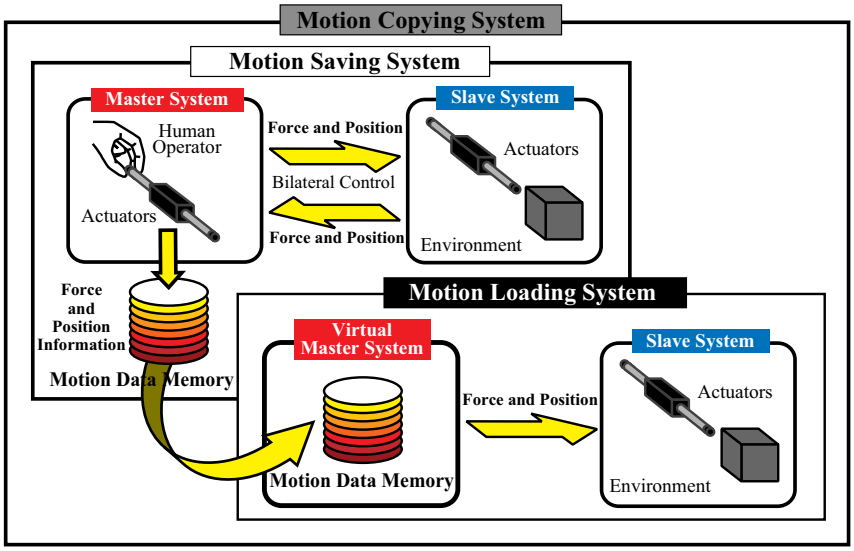

Fig. 3.10. Conceptual diagram of motion-copying system.

The motion-saving system is realized by bilateral controller to measure the force between a master system and a slave system. A human operator moves multi degree-of-freedom actuators in the master side, and is able to grasp the environmental sense in the slave side through the bilateral controller. The motion-saving system stores the force and position information to the motion data memories, in order to achieve storage of the human motion. The motion of the human operator stored in the motion data memories will be utilized to reproduce the human motion in the motion-loading system.

The aim of the motion-loading system is reproduction of the human motion without the human operator. The motion-loading system is able to reproduce the force and position, which represents the human motion stored by the motion-loading system. The reproduced force and position corresponds to the stored ones by using the motion-copying system. In this system,

mathematical model of the environment is not used at all. Therefore, the motion-loading system generates the force and position according to the motion data memories without modeling. In addition, detection of contact to the environment and switching of control are not required.

To store and reproduce the multi degree-of-freedom human motion, this thesis utilizes several motion-copying systems. These motion-copying systems copies respectively independently the human motion of respective degrees of freedom. The number of the motion-copying system depends on the number of degrees of freedom.

In this manner, the motion-copying system realizes copy of the human motion beyond time and space. The thesis treats the motion-copying system considering multi degree-of-freedom systems.

3.1.2.3 Motion-Saving System

A control method for the motion-saving system is described in this section. The thesis mentions also storage method for the human motion of the human operator in the real-world.

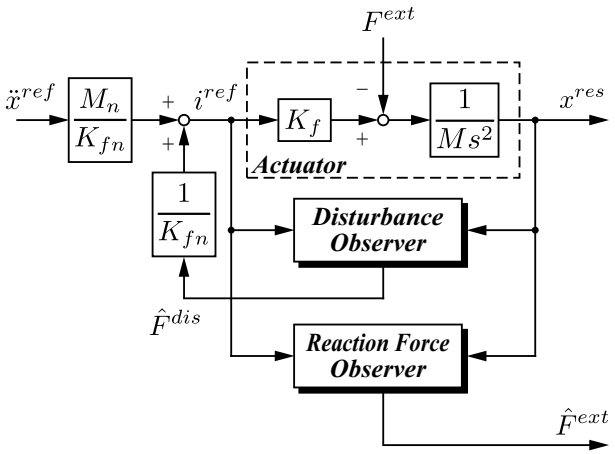

Fig. 3.11. Block diagram of the master system and the slave system.

Motion Control Fig. 3.11 shows block diagram of the master system and the slave system. The motion-saving system utilizes the acceleration control system shown in Fig. 3.11 in order to construct bilateral controller. K_f, K_{fn}, M and M_n are force constant, nominal force constant,

mass of actuator and nominal mass. The disturbance observer [66] cancels disturbance force $\hat{F}^{dis}$ using current reference i^{ref} and position response x^{res}, so that robust acceleration control is realized. $\ddot{x}^{ref}$ in Fig. 3.11 denotes a acceleration reference, which drives the actuator. The reaction force observer [64] estimates a external force F^{ext}, which is impressed by the human operator and/or the environment without force sensors. The estimated external force $\hat{F}^{ext}$ is represented as

$$\hat{F}^{ext} = \frac{g_{reac}}{s + g_{reac}} F^{ext} \tag{3.7}$$

where, g_{reac} is bandwidth of force estimation. In the motion-copying system, the frequency characteristics of the motion which is stored and reproduced is limited by the bandwidth g_{read} shown in (3.7).

Fig. 3.12 shows block diagram of the motion-saving system. F_x, F_y, X and Y denote force of X-axis, force of Y-axis, position of X-axis and Y-axis. The subscript M, S, C and D denote master, slave, common mode and differential mode. The superscript ext, res and ref are external, response and reference. Though the upper and lower systems shown in this thesis are same structures, the proposed method is also useful for bilateral control considering different structure.

The motion-saving system is realized by the bilateral controller using modal decomposition [65]. The modal decomposition which decomposes motion of actuators is realized by quarry matrix [63]. In this thesis, the second-order quarry matrix $\boldsymbol{Q}_2$ is utilized in order to operate the master system and the slave system. The second-order quarry matrix is defined as

$$\boldsymbol{Q}_2 = \frac{1}{2} \begin{bmatrix} 1 & 1 \\ 1 & -1 \end{bmatrix}. \tag{3.8}$$

The force responses of X-axis direction are transformed into force responses of modal space by the quarry matrix

$$\begin{bmatrix} F_{xC}^{ext} \\ F_{xD}^{ext} \end{bmatrix} = \boldsymbol{Q}_2 \begin{bmatrix} \hat{F}_{xM}^{ext} \\ \hat{F}_{xS}^{ext} \end{bmatrix}. \tag{3.9}$$

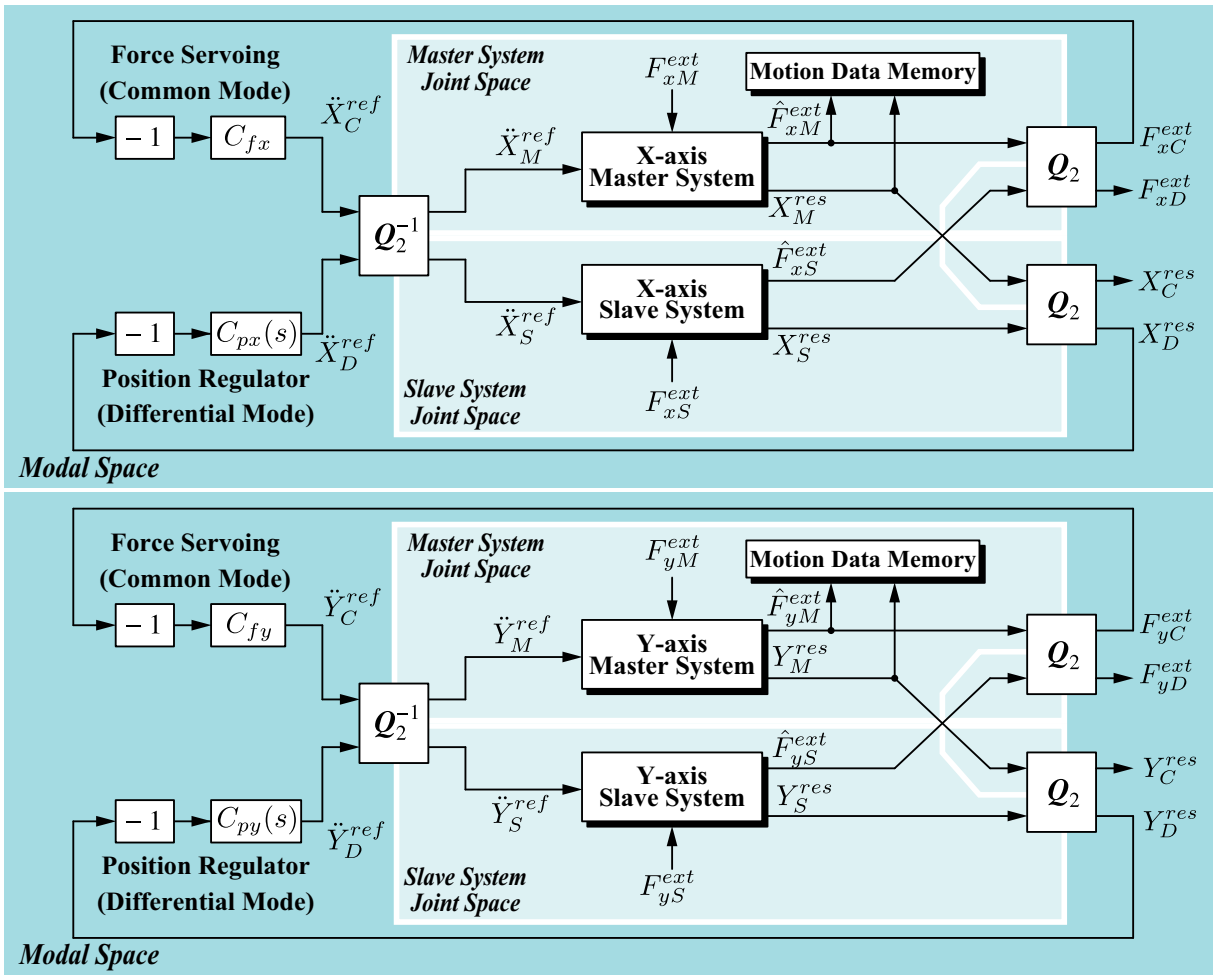

Fig. 3.12. Block diagram of motion-saving system.

The position responses of common mode and differential mode are calculated by

$$\begin{bmatrix} X_M^{res} \\ X_S^{res} \end{bmatrix} = \boldsymbol{Q}_2 \begin{bmatrix} X_C^{res} \\ X_D^{res} \end{bmatrix}. \tag{3.10}$$

The motion-saving system utilizes both the force response and the position response in modal space, in order to realize bilateral control system. A force controller of X-axis C_{fx} and a position regulator of X-axis C_{px} control the force of common mode and the position of differential mode, respectively.

$$\ddot{X}_C^{ref} = -\, C_{fx}\; F_{xC}^{ext} \tag{3.11}$$

$$\ddot{X}_D^{ref} = -\, C_{px}(s)\; X_C^{res} \tag{3.12}$$

In this thesis, these controllers are expressed as

$$C_{fx} = K_{fpx} \tag{3.13}$$

$$C_{px}(s) = K_{ppx} + \frac{s\ g_{pd}}{s + g_{pd}}\ K_{pdx} \tag{3.14}$$

where, K_{fpx}, K_{ppx}, K_{pdx} and g_{pd} denote gain of the force controller, proportional gain, differential gain of the position regulator and bandwidth of a pseudo derivative, respectively. In short, the position of differential mode is controlled by PD controller. The acceleration references calculated by (3.11) and (3.12) are transformed into joint space by using second-order inverse quarry matrix $\boldsymbol{Q}_2^{-1}$

$$\begin{bmatrix} \ddot{X}_M^{ref} \\ \ddot{X}_S^{ref} \end{bmatrix} = \boldsymbol{Q}_2^{-1} \begin{bmatrix} \ddot{X}_C^{ref} \\ \ddot{X}_D^{ref} \end{bmatrix}. \tag{3.15}$$

Finally, the master system and the slave system are operated by the acceleration references $\ddot{X}_M^{ref}$, $\ddot{X}_S^{ref}$. The control method in Y-axis direction is same as above.

By this means, the bilateral controller which is able to generate artificially the law of action and reaction is realized. The motion-saving system utilizes the bilateral controller to measure the force information, which is generated between the master system and the slave system.

Storage of Human Motion The force between the master system and the slave system is generated, when the human operator touches the environment in the slave side through the bilateral controller. Motion data memories in the motion-saving system store both the force information and the position responses of the actuators

$$\boldsymbol{M}_X^{mem} = \begin{bmatrix} \hat{F}_{xM}^{ext} \\ X_M^{res} \end{bmatrix} \tag{3.16}$$

$$\boldsymbol{M}_Y^{mem} = \begin{bmatrix} \hat{F}_{yM}^{ext} \\ Y_M^{res} \end{bmatrix}. \tag{3.17}$$

$\boldsymbol{M}_X^{mem}$ and $\boldsymbol{M}_Y^{mem}$ in (3.16) and (3.17) denote the motion data memories of X-axis and Y-axis. Therefore, the motion data memories hold time series data of the human motion. The motion data memories are utilized in the motion-loading system to reproduce the human motion.

3.1.2.4 Motion-Loading System

In this section, control scheme of the motion-loading system is explained. The reproduction method of human motion using the motion data memories is also described.

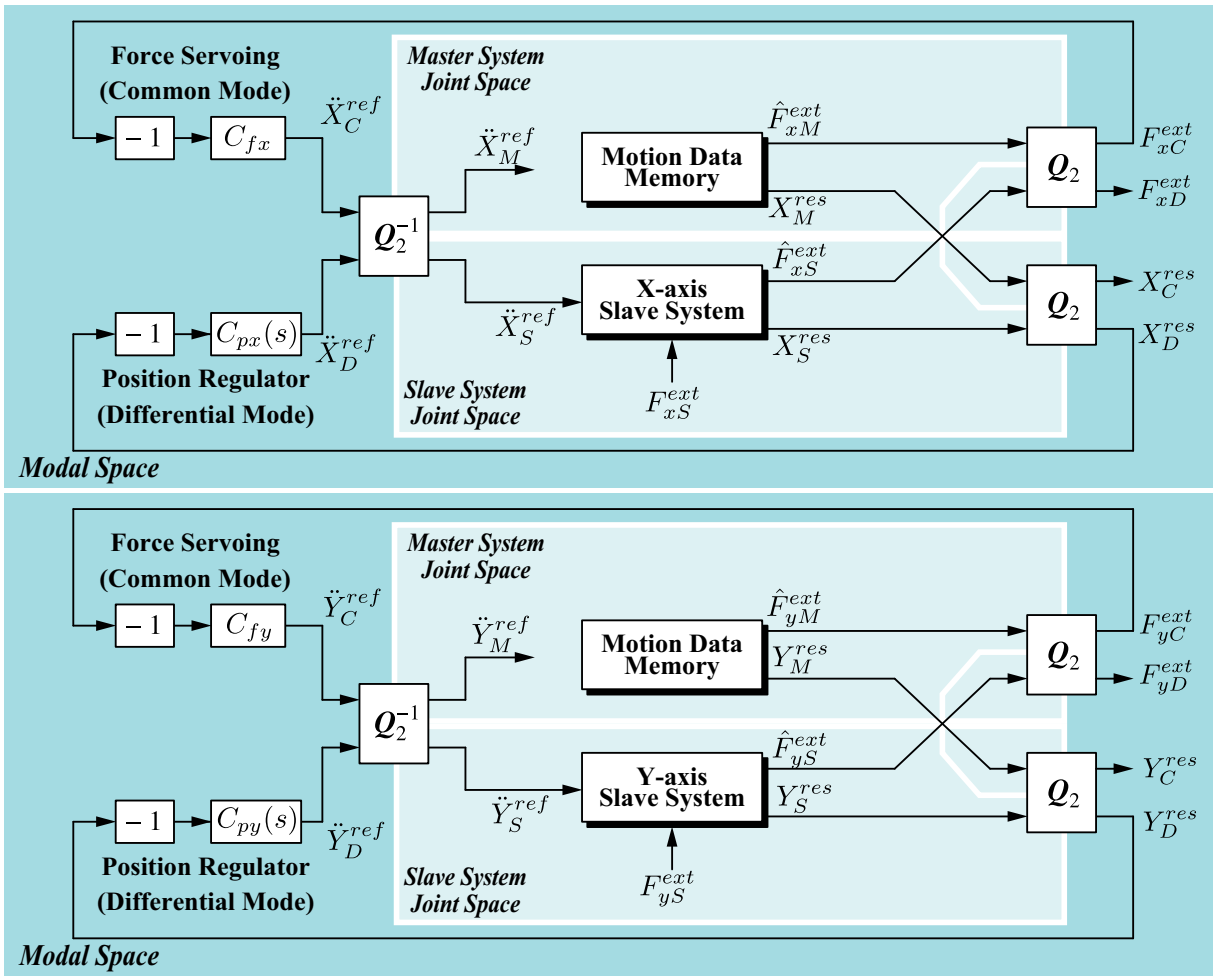

Fig. 3.13. Block diagram of motion-loading system.

Motion Control Fig. 3.13 shows block diagram of the motion-loading system. Basically, the control method of the motion-loading system is same as the motion-saving system. Thus, respective parameters of the motion-loading system are calculated by (3.9)–(3.15). However, the motion-loading system utilizes the motion data memories instead of actual master systems

in the real-world. Therefore, the actuators of the master systems are not used in the motion-loading system. In addition, since the master side consists of the motion data memories, the acceleration references of master system are unused. In this manner, the motion-loading system is constructed by singular bilateral controller.

Reproduction of Human Motion The objective of the motion-copying system is storage and reproduction of the human motion based on haptic information in the real-world. The motion-loading system achieves the reproduction of human motion. The motion data memories in the motion-loading system output the force information and the position information.

$$\begin{bmatrix} \hat{F}_{xM}^{ext} \\ X_M^{res} \end{bmatrix} = \boldsymbol{M}_X^{mem} \tag{3.18}$$

$$\begin{bmatrix} \hat{F}_{yM}^{ext} \\ Y_M^{res} \end{bmatrix} = \boldsymbol{M}_Y^{mem} \tag{3.19}$$

The bilateral controller operates the slave system according to the force information and the position information, so that the motion-loading system is able to reproduce both the force information and the position information. Therefore, the motion data memories imitate the human motion, which was stored by the motion-saving system. By the proposed method, the motion-loading system using multi degree-of-freedom systems is able to reproduce complex motion.

3.1.2.5 Experiment

Experimental Setup Fig. 3.14 shows experimental setup. The experiment uses four linear actuators to construct the bilateral control system of 2 degrees-of-freedom. These linear actuators are controlled by RTAI-3.7 and Slackware Linux. RTAI-3.7 provides real-time operating system, and realizes the motion-copying system shown in Figs. 3.12 and 3.13. In this experiment, stainless plate which is putted in the slave side is used. The distance between the slave system and the environment is few centimeters. The setup parameters of the control system is shown in Table 3.2.

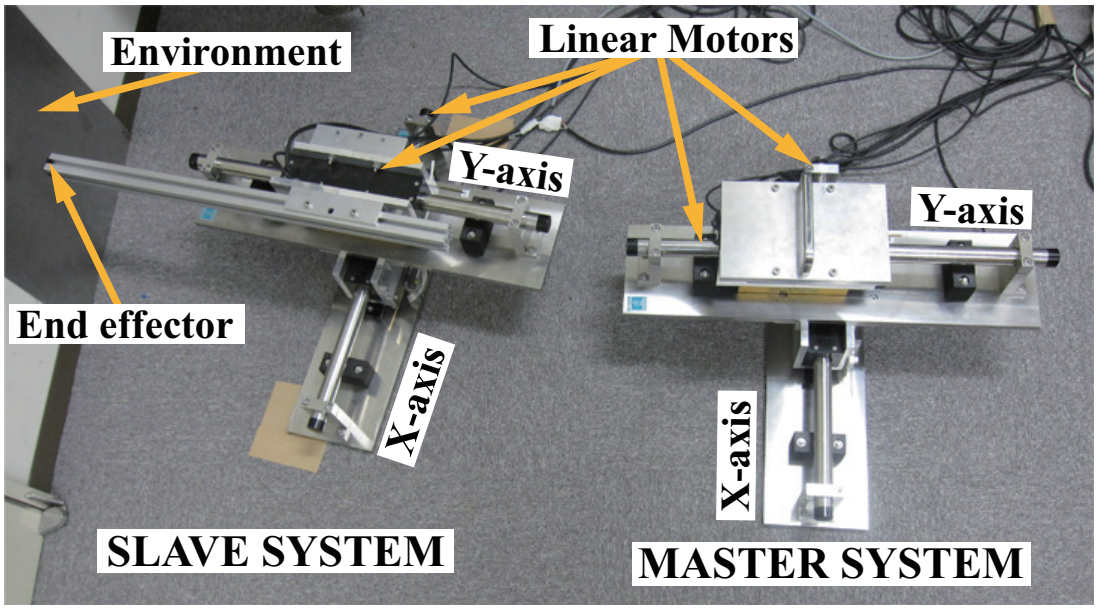

Fig. 3.14. Experimental devices. (In the case of motion-loading system, the master system is not used.)

Table 3.2. Setup Parameters

T_s	Period of control system	100	μs
K_{fn}	Force constant	57.7	N/A
M_{nx}	Mass of X-axis direction	20	kg
M_{ny}	Mass of Y-axis direction	3.5	kg
K_{fpx}	Force control gain of X-axis	$1.8/M_nx$	kg^{-1}
K_{fpy}	Force control gain of Y-axis	$1.8/M_ny$	kg^{-1}
K_{ppx}, K_{ppy}	Proportional gain of X-axis/Y-axis position control	10000	s^{-2}
K_{pdx}, K_{pdy}	Differential gain of X-axis/Y-axis position control	200	s^{-1}
g_{pd}	Pole of pseudo derivative for the position controller	10000	rad/s
g_{dis}	Pole of the disturbance observer	200	rad/s
g_{reac}	Pole of the reaction force observer	200	rad/s

Experimental Results Figs. 3.15 and 3.16 show experimental results of the motion-saving system and the motion-loading system. In this experiment, contact motion, push motion and rubbing motion were carried out by the human operator. The motion-saving system stored these motions shown in Fig. 3.15. The force and position responses shown in Fig. 3.16 are generated by the motion-loading system. The reproduced force and position corresponds to the

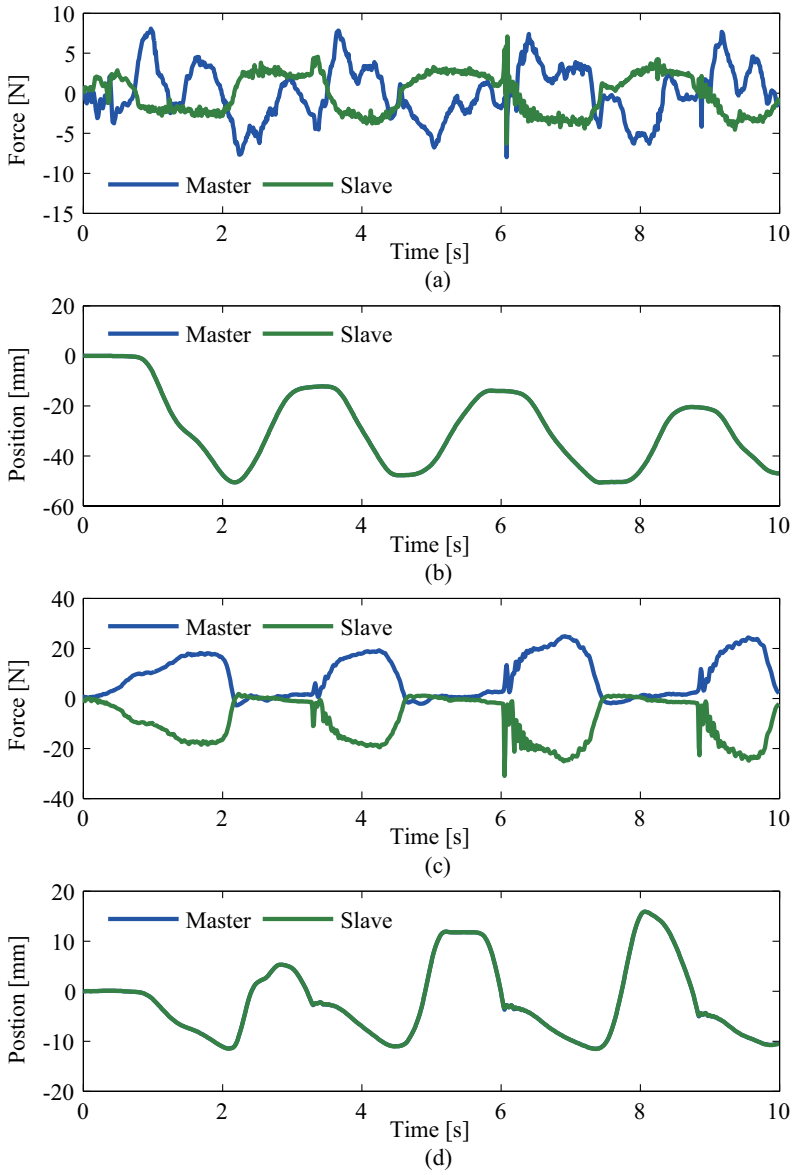

Fig. 3.15. Experimental results of the motion-saving system.
(a) Force of X-axis. (b) Position of X-axis.
(c) Force of Y-axis. (d) Position of Y-axis.

saved force and position as shown in Figs. 3.15 and 3.16. Therefore, the experimental results confirm that the motion-loading system is able to reproduce normally the human motion of the human operator. In Figs. 3.15(a) and 3.16(a), the cause of difference between the force of the master system and the force of the slave system might be effect of friction, mass of the

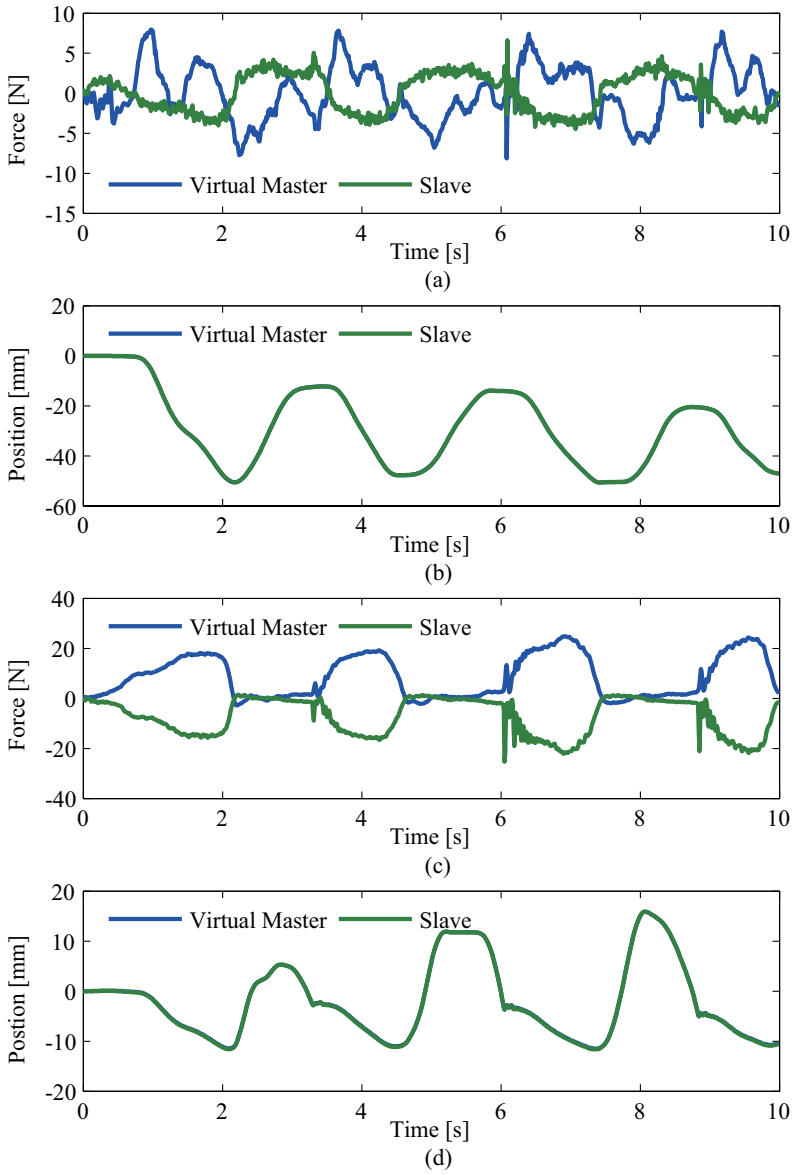

Fig. 3.16. Experimental results of the motion-loading system.
(a) Force of X-axis. (b) Position of X-axis.
(c) Force of Y-axis. (d) Position of Y-axis.

actuators, control gains and so on. However, these experiments confirmed that the reproduced force waveform corresponds to the stored ones.

3.1.2.6 Conclusion

The thesis proposes the motion-copying system considering multi degree-of-freedom human motion. In this thesis, respective motion-copying systems stores and reproduces independently motion of the respective degrees of freedom, so that the motion-copying system is able to treat multi degree-of-freedom motion. The motion-copying system consists of the motion-saving system and the motion-loading system. The motion-saving system stores the human motion of the human operator to the motion data memories by using the bilateral controller. The motion-loading system reproduces the force and position information, which is stored in the motion data memories. In other words, the motion-loading system is able to reproduce the complex motion beyond time and space. By the experiment, the validity and the reliability were confirmed in this thesis. It will be useful for industrial applications, medical and welfare human support.

3.1.3 Motion-Copying System Based on Real-World Haptics in Variable Speed

3.1.3.1 Introduction

An information processing technologies has been rapidly grown for several decades. Preservation engineering and reproduction engineering of information are developed using such technologies. Acoustic information or visual information is recorded to tape cassettes, compact disks, digital versatile discus, flash memories and so on. This stored information to media is reproduced in the real-world at any time. The player of the acoustic and visual information is able to fast-forward and/or slow down. In other words, it makes a video of rapid movement of an object slow motion video. Also, such information can be processed using various methods. On the contrary, preservation, reproduction and processing engineering of a haptic information has not been enough researched and developed. A research using a visual information acquires a motion of a human operator [29]–[31]. However, these methods are not able to detect force between the human operator and an environment. The preservation of both position information and force information is very important, in order to save the arbitrary motion. Therefore, these methods are not enough to realize preservation and reproduction of the haptic information. A control method considering both the force information and the position information has been developed [34, 35]. Though, the viewpoint of preservation and reproduction of the haptic information is nothing in the researches. Additionally, a research based on virtual environment has been proposed [72], however it is not able to treat the haptic information in the real-world. In addition, a method of reproduction according to recorded reaction force information has been developed [33].

A motion-copying system has been proposed [38], however the conventional motion-copying system does not consider in regard to variable reproduction velocity. This thesis proposes a novel motion-copying system, which is considered variable reproduction velocity. Fig. 3.17 shows the expanded motion-copying system. The motion-copying system consists of a motion-loading system and a motion-saving system using quarry matrix [63]. The motion-saving system is operated by bilateral controller with disturbance observer [66]. The motion-saving system

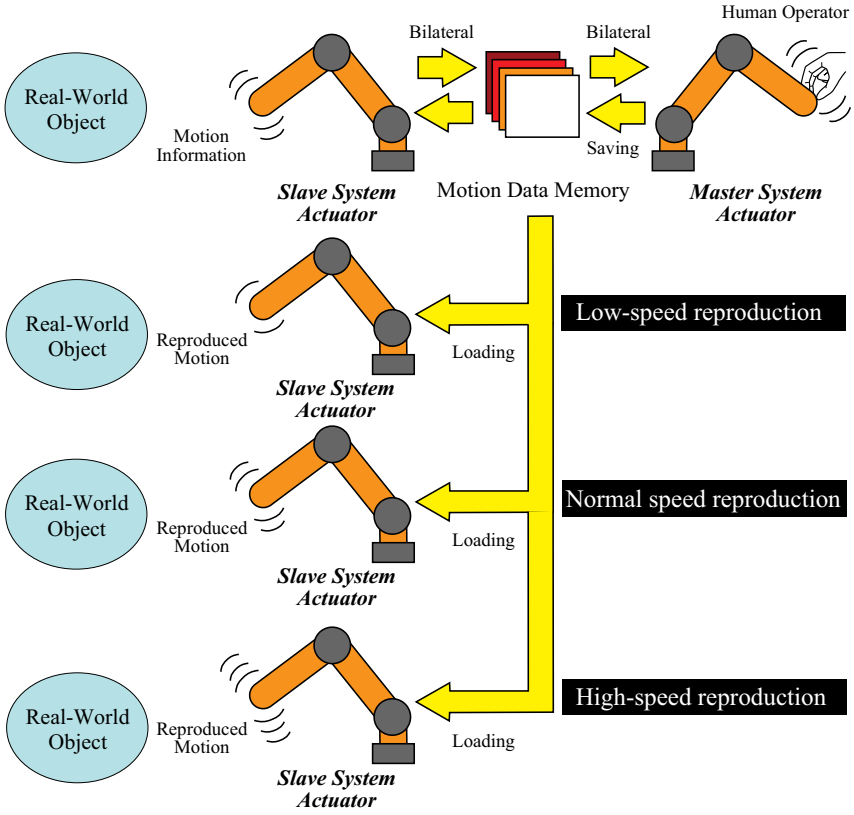

Fig. 3.17. Motion-copying system considering variable reproduction velocity.

measures position and reaction force of a master motor by a linear encoder and reaction force observer [64], and saves it to a motion data memory.

On the other hand, the motion-loading system is operated by a virtual bilateral controller. The virtual bilateral controller dose not has master motor in the real-world. The motion-loading system reproduces the motion of the human operator according to the stored motion data in the motion data memory. The reproduced position and force by the motion-loading system corresponds to the stored motion data. Therefore, the motion-copying system realizes reproduction of the motion. Also, a reproduction velocity can be freely changed, when the motion-loading system reproduces the motion. Thus, this system shifts the saved motion of the human operator to low speed or high speed. In other words, slow motion or rapid motion of a object in the real-world is obtained by the proposed method as with a sound or video player.

This research is organized as follows. A concept of the motion-copying system considering variable reproduction velocity is described in 3.1.3.2. In 3.1.3.3, a motion control for the motion-saving system is shown. Subsection 3.1.3.4 explains the motion-loading system considering variable reproduction velocity. Subsection 3.1.3.5 shows the experimental results of the proposed method. The last subsection summarizes this research.

3.1.3.2 Concept of Motion-Copying System in Variable Speed

The proposed method in this thesis utilizes the motion-copying system to save and reproduce the motion of the human operator. Fig. 3.18 shows conceptual diagram of the motion-copying

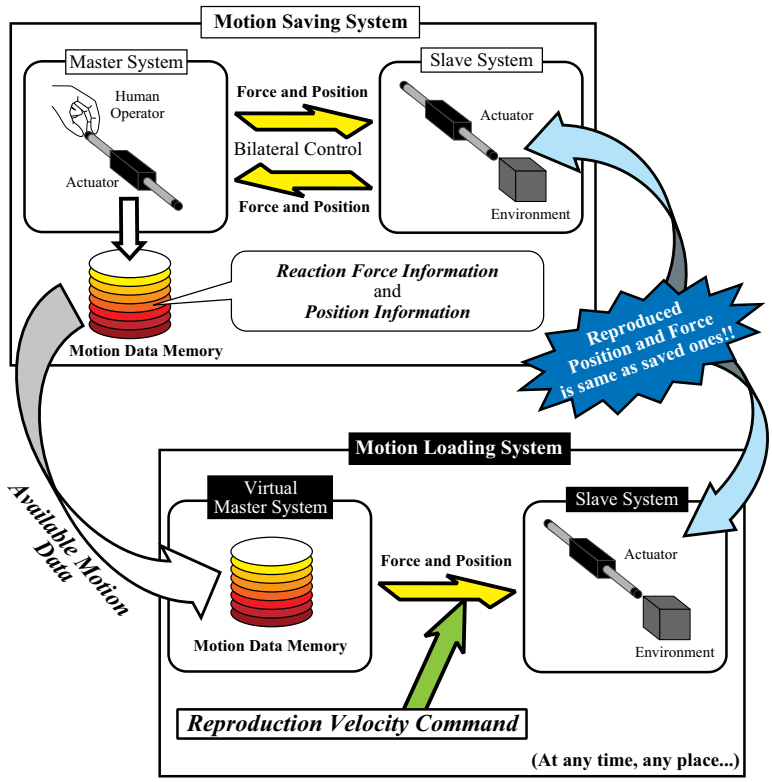

Fig. 3.18. Conceptual diagram of motion-copying system in variable reproduction velocity.

system in variable speed. The motion-copying system consists of two systems. First system is the motion-saving system; other system is the motion-loading system. This section explains the motion-saving system and the motion-loading system considering variable reproduction velocity.

Motion-Saving System A master system and a slave system constitute the motion-saving system. The human operator impresses force and moves position of an actuator in the master side, at the same time, an actuator in the slave side synchronizes it. In short, the human operator is able to grasp haptic information of an environment in the master side. The motion-saving system stores the impressed force and position of the actuator to a motion data memory, when the human operator operates the master system. The motion data in the motion data memory is used to reproduce the motion of the human operator using the motion-loading system. Fundamentally, the utilized motion-saving system in this thesis is same as the conventional motion-saving system. Therefore, the stored motion data by the conventional motion-copying system is available to the proposed system.

Motion-Loading System considering Variable Reproduction Velocity The motion-loading system is constructed by a bilateral controller. However, the motion-loading system does not utilize the actuator in the master side, because the motion data memory is used instead of the actuator in the master system. The motion data memory outputs stored the force and position information, which operates the slave system. The reproduced force and position in the slave system correspond to saved ones. Therefore, the actuator in the slave system is operated according to the saved motion of the human operator. The critical difference between the proposed method and the conventional motion-copying system is the reproduction velocity can be freely changed. Fig. 3.19 shows the method of variable reproduction velocity. If a reproduction velocity command is set to normal speed, the virtual master system outputs force and position information to the quarry matrix without change. The detailed explanation of the quarry matrix is consequent section. In the case of the reproduction velocity is double speed, the force and position information in the motion data memory are contracted before output. On the contrary, the motion-loading system extends the force and position in the memory, when the velocity command is set to half speed. A zero-order hold, linear interpolation and spline interpolation are available in this processing. Finally, the proposed motion-loading system is

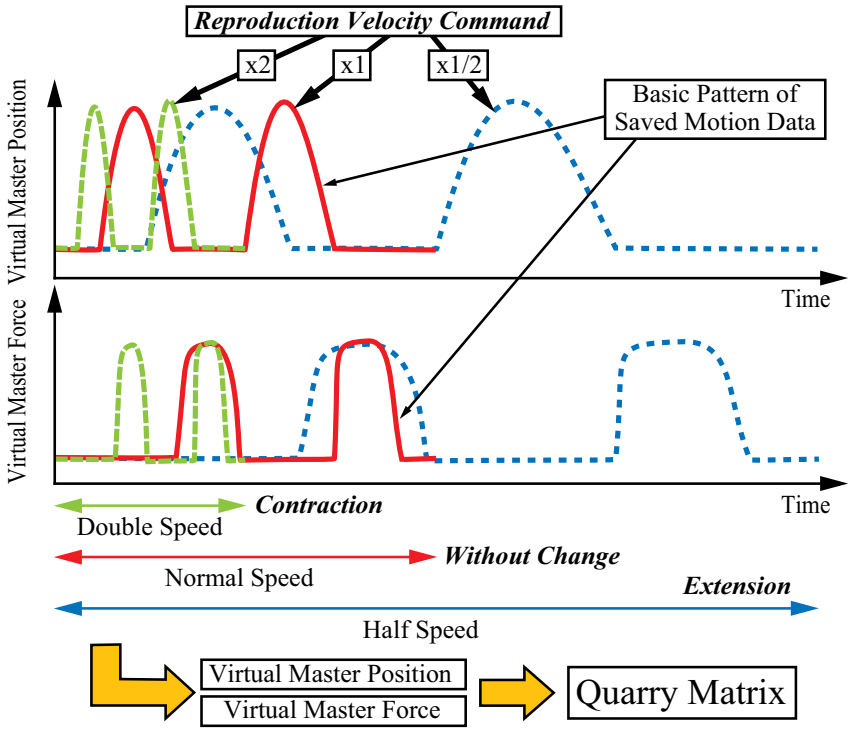

Fig. 3.19. Processing of force and position information in a motion data memory.

able to vary the reproduction velocity of the stored motion.

3.1.3.3 Motion-Saving System using Bilateral Controller

Fig. 3.20 shows block diagram of the motion-saving system. The system preserves the motion of the human operator. The master and slave system constitute the motion-saving system. A force controller and a position controller control the force of the common mode and the position of the differential mode between respective systems. F, $\hat{F}$, x and $\ddot{x}$ are force, estimated force, position and acceleration. The subscripts M, S, C and D of the paramerters are master system, slave system, common mode and differential mode, respectively. The superscripts res, ref, dis and ext show response, reference, disturbance and external, respectively. M_n is mass of actuator components.

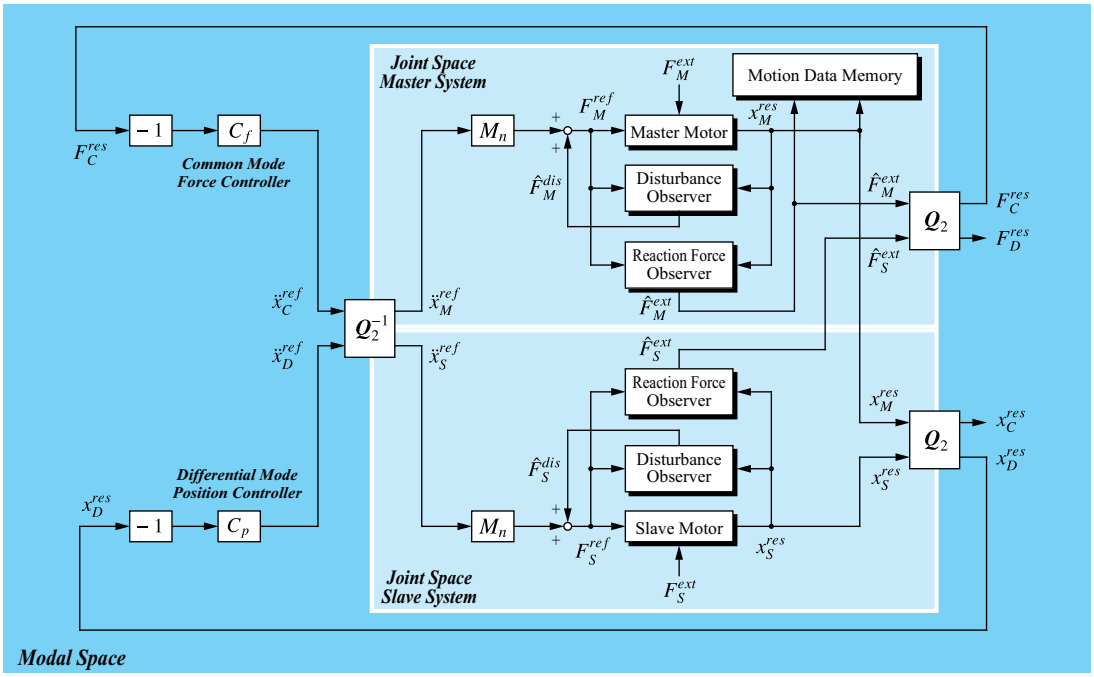

Fig. 3.20. Block diagram of motion-saving system using bilateral control system.

The quarry matrix is defined as [63, 65]

$$\boldsymbol{Q}_2 = \frac{1}{2}\begin{bmatrix} 1 & 1 \\ 1 & -1 \end{bmatrix}. \tag{3.20}$$

The expressed quarry matrix is used to control the force of the common mode and the position of the differential mode, independently. The quarry matrix $\boldsymbol{Q}_2$ decompose the reaction force of the master side actuator F_M^{ext} and the slave side actuator F_S^{ext} to the each mode F_C^{res}, F_D^{res}

$$\begin{bmatrix} F_C^{res} \\ F_D^{res} \end{bmatrix} = \boldsymbol{Q}_2 \begin{bmatrix} \hat{F}_M^{ext} \\ \hat{F}_S^{ext} \end{bmatrix}. \tag{3.21}$$

In the case of treating the position of the common mode x_C^{res} and differential mode x_M^{res}, the calculation method is same

$$\begin{bmatrix} x_C^{res} \\ x_D^{res} \end{bmatrix} = \boldsymbol{Q}_2 \begin{bmatrix} x_M^{res} \\ x_S^{res} \end{bmatrix}. \tag{3.22}$$

where, x_M^{res} is the position response of the master side actuator, x_S^{res} is the slave side actuator position response. A force controller of the common mode C_f calculates a acceleration reference

of the common mode $\ddot{x}_C^{ref}$

$$\ddot{x}_C^{ref} = - C_f \; F_C^{res} \; . \tag{3.23}$$

An acceleration reference of differential mode $\ddot{x}_D^{ref}$ calculated using a position controller of differential mode C_p

$$\ddot{x}_D^{ref} = - C_p \; x_D^{res} \; . \tag{3.24}$$

In this thesis, the force controller C_f and the position controller C_p are determined by

$$C_f = K_f \tag{3.25}$$

$$C_p = K_p + \frac{s \; g_{pd}}{s + g_{pd}} \; K_{d.} \tag{3.26}$$

where, K_f is force servoing gain, K_p and K_d is proportional gain and differential gain, g_{pd} is pole of a pseudo derivative. In short, the position controller is PD controller. Also, the disturbance observer estimates and compensates the disturbance force so as to realize acceleration control [66]. The control system in Fig. 3.20 does not use the force response of differential mode F_D^{res} and the position response of common mode x_C^{res}. In addition, the 2nd-order inverse quarry matrix $\boldsymbol{Q}_2^{-1}$ transforms to the acceleration reference in the joint space $\ddot{x}_M^{ref}$, $\ddot{x}_S^{ref}$ using the calculated acceleration reference in the modal space by the controller as follows:

$$\begin{aligned} \begin{bmatrix} \ddot{x}_M^{ref} \\ \ddot{x}_S^{ref} \end{bmatrix} &= \boldsymbol{Q}_2^{-1} \begin{bmatrix} \ddot{x}_C^{ref} \\ \ddot{x}_D^{ref} \end{bmatrix} \\ &= \begin{bmatrix} 1 & 1 \\ 1 & -1 \end{bmatrix} \begin{bmatrix} \ddot{x}_C^{ref} \\ \ddot{x}_D^{ref} \end{bmatrix}. \end{aligned} \tag{3.27}$$

The acceleration reference of respective systems $\ddot{x}_C^{ref}$, $\ddot{x}_D^{ref}$ drives the master side actuator and the slave side actuator. The presented method in this section achieves the bilateral control system, which is able to convey the haptic information of the environment in the slave side to the human operator in the master side. The motion-saving system stores the reaction force F_M^{ext} and the position x_M^{res} in the master side to the motion data memory during operating the bilateral controller. More specifically, the system preserves the motion of the human operator. This saved motion data is utilized for the motion-loading system.

3.1.3.4 Motion-Loading System considering Variable Reproduction Velocity

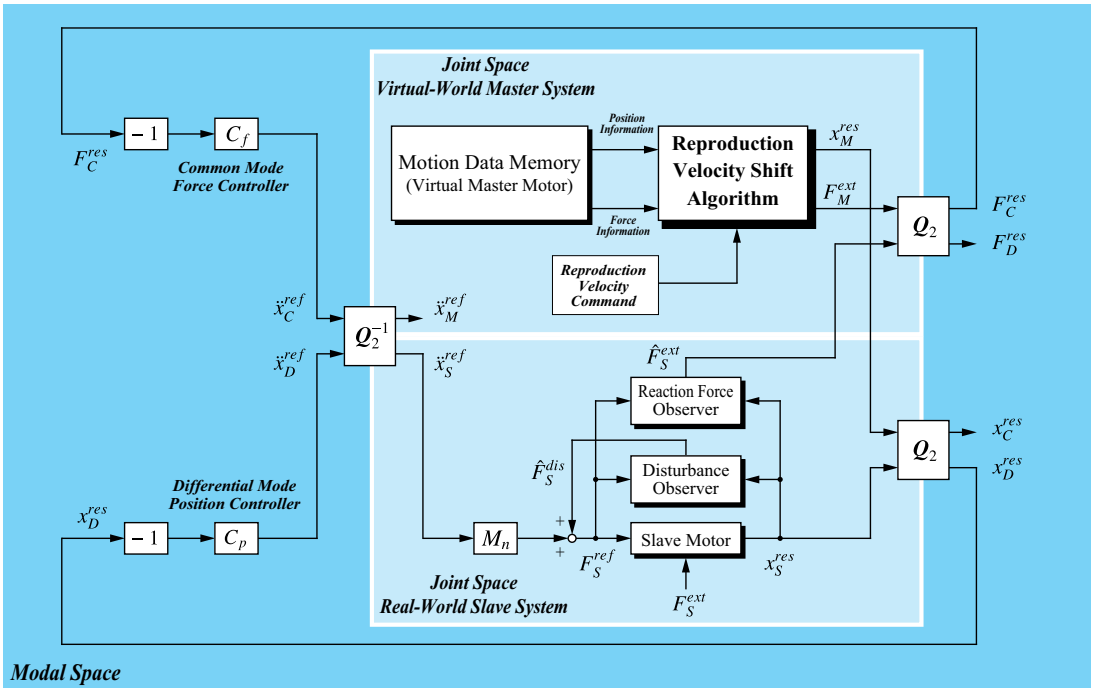

Fig. 3.21. Block diagram of motion-loading system considering variable reproduction velocity.

Fig. 3.21 shows block diagram of the motion-loading system considering variable reproduction velocity. The calculation method of parameters in the block diagram is same as previous section. However, the critical difference between the motion-saving system and the motion load system is the master system. The actuator in the master side is unused; alternatively, the system uses the motion data memory. The motion data memory outputs the stored reaction force and position information to the quarry matrix. In the motion-loading system, the actuator in the slave side reproduces the motion according to the information. A reproduction velocity of the virtual master motor depends on a reproduction velocity command. The reproduction velocity command can be freely changed, and is set to low speed or normal speed or high speed. If the reproduction velocity command is set to low speed, number of sample of saved motion data is lower than in case of reproduction motion. Accordingly, a interval of sample of saved motion

data should be interpolated. A zero-order hold interpolates the interval of sample in this thesis. On the contrary, several sampling data is ignored on condition that the reproduction velocity command is set to high speed. Thus, the motion-loading system shifts saved motion of human operator to low speed or high speed.

3.1.3.5 Experiment

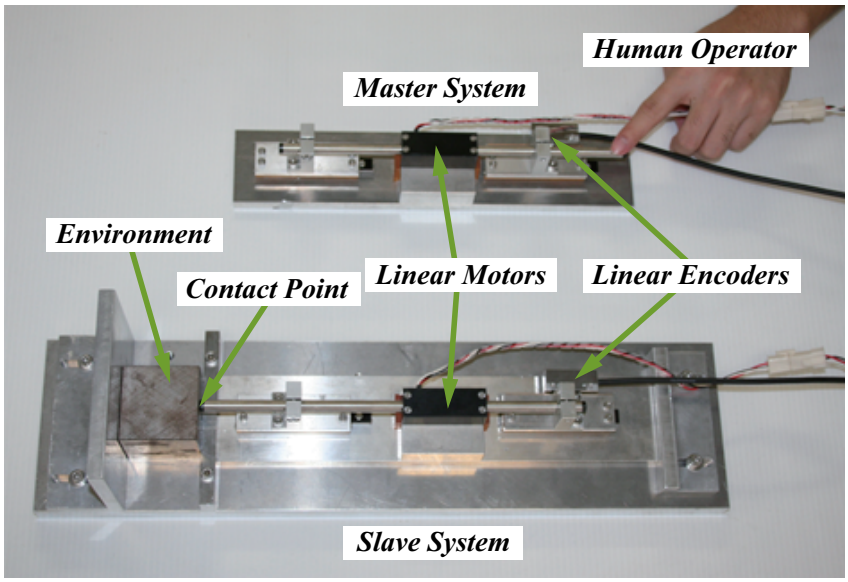

Fig. 3.22. Experimental device of motion-saving system.

Experimental Setup Figs. 3.22 and 3.23 show the experimental device of respective systems. The device of the motion-saving system consists of two linear motor and two linear encoder. On the contrary, a linear motor and a linear encoder are used in the motion-loading system as previously noted. A tip of the slave motor is able to contact to the environment. The slave motor of the motion-saving system is moved according to a master motor. The human operator moves the master motor, and grasps the environment of the slave motor side. In this thesis, the environment is an iron block.

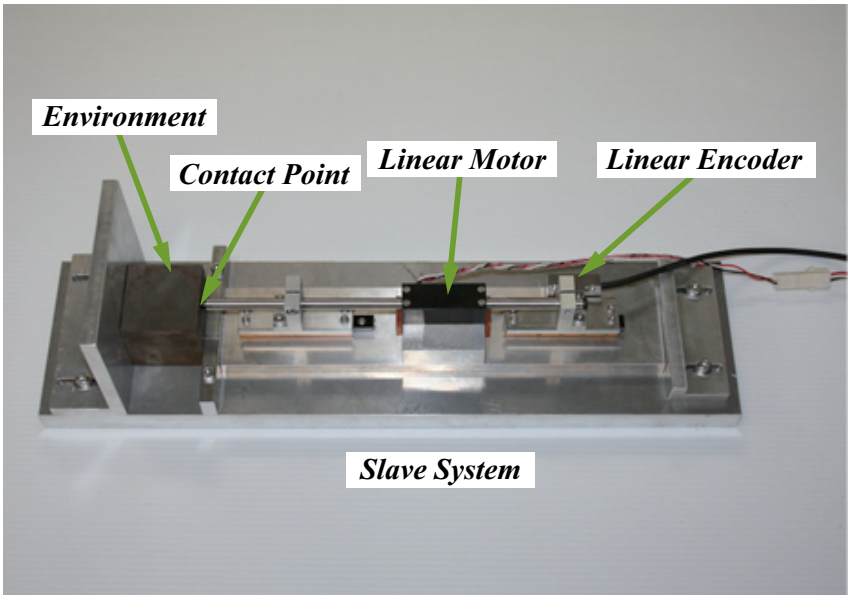

Fig. 3.23. Experimental device of motion-loading system in variable speed.

Experimental Results Fig. 3.24 shows saved motion data by the motion-saving system in the experiment. Fig. 3.24(a) and Fig. 3.24(b) show the position and force, respectively. The experiment of contact motion to the iron block are carried out. The motion-saving system using bilateral controller contrives law of action and reaction.

The experimental result of the motion-loading system in the case of normal speed is shown in Fig. 3.25. The reproduced position and force by the motion-loading system corresponds to the saved motion, which is shown in Fig. 3.24. Therefore, the motion-loading system realizes reproduction of the motion of the human operator. Additionally, Figs. 3.26 and 3.27 show that the motion-loading system reproduces the motion. In this case, the reproduction velocity is set to double or triple. Even then, these results confirm that the position and force are reproduced corresponding to stored motion data. Fig. 3.28 shows experimental results of the motion-loading system in cases where the reproduction velocity command is one-half. The motion-loading system normally operates even where reproduction velocity is low.

In this way, the motion-saving system saves the motion of the human operator, and the

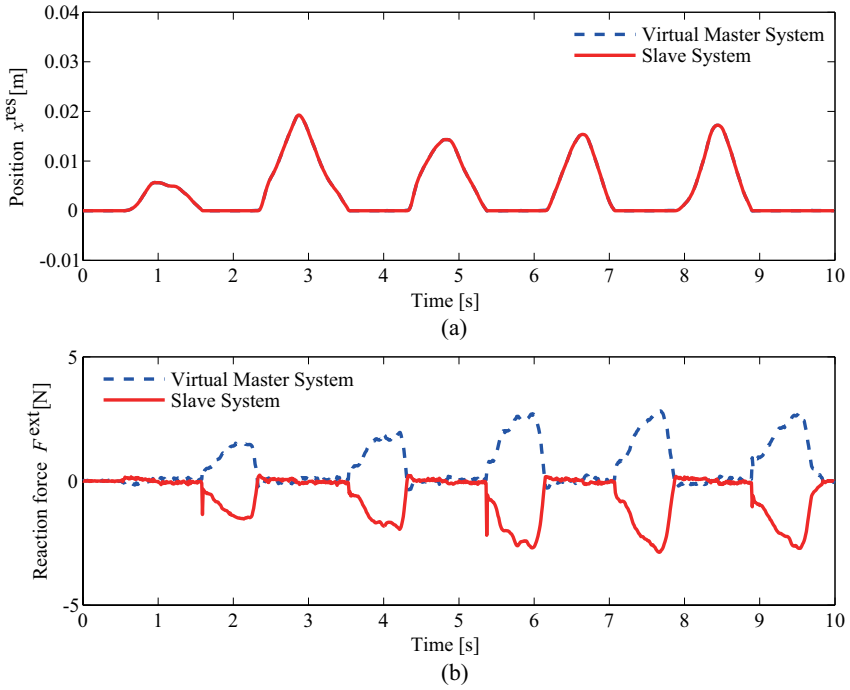

Fig. 3.24. Saved motion data using motion-saving system.
(a) Saved position (b) Saved force

motion-loading system reproduces the motion. Moreover, the motion-loading system is able to reproduce the saved motion even if the reproduction velocity is changed.

3.1.3.6 Conclusions

The thesis proposes a novel motion-copying system considering variable reproduction velocity. The motion-copying system is constructed by the motion-saving system and the motion-loading system. The bilateral controller using the quarry matrix controls the motion-saving system. The motion-saving system observes position and force of the master motor, and saves the motion of the human operator. The motion-loading system is operated by the virtual master-slave controller according to the saved motion data. The reproduced position and force of the slave motor in the motion-loading system corresponds to saved position and force. This thesis confirms that the motion-copying system normally operates. Additionally, the reproduction ve-

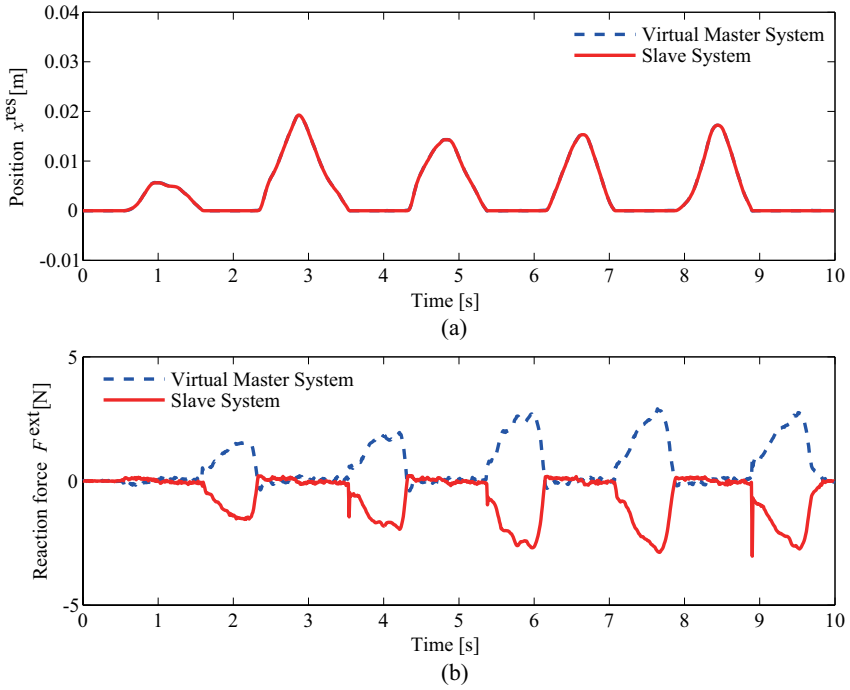

Fig. 3.25. Loaded motion data using motion-loading system.
(Reproduction velocity is normal) (a) Loaded position (b) Loaded force

locity can be freely changed when the motion-loading system reproduces the motion. Thus, the motion-copying system considering variable reproduction velocity is realized. The motion copying technology will be useful for industrial applications, medical and welfare human assistance and so on.

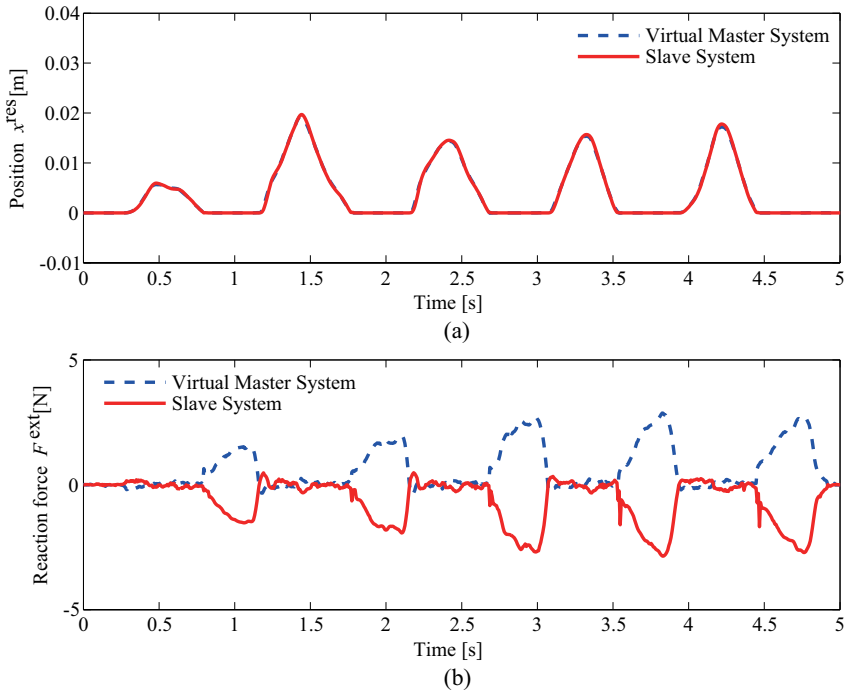

Fig. 3.26. Loaded motion data using motion-loading system.
(Reproduction velocity is twice) (a) Loaded position (b) Loaded force

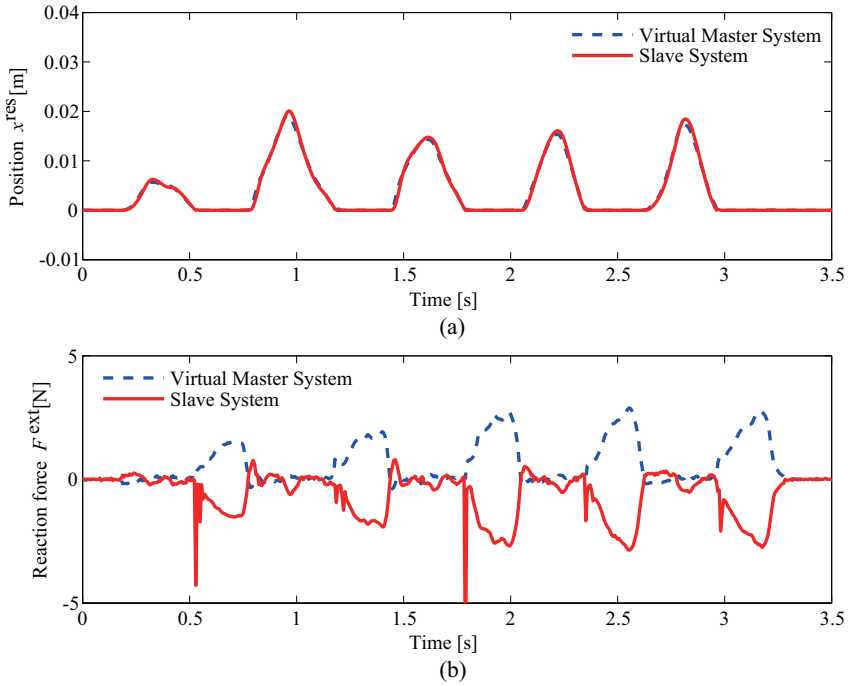

Fig. 3.27. Loaded motion data using motion-loading system.
(Reproduction velocity is third-time) (a) Loaded position (b) Loaded force

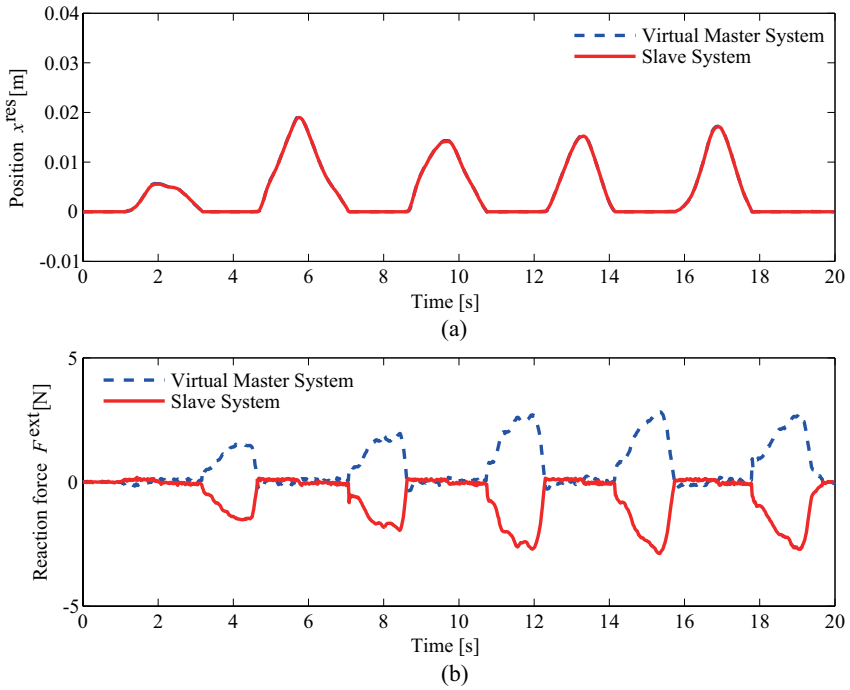

Fig. 3.28. Loaded motion data using motion-loading system.
(Reproduction velocity is one-half) (a) Loaded position (b) Loaded force

3.1.4 Realization of Motion-Copying System Based on Multilateral Control

3.1.4.1 Introduction

Recently, an aging society is progressing in several countries. In this situation, various ability of motion control technology is required to maintain technical capabilities of industrial engineering and medical engineering. Motion control for robot using acoustic and visual information has been developed. However, research of the motion control technology for treating haptic information has not been enough. The motion control based on real-world haptics should be provided for human society in order that the robot carry out complicate and dexterous tasks. To provide human skill to robot, this thesis proposes a motion-copying system using multilateral control [73]–[83]. The motion-copying system realizes storage of the motion of human operators and reproduction of the stored motion. Once such a system is constructed, the motion-copying system is capable of copying motion of expert engineers in various fields. Therefore, the proposed system will be useful for aging society.

Fig. 3.29 shows Conceptual diagram of motion-copying system using multilateral controller. The motion-copying system consists of motion-saving system and motion-loading system based on multilateral controller in order to reproduce motion of human operators. The motion-saving system stores the motion of slave system when human operator moves actuators of master systems. At the same time, identity ratio of the each master system is calculated by force of the all master systems, and are stored to motion data memory. On the other hand, the real-world master systems and virtual-world slave system realize the motion-loading system. Using the stored motion data and stored value of the identity ratio, the motion-loading system reproduces the motion.

The experimental results confirms that the reproduced position and force correspond to the stored ones. Thus, the motion-copying system based on multilateral controller is verified. The proposed method will be useful for industrial application, medical and welfare human assistance.

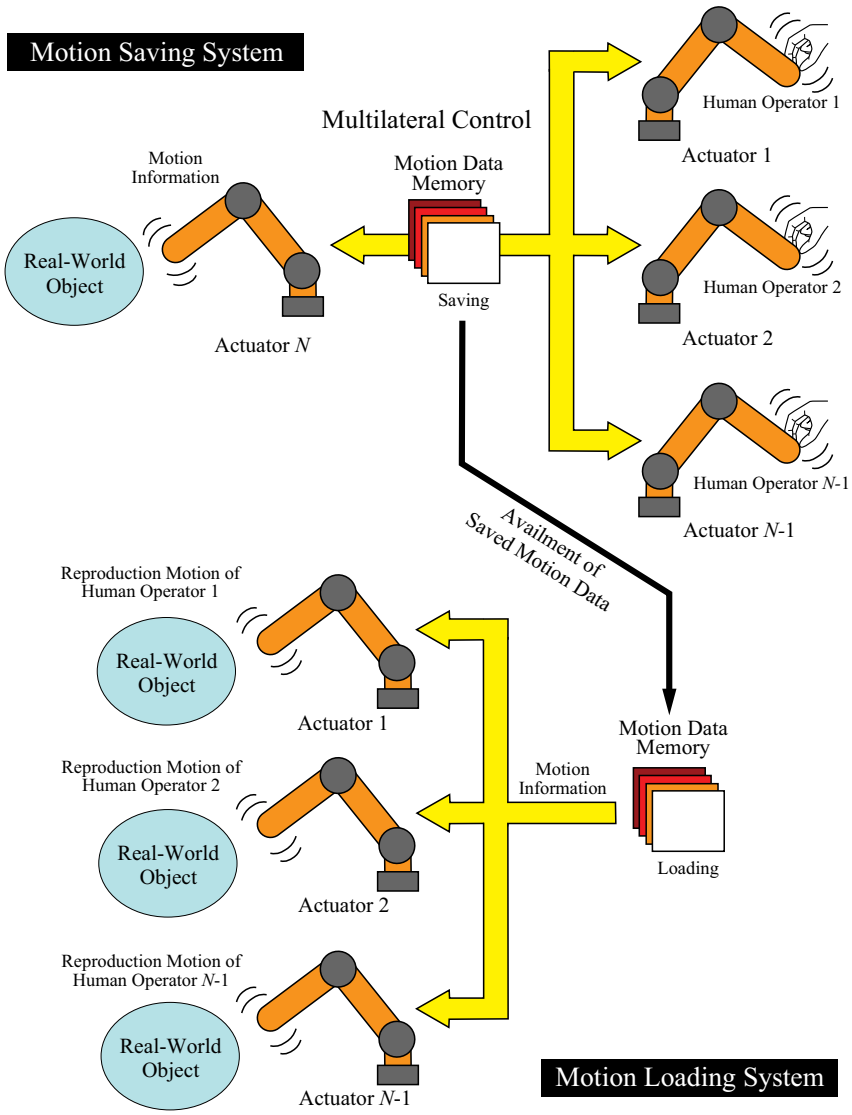

Fig. 3.29. Conceptual diagram of motion-copying system using multilateral controller.

3.1.4.2 Multilateral Control considering Identity Ratio

The multilateral control can share the haptic sensation between the actuator systems. In the basic multilateral control, position responses of the all actuators are same. Therefore, the human operators in the each system grasp motion of the other operators. In order to construct haptic broadcasting system, multilateral control using identity ratio has been proposed [84]. Fig. 3.30

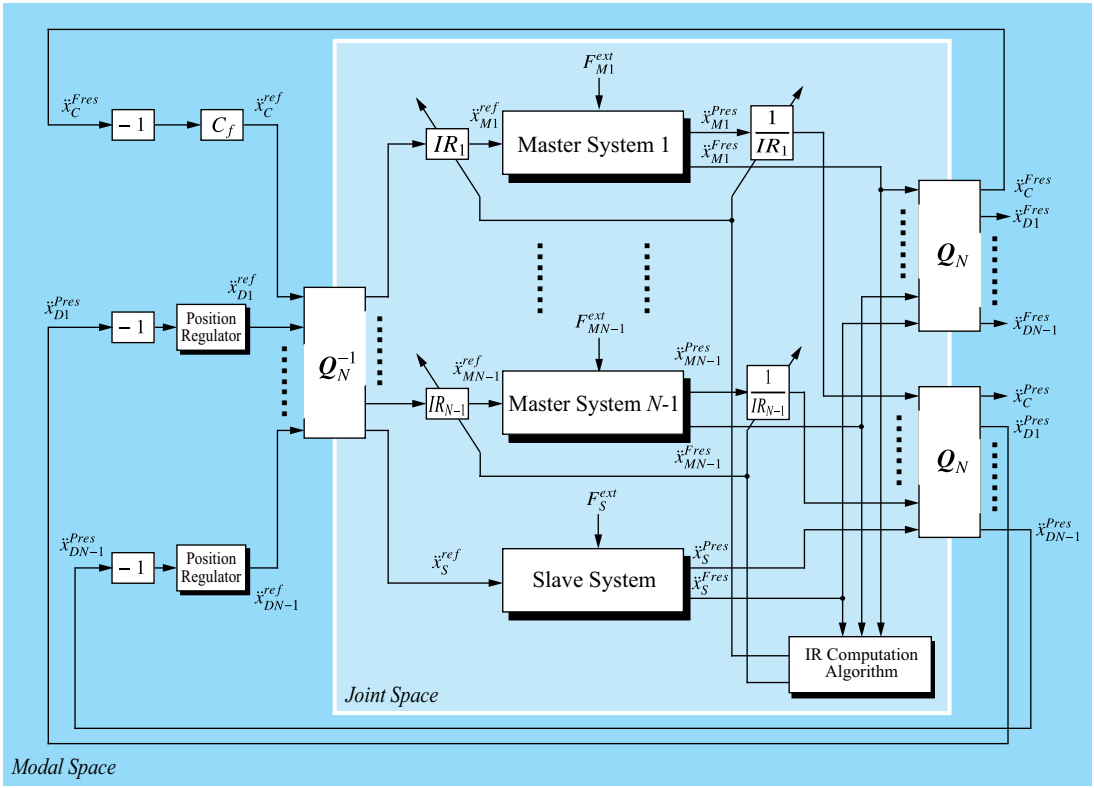

Fig. 3.30. Block diagram of multilateral control system with identity ratio.

shows block diagram of multilateral control system with identity ratio. $\ddot{x}$, subscripts M, N, and S mean acceleration, master, number of system, and slave. The superscripts $Pres$ and $Fres$ denote response and equivalent. Fundamentally, the control method of the multilateral controller is similar to the control method of the bilateral controller. However, the multilateral control utilizes N-order quarry matrix $\boldsymbol{Q}_N$ defined in [63, 65]. The force controller C_f calculates the acceleration reference $\ddot{x}_C^{Fres}$ as follows:

$$\ddot{x}_C^{ref} = -\, C_f\, \ddot{x}_C^{Fres}. \tag{3.28}$$

On the other hand, the acceleration references $\ddot{x}_{D1}^{Pres} \sim \ddot{x}_{DN-1}^{Pres}$ are also calculated as

$$\begin{array}{ccc} \ddot{x}_{D1}^{ref} & = & -\left(K_p \frac{1}{s^2} + K_v \frac{1}{s}\right) \ddot{x}_{D1}^{Pres} \\ \ddot{x}_{D2}^{ref} & = & -\left(K_p \frac{1}{s^2} + K_v \frac{1}{s}\right) \ddot{x}_{D2}^{Pres} \\ \vdots & \vdots & \vdots \\ \ddot{x}_{DN-1}^{ref} & = & -\left(K_p \frac{1}{s^2} + K_v \frac{1}{s}\right) \ddot{x}_{DN-1}^{Pres}. \end{array} \tag{3.29}$$

where K_p and K_v are gain of the position regulators. The acceleration references in the modal space are transformed into the joint space by using inverse quarry matrix $\boldsymbol{Q}_N^{-1}$ as follows:

$$\begin{bmatrix} \ddot{x}_{M1}^{ref} \\ \vdots \\ \ddot{x}_{MN-1}^{ref} \\ \ddot{x}_{S}^{ref} \end{bmatrix} = \boldsymbol{Q}_N^{-1} \begin{bmatrix} \ddot{x}_{C}^{ref} \\ \ddot{x}_{D1}^{ref} \\ \vdots \\ \ddot{x}_{DN-1}^{ref} \end{bmatrix}. \tag{3.30}$$

In addition, the identity ratio IR_i in the master system i is derived as

$$IR_i = \frac{\hat{F}_{Mi}^{ext}}{\sum_{k=1}^{N-1} \hat{F}_{Mk}^{ext}} \qquad (i = 1, 2, \cdots, N-1) \tag{3.31}$$

where $\hat{F}_{Mi}^{ext}$ denote force response of the master system i. Using the identity ratio, the motion of the operators in the each system is able to be decoupled.

3.1.4.3 Motion-Copying System Based on Multilateral Control

Fig. 3.31 shows block diagram of motion-saving system based on multilateral control and identity ratio. Basically, the control scheme of the motion-saving system is same as the multilateral control with identity ratio. In Fig. 3.31, 3rd-order quarry matrix $\boldsymbol{Q}_3$ [63] is defined as

$$\boldsymbol{Q}_3 = \frac{1}{3} \begin{bmatrix} 1 & 1 & 1 \\ 0 & 1 & -1 \\ 2 & -1 & -1 \end{bmatrix}. \tag{3.32}$$

In the motion-saving system, the motion data memory stores not only the equivalent acceleration $\ddot{x}_S^{Fres}$ and responses $\ddot{x}_S^{Pres}$ but also the identity ratio IR_1 and IR_2. The stored data is used for the motion-loading system. Fig. 3.32 shows block diagram of the motion-loading system using the multilateral controller. In the reproduction phase, the motion data memory is used instead

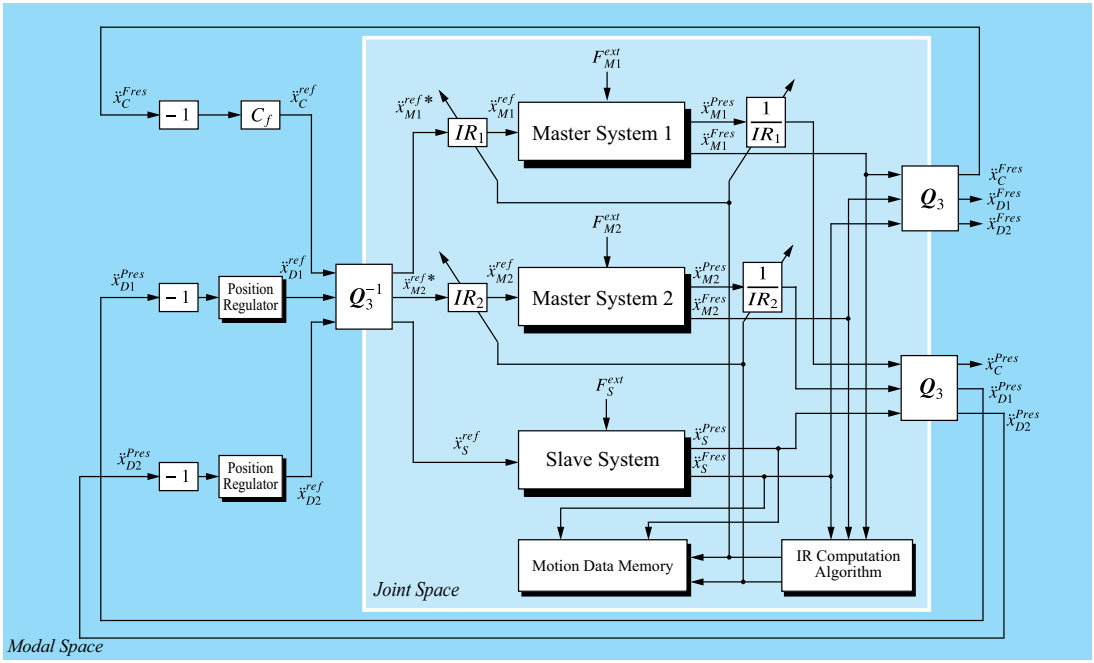

Fig. 3.31. Block diagram of motion-saving system based on multilateral control and identity ratio.

of the real slave system. Thus, the actuators in the slave side is unused. The virtual slave system outputs the acceleration to the master systems. In addition, the identity ratio IR_1 and IR_2 is changed by the motion data memory. By this means, the motion of the human operators are able to be reproduced independently.

3.1.4.4 Experiment

Experimental Setup Figs. 3.33 and 3.34 shows experimental setup of the motion-saving system and of the motion-loading system. In this experiment, the sponge block for environmental object in the slave side is used. These linear actuators are controlled by RT-Linux.

Experiment Results Figs. 3.35 and 3.36 shows experimental results of the motion-saving system and of the motion-loading system. In the reproduction phase, the experimental results exhibit that the force and the position is able to be reproduced according to the stored force, po-

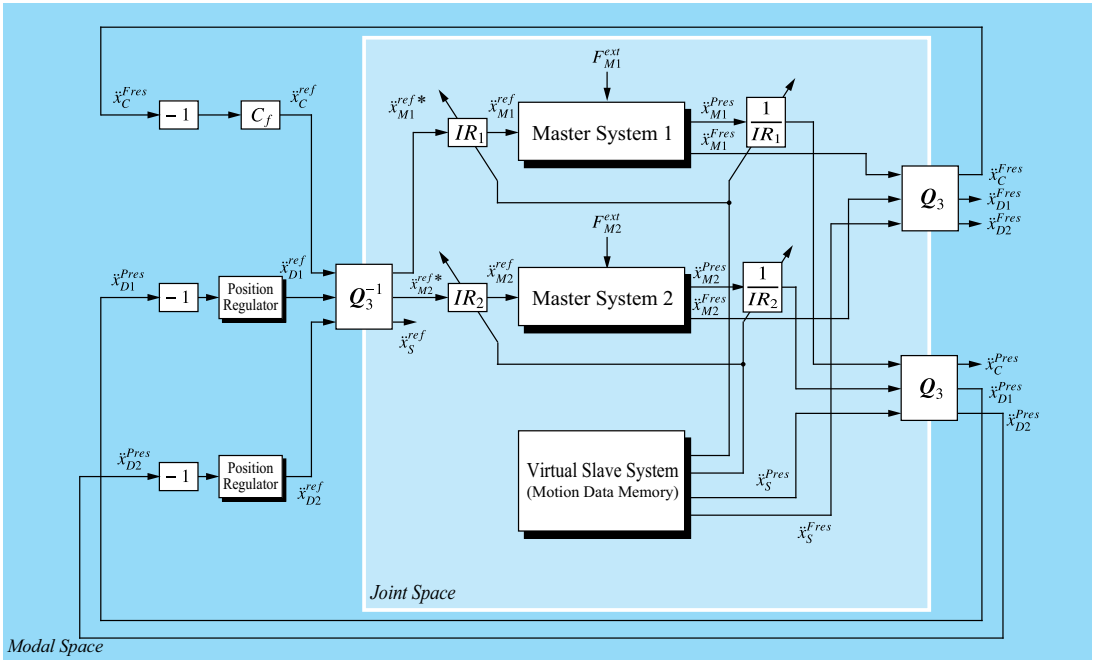

Fig. 3.32. Block diagram of motion-loading system using multilateral controller.

sition, and identity ratio. Therefore, the multiple motion of the human operators are reproduced independently by the proposed system. By the experiment, validity of the proposed method is verified.

3.1.4.5 Conclusion

This thesis proposed a motion-copying system in order to reproduce motion of human operators. The motion-copying system consists of motion-saving system and motion-loading system based on multilateral controller. The motion-saving system, which is realized by master systems and slave system, stores the motion of the slave system when human operator moves the master systems. At the same time, identity ratio is introduced to decouple the master system. The identity ratio of the each master system is calculated by force of the all master systems, and are stored to the memory. On the other hand, the real-world master systems and virtual-world slave system realize the motion-loading system. The motion-loading system reproduces the motion using the stored motion and the value of the identity ratio. The thesis confirms that the

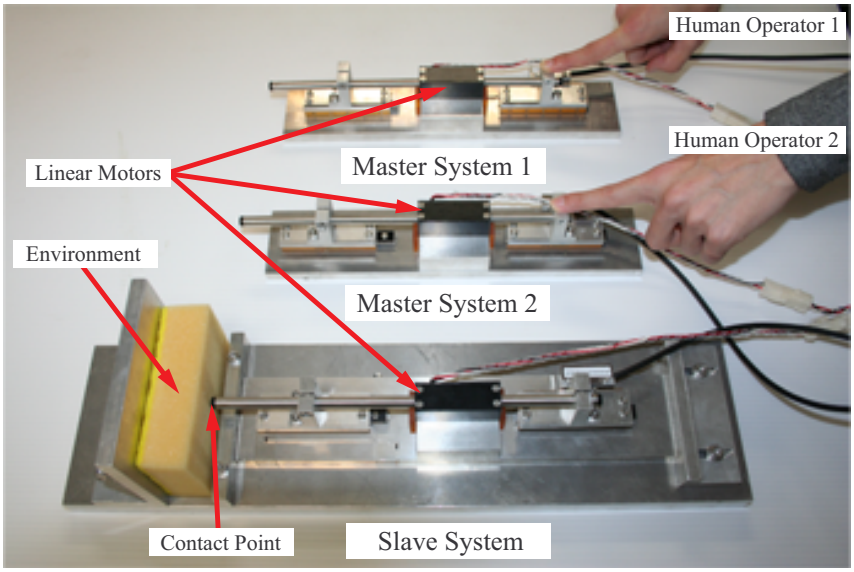

Fig. 3.33. Experimental setup of motion-saving system

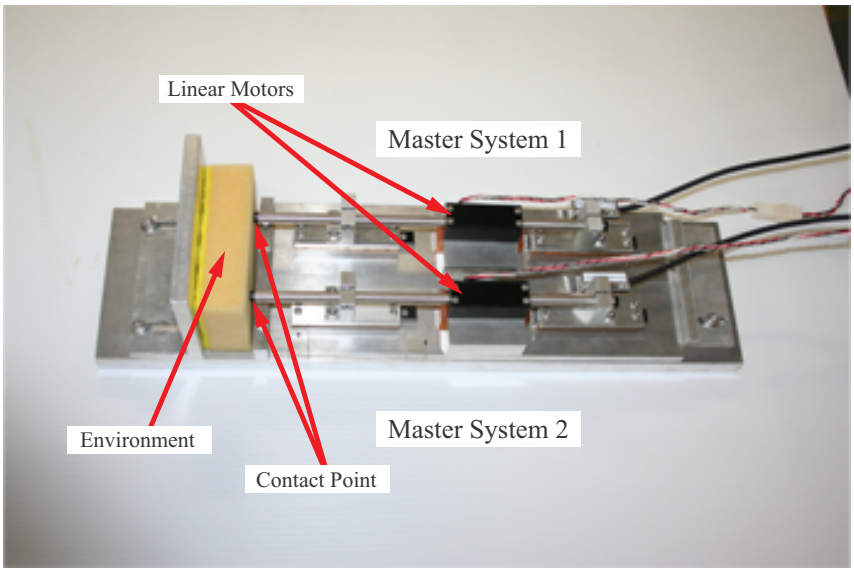

Fig. 3.34. Experimental setup of motion-loading system

motion-saving system and motion-loading system based on multilateral controller is verified. The reproduced position and the reproduced force are able to be corresponded to the stored ones.

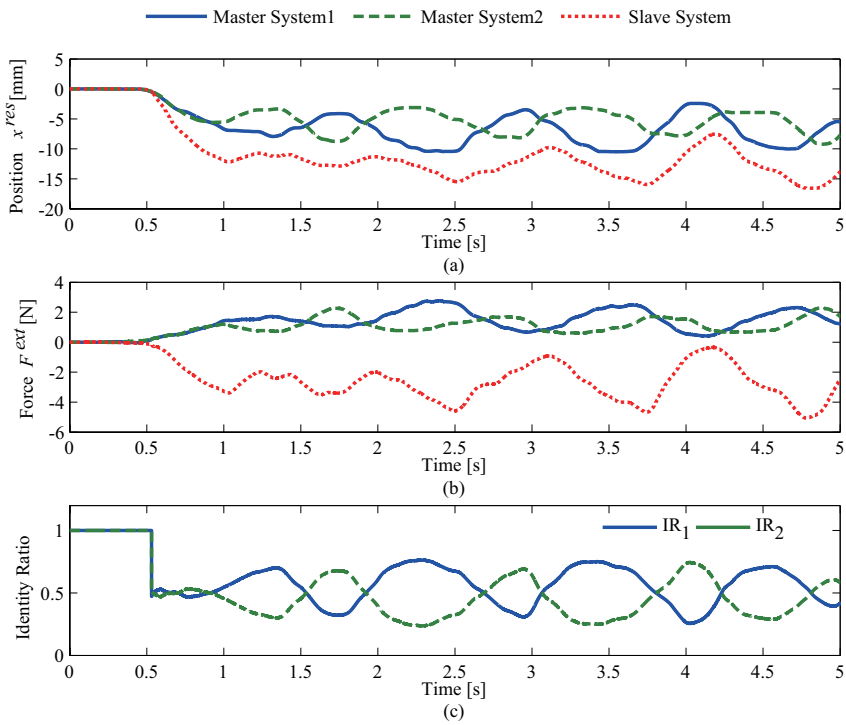

Fig. 3.35. Saved motion data using motion-saving system (a) Position (b) Force (c) Identity ratio

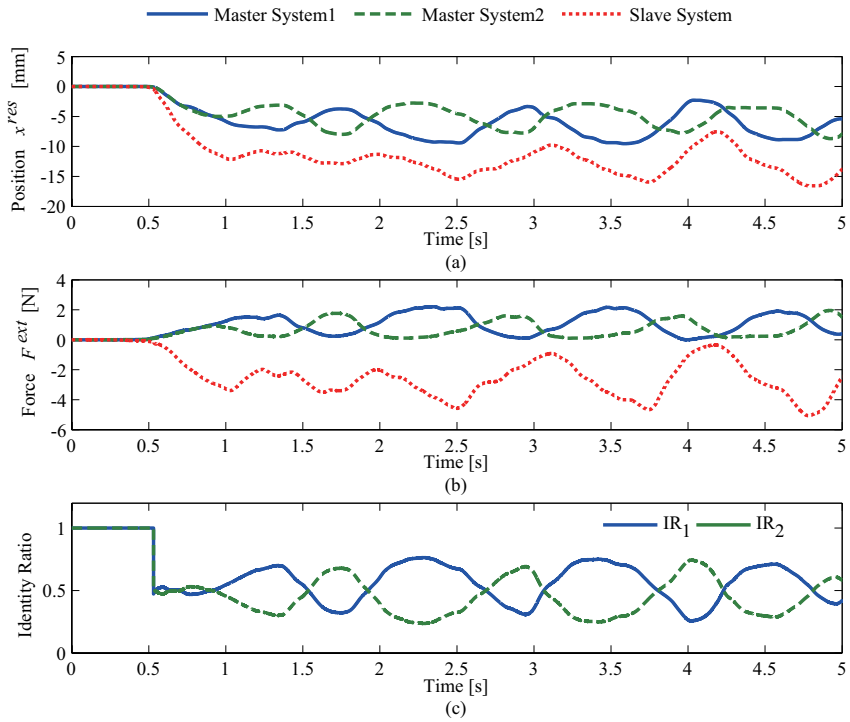

Fig. 3.36. Loaded motion data using motion-loading system (a) Position (b) Force (c) Identity ratio

3.1.5 Stability Analysis and Experimental Validation of Motion-Copying System

3.1.5.1 Introduction

In order to increase the amount and variety of available information in the human society, not only the acoustic and visual, but also haptic informational preservation and/or reproduction technique should be researched and developed, because the human utilizes the information, which is given by the five organs. In the practical use, microphone catches air vibration, which comes from the environment in the real-world. The acoustic information is stored to the memory, and can be reproduced to the real-world by the speaker systems. Additionally, the camera or video camera takes the pictures of the environment. The display system plays the visual information according to the memory. There are much researched and developed, however the research and development in regard to the haptic information is not enough.

The acoustic information and visual information are unilateral information. On the other hand, the haptic informational handling is difficult, because it is bilateral information. The environment is formed by the motion of the human, if the human touches to the environment. Thus, the mutual characteristics are influenced. This situation makes difficult to realize preservation and reproduction of the haptic information. The acquisition methods of the human motion based on visual information are researched [29]–[32]. Also, the method using reaction force between the environment and the human has been proposed [33]. However, these methods consider only either position information or force information. Therefore, it is hard to extract the motion of the human operator. The research considering both the position/velocity and the force has been proposed [34]–[37], though the point of view with respect to saving and loading of the haptic information is not presented.

We have already proposed the motion-copying system, which preserves and reproduces the motion of the human operator [38]. A motion-loading system which composes the motion-copying system replays force and position using information stored by a motion-saving system. In the case of industrial applications or medical applications, the proposed system is applied

to numerical controlled machine tools, industrial robots or surgical robots. There are able to regenerate motions of expert engineers or operators based on both force information and position information.

The proposed motion-loading system in [38] is able to reproduce the haptic information of a human operator under the passive environments. The system imitates the motion of the human operator beyond time and space. In short, the motion-copying system copies the human motion. However, the research does not consider the environmental transition. The thesis examines stability of the motion-copying system in terms of the environmental mechanical impedance. The motion-copying system consists of the motion-saving system and the motion-loading system. They preserve and reproduce the motion, respectively. The stability is investigated by displacement of the poles with transition of environmental stiffness and damper in the motion-loading system. By the experiments, the influences from the environment are confirmed in this thesis.

This research is organized as follows. Subsection 3.1.5.2 presents concept and motion control of the motion-copying system. Subsection 3.1.5.3 derives a transfer function of the system and examines stability of the system in case that the environmental mechanical impedance is changed. The experimental setup and results are shown in 3.1.5.4. The last section concludes this research.

3.1.5.2 Motion-Copying System

Concept Fig. 3.37 shows conceptual diagram of the motion-copying system. The motion-copying system consists of two systems. The first system is the motion-saving system; the other system is the motion-loading system. The motion-saving system is controlled by the bilateral controller. The human operator in the master side is able to touch the environment in the slave side through the bilateral controller. On this occasion, the motion-saving system stores both force impressed by the human operator and position of the master side actuator to a motion data memory. This information in the motion data memory is utilized, when the motion-loading system reproduces the motion of the human operator.

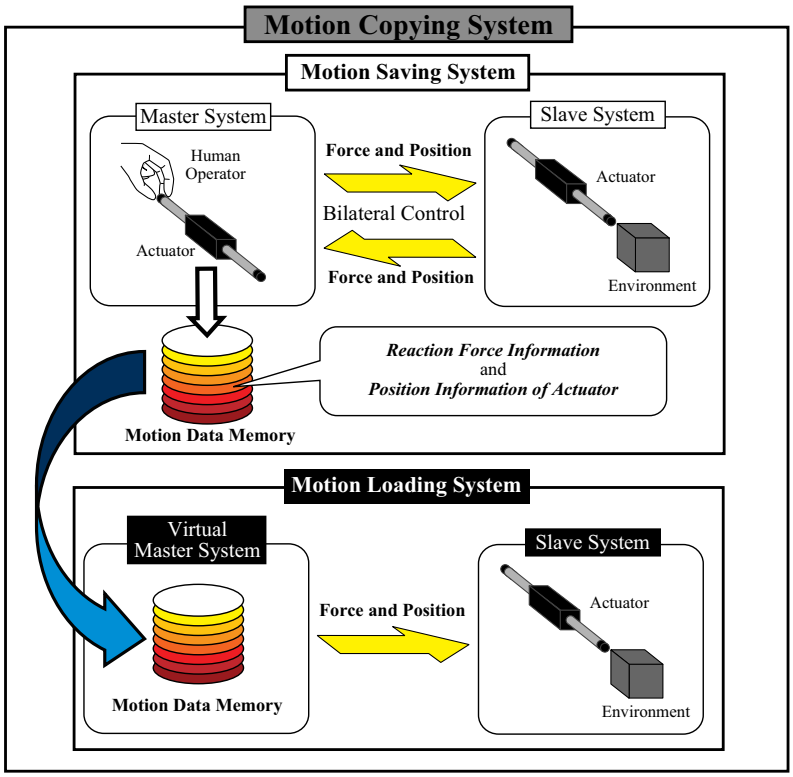

Fig. 3.37. Conceptual diagram of motion-copying system.

Meanwhile, the motion-loading system consists of a virtual master system and a slave system. In other words, the motion-loading system uses only one actuator, because the motion data memory is used in stead of the actuator in the master side. The motion data memory outputs force and position information. The reproduced force and position are accorded to the saved ones by the motion-loading system. Since the haptic information is subject to the law of action and reaction, a bilateral controller is utilized in order that the motion-saving system preserves the both force and position responses of the master and slave systems. In addition, the motion-loading system which is composed of only the slave system reproduces the force and position beyond time and space. The thesis assume that the motion of the human operator consists of the force and position information. To acquire such haptic data, bilateral system is requisite. Since the actual master system has time-varying dynamic components, the thesis uses the same

structure for the master and slave to reflect the dynamics to the operator. Furthermore, the disturbance observer compensates the dynamic variations.

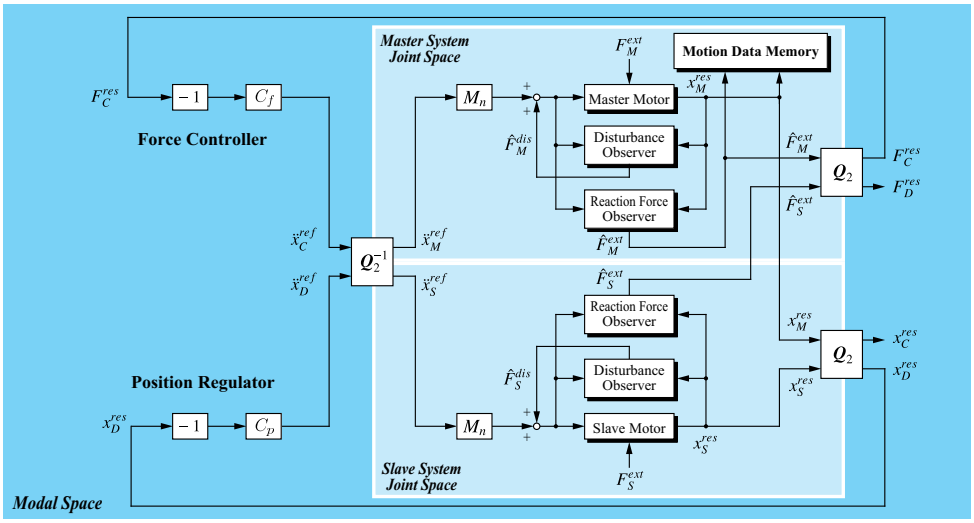

Fig. 3.38. Block diagram of motion-saving system using bilateral control system.

Motion Control Fig. 3.38 shows block diagram of the motion-saving system. M_n in the figure is nominal mass of the actuator. The motion-saving system consists of the master and slave actuators, and controlled by the bilateral control system. The motion-saving system includes a modal space section, a joint space of the master system section and a joint space of the slave system section. The conversion from the real-world joint space to the virtual-world modal space achieves using a quarry matrix [65]. The quarry matrix carries out modal decomposition on condition that the several actuators are operated. The quarry matrix abstracts independent modes. By using the quarry matrix, it is possible to extend to the infinity order. The generalized

quarry matrix is given as follows,

$$\boldsymbol{Q}_n = \frac{1}{n}\begin{bmatrix} 1 & \cdots & 1 & 1 & 1 & 1 & 1 \\ 0 & \cdots & 0 & 0 & 0 & 1 & -1 \\ 0 & \cdots & 0 & 0 & 2 & -1 & -1 \\ 0 & \cdots & 0 & 3 & -1 & -1 & -1 \\ 0 & \cdots & 4 & -1 & -1 & -1 & -1 \\ \vdots & \ddots & \vdots & \vdots & \vdots & \vdots & \vdots \\ n-1 & \cdots & -1 & -1 & -1 & -1 & -1 \end{bmatrix}. \tag{3.33}$$

In the equation (1), the first row represents a common mode; the other row represents differential modes. The common mode means sort of overall movement such as bias. Moreover, the differential mode represents movement between each actuator. As a result, the quarry matrix is one of good candidates for modal decomposition.

The second-order quarry matrix $\boldsymbol{Q}_2$ is defined by (3.34) [63]

$$\boldsymbol{Q}_2 = \frac{1}{2}\begin{bmatrix} 1 & 1 \\ 1 & -1 \end{bmatrix}. \tag{3.34}$$

The second order quarry matrix $\boldsymbol{Q}_2$ transforms from the reaction force of the master and slave actuators $\hat{F}_M^{ext}$, $\hat{F}_S^{ext}$ estimated by the reaction force observer [64] to the common mode force response F_C^{res} and the differential mode force response F_D^{res}.

$$\begin{bmatrix} F_C^{res} \\ F_D^{res} \end{bmatrix} = \boldsymbol{Q}_2 \begin{bmatrix} \hat{F}_M^{ext} \\ \hat{F}_S^{ext} \end{bmatrix} \tag{3.35}$$

In addition, the quarry matrix $\boldsymbol{Q}_2$ transforms from the position response of respective actuators x_M^{res} , x_S^{res} to the common mode position response x_C^{res} and the differential mode position x_D^{res}.

$$\begin{bmatrix} x_C^{res} \\ x_D^{res} \end{bmatrix} = \boldsymbol{Q}_2 \begin{bmatrix} x_M^{res} \\ x_S^{res} \end{bmatrix} \tag{3.36}$$

The force controller C_f and position regulator C_p calculate the common mode acceleration reference $\ddot{x}_C^{ref}$ and the differential mode acceleration reference $\ddot{x}_D^{ref}$ using the transformed force and position response.

$$\ddot{x}_C^{ref} = -C_f\, F_C^{res} \tag{3.37}$$

$$\ddot{x}_D^{ref} = -C_p\, x_D^{res} \tag{3.38}$$

In this thesis, the force controller and the position regulator is expressed as

$$C_f = K_{pf} \tag{3.39}$$

$$C_p = K_{pp} + sK_{dp} \tag{3.40}$$

where, K_{pf} is proportional gain of the force controller, K_{pp} and K_{dp} are proportional and differential gain of the position controller. The inverse quarry matrix $\boldsymbol{Q}_2^{-1}$ transforms from the acceleration references calculated by (3.39) and (3.40) to the acceleration references of the master actuator $\ddot{x}_M^{ref}$ and the slave actuator $\ddot{x}_S^{ref}$.

$$\begin{aligned} \begin{bmatrix} \ddot{x}_M^{ref} \\ \ddot{x}_S^{ref} \end{bmatrix} &= \boldsymbol{Q}_2^{-1} \begin{bmatrix} \ddot{x}_C^{ref} \\ \ddot{x}_D^{ref} \end{bmatrix} \\ &= \begin{bmatrix} 1 & 1 \\ 1 & -1 \end{bmatrix} \begin{bmatrix} \ddot{x}_C^{ref} \\ \ddot{x}_D^{ref} \end{bmatrix} \end{aligned} \tag{3.41}$$

The respective actuators are operated by the acceleration references, so that the bilateral controller is constructed. The disturbance observer estimates and compensates the disturbance force $\hat{F}_M^{dis}$, $\hat{F}_S^{dis}$, and realizes acceleration control [66],[85]–[88]. The control system of the thesis implements dual feedback loops of the disturbance observer. The inner one is to achieve the robust acceleration control. On the contrary, the outer one estimates the external forces to realize force servoing. In the thesis, we use linear motors, which do not have the friction in the experiment. Thus, coulomb friction and viscous friction are not considered in the experiment. As a result, the construction of the reaction force observer is same as the disturbance observer in the ideal frictionless case. The position and force responses of the master actuator x_M^{res}, F_M^{ext} are varied by the human operator. These two parameters are stored to the motion data memory in order to realize the motion-saving system.

Fig. 3.39 shows block diagram of the motion-loading system. Fundamentally, a control method of the motion-loading system is similar to the motion-saving system. The parameters in Fig. 3.39 are calculated, as with case of the motion-saving system. However, the position response x_M^{res} and force response F_M^{ext} are set to values of the stored position and force in the motion data memory. Therefore, the motion-loading system is able to reproduce the saved

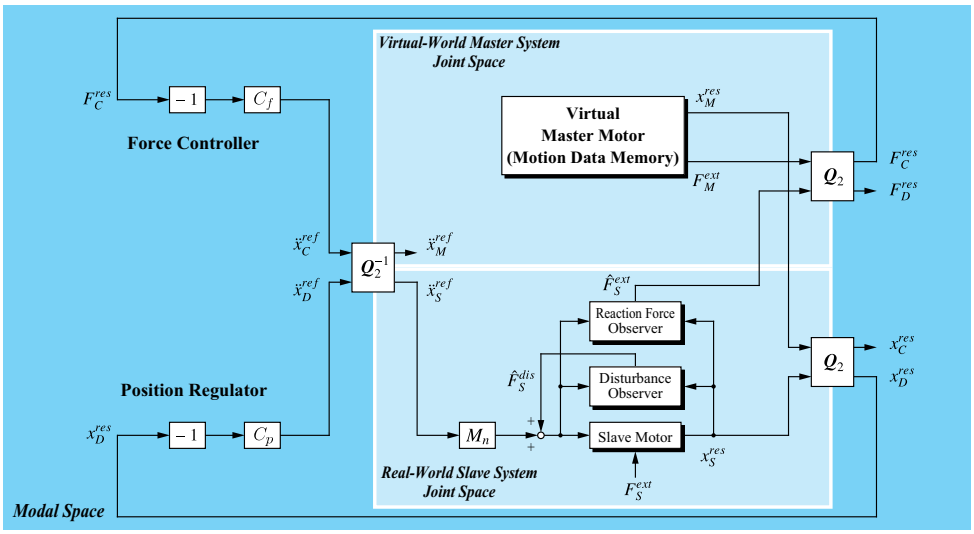

Fig. 3.39. Block diagram of motion-loading system using virtual master system.

motion of the human operator by the motion-saving system.

3.1.5.3 Stability of Motion-Copying System

This section examines stability of the motion-copying system considering environmental changing. The above concept of the proposed motion-copying system has been presented [38]. In this thesis, stability analysis of the motion-copying system has been confirmed when the environmental impedance is changed. As a result, it is possible to apply in changed environment.

Fig. 3.40 shows block diagram of the motion-loading system considering the environmental mechanical impedance without using the quarry matrix $\boldsymbol{Q}_2$ and the inverse quarry matrix $\boldsymbol{Q}_2^{-1}$. The equivalent conversion diagram of Fig. 3.40 is Fig. 3.41. M, K_f, K_{fn}, g_{dis} and g_{reac} in the figure are mass of the actuator, force constant, nominal force constant, bandwidth of the disturbance observer and the reaction force observer, respectively. The environmental mechanical impedance Z_s is defined as

$$Z_s = D_s\ s + K_s \tag{3.42}$$

where, K_s is stiffness, D_s is damper, when the motion-saving system preserves the motion. Also, when the motion-loading system reproduces the motion, the environmental impedance Z_ℓ

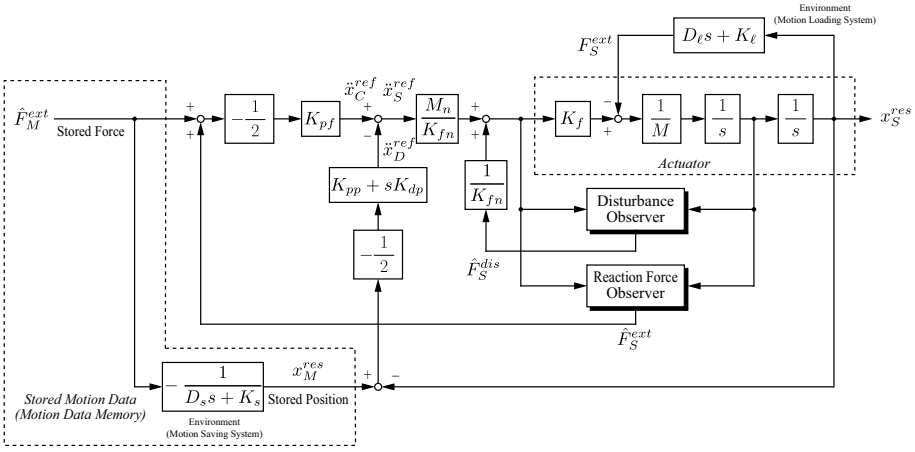

Fig. 3.40. Block diagram of motion-loading system considering the environmental impedance.

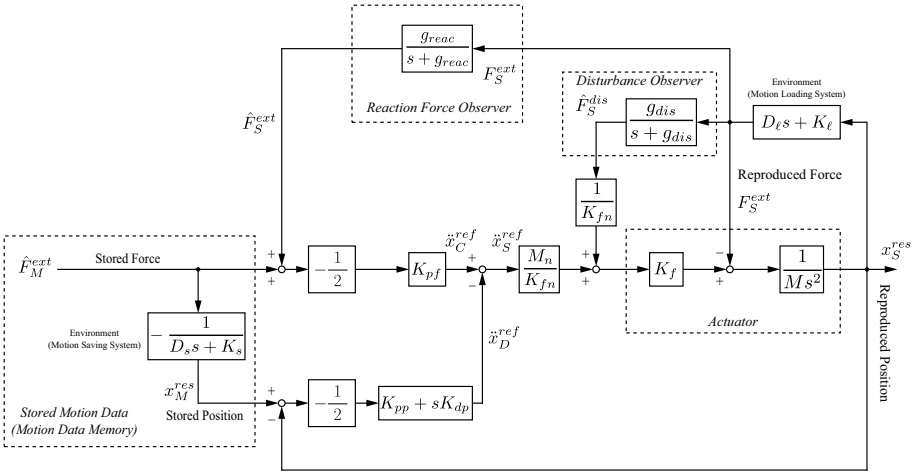

Fig. 3.41. Equivalent conversion block diagram of Fig. 3.41.

is defined as

$$Z_\ell = D_\ell \, s + K_\ell \tag{3.43}$$

where, K_ℓ is environmental stiffness, D_ℓ is environmental damper. In Fig. 3.41, the transfer function of the force in the slave side F_S^{ext} from the force in the master side F_M^{ext} is derived as

$$G_f = \frac{F_S^{ext}}{F_M^{ext}} = \frac{a_4 s^4 + a_3 s^3 + a_2 s^2 + a_1 s + a_0}{b_5 s^5 + b_4 s^4 + b_3 s^3 + b_2 s^2 + b_1 s + b_0} \tag{3.44}$$

where, the coefficients in the numerator are expressed by

$$\begin{aligned}
a_4 &= -D_\ell\ \alpha \\
a_3 &= -K_\ell\ \alpha - D_\ell\ (\beta + \alpha\ g_{dis} + \alpha\ g_{reac}) \\
a_2 &= -K_\ell\ (\beta + \alpha\ g_{dis} + \alpha\ g_{reac}) \\
&\quad -D_\ell\ (\beta\ g_{dis} + \beta\ g_{reac} + \alpha\ g_{dis}\ g_{reac}) \\
a_1 &= -K_\ell\ (\beta\ g_{dis} + \beta\ g_{reac} + \alpha\ g_{dis}\ g_{reac}) \\
&\quad -D_\ell\ \beta\ g_{dis}\ g_{reac} \\
a_0 &= -K_\ell\ \beta\ g_{dis}\ g_{reac}
\end{aligned} \tag{3.45}$$

additionally the coefficients in the denominator are shown by

$$\begin{aligned}
b_5 &= 2D_s \\
b_4 &= 2K_s + D_s\ (\gamma + 2g_{reac}) \\
b_3 &= K_s\ (\gamma + 2g_{reac}) + D_s\ (\delta + \gamma\ g_{reac} + \varepsilon) \\
b_2 &= K_s\ (\delta + \gamma\ g_{reac} + \varepsilon) + D_s\ (\delta\ g_{dis} + \eta + \varepsilon\ g_{reac}) \\
b_1 &= K_s\ (\delta\ g_{dis} + \eta + \varepsilon\ g_{reac}) + D_s\ \eta\ g_{dis} \\
b_0 &= K_s\ \eta\ g_{dis}
\end{aligned} \tag{3.46}$$

where, the respective coefficients are defined as

$$\begin{aligned}
\alpha &= K_{pf}\ D_s + K_{dp} \\
\beta &= K_{pf}\ K_s + K_{pp} \\
\gamma &= \frac{2D_\ell}{M_n} + K_{dp} + 2g_{dis} \\
\delta &= K_{pf}\ g_{reac}\ D_\ell + K_{pp} \\
\varepsilon &= g_{dis}\ K_{dp} + \frac{2K_\ell}{M_n} \\
\eta &= K_{pf}\ g_{reac}\ K_\ell + K_{pp}\ g_{reac}
\end{aligned} \tag{3.47}$$

on condition that M_n is M and K_{fn} is K_f.

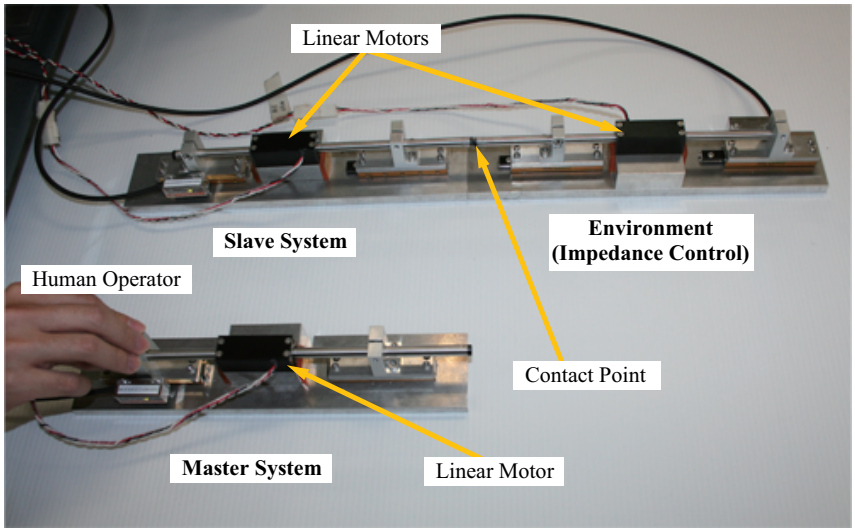

Fig. 3.42. Experimental device of motion-saving system.

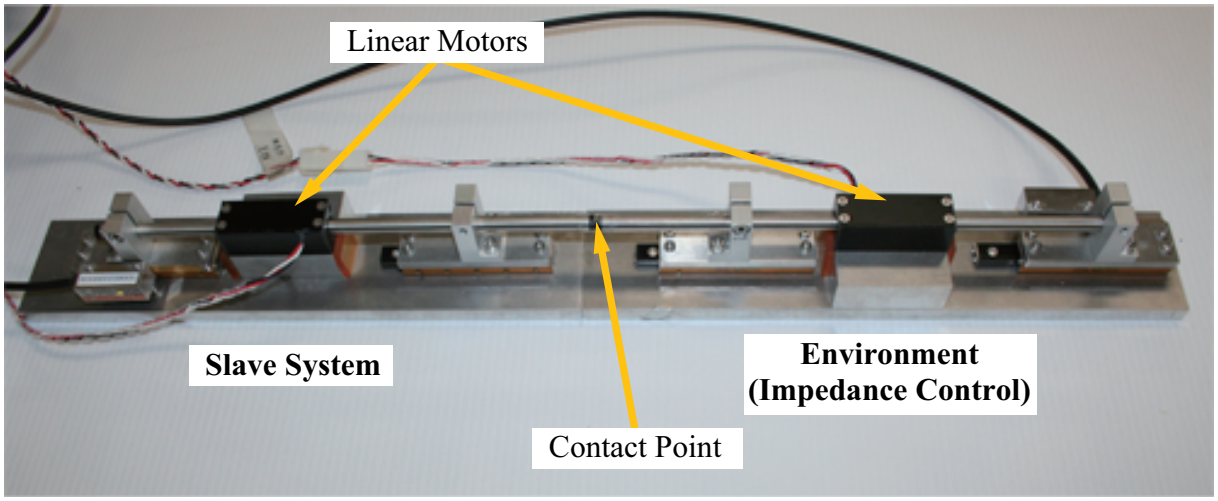

Fig. 3.43. Experimental device of motion-loading system.

In this section, the stability of the motion-copying system considering changing of the environmental impedance is examined by displacement of the poles using (3.44)–(3.47). Fig. 3.44 shows displacement of the poles with the transition of environmental stiffness K_ℓ. The displacement of the poles in the figure are obtained by changed stiffness K_ℓ using transfer function in (3.44). At this conjuncture, the stiffness and damper of the motion-saving system K_s, D_s and

the damper of the motion-loading system D_ℓ are set to constant, on the contrary, the stiffness K_ℓ is changed from 0 to 10^6 N/m. All poles in Fig. 3.44 are left side of the imaginary axis. Therfore the motion-loading system is able to stably operate even if the enviromental stiffness K_ℓ is varied. Fig. 3.45 shows displacement of the poles in case that the environmental damper D_ℓ is changed. This figure confirms that the motion-loading system also stably operates. Figs. 3.46 and 3.47 show displacement of the poles in the case of different from the stiffness K_s and damper D_s of Figs. 3.44 and 3.45. In each case, all poles in these figures exist in the left side of the imaginary axis. Thus, the operation of the motion-loading system is stable.

In consequence, even if the environmental mechanical impedance in the motion-loading system differ from the environmental mechanical impedance in the motion-saving system, the motion-copying system does not run out of the control, and is able to stably operate.

3.1.5.4 Experiment

In this section, the operation of the motion-copying system with transition of the environmental impedance is confirmed by the experiment.

Experimental Setup Figs. 3.42 and 3.43 show the experimental devices of respective systems. Fig 3.48 shows block diagram of the environmental reproduction system, which is general impedance control system using the disturbance and reaction force observer. The stiffness K_i and damper D_i of the impedance control system are set to K_s and D_s in the motion-saving system. On the other hand, the K_i and D_i are set to K_ℓ and D_ℓ in case of the motion-loading system. In the experiment of the motion-saving system, the human operator grasps the environment in the slave side via the bilateral controller. On this occasion, the motion-saving system stores the force and position to the motion data files on RT-Linux 3.2. Meanwhile, the motion-loading system reproduces the motion according to the force and position concerning the mechanical impedance control system. The setup parameters are shown in Table 3.3.

Table 3.3. Setup Parameters

T_s	Period of control system	100	μs
K_{fn}	Force constant of actuator	3.33	N/A
M_n	Mass of nominal	0.18	kg
K_{pf}	Gain of force controller	10	
K_{pp}	Proportional gain of position regulator	10000	
K_{dp}	Differential gain of position regulator	200	
g_{pd}	Pole of pseudo derivative for PD controller of position regulator	10000	rad/s
g_{dis}	Pole of disturbance observer	1000	rad/s
g_{reac}	Pole of reaction force observer	1000	rad/s

Experimental Results Fig. 3.49 shows experimental results of the motion-saving system, which was moved and given by the human operator. The results confirm that the bilateral controller artificially generates the law of action and reaction and measures the given force between the master side and the slave side. The experimental results of the motion-loading system are shown in Fig. 3.50, when the environmental stiffness K_ℓ is changed from 100 to 700 N/m. In this experiment, the motion-loading system reproduces the motion of the human operator using the motion data memory without the human oeprator. The results confirm that the motion-loading system is able to reproduce the motion. The reproduced motion does not correspond to the stored motion on condition that the stiffness K_ℓ is varied, however the overdrive of the motion-loading system is not induced by it.

The reproduced position and the reproduced force can be corresponded to the preserved ones on condition that the environmental mechanical impedance is not varied. In this regard, the record and playback system which treats acoustic information is also same. If the reproduction environment differs from the preservation environment, we can listen differently to the reproduced sounds. The purpose of the proposed system is preservation and reproduction of the haptic information under the specific environment. Therefore the haptic information should be newly stored in case that the environments are changed.

In addition, Fig. 3.51 shows the experimental results of changing of the environmental

damper D_ℓ in the motion-loading system. The damper is changed from 20 to 200 Ns/m in this experiment. The operation of the motion-loading system is also stable in this case. Fig. 3.52 shows the placement of poles in the experiment of Figs. 3.50 and 3.51.

In short, these results clarify that the motion-copying system does not become unstable, even if the environment is changed in the motion-loading system.

If the reproduction environment is changed, the waveform of position and force is also changed. In addition, in this thesis it is assumed that the reproduced position and force by the motion-loading system includes vibration on condition that the damping factor of reproduction environment is lower than the damper of preservation environment. However, the system is not unstable.

3.1.5.5 Conclusion

The thesis examines the stability of the motion-copying system, which preserves and reproduces the motion of the human operator. The motion-copying system is able to reproduce the force and position according to the stored force and position in the motion data memory. The stability is theoretically confirmed by displacement of the poles with transition of stiffness and damper using the transfer function. By the experiments, the thesis confirms that if the environmental mechanical impedance is changed, the motion-copying system does not run out of the control.

The proposed method in this thesis will be useful for industrial application, medical, welfare human support. The motion-copying system stores and reproduces specific special human motions, which are provided by expert engineers, skilled workers or medical operators in industrial or medical fields. More specifically, the numerical controlled machine tools which imitate the motions of skilled operators can be realized assuming that the proposed method is applied to industrial applications.

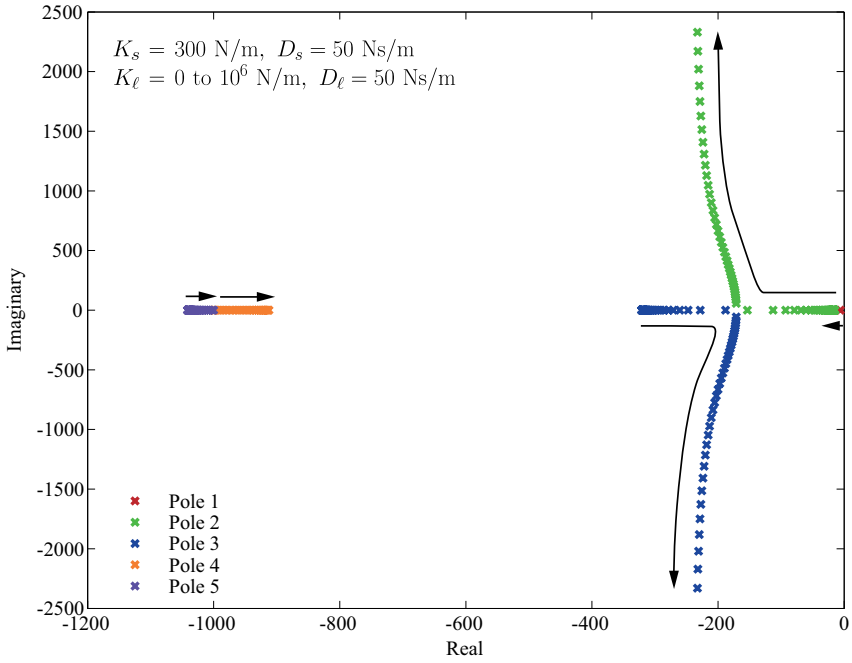

Fig. 3.44. Displacement of the poles with the transition of environmental stiffness K_ℓ.

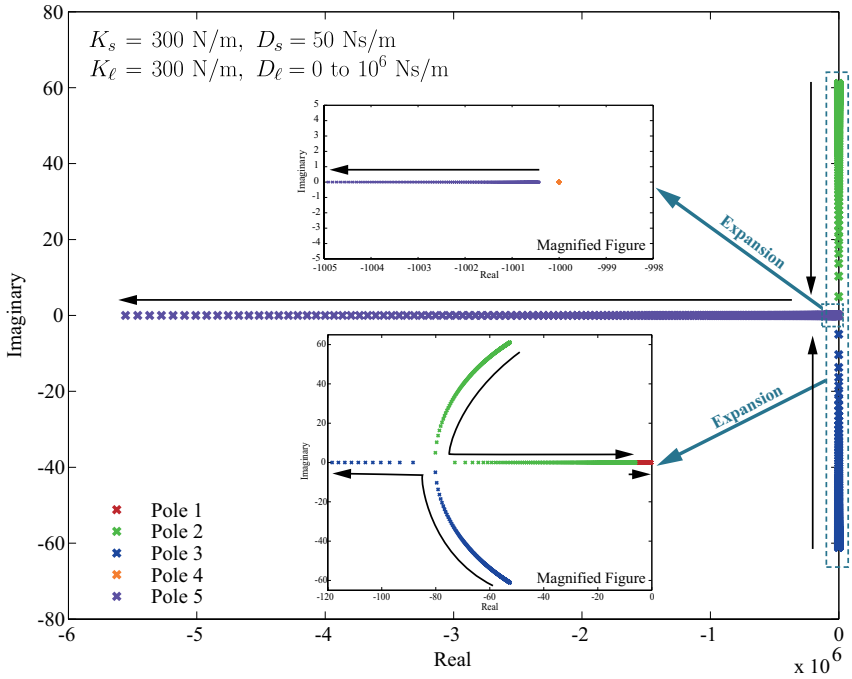

Fig. 3.45. Displacement of the poles with the transition of environmental damper D_ℓ.

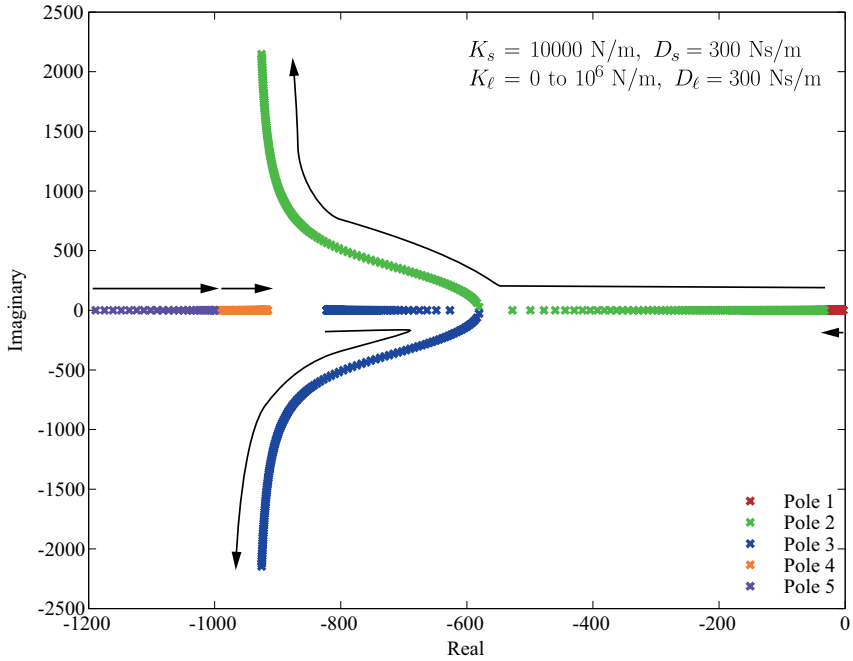

Fig. 3.46. Displacement of the poles with the transition of environmental stiffness K_ℓ.

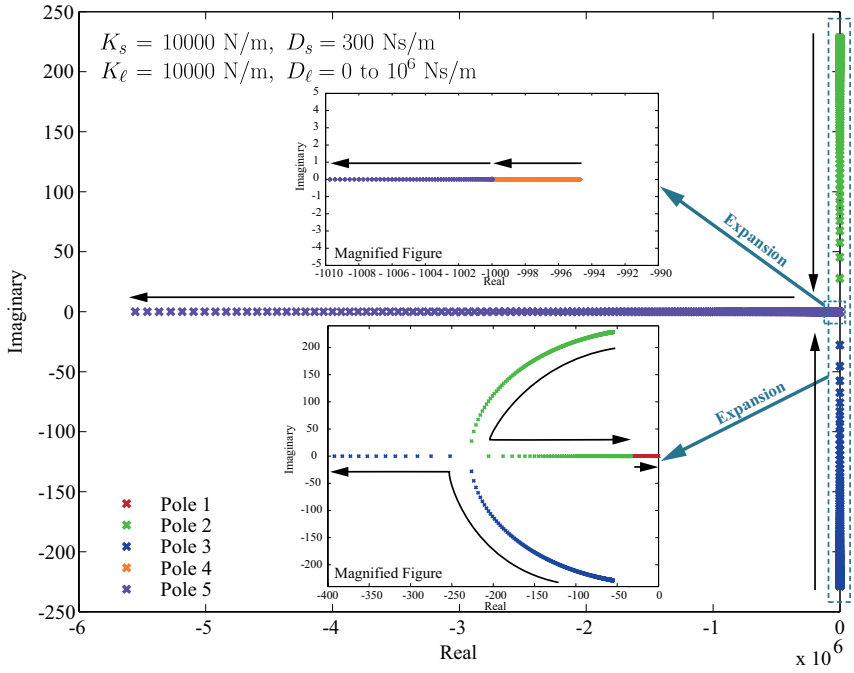

Fig. 3.47. Displacement of the poles with the transition of environmental damper D_ℓ.

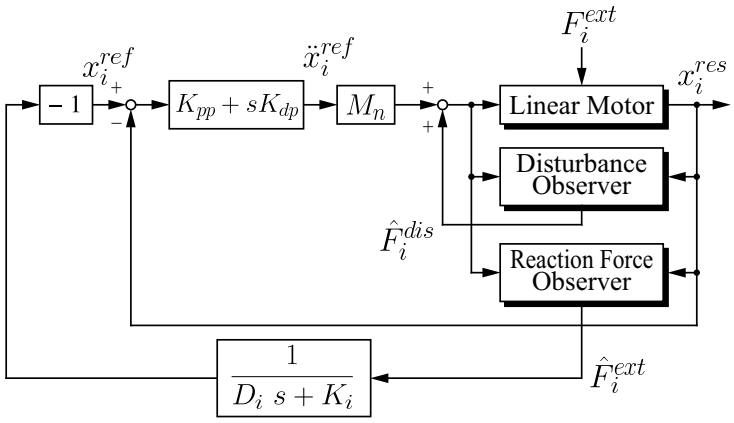

Fig. 3.48. Block diagram of environments reproduction system.(Impedance control)

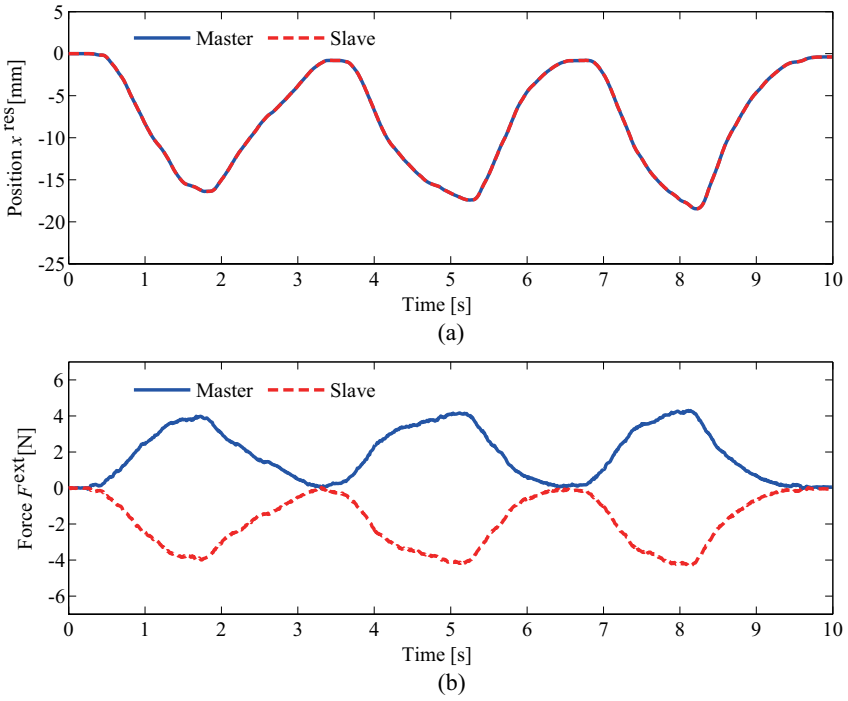

Fig. 3.49. Experimental result of motion-saving system. (a) position (b) force (Environmental stiffness K_s is 300, damper D_s is 50)

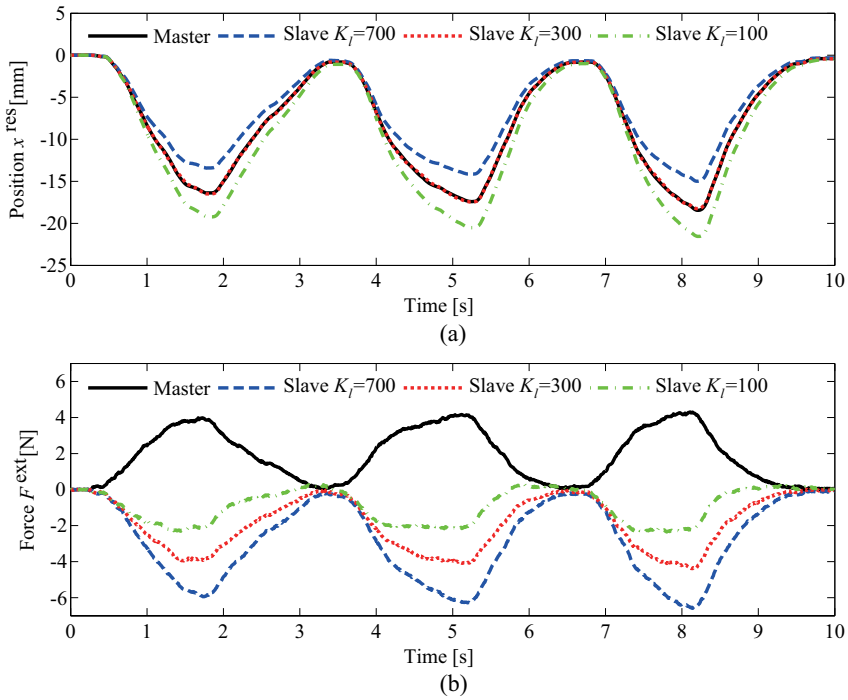

Fig. 3.50. Experimental result of motion-loading system. (a) position (b) force (Environmental stiffness K_ℓ is 100 to 700, damper D_ℓ is 50)

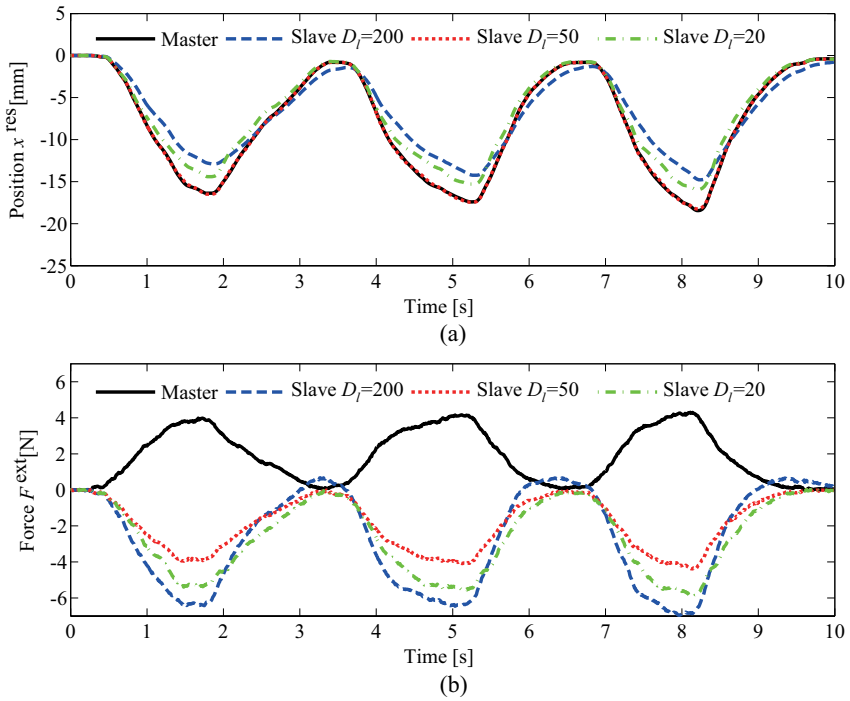

Fig. 3.51. Experimental result of motion-loading system. (a) position (b) force (Environmental stiffness K_ℓ is 300, damper D_ℓ is 20 to 200)

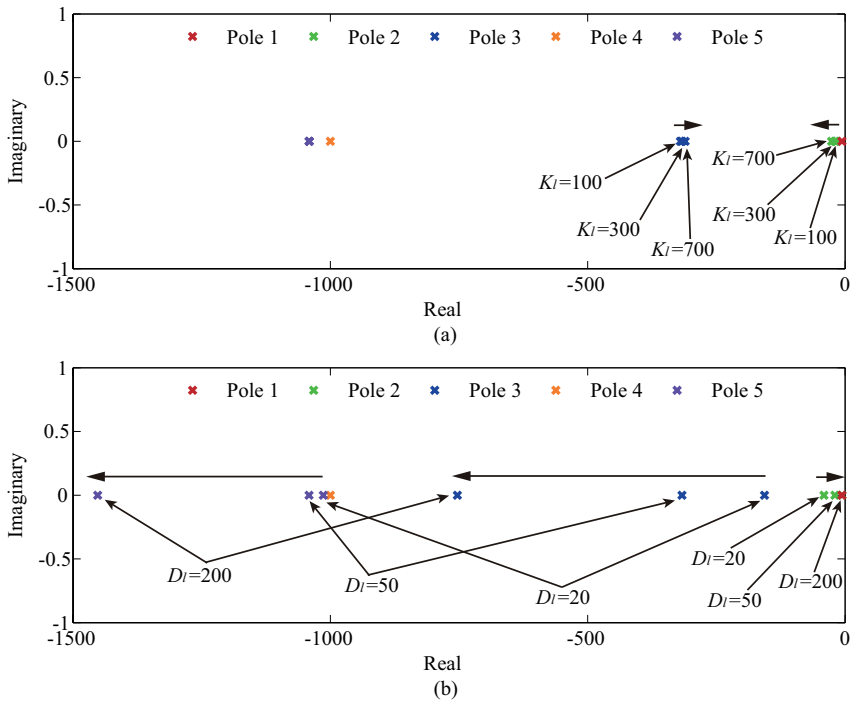

Fig. 3.52. The actual pole placement in the experiment. (a) Transition of the stiffness K_ℓ (The experiment of Fig. 3.50) (b) Transition of the damper D_ℓ (The experiment of Fig. 3.51)

3.1.6 Improvement of Force Reproducibility for Motion-Copying System

3.1.6.1 Introduction

In recent years, information and communication technology has been continuously grown. The current information technology treats acoustic information and visual information such as JPEG documents, mp3 files and video files and so on. The acoustic and visual information are considered in the practical techniques. However, the human has five organs, which recognize acoustic, visual, olfactory, gustatory and haptic information. Therefore, the information technology should treat residual information in order to provide realistic environment in the distant place.

In this thesis, the haptic information is considered. The acquisition method of the human motion based on visual information has been proposed [29]–[31]. However, these methods are not able to obtain the force information between the human and the environment. In addition, the abstraction method of human motion using the force information is proposed [33]. The hybrid control which treats both the force information and the position information has been proposed [34]–[35]. However, treatment of the haptic information in the real-world is not considered in the research. Though the method using virtual environment was proposed [72], the error of environmental model might be induced.

In addition, motion-copying system has been proposed [38]. The motion-copying system stores the motion of the human operator. Moreover, the motion-copying system is able to reproduce not only position but also force without mathematical model of the environment. Therefore, the motion-copying system can imitate the human motion.

However, the force reproduced by the motion-copying system is not corresponding to the stored force due to performance of force controller included in the motion-copying system. Thus, the force reproducibility of the conventional motion-copying system should be improved. Consequently, this thesis proposes the novel motion-copying system which the force reproducibility is enhanced. In addition, the force reproducibility of the proposed motion-copying system is compared to the conventional one by using three evaluation methods.

This research is organized as follows. In 3.1.6.2, control scheme of the conventional motion-copying system is explained. The acceleration observer which is capable of estimating acceleration response is explained in 3.1.6.3. In 3.1.6.4, improved force controller with acceleration observer is described. The novel motion-copying system proposed in this thesis is mentioned in 3.1.6.5. In 3.1.6.6, evaluation method for the motion-copying system is explained. Subsection 3.1.6.7 concludes this research.

3.1.6.2 Conventional Motion-Copying System

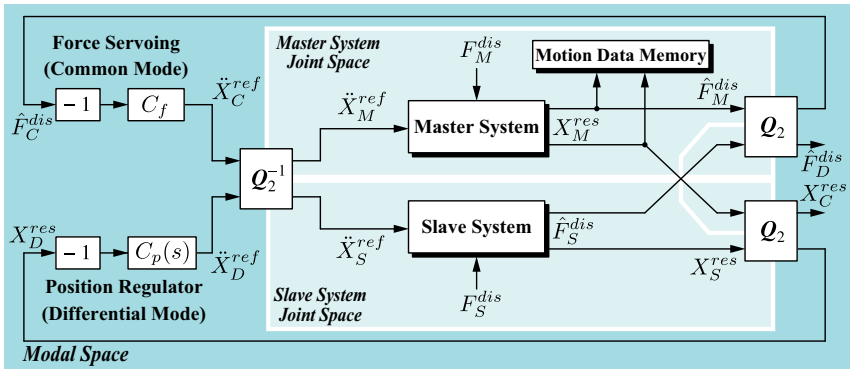

(a) Motion-Saving System

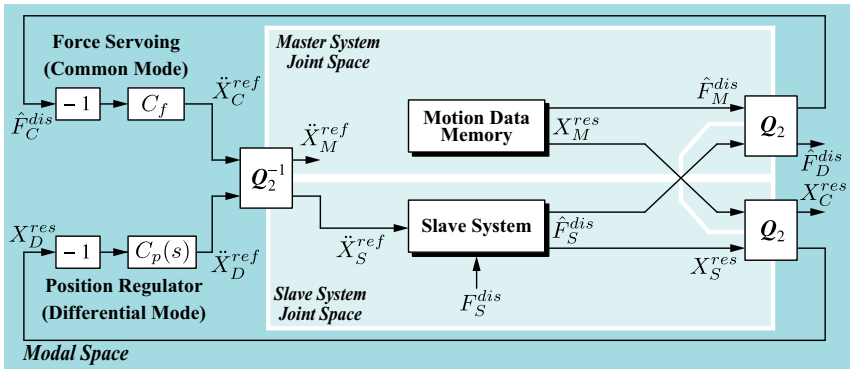

(b) Motion-Loading System

Fig. 3.53. Conventional Motion-Copying System

Fig. 3.53 shows block diagram of the motion-copying system, which can store and reproduce

motion of human operator. F, X, and $\ddot{X}$ represent force, position, and acceleration, respectively. The superscripts res, dis, and ref mean response, disturbance, and reference. The subscripts M, S, C, and D are master, slave, common mode, and differential mode. The motion-copying system consists of the motion-saving system shown in Fig. 3.53(a) and the motion-loading system shown in Fig. 3.53(b). In this section, control scheme of the motion-copying system is briefly described.

Motion-Saving System In Fig. 3.53(a), the disturbance observers [66] which estimate and reject the disturbance force are implemented in the master system and the slave system. The force and position responses of the actuators are transformed into modal space by using second order quarry matrix $\boldsymbol{Q}_2$ [65, 63] defined as

$$\boldsymbol{Q}_2 = \frac{1}{2}\begin{bmatrix} 1 & 1 \\ 1 & -1 \end{bmatrix}. \tag{3.48}$$

After that, force controller and position regulator calculate acceleration references in modal space. The force controller C_f and the position regulator $C_p(s)$ are given by

$$C_f = K_{fp} \tag{3.49}$$

$$C_p(s) = K_{pp} + \frac{sg_{pd}}{s + g_{pd}} K_{pd} \tag{3.50}$$

where K_{fp}, K_{pp}, K_{pd}, and g_{pd} denote gain of the force controller, proportional gain, differential gain of the position regulator, and bandwidth of pseudo derivative. Using inverse quarry matrix $\boldsymbol{Q}_2^{-1}$, the acceleration references calculated by the controllers are transformed into joint space. Finally, the actuators in master side and slave side are operated by the acceleration references in joint space.

At the same time, the motion data memory stores the force and position responses in the master side. By this means, the motion-saving system is constructed.

Motion-Loading System Basically, control method of the motion-loading system is almost same as the control method of the motion-saving system. However, the motion data memory is

used in the master side instead of the real master system. The motion data memory outputs the stored force and position responses. Thus, the motion of the human operator can be reproduced by the motion-loading system.

Issue However, the conventional motion-copying system cannot reproduce normally the human motion, if the operator conducts very fast free motion. In concrete terms, the reproduced force is not corresponding to the stored force. This thesis considers the issue of the reproduction. Since the force reproducibility is considered, the force controller in the modal space is examined in this section.

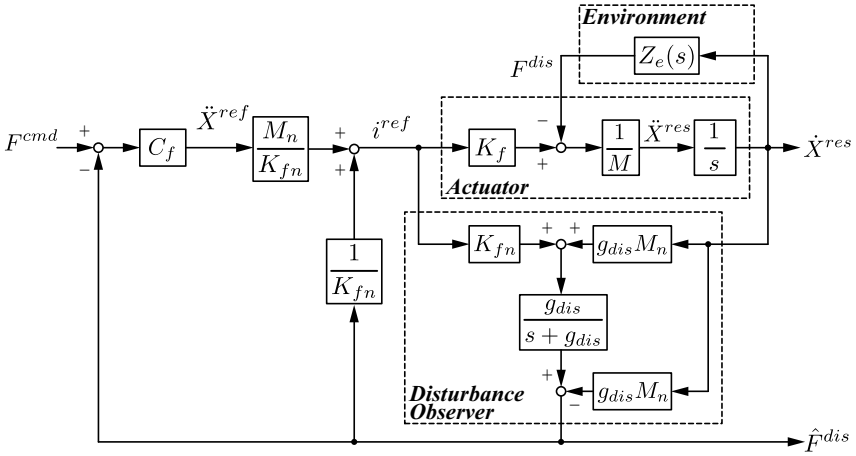

Fig. 3.54. Block diagram of force controller.

Fig. 3.54 shows the block diagram of the force controller. K_f, M, g_{dis}, and $Z_e(s)$ represent force constant, mass, bandwidth of the disturbance observer, and environmental mechanical impedance, respectively. The subscript n means nominal value. In Fig. 3.54, position response X^{res} can be calculated as

$$X^{res}=\left[\left\{\left(F^{cmd}-\hat{F}^{dis}\right)C_f\frac{M_n}{K_{fn}}+\frac{\hat{F}^{dis}}{K_{fn}}\right\}K_f-F^{dis}\right]\frac{1}{Ms^2} \tag{3.51}$$

where F^{cmd} denote force command. In case that bandwidth of disturbance observer g_{dis} is very large, $K_{fn}=K_f$, and $M_n=M$, the force command is expressed as

$$F^{cmd} = \hat{F}^{dis}+\frac{1}{C_f}s^2X^{res}. \tag{3.52}$$

Thus, the force response cannot follow the force command as follows:

$$F^{cmd} \neq \hat{F}^{dis}. \tag{3.53}$$

If C_f is set to large value, second term of right side member in Eq. (3.52) disappear. However, the force gain C_f is limited depending on effect of mechanical systems such as inertia of the actuators. Therefore, C_f cannot be set to large value. Using the acceleration response, the rejection of the right side member in Eq. (3.52) is carried out as follows:

$$\begin{aligned} F^{cmd} &= \hat{F}^{dis} + \frac{1}{C_f} s^2 X^{res} - \frac{1}{C_f} \ddot{X}^{res} \\ F^{cmd} &= \hat{F}^{dis}. \end{aligned} \tag{3.54}$$

By this method, the force controller can be improved.

3.1.6.3 Acceleration Observer

As mentioned above, to improve the force reproducibility, measurement of the acceleration response is required. However, acceleration sensor would not be used because of cost. In addition, the second order pseudo derivative of position response might be available. However, since second order LPF is implemented in the pseudo derivative, phase shift related to stability is also large. Consequently, this thesis uses acceleration observer, which is able to estimate the acceleration response.

Estimation Method In Fig. 3.54, using acceleration reference $\ddot{X}^{ref}$ and estimated force $\hat{F}^{dis}$, the acceleration response $\ddot{X}^{res}$ is derived as

$$\ddot{X}^{res} = \ddot{X}^{ref} - \frac{s}{g_{dis} M} \hat{F}^{dis}. \tag{3.55}$$

To reduce influence of noise and configure bandwidth of the acceleration observer, first order LPF is implemented. Thus, estimated acceleration response $\hat{\ddot{X}}^{res}$ is given by

$$\hat{\ddot{X}}^{res} = \left(\ddot{X}^{ref} - \frac{s}{g_{dis} M_n} \hat{F}^{dis} \right) \frac{g_{acc}}{s + g_{acc}} \tag{3.56}$$

where g_{acc} denote bandwidth of the acceleration observer. However, Eq. (3.56) includes derivation of estimated force. To prevent derivation, Eq. (3.56) is rewritten to

$$\hat{\ddot{X}}^{res} = \left(\ddot{X}^{ref} + \frac{g_{acc}}{g_{dis} M_n} \hat{F}^{dis} \right) \frac{g_{acc}}{s + g_{acc}} - \frac{g_{acc}}{g_{dis} M_n} \hat{F}^{dis}. \tag{3.57}$$

The acceleration observer based on Eq. 3.57 is constructed. Fig. 3.55 shows block diagram of

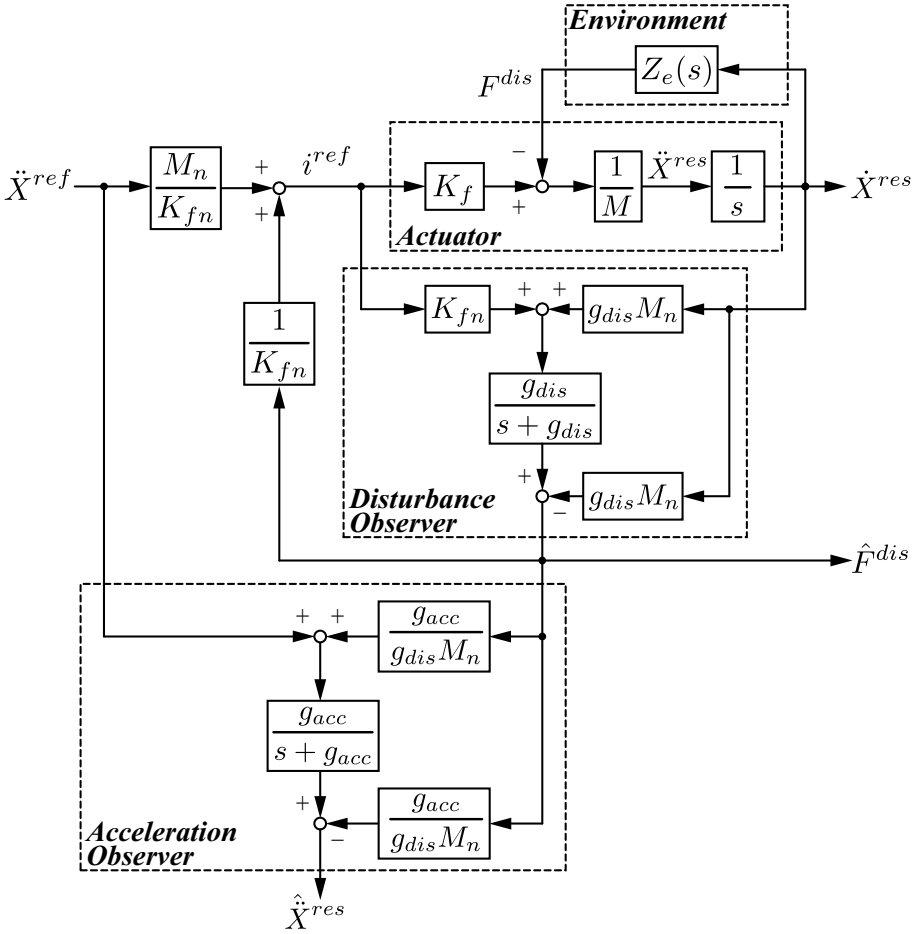

Fig. 3.55. Block diagram of acceleration observer.

the actuator, the disturbance observer, and the acceleration observer. In this situation, the acceleration response estimated by the observer is expressed as

$$\hat{\ddot{X}}^{res} = \frac{g_{acc}}{s + g_{acc}} \ddot{X}^{res}. \tag{3.58}$$

In Eq. (3.58), environmental mechanical impedance $Z_e(s)$ disappear. Therefore, acceleration observer is not depending on influence of the environmental characteristics. Moreover, transfer function from the acceleration response to the estimated acceleration is equal to first order LPF. On the other hand, in the case of the pseudo derivative, acceleration response from the pseudo derivative $\hat{\ddot{X}}_{pd}^{res}$ is expressed as

$$\begin{aligned} \hat{\ddot{X}}_{pd}^{res} &= \frac{s^2 g_{acc}^2}{s^2 + 2g_{acc}s + g_{acc}^2} X^{res} \\ &= \frac{g_{acc}}{s + g_{acc}} \frac{g_{acc}}{s + g_{acc}} \ddot{X}^{res}. \end{aligned} \tag{3.59}$$

In other words, compared with the pseudo derivative, the number of order of the observer and phase shift can be decreased.

By this means, using the acceleration reference and the estimated force, the acceleration observer is able to estimate the acceleration response without sensor.

Experiment The experiment is carried out to verify validity of the acceleration observer. The actuator is controlled by position regulator with acceleration control using the disturbance observer. The position command X^{cmd} is set to sinusoidal wave as follows:

$$X^{cmd} = X_{max} \sin \omega t. \tag{3.60}$$

Therefore, theoretical ideal value of acceleration response is derived as

$$\begin{aligned} \ddot{X}_{ideal}^{res} &= \frac{d^2}{dt^2} X^{res} = \frac{d^2}{dt^2} X_{cmd} \\ &= -\omega^2 X_{max} \sin \omega t. \end{aligned} \tag{3.61}$$

In this experiment, the acceleration response from the observer is compared to the ideal value of acceleration.

Fig. 3.56 shows experimental results. The acceleration observer is capable of calculating the acceleration response. The phase shift of the acceleration observer is smaller than the pseudo derivative. By the experiment, the validity of the acceleration observer is verified.

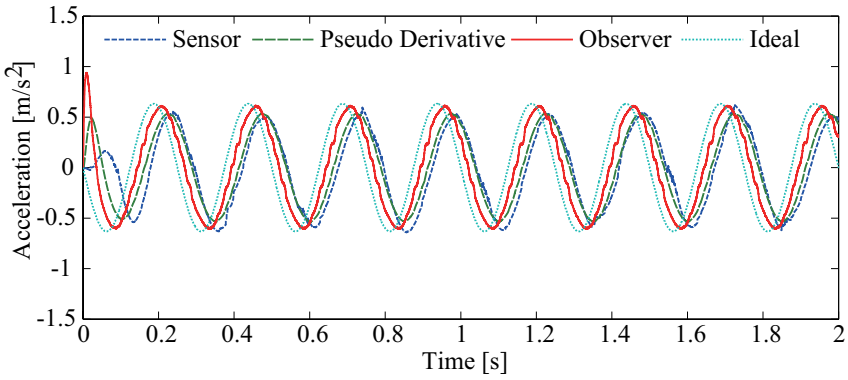

Fig. 3.56. Experimental results of acceleration observer.

3.1.6.4 Force Controller with Acceleration Observer

The improvement method for the force controller using the acceleration observer is explained in this section.

Improvement In the force controller shown in Fig. 3.54, the acceleration reference is calculated as

$$\ddot{X}^{ref} = \left(F^{cmd} - \hat{F}^{dis}\right) C_f. \tag{3.62}$$

As mentioned in section 3.1.6.2, effect of second term of right side member in Eq. (3.52) appears. In order to achieve the rejection as shown in Eq. (3.54), novel acceleration reference for improvement $\tilde{\ddot{X}}^{ref}$ is calculated as

$$\begin{aligned} \tilde{\ddot{X}}^{ref} &= \left\{F^{cmd} - \left(\hat{F}^{dis} - \frac{1}{C_f}\hat{\ddot{X}}^{res}\right)\right\} C_f \\ &= \ddot{X}^{ref} + \hat{\ddot{X}}^{res}. \end{aligned} \tag{3.63}$$

As a result, the actuator is operated by the novel acceleration reference. By this method, Eq. (3.54) is able to be realized.

Stabilization However, the force controller become unstable because of the rejection shown in Eq. (3.63). Thus, in order to prevent unstable operation, the acceleration reference is calculated

as

$$\tilde{\ddot{X}}^{ref} = \ddot{X}^{ref} + \hat{\ddot{X}}^{res} - \beta \frac{g_{hpf}}{s + g_{hpf}} \dot{X}^{res} \tag{3.64}$$

where β and g_{hpf} represent damping factor and bandwidth of HPF for stabilization. In short, the damping effect is artificially injected at high-frequency region, so that total system become stable. Since operation of the damper is limited by the HPF, degradation of performance of the force controller is prevented. The improved force controller based on Eq. (3.64) is shown in

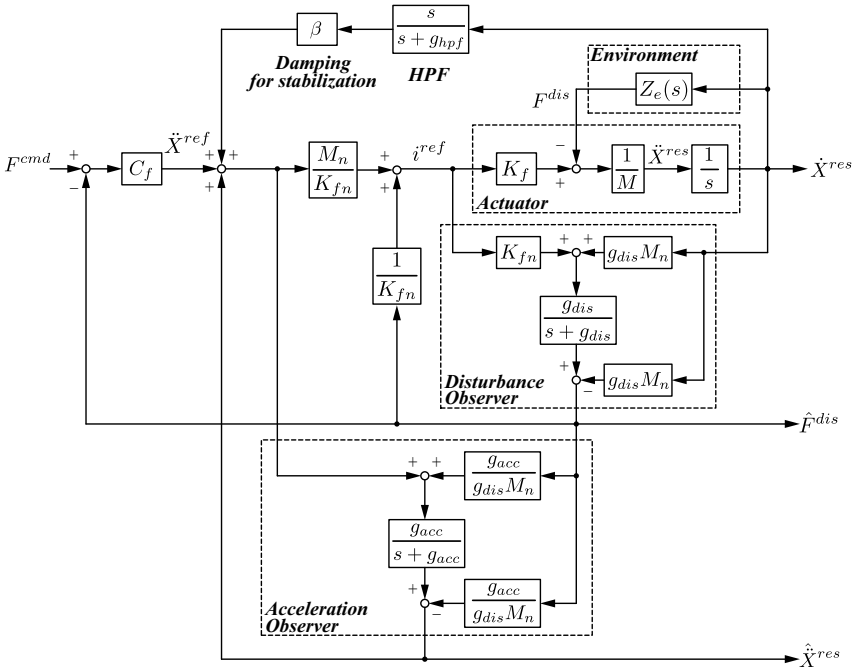

Fig. 3.57. Block diagram of improved force controller.

Fig. 3.57.

Experiment In order to verify validity of the improved force controller shown in Fig. 3.57, the experiment is conducted. In this experiment, the force command F_{cmd} is set to 0 N, and human operator moves the linear actuator. The respective parameters are set as follows; the gain of force controller $C_f = 1.5$; the damping factor $\beta = 80$; the each bandwidth $g_{dis} = g_{acc} = g_{hpf} = 1000$ rad/s.

Figs. 3.58 and 3.59 show the experimental results of force controller and improved force

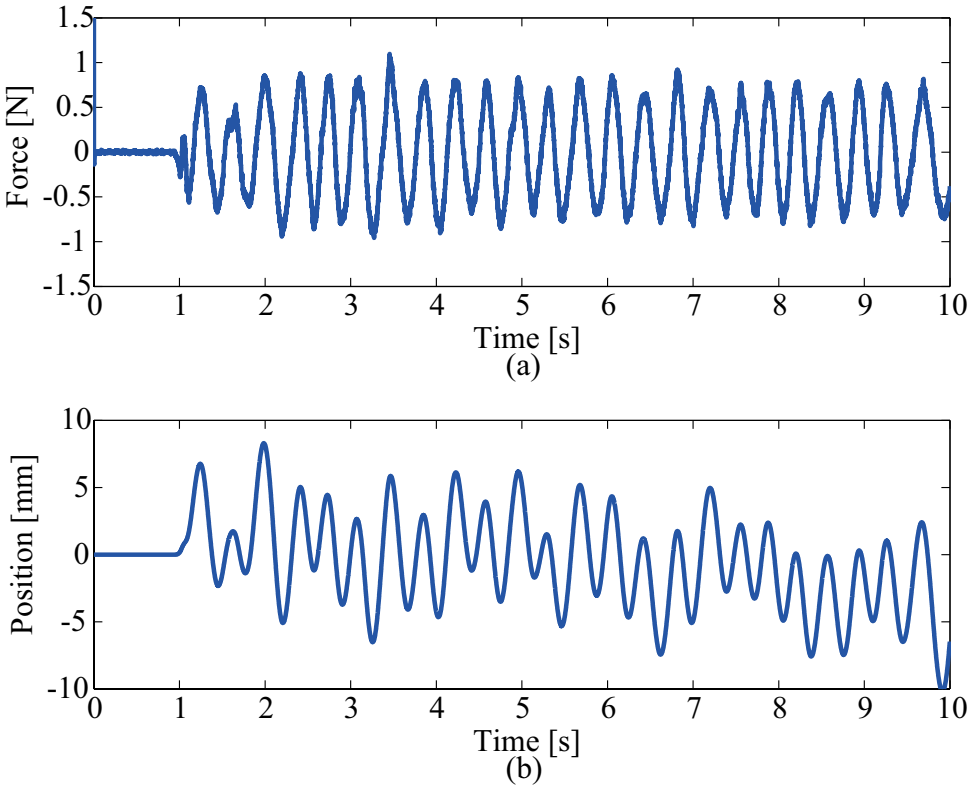

Fig. 3.58. Experimental results of force controller.

controller. The undesired force occurs in the case of normal force controller. On the other hand, the force response of the improved force controller is roughly 0. Therefore, the force response follows the force command.

3.1.6.5 Proposed Motion-Copying System

This thesis proposes the novel motion-copying system. The improved force controller as mentioned in previous section is applied to the novel motion-copying system, so that the force reproducibility is enhanced.

Motion-Saving System Fig. 3.60(a) shows block diagram of the proposed motion-saving system. In the proposed motion-saving system, the motion data memory stores the acceleration

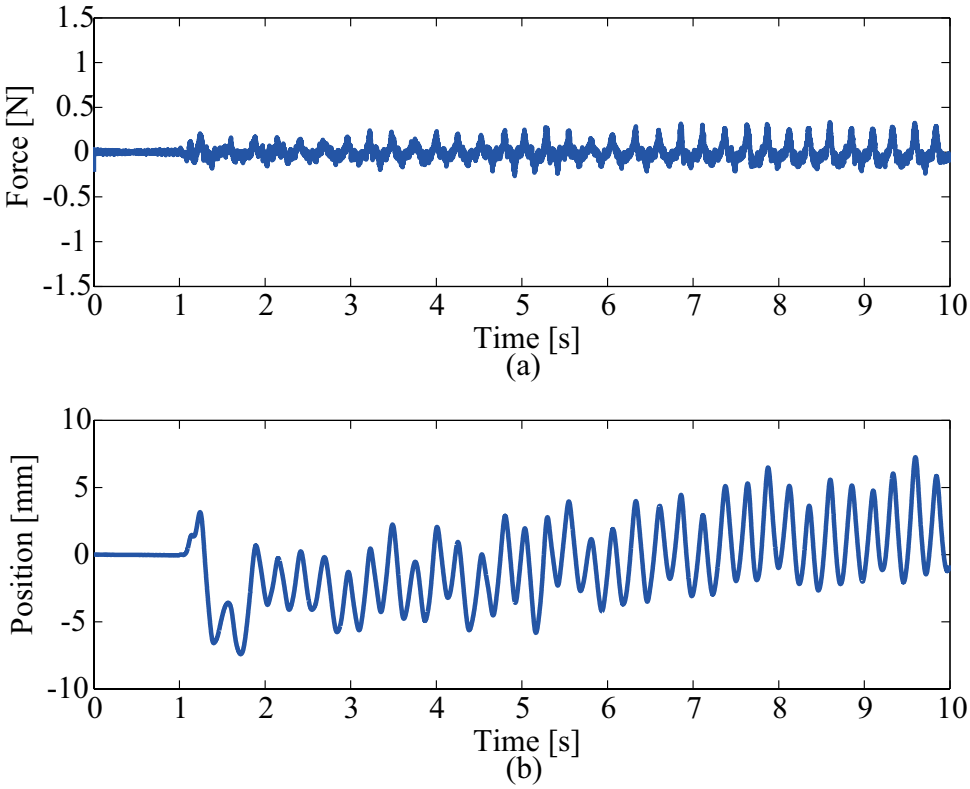

Fig. 3.59. Experimental results of improved force controller.

response as well as the force response and the position response as follows:

$$M_F[n] = \hat{F}_M^{dis}[n] \tag{3.65}$$

$$M_X[n] = X_M^{res}[n] \tag{3.66}$$

$$M_{\ddot{X}}[n] = \hat{\ddot{X}}_M^{res}[n] \tag{3.67}$$

$$(n = 1, 2, \cdots, N_n)$$

where M_F, M_X, and $M_{\ddot{X}}$ mean the motion data memory. n and N_n are discrete time and length of discrete time. As with the force and the position, the acceleration responses of master $\hat{\ddot{X}}_M^{res}$ and of slave $\hat{\ddot{X}}_S^{res}$ is transformed into the modal space by using quarry matrix. Thus, the acceleration responses of common mode $\hat{\ddot{X}}_C^{res}$ and of differential mode $\hat{\ddot{X}}_D^{res}$ is given by

$$\begin{bmatrix} \hat{\ddot{X}}_C^{res} \\ \hat{\ddot{X}}_D^{res} \end{bmatrix} = \boldsymbol{Q}_2 \begin{bmatrix} \hat{\ddot{X}}_M^{res} \\ \hat{\ddot{X}}_S^{res} \end{bmatrix}. \tag{3.68}$$

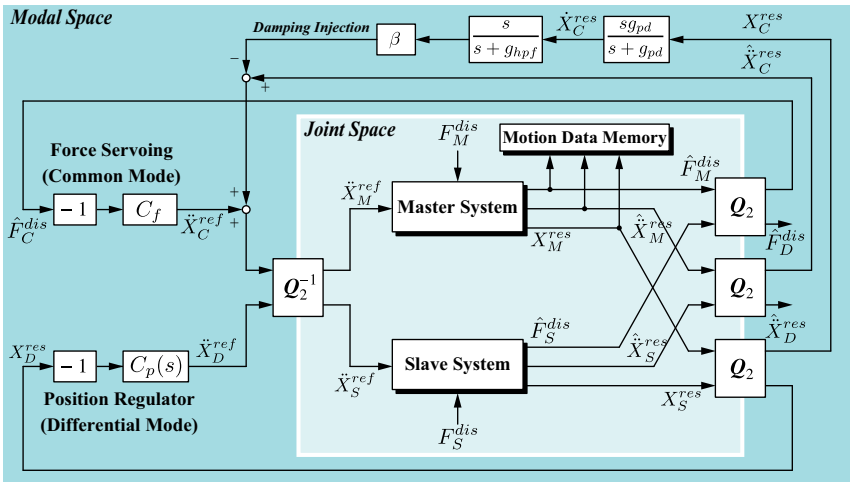

(a) Block diagram of proposed motion-saving system.

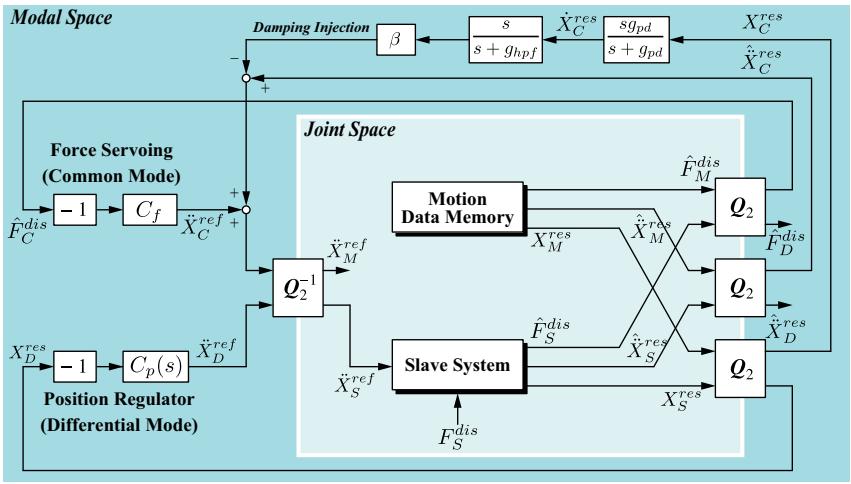

(b) Block diagram of proposed motion-loading system.

Fig. 3.60. Motion-copying system proposed in this thesis.

In order to enhance the force reproducibility and stabilize the system, the acceleration reference of common mode is newly calculated as

$$\tilde{\ddot{X}}_C^{ref} = \ddot{X}_C^{ref} + \hat{\ddot{X}}_C^{res} - \beta \frac{g_{hpf}}{s+g_{hpf}} \frac{s g_{pd}}{s+g_{pd}} X_C^{res}. \tag{3.69}$$

In other words, force controller in the modal space is able to be improved.

Motion-Loading System Fig. 3.60(b) shows block diagram of the proposed motion-saving system. Fundamentally, the control method is almost equal to the control method of the motion-saving system. However, the motion data memory is implemented in the master side instead of the actuator in the master system. The motion data memory provides the force response, the position response, and the acceleration response depending on the discrete time as follows:

$$\hat{F}_M^{dis}[n] = M_F[n] \tag{3.70}$$

$$X_M^{res}[n] = M_X[n] \tag{3.71}$$

$$\hat{\ddot{X}}_M^{res}[n] = M_{\ddot{X}}[n] \tag{3.72}$$

$$(n = 1, 2, \cdots, N_n)$$

In short, the motion data memory reproduces and imitates the human motion, which was stored by the motion-saving system. At the same time, the proposed system uses the acceleration response stored in the motion data memory in order to enhance the force reproducibility.

Experiment Figs. 3.61 and 3.62 show the experimental results of the conventional motion-copying system and the proposed motion-copying system. In the case of the conventional system, the reproduced force is not corresponding to the stored force. Thus, the reproduction of human motion cannot be realized. On the other hand, the force reproduced by the proposed motion-copying system is corresponding to the stored one. By the experiment, validity of the proposed method is verified.

3.1.6.6 Evaluation of Force Reproducibility

In this section, three evaluation methods which provide indicators of force reproducibility are described. The force reproducibility represents performance of the motion-copying system.

Correlation Coefficient One of the evaluation methods calculates correlation coefficient between stored force and reproduced force. The correlation coefficient of the force ρ is able to be

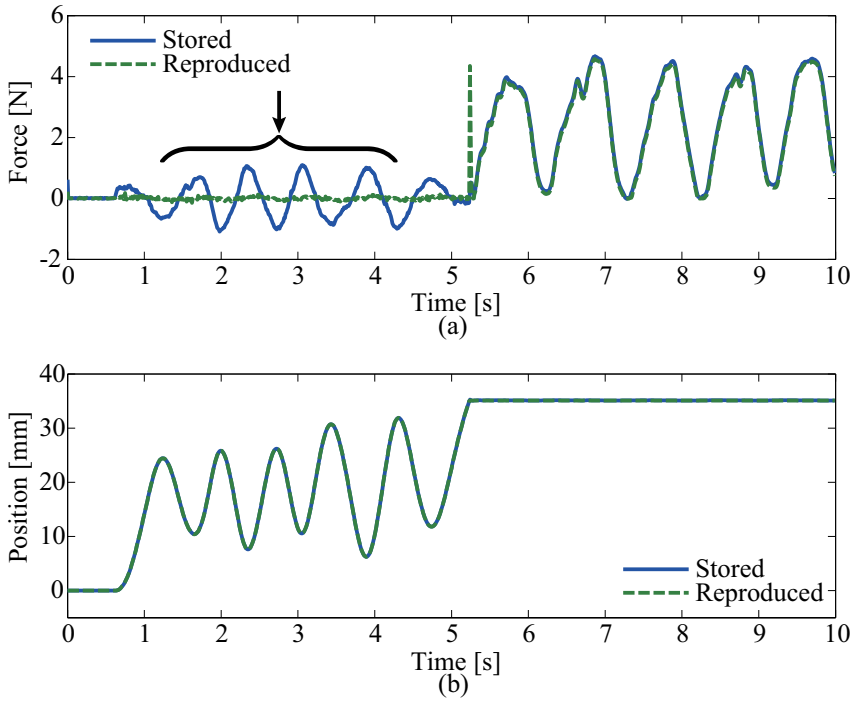

Fig. 3.61. Experimental results of conventional motion-loading system.

calculated as

$$\rho = \frac{\sum_{n=0}^{N_n} \left(\hat{F}_M^{dis}[n] - \overline{\hat{F}}_M^{dis} \right) \left(\hat{F}_S^{dis}[n] - \overline{\hat{F}}_S^{dis} \right)}{\sqrt{\sum_{n=0}^{N_n} \left(\hat{F}_M^{dis}[n] - \overline{\hat{F}}_M^{dis} \right)^2} \sqrt{\sum_{n=0}^{N_n} \left(\hat{F}_S^{dis}[n] - \overline{\hat{F}}_S^{dis} \right)^2}} \tag{3.73}$$

where $\overline{\hat{F}}^{dis}$ means average value of the force. In the conventional motion-copying system, the correlation coefficients of force is calculated as

$$\rho = 0.970. \tag{3.74}$$

On the other hand, the correlation coefficients of the proposed motion-copying system is calculated as

$$\rho = 0.999. \tag{3.75}$$

Therefore, compared with the conventional motion-copying system, this evaluation method confirms that the force reproducibility of the proposed system was improved.

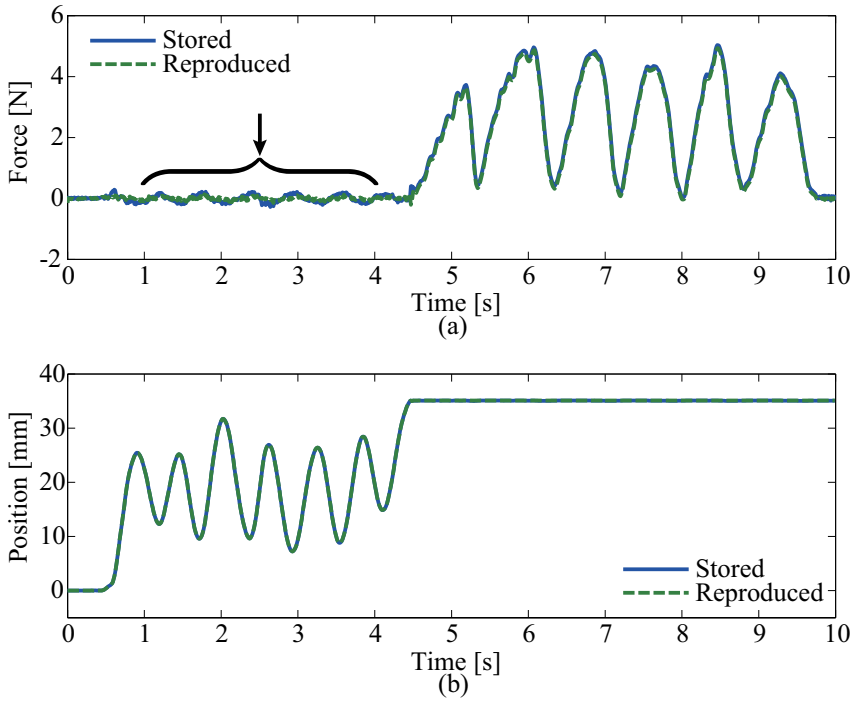

Fig. 3.62. Experimental results of improved motion-loading system.

Power Spectrum Density In order to evaluate performance of the motion-copying systems, this thesis uses power spectrum density. The force in the time domain $\hat{F}^{dis}$ is transformed into the force in the frequency domain Φ by using DFT as follows:

$$\Phi[k] = \sum_{n=1}^{N_n} \hat{F}^{dis}[n] \exp\left\{\frac{-j2\pi(k-1)(n-1)}{N_n}\right\} \tag{3.76}$$

where n, k, and N_n represent discrete time, frequency, and number of data. The power spectrum density P_d is calculated as

$$P_d[k] = \frac{\Phi[k]\Phi^*[k]}{N_n} \tag{3.77}$$

where superscript $*$ means complex conjugate. Using the power spectrum density, the force reproducibility in the frequency domain is able to be expressed.

Figs. 3.63 and 3.64 show the power spectrum density of the conventional motion-copying system and the proposed motion-copying system. In this evaluation, the calculated power spectrum density confirmed that the force reproducibility increased around 100 rad/s.

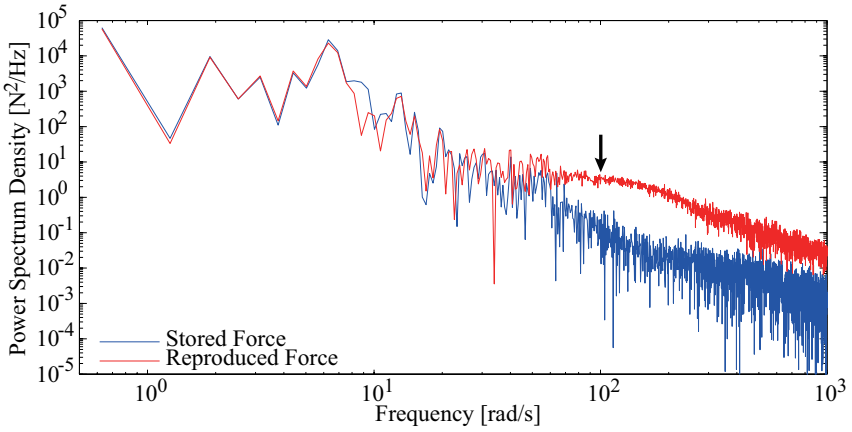

Fig. 3.63. Power spectrum density (conventional).

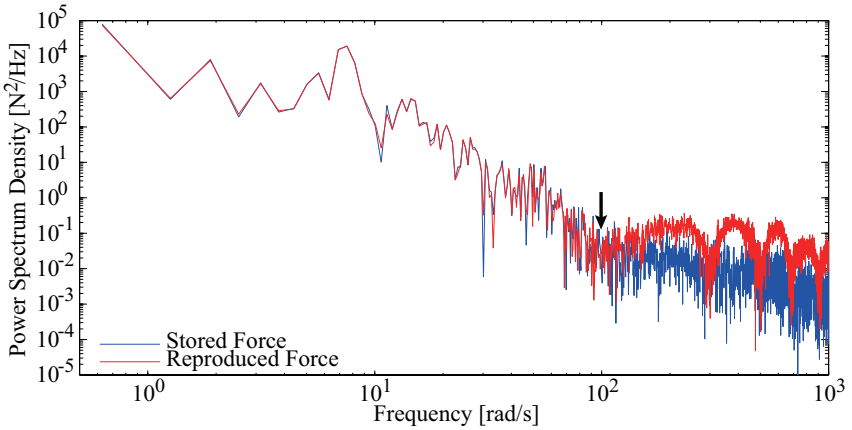

Fig. 3.64. Power spectrum density (proposed).

Histogram of Force Error Besides, this thesis utilizes evaluation method using histogram of force error for the motion-copying system. At first, error of force F_{err} is calculated as

$$F_{err}[n] = F_M^{dis}[n] - F_S^{dis}[n]. \tag{3.78}$$

Secondly, quantized force error e is given by

$$e[n] = \begin{cases} \left\lfloor \frac{F_{err}[n]-F_{min}}{F_{max}-F_{min}} N_{div} + 0.5 \right\rfloor & (\ F_{err}[n] > 0\ ) \\ \left\lceil \frac{F_{err}[n]-F_{min}}{F_{max}-F_{min}} N_{div} - 0.5 \right\rceil & (\ F_{err}[n] \leq 0\ ) \end{cases} \tag{3.79}$$

where F_{max}, F_{min}, and N_{div} are maximum value of force, minimum value of force, and number of division, respectively. Finally, histogram H with respect to the force error is obtained by

$$H[e[n]] := H[e[n]] + \frac{1}{N_n} \quad (\ n = 1, 2, \cdots, N_n \ ). \tag{3.80}$$

The force reproducibility is able to be measured by peak value and shape of histogram. For example, ideal shape of histogram is expressed as

$$H[e[n]] = \begin{cases} 1 & (\ F_{err}[n] = 0 \ ) \\ 0 & (\ \text{otherwise} \ ) \end{cases} \tag{3.81}$$

In this case, the force reproducibility is obviously perfect. The histogram of the motion-copying

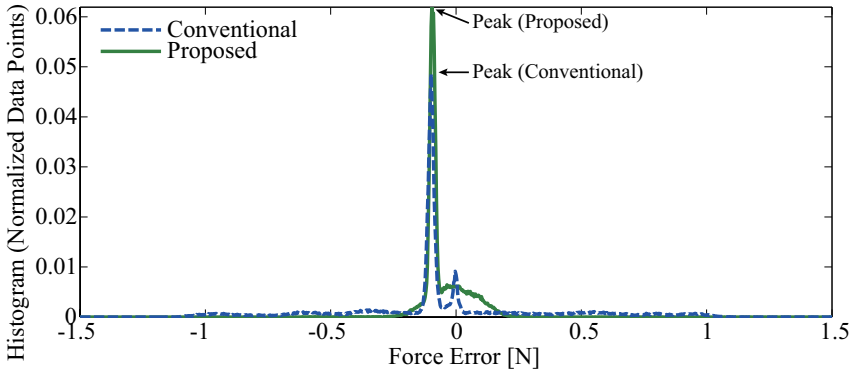

Fig. 3.65. Histogram of force error.

systems is shown in Fig. 3.65. In Fig. 3.65, peak of the histogram of the proposed system is higher than the conventional one. Moreover, Fig. 3.66 shows magnified figure of the histogram. In the case of the conventional motion-copying system, side lobe appears in a wide range. Therefore, compared with the conventional one, the histogram of the proposed motion-copying system is close to the ideal histogram. Hence, the evaluation method which utilizes the histogram of force error is able to verify validity of the proposed system.

3.1.6.7 Conclusion

This thesis proposed the novel motion-copying system. The motion-copying system proposed in this thesis used the acceleration response provided by the acceleration observer, so that the

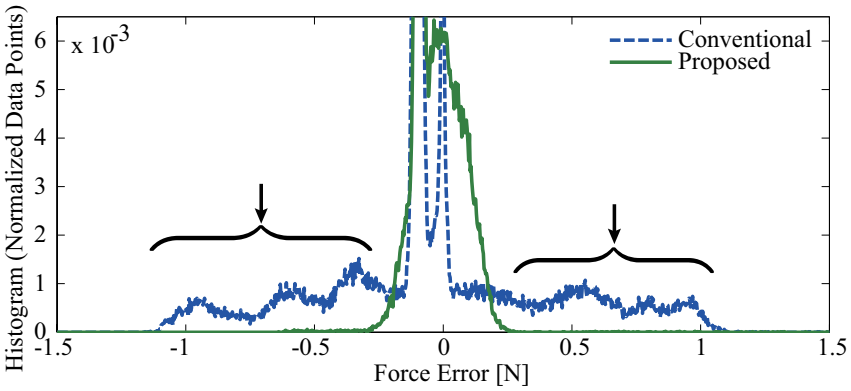

Fig. 3.66. Magnified figure of Fig. 3.65.

force reproducibility in the reproduction phase is improved. By the experiment, validity of the proposed method was verified. In addition, the force reproducibility was evaluated by using three evaluation methods. It will be useful for industrial applications, medical and welfare human support.

3.1.7 Construction of Motion Database using Motion-Copying System

3.1.7.1 Introduction

Practical database systems are available to handle text information. For example, insertion, updating, retrieval, and deletion of text are achieved by using a text database system. Moreover, the text database system is used in various systems in human society. In addition, auditory databases are also used, especially in voice synthesis. Image databases have also been researched and developed. However, since human has haptic organ as well as acoustic organs and visual organs, a practical system cannot treat haptic information. Consequently, this thesis proposes a motion database based on real-world haptics.

3.1.7.2 Concept of Motion Database System

Fig. 3.67 shows a conceptual diagram of a motion database system and an application system. On the application system side, a haptic device in the master side and haptic devices

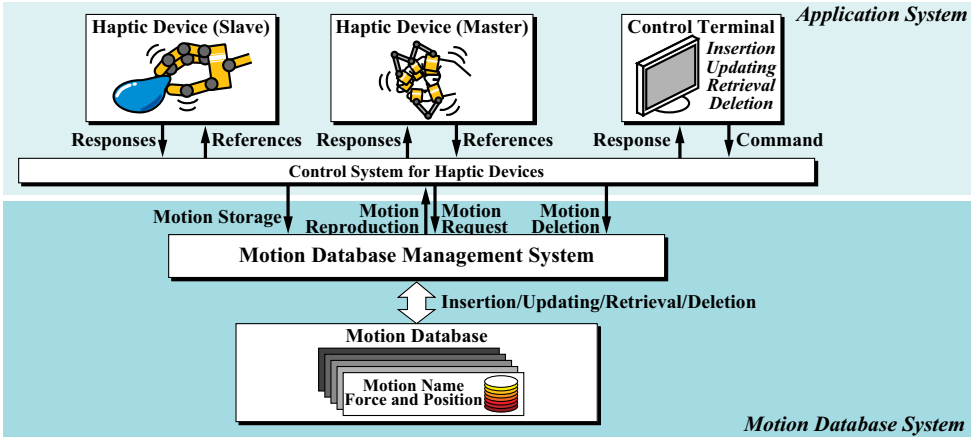

Fig. 3.67. Conceptual diagram of motion database system and control system.

in the slave side are controlled by the control system. The control system carries out various functions according to requests from the operator through the control terminal. Additionally, the requests from the control system on the application side is sent to the motion database system. The motion database system consists of a motion database management system and a motion database. The motion database is constructed and managed by the motion database

management system, which performs the tasks of inserting, updating, retrieving, and deleting information pertaining to human motion.

Fig. 3.68 shows structure of the motion database. In order to treat advanced types of haptic

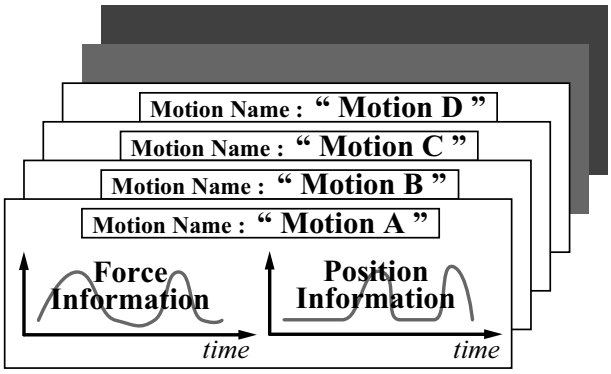

Fig. 3.68. Structure of motion database.

information, the motion database contains not only the name of motion and position trajectory of a human operator but also force information. The system proposed in this thesis is able to treat force information and position information.

3.1.7.3 Motion Control

Figs. 3.69 and 3.70 shows block diagram of the control system in the insertion phase and the retrieval phase. Fundamentally, the control method is same as the general motion-copying system. However, the motion database management system is implemented in the systems, so that the motion database management system performs the tasks of inserting, updating, retrieving, and deleting information pertaining to human motion.

3.1.7.4 Experiment

Figs. 3.71 and 3.73 show experimental results of motion insertion in the motion database. In this experiment, force responses and position responses are obtained by a reaction force observer and an encoder, respectively. Fig. 3.75 shows experimental results of motion retrieval. The reproduced force and the reproduced position are almost the same as those stored. In

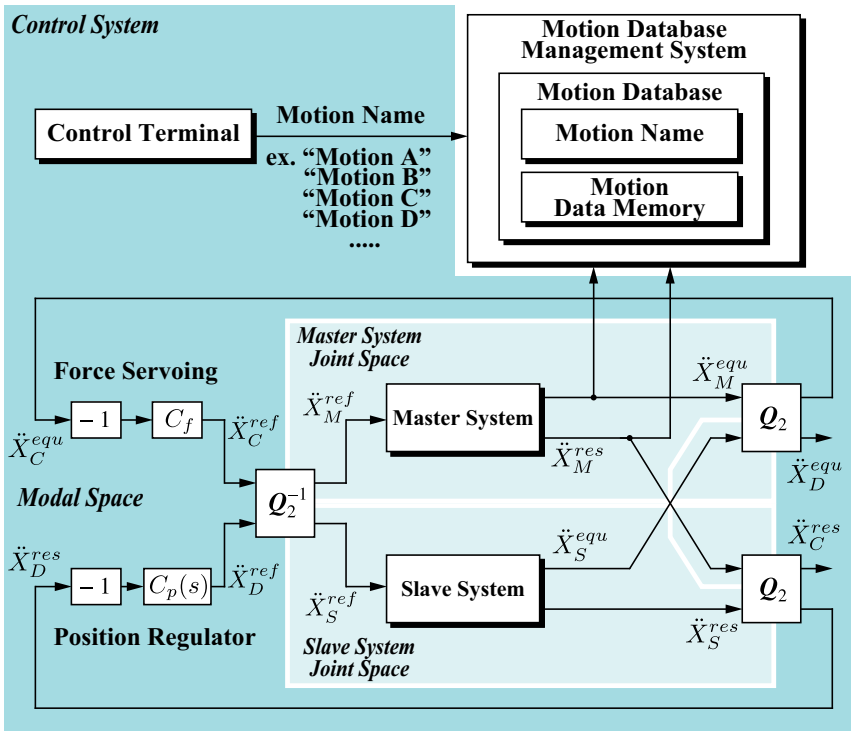

Fig. 3.69. Block diagram of motion insertion.

addition, the proposed system is able to accurately reproduce the motions A to D corresponding to the motion request.

3.1.7.5 Conclusion

In this research, the validity and feasibility of the proposed method are verified. By using the proposed method, the motion of a human operator in the industrial and medical fields is able to be stored, retrieved, and reproduced. The proposed method is expected to be useful in the industrial applications and for providing medical and human support to patients.

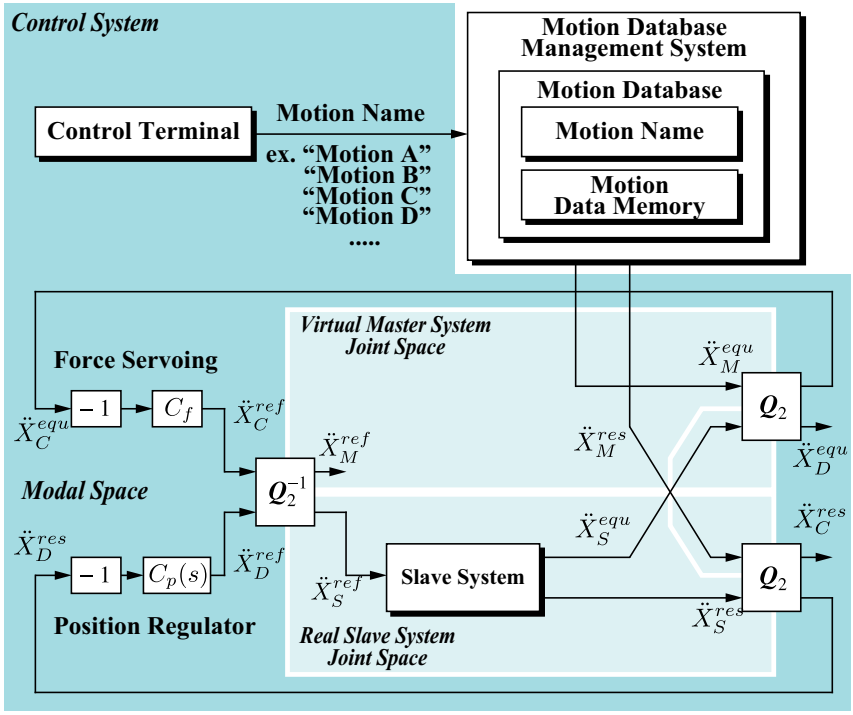

Fig. 3.70. Block diagram of motion retrieval.

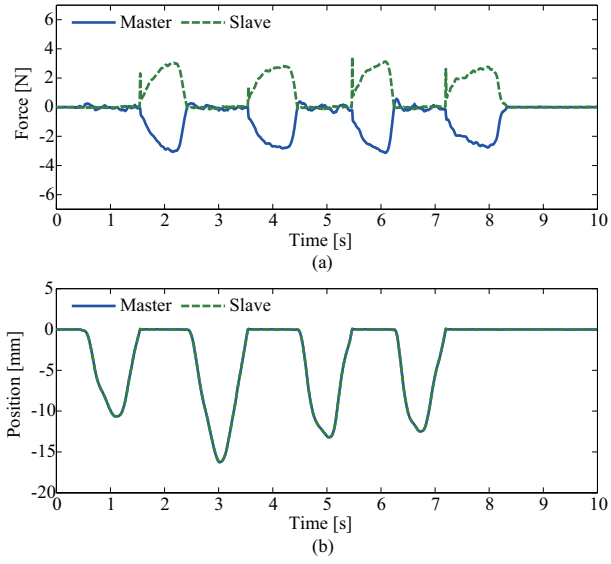

Fig. 3.71. Insertion of "Motion A."

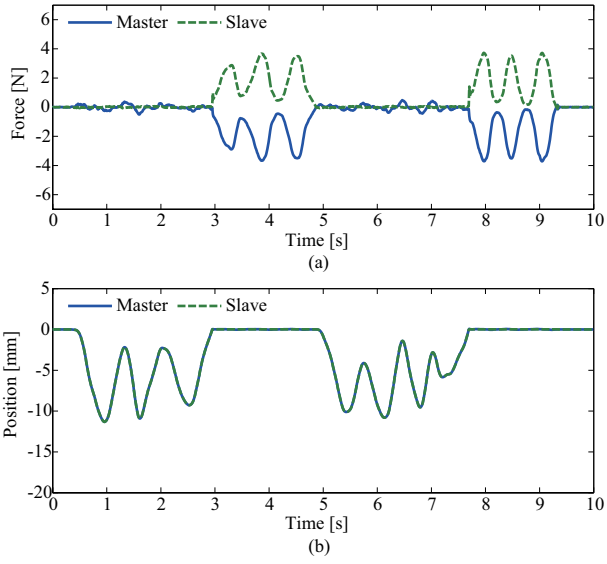

Fig. 3.72. Insertion of "Motion B."

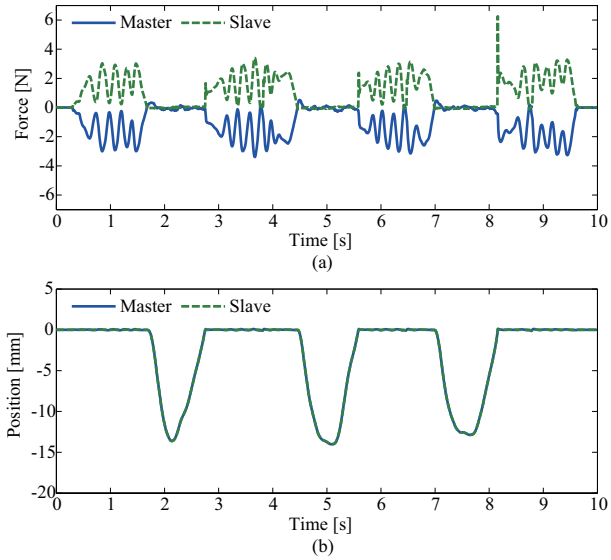

Fig. 3.73. Insertion of "Motion C."

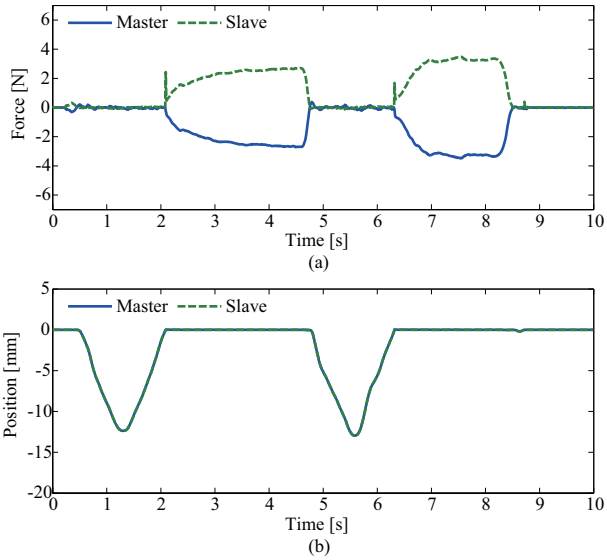

Fig. 3.74. Insertion of "Motion D."

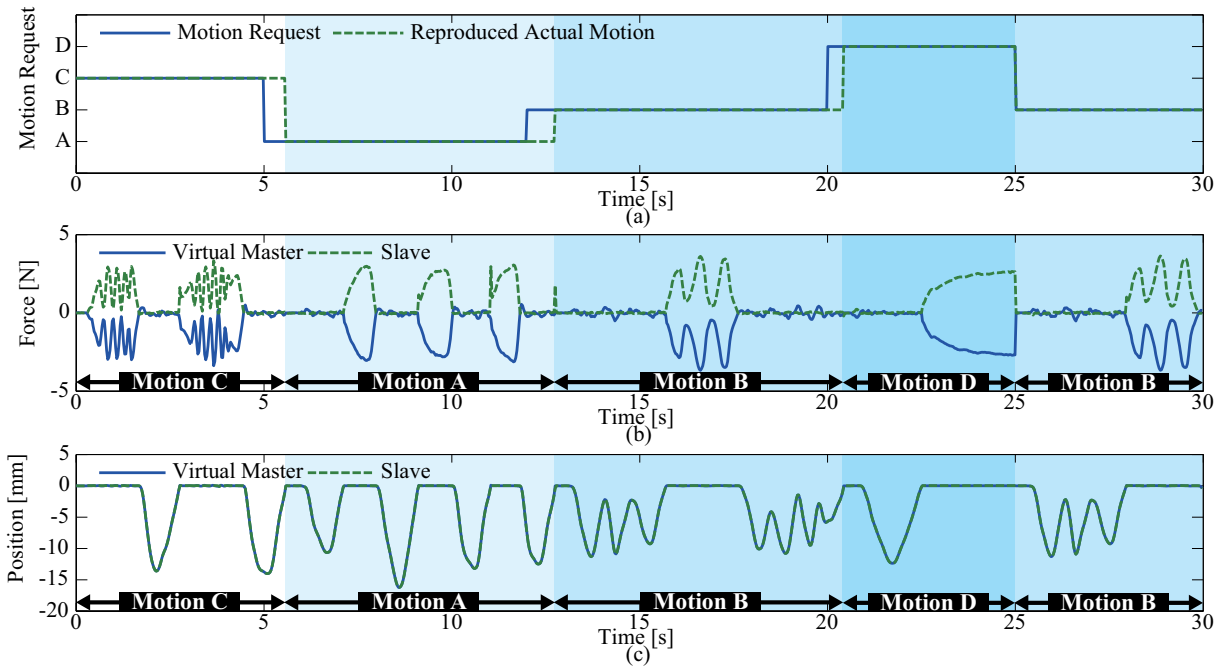

Fig. 3.75. Motion retrieval. (a) Motion request. (b) Force responses. (c) Position responses.

3.1.8 Motion-Copying System in Work Space

In order to store and reproduce complicated motion, the motion-copying system mentioned above is expanded. The control system of the motion-copying system in the previous subsection is operated in joint space. Therefore, the complicated human motion cannot be treated. In this subsection, the human motion is stored and reproduced in work space by using the extended motion-copying system.

3.1.8.1 Motion-Saving System

Fig. 3.76 shows block diagram of the motion-copying system in the work space. The torque

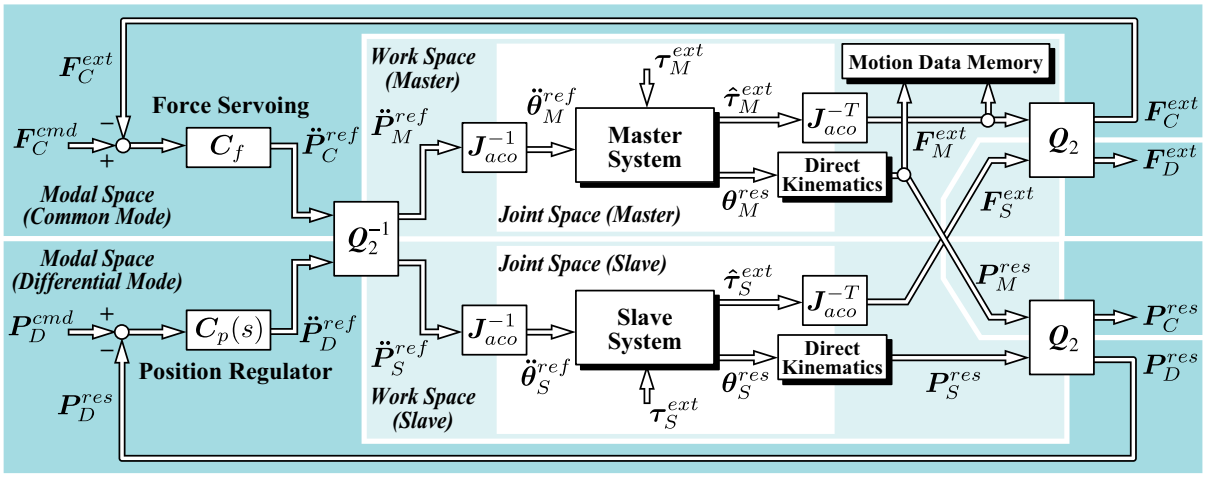

Fig. 3.76. Block diagram of motion-saving system.

responses in joint space $\hat{\boldsymbol{\tau}}^{ext} = \left[\hat{\tau}_1^{ext}\ \hat{\tau}_2^{ext}\ \cdots\ \hat{\tau}_N^{ext}\right]^T$ are transformed into force responses in work space $\boldsymbol{F}^{ext} = \left[F_X^{ext}\ F_Y^{ext}\ F_Z^{ext}\right]^T$ as follows:

$$\boldsymbol{F}^{ext} = \boldsymbol{J}_{aco}^{-T}\hat{\boldsymbol{\tau}}^{ext} \tag{3.82}$$

where $\boldsymbol{J}_{aco}^{-T}$ represents Jacobian matrix. In this thesis, number of joint is set as $N = 2$, and parallel link robot systems is used. Moreover, the thesis considers X–Y plane. Thus, the Jacobian matrix is derived as

$$\boldsymbol{J}_{aco} = \begin{bmatrix} -\ell\sin\theta_1 & -\ell\sin\theta_2 \\ \ell\cos\theta_1 & \ell\cos\theta_2 \end{bmatrix} \tag{3.83}$$

where θ_1 and θ_2 are angle of the link 1 and of the link 2, respectively. ℓ mean length of the each link. The angle of the actuators $\boldsymbol{\theta}^{res} = [\theta_1^{res}\ \theta_2^{res}\ \cdots\ \theta_N^{res}]^T$ are also transformed into the position in the work space $\boldsymbol{P}^{res} = [X^{res}\ \ Y^{res}\ \ Z^{res}]^T$ as follows:

$$\begin{bmatrix} X^{res} \\ Y^{res} \end{bmatrix} = \begin{bmatrix} \ell\cos\theta_1 + \ell\cos\theta_2 \\ \ell\sin\theta_1 + \ell\sin\theta_2 \end{bmatrix}. \tag{3.84}$$

In the next step, the force responses in the work space are transformed into the modal space by using the quarry matrix $\boldsymbol{Q}_2$ as follows:

$$\begin{bmatrix} {}^{C}F^{ext} \\ {}^{D}F^{ext} \end{bmatrix} = \boldsymbol{Q}_2 \begin{bmatrix} {}^{M}F^{ext} \\ {}^{S}F^{ext} \end{bmatrix} \tag{3.85}$$

where superscript of left side C and D mean the common mode and the differential mode. The superscript of left side M and S represent the master and the slave. The superscript ext is external force. In addition, the position responses in x-axis are are also converted to the position responses in the modal space

$$\begin{bmatrix} {}^{C}X^{res} \\ {}^{D}X^{res} \end{bmatrix} = \boldsymbol{Q}_2 \begin{bmatrix} {}^{M}X^{res} \\ {}^{S}X^{res} \end{bmatrix} \tag{3.86}$$

where superscript res means response. As with the x-axis, the position responses in y-axis and z-axis are transformed into the modal space. In this thesis, the each parameters are defined as $\boldsymbol{F}_C^{ext} = \left[{}^{C}F_X^{ext}\ {}^{C}F_Y^{ext}\ {}^{C}F_Z^{ext}\right]^T$, and $\boldsymbol{P}_D^{res} = \left[{}^{D}X^{res}\ \ {}^{D}Y^{res}\ \ {}^{D}Z^{res}\right]^T$.

In the modal space, the acceleration references $\ddot{\boldsymbol{P}}_C^{ref} = \left[{}^{C}\ddot{X}^{ref}\ \ {}^{C}\ddot{Y}^{ref}\ \ {}^{C}\ddot{Z}^{ref}\right]^T$ are calculated as

$$\ddot{\boldsymbol{P}}_C^{ref} = \boldsymbol{C}_f\left(\boldsymbol{F}_C^{cmd} - \boldsymbol{F}_C^{ext}\right) \tag{3.87}$$

where $\boldsymbol{C}_f$ represents the force controllers, which is expressed as

$$\boldsymbol{C}_f = \begin{bmatrix} K_{fX} & 0 & 0 \\ 0 & K_{fY} & 0 \\ 0 & 0 & K_{fZ} \end{bmatrix} \tag{3.88}$$

where K_{fX}, K_{fY}, and K_{fZ} are gain of the force controllers. The force command in the common mode is set as $\boldsymbol{F}_C^{cmd} = \boldsymbol{0}$. Additionally, the acceleration references in the differential mode $\ddot{\boldsymbol{P}}_D^{ref} = \left[{}^{D}\ddot{X}^{ref}\ \ {}^{D}\ddot{Y}^{ref}\ \ {}^{D}\ddot{Z}^{ref}\right]^T$ are calculated as

$$\ddot{\boldsymbol{P}}_D^{ref} = \boldsymbol{C}_p(s)\left(\boldsymbol{P}_D^{cmd} - \boldsymbol{P}_D^{res}\right) \tag{3.89}$$

where $\boldsymbol{C}_p(s)$ is position controllers, which is represented as

$$\boldsymbol{C}_p(s) = \begin{bmatrix} C_{pX}(s) & 0 & 0 \\ 0 & C_{pY}(s) & 0 \\ 0 & 0 & C_{pZ}(s) \end{bmatrix} \tag{3.90}$$

where $C_{pX}(s)$, $C_{pY}(s)$, and C_{pZ} are position controllers. In this thesis, the position controllers are PD controllers, and the position command in the differential mode is set as $\boldsymbol{P}_D^{cmd} = \boldsymbol{0}$.

The acceleration references in the modal space are transformed into the acceleration references in the work space $\ddot{\boldsymbol{P}}^{ref} = \begin{bmatrix} \ddot{X}^{ref} & \ddot{Y}^{ref} & \ddot{Z}^{ref} \end{bmatrix}^T$ as follows:

$$\begin{bmatrix} {}^M\ddot{X}^{ref} \\ {}^S\ddot{X}^{ref} \end{bmatrix} = \boldsymbol{Q}_2^{-1} \begin{bmatrix} {}^C\ddot{X}^{ref} \\ {}^D\ddot{X}^{ref} \end{bmatrix} \tag{3.91}$$

where superscript ref means reference. As with x-axis, the acceleration references in y-axis and z-axis are also converted. The acceleration references in the joint space $\ddot{\boldsymbol{\theta}}^{ref} = \begin{bmatrix} \ddot{\theta}_1^{ref} & \ddot{\theta}_2^{ref} & \cdots & \ddot{\theta}_N^{ref} \end{bmatrix}^T$ are calculated as

$$\ddot{\boldsymbol{\theta}}^{ref} = \boldsymbol{J}_{aco}^{-1} \ddot{\boldsymbol{P}}^{ref}. \tag{3.92}$$

The torque references $\boldsymbol{\tau}^{ref} = \begin{bmatrix} \tau_1^{ref} & \tau_2^{ref} & \cdots & \tau_N^{ref} \end{bmatrix}$ are calculated as

$$\boldsymbol{\tau}^{ref} = \boldsymbol{M}\left(\boldsymbol{\theta}^{res}\right) \ddot{\boldsymbol{\theta}}^{ref} + \boldsymbol{H}\left(\boldsymbol{\theta}^{res}, \dot{\boldsymbol{\theta}}^{res}\right) \tag{3.93}$$

where $\boldsymbol{M}$ represents inertia matrix, which is derived as

$$\boldsymbol{M}\left(\boldsymbol{\theta}^{res}\right) = \begin{bmatrix} \ell^2(m_1 + m_2) + J_n & \ell^2 m_2 \cos(\theta_2^{res} - \theta_1^{res}) \\ \ell^2 m_2 \cos(\theta_2^{res} - \theta_1^{res}) & \ell^2(m_1 + m_2) + J_n \end{bmatrix}. \tag{3.94}$$

where J_n represents nominal inertia of the each motors. $\boldsymbol{H}$ in the thesis is derived as

$$\boldsymbol{H}\left(\boldsymbol{\theta}^{res}, \dot{\boldsymbol{\theta}}^{res}\right) = \begin{bmatrix} -\ell^2 m_2 \dot{\theta}_2^{res^2} \sin(\theta_2^{res} - \theta_1^{res}) \\ \ell^2 m_2 \dot{\theta}_2^{res^2} \sin(\theta_2^{res} - \theta_1^{res}) \end{bmatrix} \tag{3.95}$$

where m_1 and m_2 are mass of tip of the each link. Finally, the current references of the each actuators $\boldsymbol{i}^{ref} = \begin{bmatrix} i_1^{ref} & i_2^{ref} & \cdots & i_N^{ref} \end{bmatrix}^T$ are calculated as

$$\boldsymbol{i}^{ref} = \boldsymbol{K}_{tn}^{-1} \boldsymbol{\tau}^{ref} \tag{3.96}$$

where $\boldsymbol{K}_{tn}$ means torque constant of the actuators. $\boldsymbol{K}_{tn}$ is expressed as

$$\boldsymbol{K}_{tn} = \begin{bmatrix} K_{tn1} & 0 & \cdots & 0 \\ 0 & K_{tn2} & \cdots & 0 \\ \vdots & \vdots & \ddots & \vdots \\ 0 & 0 & \cdots & K_{tnN} \end{bmatrix} \tag{3.97}$$

where K_{tn1} to K_{tnN} are nominal value of the torque constant. The respective actuators are controlled by the current references.

To store the motion of the human operator, the force and position responses are stored as follows:

$$\boldsymbol{M}_{DAT}[k] = \begin{bmatrix} \boldsymbol{F}_M^{ext}[k] \\ \boldsymbol{P}_M^{res}[k] \end{bmatrix} \qquad (k = 0, 1, 2, \cdots, N_k) \tag{3.98}$$

where $\boldsymbol{M}_{DAT}$, k, and N_k are the motion data memory, discrete time, and number of the motion data, respectively.

3.1.8.2 Motion-Loading System

Fig. 3.77 shows block diagram of the motion-loading system. Fundamentally, the control

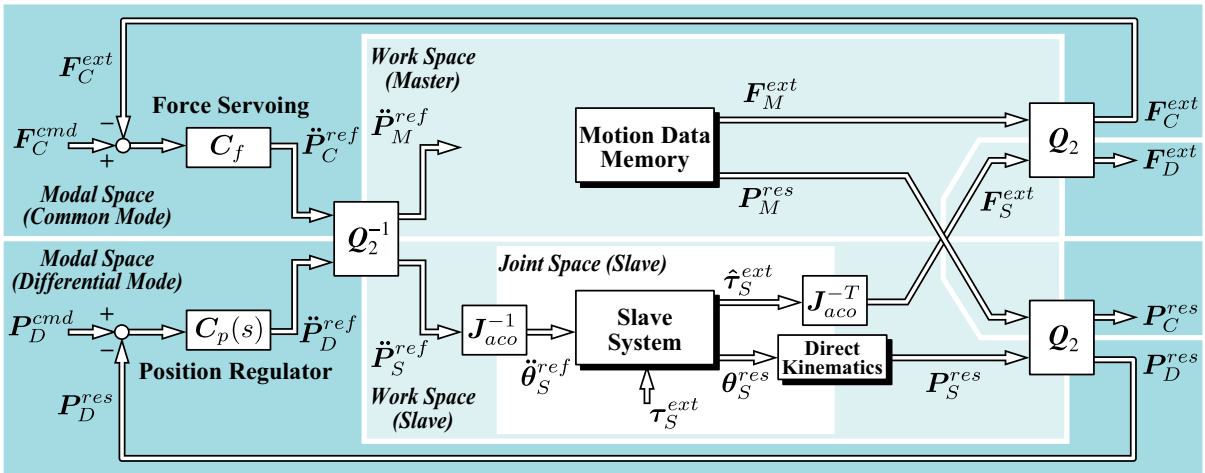

Fig. 3.77. Block diagram of motion-loading system.

method in the motion-loading system is almost same as the control system of the motion-saving system. However, the motion-loading system does not use the master system. The motion data memory is used instead of the actuators. In the motion-loading system, to reproduce the human

motion, the force and position in the master side is set as

$$\begin{bmatrix} \boldsymbol{F}_M^{ext}[k] \\ \boldsymbol{P}_M^{res}[k] \end{bmatrix} = \boldsymbol{M}_{DAT}[k] \qquad (k = 0, 1, 2, \cdots, N_k) \tag{3.99}$$

By this means, the storage and reproduction of the human motion is realized.

3.1.8.3 Experiment

Experimental Setup Fig. 3.78 shows model of the parallel link robot systems. Moreover,

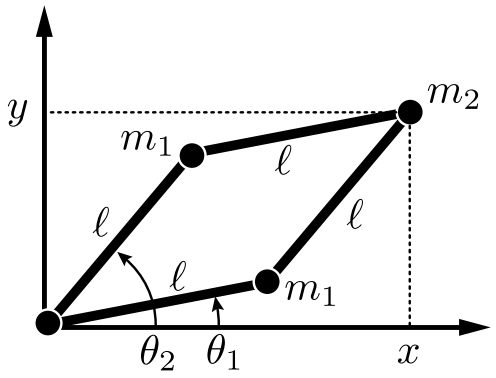

Fig. 3.78. Model of parallel link robot.

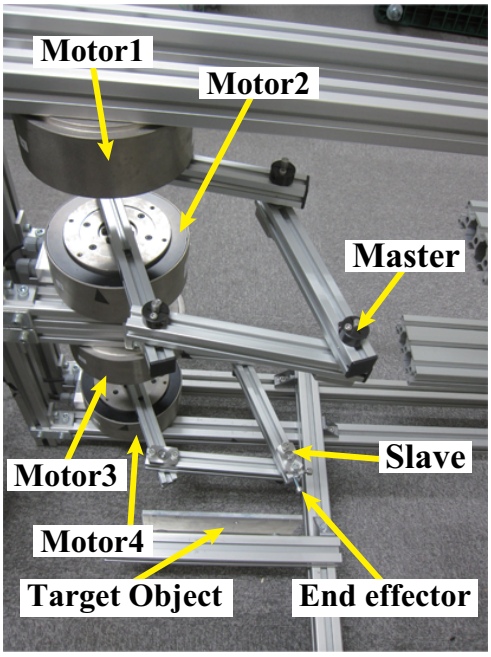

Fig. 3.79. Experimental setup.

Fig. 3.79 shows experimental setup. In the thesis, the systems consist of the 2 direct drive motors. The target object in the slave side is the aluminum plate. The plate is put on the slave side in the storage phase and reproduction phase.

Experimental Results The experimental results are shown in Fig. 3.80 and 3.81. In this experiment, the position trajectory of the end effector is normally reproduced. Additionally, the force reproduced by the motion-loading system is corresponding to the force stored by the motion-saving system. Therefore, this experimental results confirm that the motion-copying

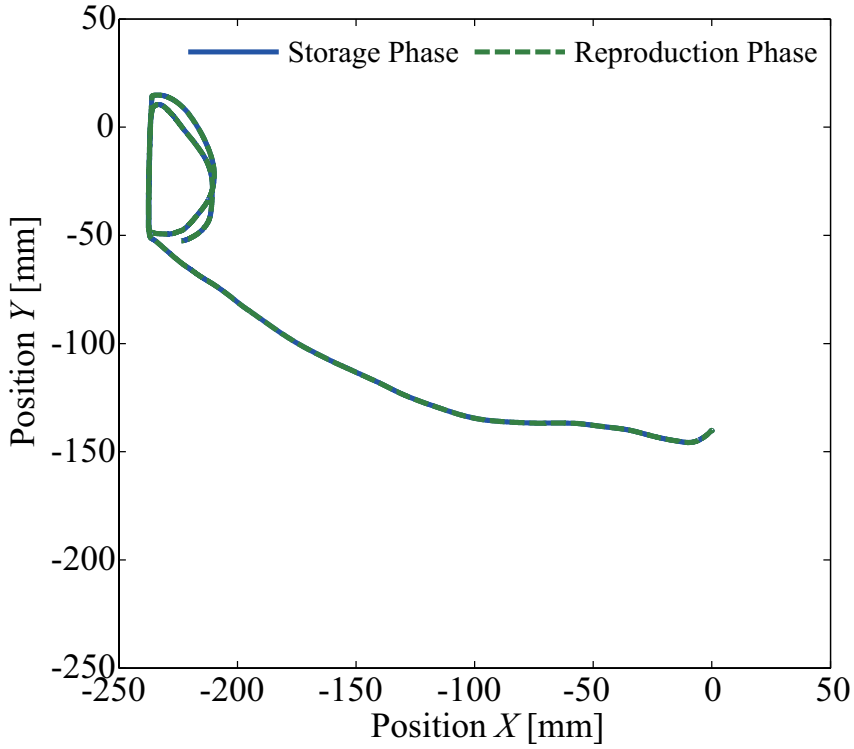

Fig. 3.80. Trajectory of storage phase and trajectory of reproduction phase.

system in the work space is able to store and reproduce the complicated motion of the human operators.

3.1.8.4 Conclusion

The thesis proposed the motion-copying system, which is capable of storing and reproducing the human motion in work space. By using the proposed method, complicated motion of the human operator is able to be treated because of multi-degree of freedom systems. In the experiment, the validity of the proposed motion-copying system was verified.

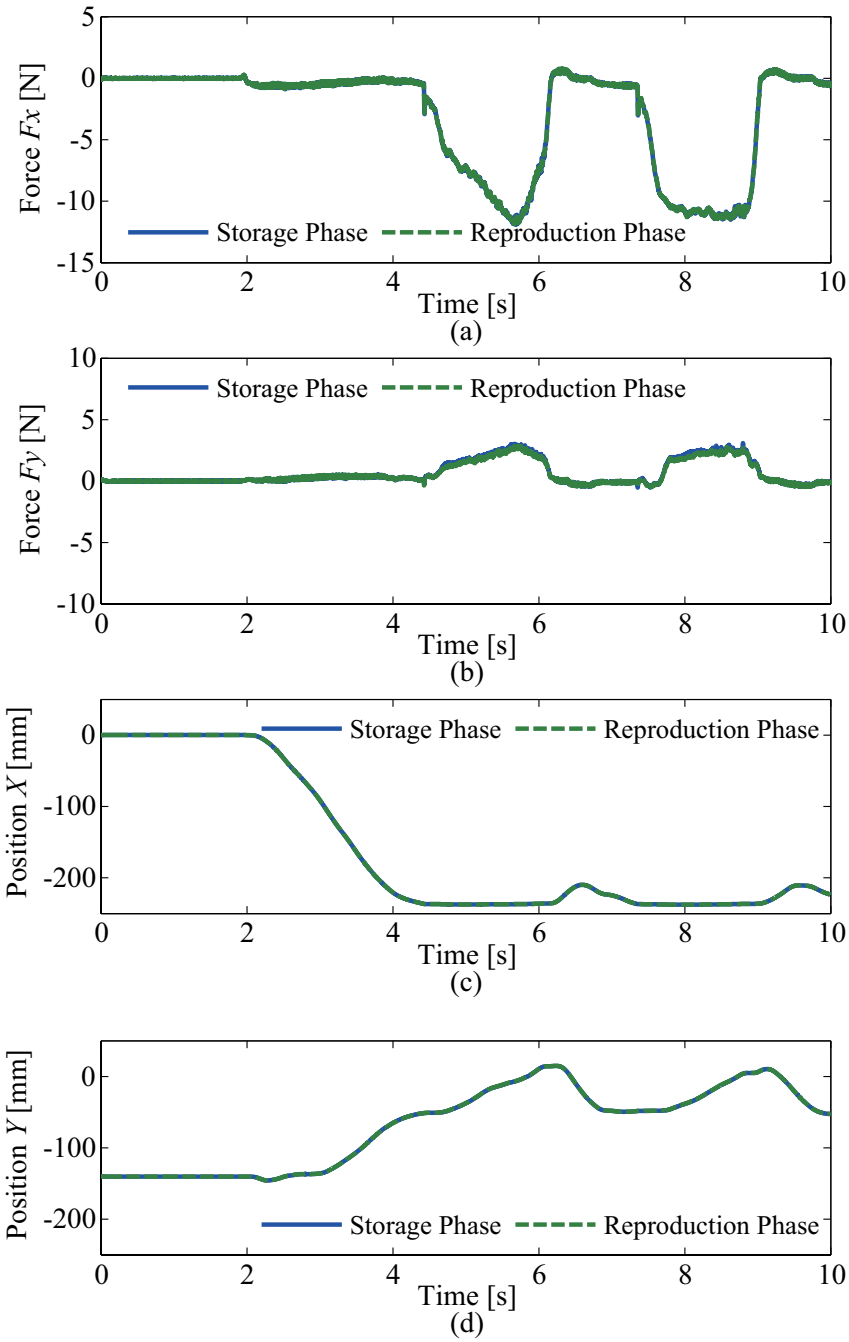

Fig. 3.81. Experimental results of motion-saving system and motion-loading system. (a) Force (X-axis). (b) Force (Y-axis). (c) Position (X-axis). (d) Position (Y-axis).

3.2 Environmental Copying System

3.2.1 Introduction

In recent years, electrical engineering, electronics, computer science, information and communication technology has been rapidly grown, so that information of the entire world can be provided to human. Fig. 3.82 shows storage and reproduction technology of acoustic informa-

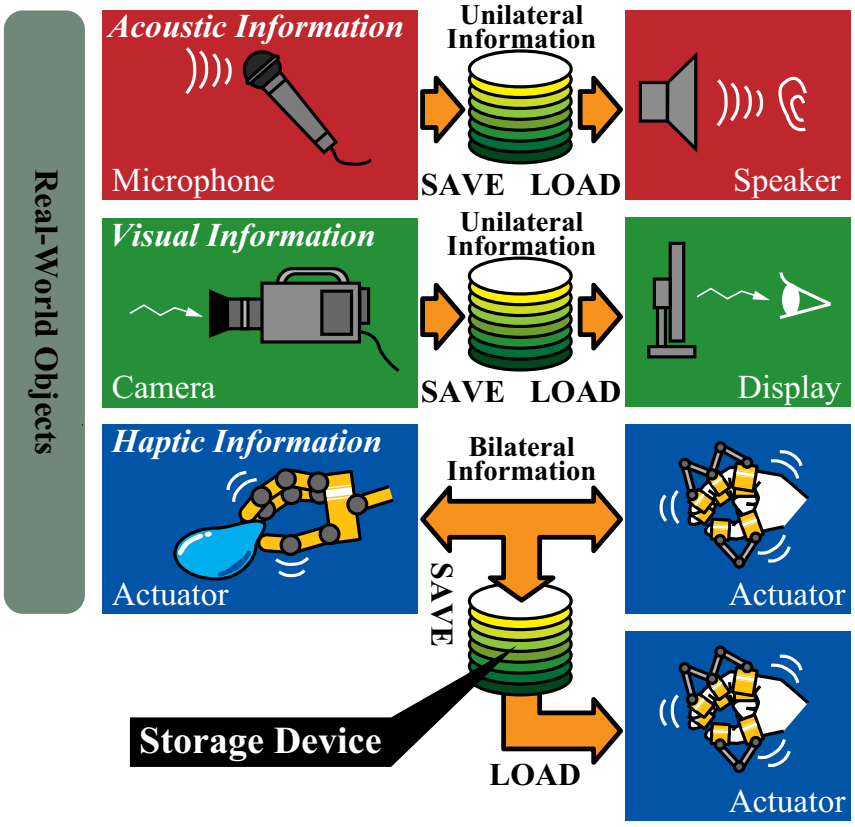

Fig. 3.82. Preservation and reproduction system of acoustic, visual and haptic information.

tion and of visual information. A microphone catches vibration of air and converts to electronic information. After that, the converted electronic signal which has the acoustic information is stored to the memory. Moreover, a speaker system reproduces the acoustic information according to sound data stored to storage device. In addition, video recorder/player, CD, MD, DVD, telephone and television provide acoustic information and/or visual information in the

real world. These are useful for communication devices between human and human. Additionally, sound radio and television are broadcasting environmental situation in the distant place based on acoustic and visual information.

However, the human has five organs. Though these are visual, auditory, olfactory, gustatory, and tactile organs, the practical broadcasting technology and recorder/player system are considering only two organs. In this situation, the conventional broadcasting technology and recorder/player system are not able to reproduce realistic remote environment. Therefore, the saving and loading system and communication technology should be expanding to treat haptic information by using novel scheme and techniques.

To realize the haptic communication and broadcasting system, compensation method of time delay which occurs in communication network is very important element. Since haptic information is bilateral information different from acoustic information and visual information, the haptic communication and broadcasting system are very sensitive to the time delay. The compensation method for the haptic communication has been proposed [89, 90, 91].

In addition, the storage system and the reproduce system for the haptic information should be considered along with the acoustic information and the visual information. The various methods for acquisition and/or reproduction of human motion are being researched. The research of motion acquisition based on visual information were developed [29]–[32]. However, the motion acquisition system by the visual information is not able to detect force. Therefore, it is hard to extract the human motion. Also, a method of obtaining the reaction force from environment using master-slave system was already proposed [33]. This method reproduces motion by recorded reaction force from environment. In addition, methods using a virtual-world environment [72] or hybrid control of position and force [34]–[35] has been proposed. Haptic camera has been proposed to obtain the impedance parameter of the contact environment [92]. However, the haptic camera obtains simply the value of the mechanical impedance. Additionally, the motion-copying system has been proposed [38]. The motion-copying system stores and reproduces the motion of human operator by using both environmental force response and position response. Though the

human motion of the human operator is able to be treated, the motion-copying system cannot provide the environmental haptic sensation.

Hence, this thesis proposes environmental copying system, which preserves and reproduces the haptic information of the environment. The environmental copying system proposed in this thesis realizes storage and reproduction of haptic information of environment in the real world, so that the human operator feels the environmental haptic sense. In other words, haptic sense of real-world objects is able to be provided freely beyond time and space.

This research is organized as follows. Subsection 3.2.2 explains concept of the environmental copying system. In 3.2.3, concept and motion control of the environmental saving system is presented. The concept and motion control system of environmental loading system is described in Section 3.2.4. The experimental result of the proposed method is shown in Section 3.2.5. The last subsection concludes this study.

3.2.2 Concept of Environmental Copying System

In this section, fundamental concept of the environmental copying system proposed in this thesis is explained.

The environmental copying system consists of two systems. The first system is the environmental saving system; the other system is the environmental loading system. The environmental saving system is operated by bilateral controller to measure the force between the master system and the slave system. Meanwhile, the environmental saving system stores the force response to the environmental data memory corresponding to the position response and the velocity response.

Additionally, the environmental loading system reproduces the force according to the environment data memory, which was generated by the environmental saving system, in order to provide haptic sense of the environment to the human operator in the master side.

By the proposed method, the human operator is able to feel the environmental sense beyond time and space without the environmental mathematical models.

3.2.3 Environmental Saving System

This section describes concept and motion control of the environmental saving system.

3.2.3.1 Concept

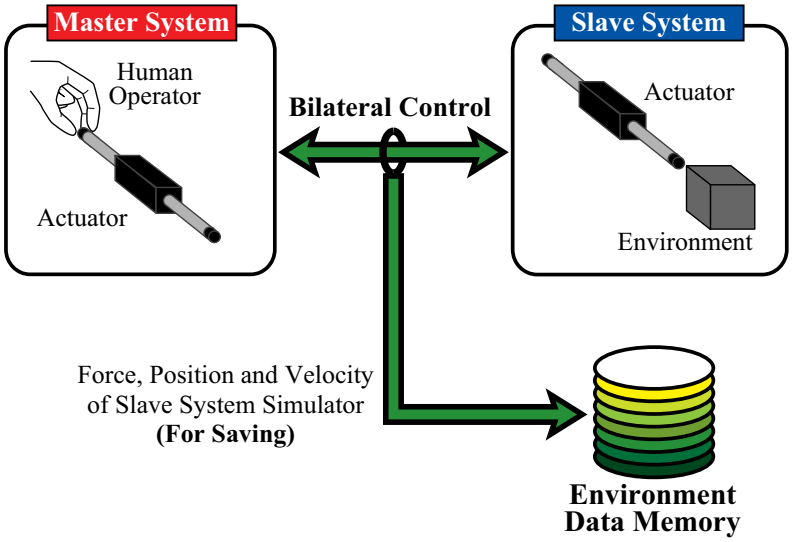

Fig. 3.83. Conceptual diagram of the environmental saving system.

Fig. 3.83 shows a conceptual diagram of the environmental saving system. The environmental saving system consists of a master system and a slave system, which are operated by a bilateral control. The bilateral controller utilized in this thesis generates artificially the law of action and reaction according to

$$F_M + F_S = 0 \tag{3.100}$$

where, F_M and F_S denote a force of the master system and a force of the slave system. The position of the master system and the position of the slave system are also synchronized by the controller.

$$x_M - x_S = 0 \tag{3.101}$$

where, x_M is position of the master, x_S is position of the slave. By this means, human operator which is in the master side is able to grasp sensation of environment in the slave side without environmental mathematical model.

In order to express the environmental characteristics of the slave side, the environmental saving system stores the force response, the velocity and the position response of a actuator in the slave side to a environment data memory during operation of the bilateral controller. The force information stored to the environment data memory is utilized, when the environmental loading system reproduces the environment.

3.2.3.2 Motion Control

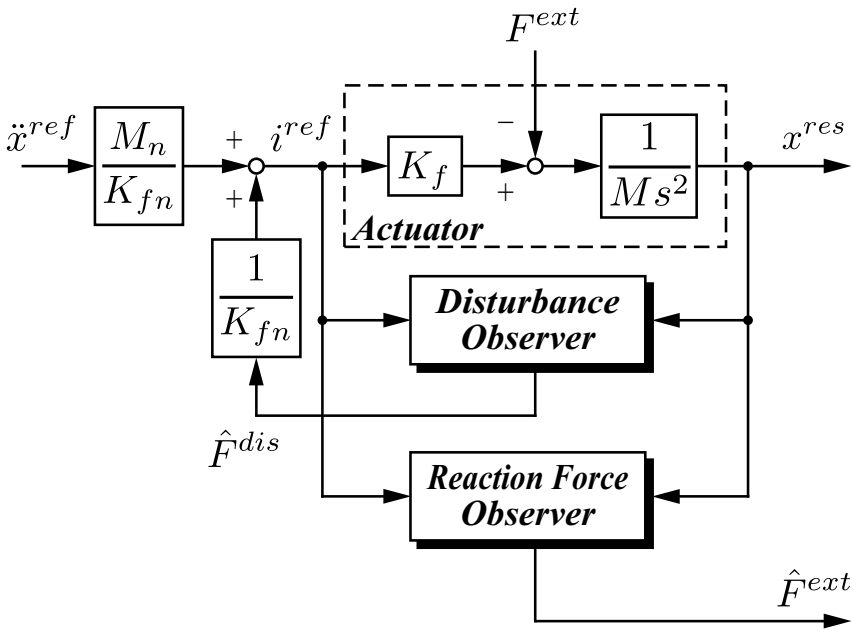

Fig. 3.84. Block diagram of the master system and the slave system.

Fig. 3.84 shows block diagram of the master and slave systems. M, M_n, K_f and K_{fn} in Fig. 3.84 are mass, nominal mass, force constant and nominal force constant of a actuator. $\ddot{x}^{ref}$ and F^{ext} denote acceleration reference and estimated reaction force. A disturbance observer calculates and compensates the disturbance force $\hat{F}^{dis}$, and realizes robust acceleration control [66]. A reaction force observer estimates reaction force $\hat{F}^{ext}$ using a position response x^{res} and current i^{ref} [64].

In this thesis, the bilateral control based on modal decomposition is utilized by quarry matrix

[65, 63]. The second-order quarry matrix is defined as

$$\boldsymbol{Q}_2 = \frac{1}{2}\begin{bmatrix} 1 & 1 \\ 1 & -1 \end{bmatrix}. \tag{3.102}$$

The quarry matrices of third-order or more higher-order which are utilized in multi-lateral control [93] has been also defined. Therefore, the proposed method in this thesis can be easily expanded to the multi-lateral control.

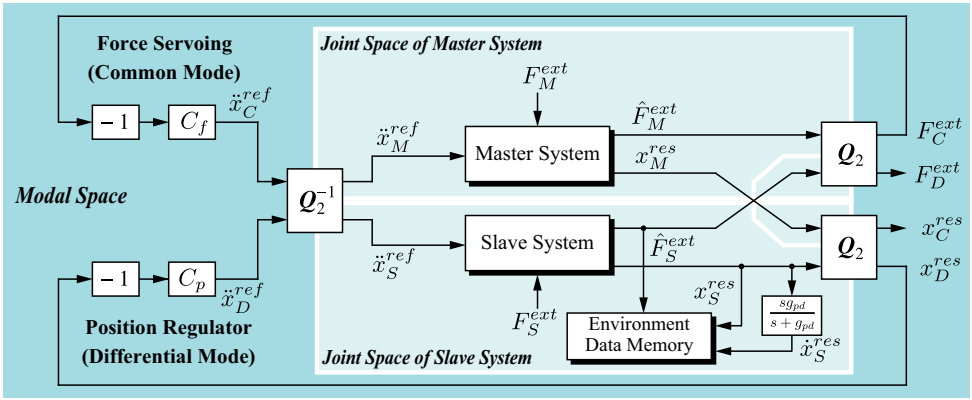

Fig. 3.85. Block diagram of the environmental saving system.

Fig. 3.85 shows block diagram of the environmental saving system. The subscripts $_M$, $_S$, $_C$, $_D$ of parameters in Fig. 3.85 denote master, slave, common mode, differential mode. The force responses of the master and slave system are transformed into the modal space by the quarry matrix.

$$\begin{bmatrix} F_C^{ext} \\ F_D^{ext} \end{bmatrix} = \boldsymbol{Q}_2 \begin{bmatrix} \hat{F}_M^{ext} \\ \hat{F}_S^{ext} \end{bmatrix} \tag{3.103}$$

The quarry matrix transforms the position responses in the joint space into the position responses in the modal space.

$$\begin{bmatrix} x_C^{res} \\ x_D^{res} \end{bmatrix} = \boldsymbol{Q}_2 \begin{bmatrix} x_M^{res} \\ x_S^{res} \end{bmatrix}. \tag{3.104}$$

A force controller C_f and a position regulator C_p calculate acceleration references $\ddot{x}_C^{ref}$, $\ddot{x}_D^{ref}$ in the modal space.

$$\ddot{x}_C^{ref} = -C_f\, F_C^{res} \tag{3.105}$$

$$\ddot{x}_D^{ref} = -C_p(s)\, x_D^{res} \tag{3.106}$$

In short, the bilateral control system controls independently the force in the common mode and the position in the differential mode. C_f and C_p are defined as

$$C_f = K_{fp} \tag{3.107}$$

$$C_p(s) = K_{pp} + \frac{s\ g_{pd}}{s + g_{pd}}\ K_{pd} \tag{3.108}$$

where, K_{fp}, K_{pp}, K_{pd} and g_{pd} are gain of the force controller, proportional gain, differential gain and pole of the position regulator. The calculated acceleration references are transformed into the joint space as

$$\begin{bmatrix} \ddot{x}_M^{ref} \\ \ddot{x}_S^{ref} \end{bmatrix} = \boldsymbol{Q}_2^{-1} \begin{bmatrix} \ddot{x}_C^{ref} \\ \ddot{x}_D^{ref} \end{bmatrix} \tag{3.109}$$

where, Q_2^{-1} is inverse quarry matrix. The actuators of the master and slave systems are controlled by the acceleration references $\ddot{x}_M^{ref}$, $\ddot{x}_S^{ref}$. By this means, the bilateral control for real-world haptics is achieved.

The environmental saving system stores the force information of the actuator in the slave side according to

$$F^{env}\left(\dot{x}_S^{res}, x_S^{res}\right) = \hat{F}_S^{ext} \tag{3.110}$$

where, F^{env} denotes force information preserved in the environment data memory. $\dot{x}_S^{res}$ is a velocity response of the actuator in the slave side. The velocity response is calculated by

$$\dot{x}_S^{res} = \frac{s g_{pd}}{s + g_{pd}} x_S^{res}. \tag{3.111}$$

In other words, the environmental saving system fills in second dimensional table of the force by using the position and velocity responses.

3.2.4 Environmental Loading System

3.2.4.1 Concept

A conceptual diagram of the environmental loading system is shown in Fig. 3.86. The environmental loading system is also operated by the bilateral controller. However, the slave

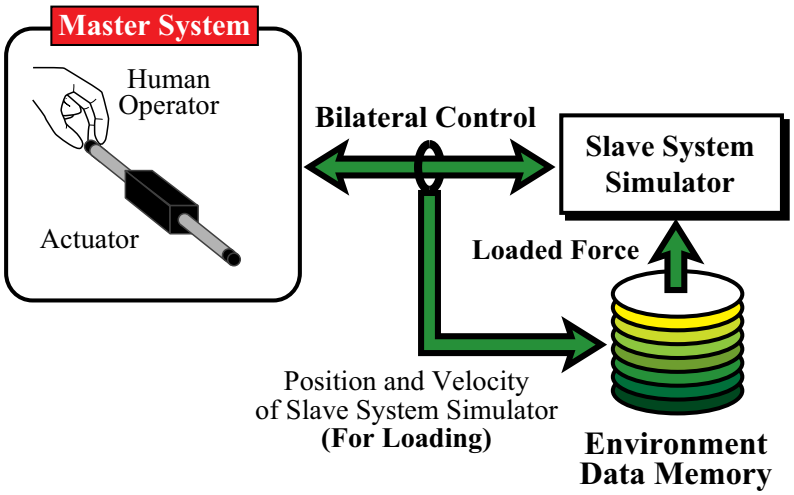

Fig. 3.86. Conceptual diagram of the environmental loading system.

system is unused. In the environmental loading system, a slave system simulator is utilized instead of the real slave system. Therefore, the bilateral controller controls both the master system and the slave system simulator. In addition, the environment data memory outputs a force signal according to the position and velocity responses of the slave system simulator. The environment data memory which contains the environmental characteristics stored by the environmental saving system imitates the real-world environment in the slave side, so that the environmental loading system stimulates the human operator in the master side.

3.2.4.2 Motion Control

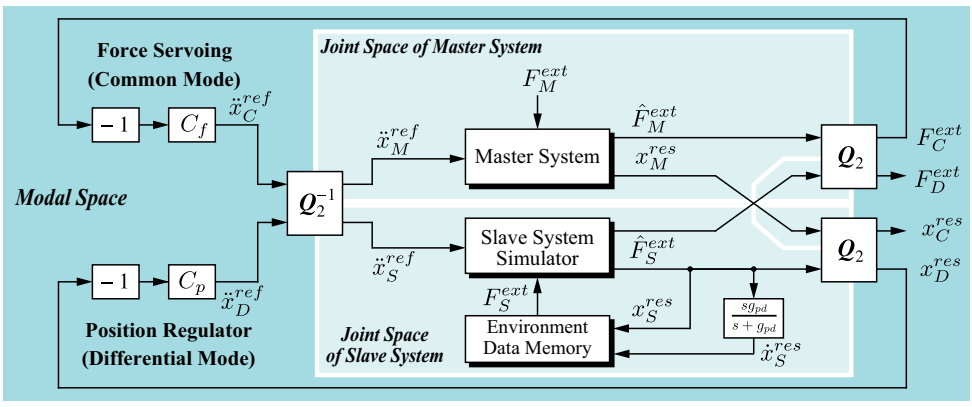

Fig. 3.87. Block diagram of the environmental loading system.

Fig. 3.87 shows a block diagram of the environmental loading system. In this system, respective parameters shown in Fig. 3.87 are calculated by (3.103)–(3.109). Fundamentally, the control method of the environmental loading system is same as the environmental saving system. However, the slave system does not exist in the real-world. The environmental loading system utilizes the slave system simulator, which has the control block shown in Fig. 3.84, in order to reproduce interference force between the master system and the slave system. Thus, operation of the slave system simulator is same as the operation of the real slave system.

The reaction force which gives to the slave system simulator is calculated by

$$F_S^{ext} = F^{env}\left(\dot{x}_S^{res}, x_S^{res}\right). \tag{3.112}$$

Actually, the control system utilizes generated lookup table including the force information, which was measured by the environmental saving system. In short, the slave system simulator is operated according to the environment characteristics.

In general, environmental haptic sensation is represented as mechanical impedance including stiffness and damper. In the environment data memory, the environmental stiffness K and damper factor D are expressed as

$$K = \frac{\partial F^{env}}{\partial x^{res}} \tag{3.113}$$

$$D = \frac{\partial F^{env}}{\partial \dot{x}^{res}}. \tag{3.114}$$

Fig. 3.88 shows force information in the environment data memory in case where the environment consists of pure stiffness and/or damper. The conventional linear impedance controller operates on the plane in Fig. 3.88. On the other hand, the proposed method is able to operate under unmodeled environment, because the system treats raw force data. Moreover, haptic sensation of nonlinear environment can be reproduced by the proposed method. In this point, the environmental copying system has large advantage.

In fact, the deformation of a target object in the real-world might be plastic deformation. However, this paper assumes that the environment is not depending on time variance. Therefore, this method cannot treat about the plastic deformation.

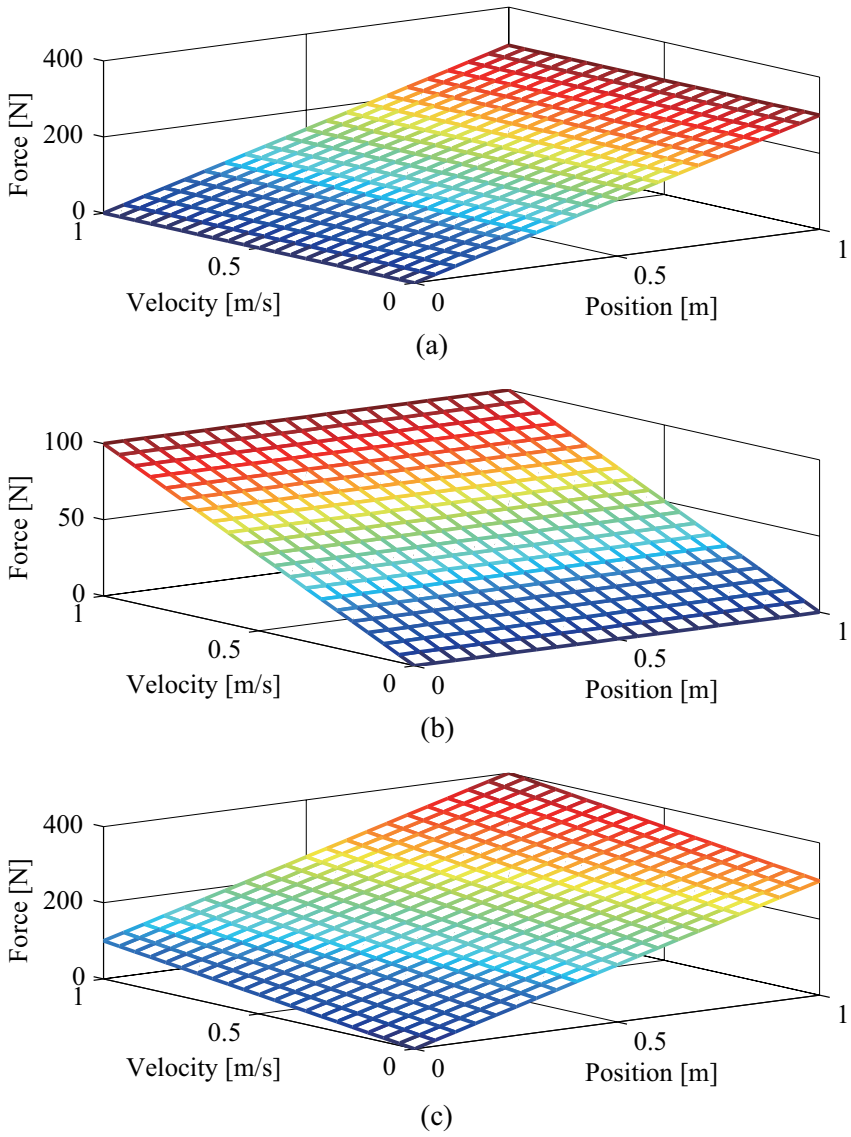

Fig. 3.88. Force information in the environment data memory. (a) In case of stiffness. (b) In case of damper. (c) In case of stiffness and damper.

3.2.5 Experiment

3.2.5.1 Experimental Setup

In this thesis, two experiments are carried out. The first experiment is environmental saving system; the other experiment is environmental loading system. Fig. 3.89 shows experimental devices. In case of the environmental saving system, two actuators are utilized. On the other

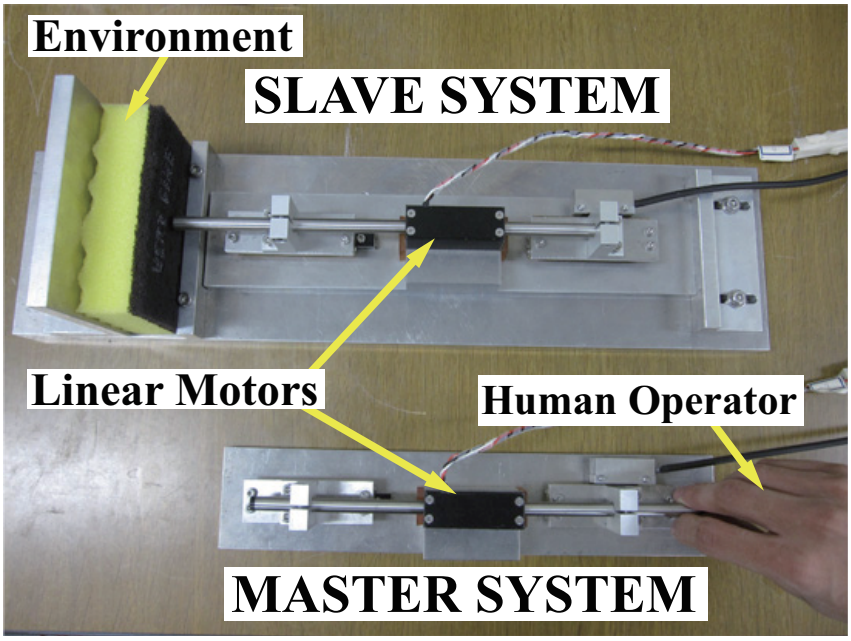

Fig. 3.89. Experimental setup (In case of environmental loading system, the slave system is unused).

hand, the actuator of the slave system is not used in the experiment of the environmental loading system. The actuators used in this experiment are the linear motors, which are controlled by RTAI 3.7. In the experiment, the human operator moves the actuator of the master system, and impresses the force. The environment in the slave side is a sponge. The setup parameters are shown in Table 3.4

Table 3.4. Setup Parameters

T_s	Period of control system	100	μs
K_{fn}	Force constant	3.33	N/A
M_n	Mass of nominal	0.245	kg
K_{fp}	Gain of force controller	5	
K_pp	Proportional gain of position controller	10000	
K_pd	Differential gain of position controller	200	
g_{pd}	Pole of pseudo derivative for the PD controller	10000	rad/s
g_{dis}	Pole of the disturbance observer	1000	rad/s
g_{reac}	Pole of the reaction force observer	1000	rad/s

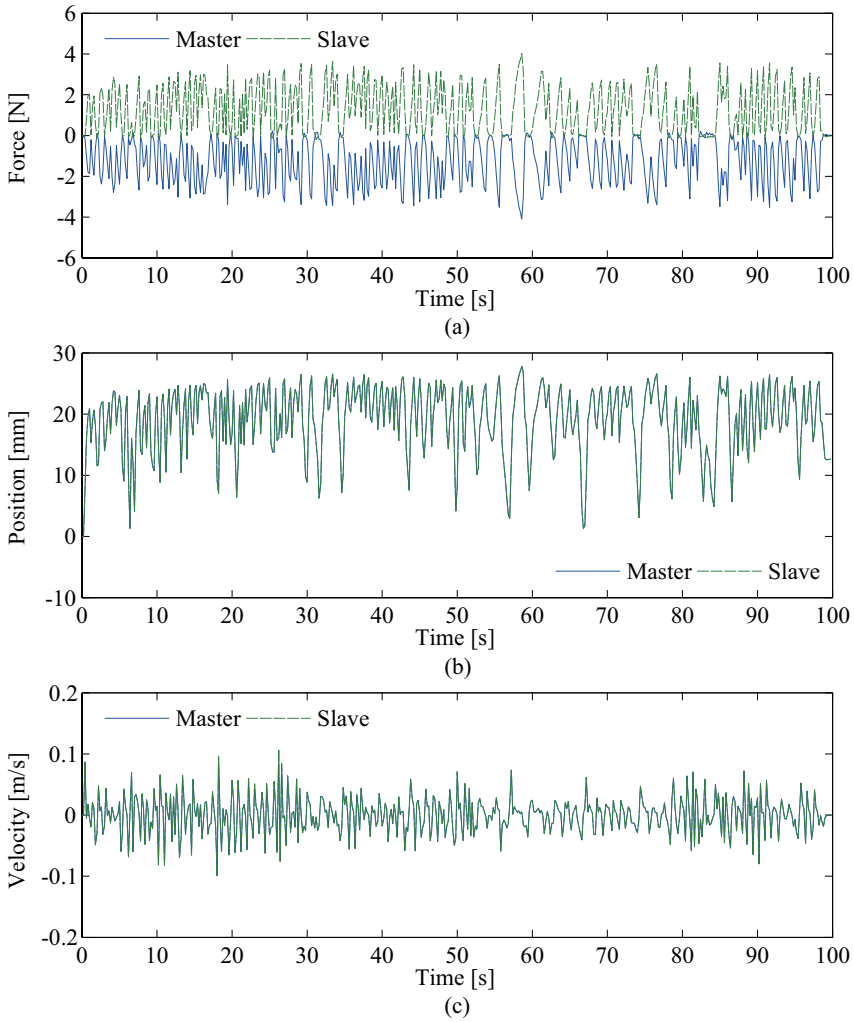

Fig. 3.90. Experimental results of the environmental saving system. (a) Force responses. (b) Position responses. (c) Velocity responses.

3.2.5.2 Experimental Results

Figs. 3.90 and 3.91 show the experimental results in case of the environmental saving system. The preserving time is 100 s. The reaction forces, position responses and velocity responses of the master and slave system are shown in Fig. 3.90. Fig. 3.91 shows force information of the environment data memory, which is generated by Fig. 3.90. The experimental results of Fig. 3.91 confirms that the proposed method is able to express the environmental characteristics.

Figs. 3.92 and 3.93 show the experimental results of the environmental loading system. In

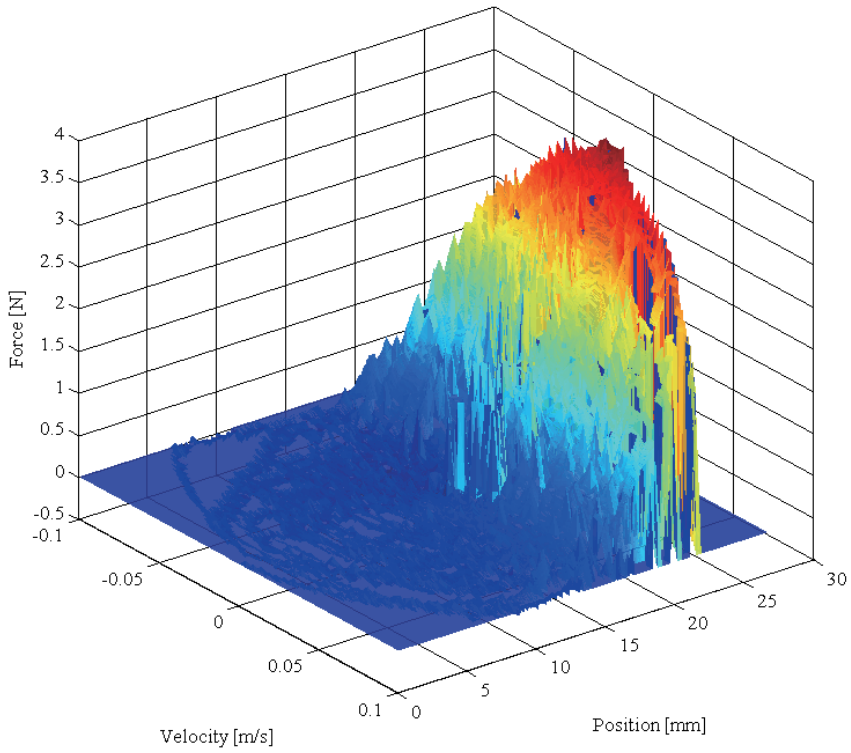

Fig. 3.91. The force information in the environment data memory.

Fig. 3.92, the bilateral controller using the environment data memory artificially generates the law of action and reaction. Fig. 3.93 shows comparison between the stored force in the environment data memory and the reproduced force by the environmental loading system. The reproduced force corresponds to the stored ones. The experiment confirms that the environmental loading system normally reproduces the environment in the slave side. Therefore, the human operator is able to grasp the environmental senses.

3.2.6 Conclusion

This thesis proposes novel environmental copying system based on real-world haptics. The proposed system consists of the environmental saving system and the environmental loading system. The environmental saving system stores haptic information of the environment in order to reproduce the environmental haptic sensation by using the environmental loading system, which stimulates the human operator at any time and at any place. The environmental copying system

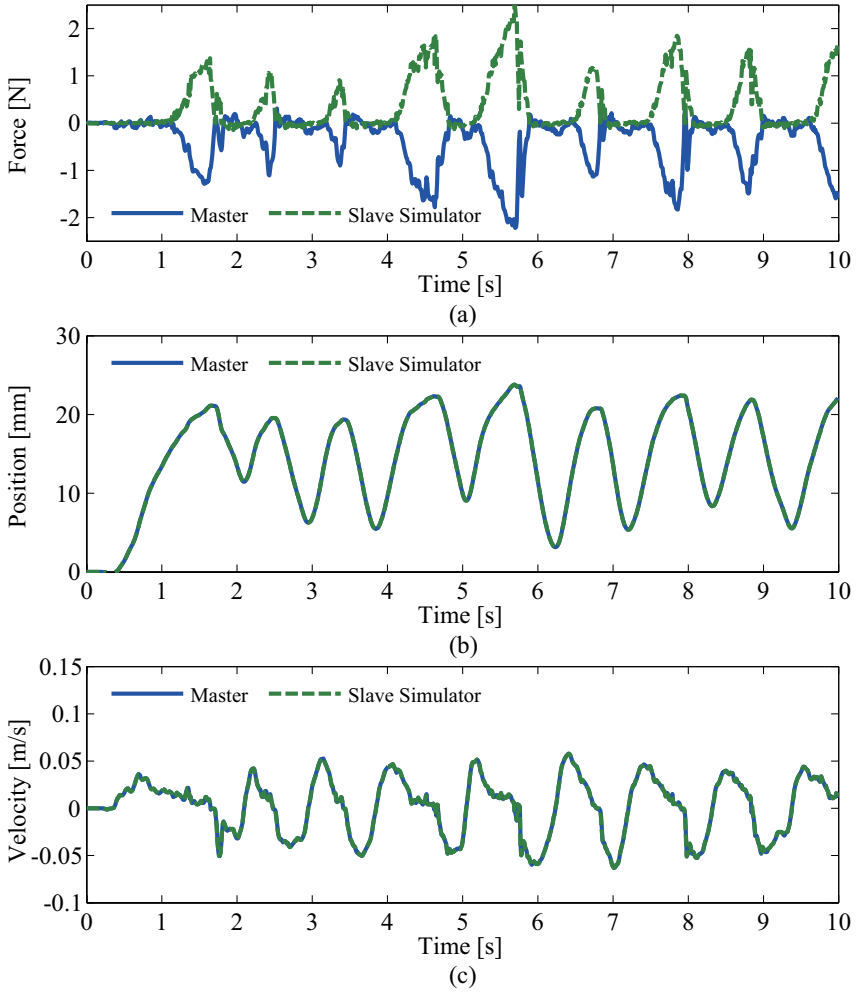

Fig. 3.92. Experimental results of the environmental loading system. (a) Force responses. (b) Position responses. (c) Velocity responses.

proposed in this thesis realizes saving and loading of haptic information. By the experiments, the validity of the proposed method was confirmed. It will be useful for industrial applications, medical and welfare human assistance.

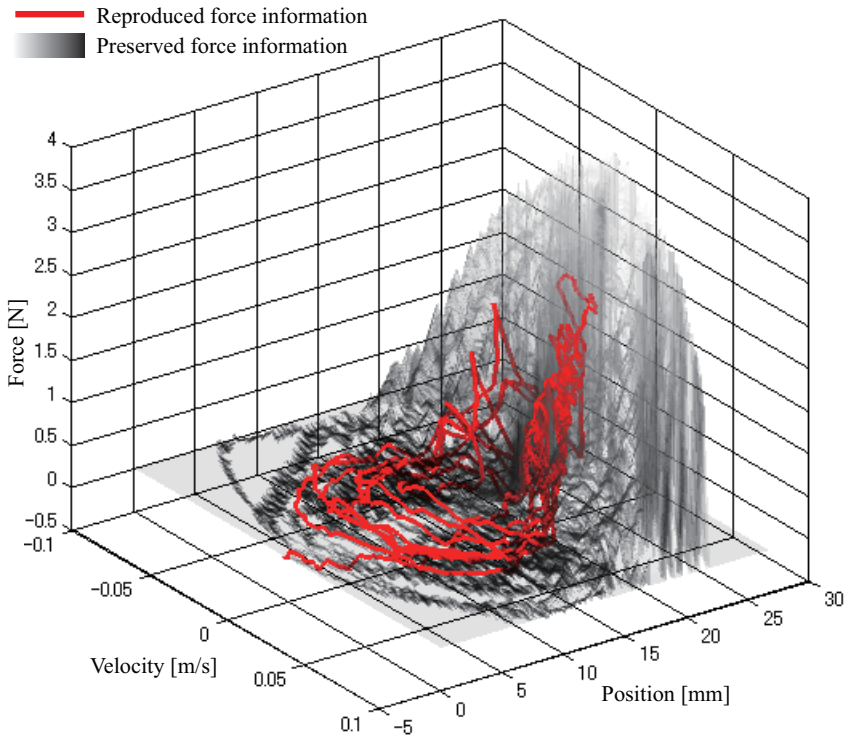

Fig. 3.93. Experimental results of the environmental loading system.

Chapter 4

Haptic Recognition on Remote Environment

Abstract

In order to realize communication and broadcasting of haptic information, bilateral/multilateral control with communication time delay is important element. The thesis proposes a novel bilateral/multilateral control method for communication time delay. To compensate the effect of communication time delay, the proposed method applies a motion-copying system. The motion-copying system is able to save and reproduce motion of human operator. The reproduced position and force by the motion-copying system corresponds to saved position and force. The motion-copying system copies local motion to other side, in order to realize compensation of communication time delay. The thesis confirms that the communication time delay compensation using the motion-copying system normally operates.

In addition, this thesis also proposes a novel bilateral control system using environmental data memory and slave system simulator in order to eliminate effect of the time delay, which exist in the communication network. The slave system simulator imitates the real slave system by using the environmental data memory without environmental mathematical model. Thus, non-linear environment and unknown environment can be treated, since raw force information is utilized. In addition, responses of the slave system in the real-world are not returned directly to the master side. By the proposed method, the bilateral controller operates normally under

the time delay, which causes vibration and/or overdrive. Therefore, the human operator in the master side is able to grasp the environmental sense through the bilateral controller, even if the environment exists in the distant place. By the experiments, validity of the proposed method is confirmed in the case that the time delay is set to 0 to 10 s.

Additionally, the thesis proposes the transfer technique of haptic information under the narrow-band network. The bilateral controller through the low-rate network encounters the influence. In this thesis, the compressors and the decompressors is implemented to the bilateral controller based on a motion-copying system in order to solve the problems. The data compressors reduce an amount of the data, which flows between a master system and a slave system in the bilateral controller. The reaction force between the master and the slave becomes stable even if the data transfer rate is low in the network.

4.1 Bilateral Control over Network

4.1.1 Bilateral Control with Communication Time Delay by Using Motion-Copying System

4.1.1.1 Introduction

An electrical communication technology and engineering of telecommunication network has been rapidly grown. Thus, information of the entire world can be provided to human. Telephone and television provide acoustic information and visual information, respectively. These are useful for communication devices between human and human. Also, sound radio and television broadcast information based on acoustic and visual information. However, the human has five organs. These are visual, auditory, olfactory, gustatory, and tactile organs. At this moment, the broadcasting of information considers only two organs. In this situation, the conventional broadcasting technology is not able to reproduce realistic remote environment. Consequently, the communication and broadcasting technology should be expanding to treat haptic information. A compensation of communication time delay is very important element, in order that a communication system normally transmits information. Fig. 4.1 shows appearance of information transmission. A microphone catches vibration of air, converts to electronic information.

The converted electronic information is transmitted to other side. A speaker system reproduces acoustic information according to transmitted electronic information. At the same time, the time delay of between transmission and reception exists. In the case of visual information, the situation is same. The acoustic and visual information are unilateral information. Therefore, the communication time delay does not become an issue in this case. However, the haptic information is bilateral information. More specifically, the environment in local side and remote side are influenced by mutual environments. Thus, haptic communication and broadcasting system are very sensitive to the time delay. Hence, compensation of communication time delay for haptic communication and broadcasting is required. The compensation method using scattering theory has been proposed [89, 90]. Though, such method can not normally compensate, when the time delay is varied. A communication disturbance observer has been proposed [94]–[99]. However, calculated communication disturbance includes contact force of between slave system and environment, when the communication disturbance observer calculates communication disturbance. Also, to compensate communication time delay, the compensation method using smith predictor and neural network has been already proposed [91].

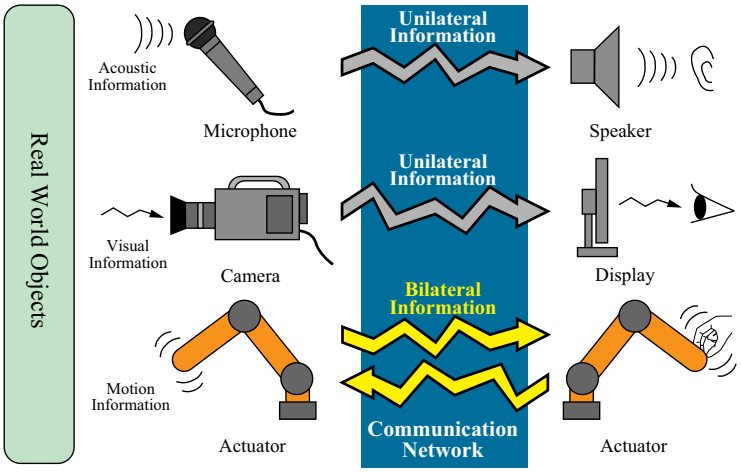

Fig. 4.1. Transmission of acoustic and visual, haptic information.

The thesis proposes a novel compensation method for communication time delay. Bilateral and/or multilateral controls are used to share haptic information of the environment. The

proposed method applies a motion-copying system [38] in order to compensate communication time delay. The motion-copying system consists of a motion-saving system and motion-loading system, and is able to store and reproduce the motion of human operator. The motion-saving system saves position and force of human operator and/or environment. The motion-loading system reproduces the position and the force according to saved motion. The reproduced position and force corresponds to the saved position and force. To realize compensation of communication time delay, the motion-copying system copies local motion to other side.

This research is organized as follows. Subsection 4.1.1.2 explains bilateral control with time delay. In 4.1.1.3, concept of the motion-copying system is presented. The concept and motion control system of time delay compensation using motion-copying system is shown in 4.1.1.4. The experimental result of conventional and proposed method is shown in 4.1.1.5. The last subsection concludes this study.

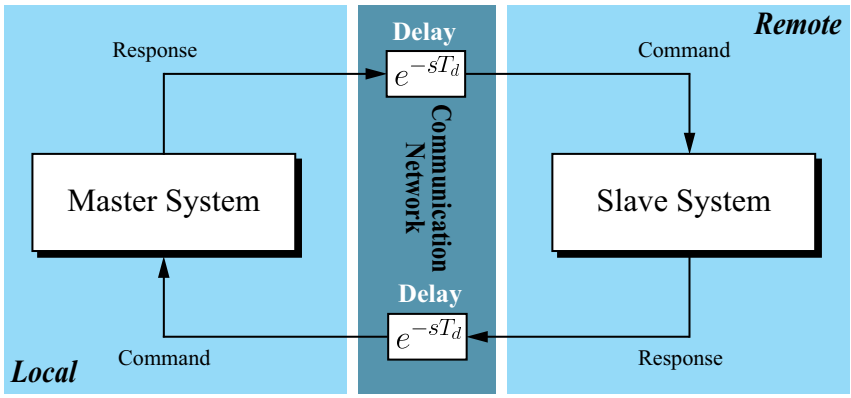

Fig. 4.2. Bilateral control system with communication time delay.

4.1.1.2 Bilateral Control with Time Delay

Fig. 4.2 shows bilateral control system including time delay of communication. In this thesis, sharing of haptic information is carried out using a bilateral control system. The bilateral control system consists of a master system and a slave system. If a human operator impresses force and moves position of the master motor, a motor of the slave side is operated by bilateral

controller according to it. The bilateral controller generates hypothetical law of action and reaction. Therefore, the bilateral control system realizes propagation of haptic information. However, the bilateral control system can not operate when communication delay exists in communication network. The communication time delay makes the controller unstable, and poses vibration of position and force response. Thus, in order to realize the bilateral control system via communication network, the compensation of communication time delay is required.

4.1.1.3 Motion-Copying System

This section explains concept of the motion-copying system. The motion-copying system consists of both the motion-saving system and the motion-loading system. In this thesis, the motion-copying system is applied to compensate delay of communication network.

Motion-Saving System Fig. 4.3 shows conceptual diagram of the motion-saving system. The motion-saving system is constructed by general bilateral controller. The human operator grasps the environment of other side using the control system. At the same time, impressed force by the human operator and position of the master motor is stored to motion data memory. The saved force and position information is used when the motion-loading system reproduces saved motion of the human operator. More specifically, the motion-saving system realizes save of the human operator motion.

Motion-Loading System Conceptual diagram of the motion-loading system is shown in Fig. 4.4. The motion-loading system is operated by master-slave controller. A calculation method of controller value for realization of the motion-loading system is similar to the case of the motion-saving system. Though, the motion-loading system does not have a motor in the master-system side, because the motion data memory is used instead of the master system. The motion data memory holds the impressed force by the human operator and the position information of the master motor. In the motion-loading system, a motor of the slave system is operated by the motion data memory. The reproduced position and force by the motion-loading

system corresponds to the saved ones.

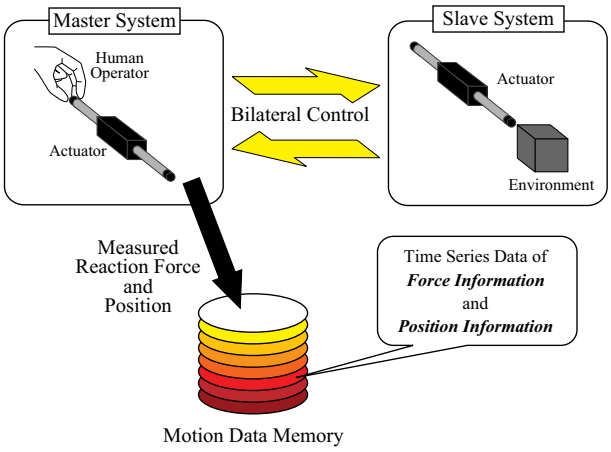

Fig. 4.3. Conceptual diagram of motion-saving system.

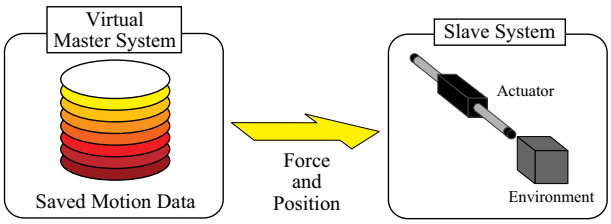

Fig. 4.4. Conceptual diagram of motion-loading system.

4.1.1.4 Communication Delay Compensation Based on Motion-Copying System

Concept The conceptual diagram of time delay compensation for bilateral controller based on motion-copying system is shown in Fig. 4.5. Both the master system and the slave system have the motion-copying system. The motion data memory is installed to these systems instead of a slave system in the master side or a master system in the slave side. These data memories are used as with a virtual slave system or a virtual master system. In the master side, the motion-saving system saves impressed force by the human operator and position of the motor to the motion data memory. On the contrary, the motion-loading system reproduces force and position using held data by the motion data memory. Additionally, the motion-saving system in the slave

side saves position and force of between the slave motor and the environment as with the case of the master side. The motion-loading system reproduced motion according to the motion data memory. The value of the motion data memory of each side is exchanged via communication network at all times, when the bilateral controller is operating. Also, since reproduced the force and position in each side corresponds to held force and position by the memory, the bilateral controller is realized even if the motion data memory exists between the master system and slave system. The force and position data are stored by the motion data memory in each system. These are reproduced by the motion-loading system of respective systems at any time. Therefore, the bilateral controller using the motion-copying system normally operates even if the system includes communication delay. More specifically, the human operator is able to grasp haptic information of the environment by the bilateral controller using the proposed method.

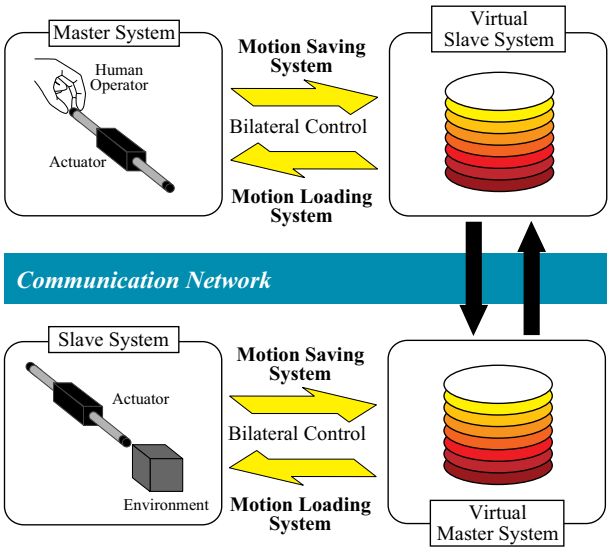

Fig. 4.5. Conceptual diagram of bilateral control with time delay compensation based on motion-copying system.

Motion Control The detailed block diagram of the master and the slave system is shown in Fig 4.6. In this figure, $\ddot{x}^{ref}$, M_n, F^{ext} and x^{res} denotes reference of a motor, mass of actuator, reaction force and position of the motor, respectively. The disturbance observer [66] calculates

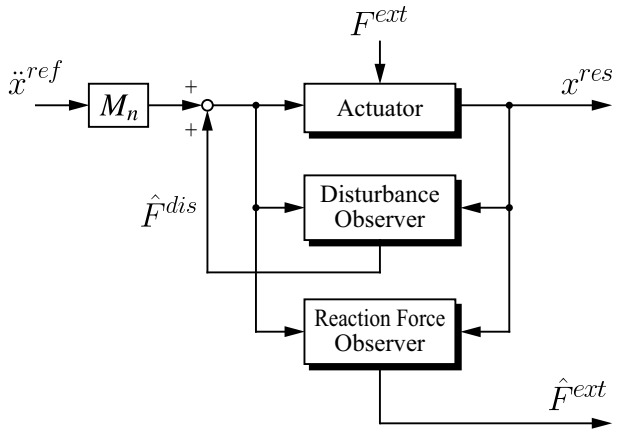

Fig. 4.6. Block diagram of master and slave system.

disturbance force F^{dis}, and realizes robust acceleration control. Also, the estimation value of reaction force $\hat{F}^{ext}$ is calculated by the reaction force observer [64].

Fig. 4.7 shows the block diagram of the bilateral control system using time delay compensation. The bilateral controller consists of two sections. The first section is master system side; the other section is slave system side. These sections are connected by communication network including time delay. In this thesis, T_d denotes delay time. The communication delay exists in the master and slave side.

$$\begin{aligned} \hat{F}^{ext}_{Ms} = e^{-sT_d}\ \hat{F}^{ext}_{Mm} \quad , \quad x^{res}_{Ms} = e^{-sT_d}\ x^{res}_{Mm} \\ \hat{F}^{ext}_{Sm} = e^{-sT_d}\ \hat{F}^{ext}_{Ss} \quad , \quad x^{res}_{Sm} = e^{-sT_d}\ x^{res}_{Ss} \end{aligned} \tag{4.1}$$

where, x^{res}_{Mm}, x^{res}_{Sm} and x^{res}_{Ms}, x^{res}_{Ss} are the position response of each system in the master and slave side.

The respective systems include both a modal space and a joint space. The mutual conversion of between the modal space and the joint space is realized using the quarry matrix [65]. The second-order quarry matrix $\boldsymbol{Q}_2$ is denoted by (4.2) [63]

$$\boldsymbol{Q}_2 = \frac{1}{2}\begin{bmatrix} 1 & 1 \\ 1 & -1 \end{bmatrix}. \tag{4.2}$$

The quarry matrix is used to realize the bilateral controller and/or the motion-copying system.

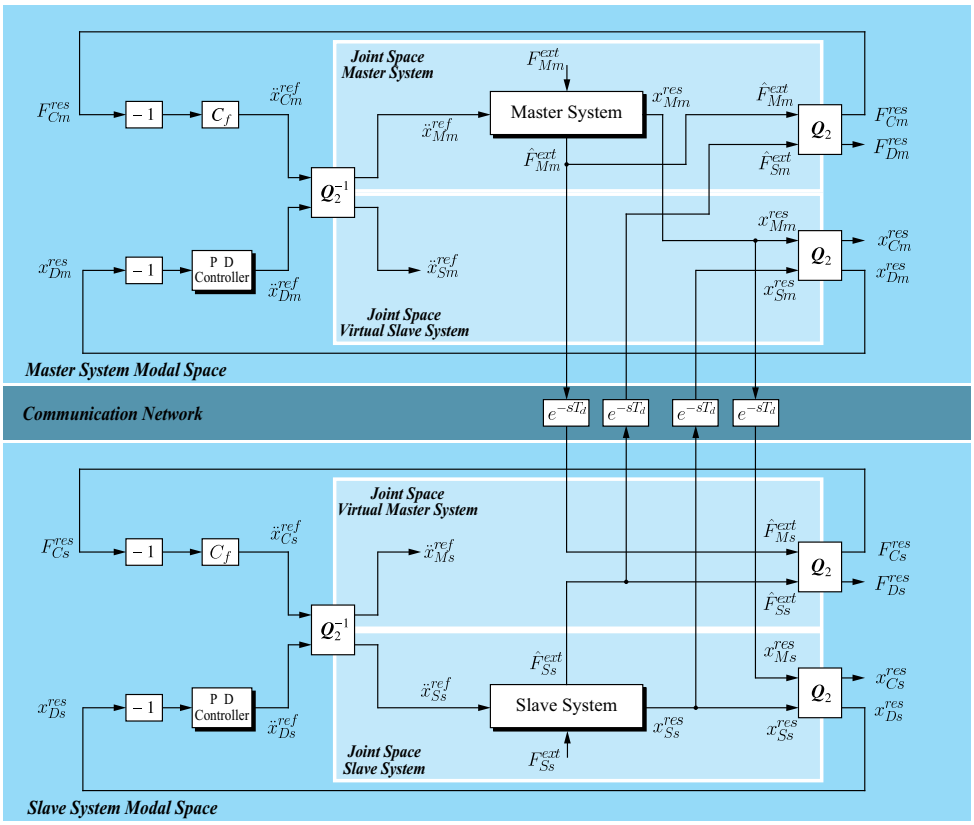

Fig. 4.7. Block diagram of bilateral control system using time delay compensation based on motion-copying system.

The estimated reaction force of the master side $\hat{F}^{ext}_{Mm}$, $\hat{F}^{ext}_{Sm}$, and the slave side $\hat{F}^{ext}_{Ms}$, $\hat{F}^{ext}_{Ss}$ are transformed by (4.3), (4.4)

$$\begin{bmatrix} F^{res}_{Cm} \\ F^{res}_{Dm} \end{bmatrix} = \boldsymbol{Q}_2 \begin{bmatrix} \hat{F}^{ext}_{Mm} \\ \hat{F}^{ext}_{Sm} \end{bmatrix} \tag{4.3}$$

$$\begin{bmatrix} F^{res}_{Cs} \\ F^{res}_{Ds} \end{bmatrix} = \boldsymbol{Q}_2 \begin{bmatrix} \hat{F}^{ext}_{Ms} \\ \hat{F}^{ext}_{Ss} \end{bmatrix} \tag{4.4}$$

where, F^{res}_{Cm} and F^{res}_{Dm} are the force response in the common mode and one in the differential mode in the master side. Also F^{res}_{Cs} and F^{res}_{Ds} are each mode force response in the slave side. On the contrary, the position response in the common mode and differential modes in the master

side x_{Cm}^{res} , x_{Dm}^{res} and the slave side x_{Cs}^{res} , x_{Ds}^{res} are derived by (4.5), (4.6)

$$\begin{bmatrix} x_{Cm}^{res} \\ x_{Dm}^{res} \end{bmatrix} = \boldsymbol{Q}_2 \begin{bmatrix} x_{Mm}^{res} \\ x_{Sm}^{res} \end{bmatrix} \tag{4.5}$$

$$\begin{bmatrix} x_{Cs}^{res} \\ x_{Ds}^{res} \end{bmatrix} = \boldsymbol{Q}_2 \begin{bmatrix} x_{Ms}^{res} \\ x_{Ss}^{res} \end{bmatrix}. \tag{4.6}$$

In order to realize bilateral control, this system controls the force in the common mode F_{Cm}^{res}, F_{Cs}^{res} and the position in the differential mode x_{Dm}^{res}, x_{Ds}^{res}. The acceleration reference of each mode $\ddot{x}_{Cm}^{ref}$, $\ddot{x}_{Dm}^{ref}$ in the master side is derived by (4.7), (4.8)

$$\ddot{x}_{Cm}^{ref} = -C_f \; F_{Cm}^{res} \tag{4.7}$$

$$\ddot{x}_{Dm}^{ref} = -(K_p + s \; K_d) \; x_{Dm}^{res} \tag{4.8}$$

where, C_f, K_p and K_d is the gain of force control, proportional gain and differential gain. In the slave side, the acceleration references $\ddot{x}_{Cs}^{ref}$, $\ddot{x}_{Ds}^{ref}$ is calculated by (4.9), (4.10)

$$\ddot{x}_{Cs}^{ref} = -C_f \; F_{Cs}^{res} \tag{4.9}$$

$$\ddot{x}_{Ds}^{ref} = -(K_p + s \; K_d) \; x_{Ds}^{res}. \tag{4.10}$$

The acceleration references $\ddot{x}_{Cm}^{ref}$, $\ddot{x}_{Dm}^{ref}$, $\ddot{x}_{Cs}^{ref}$, $\ddot{x}_{Ds}^{ref}$ are transformed into the joint space using (4.11), (4.12)

$$\begin{bmatrix} \ddot{x}_{Mm}^{ref} \\ \ddot{x}_{Sm}^{ref} \end{bmatrix} = \boldsymbol{Q}_2^{-1} \begin{bmatrix} \ddot{x}_{Cm}^{ref} \\ \ddot{x}_{Dm}^{ref} \end{bmatrix} \tag{4.11}$$

$$\begin{bmatrix} \ddot{x}_{Ms}^{ref} \\ \ddot{x}_{Ss}^{ref} \end{bmatrix} = \boldsymbol{Q}_2^{-1} \begin{bmatrix} \ddot{x}_{Cs}^{ref} \\ \ddot{x}_{Ds}^{ref} \end{bmatrix} \tag{4.12}$$

where $\boldsymbol{Q}_2^{-1}$ is the inverse quarry matrix. Also, $\ddot{x}_{Mm}^{ref}$, $\ddot{x}_{Sm}^{ref}$ are acceleration references of the master and slave systems in the master side, $\ddot{x}_{Ms}^{ref}$ and $\ddot{x}_{Ss}^{ref}$ are acceleration references of each system in the slave side. These calculated acceleration references operate the systems.

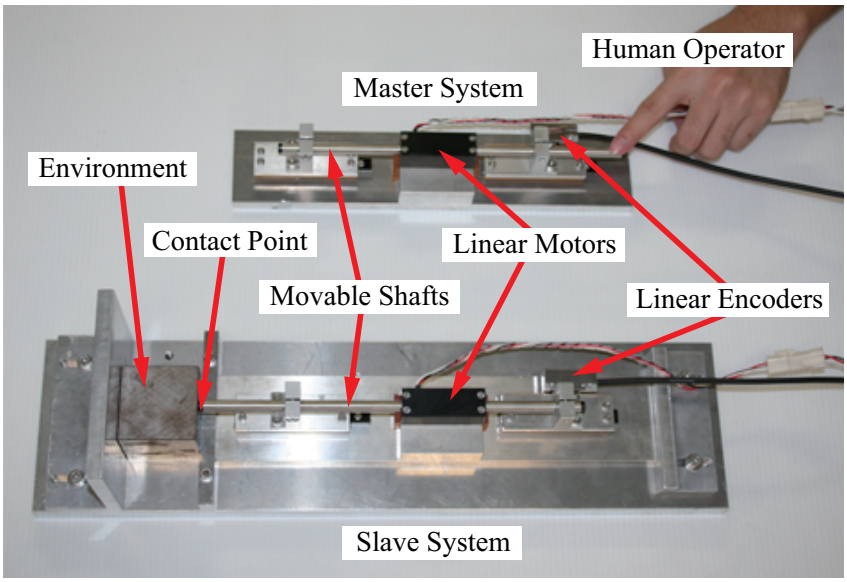

Fig. 4.8. Experimental devices.

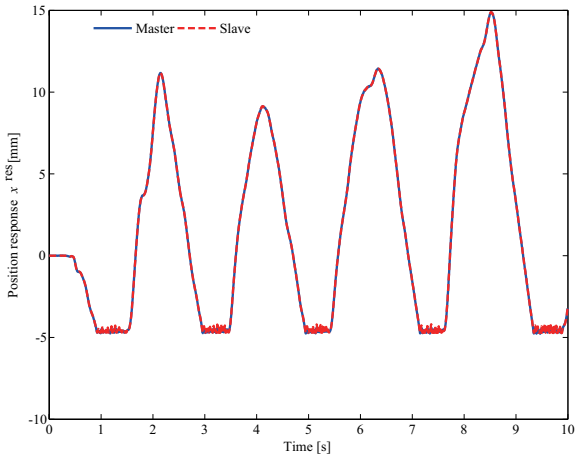

Fig. 4.9. Position response without time delay compensation (Communication delay time $T_d = 3$ ms).

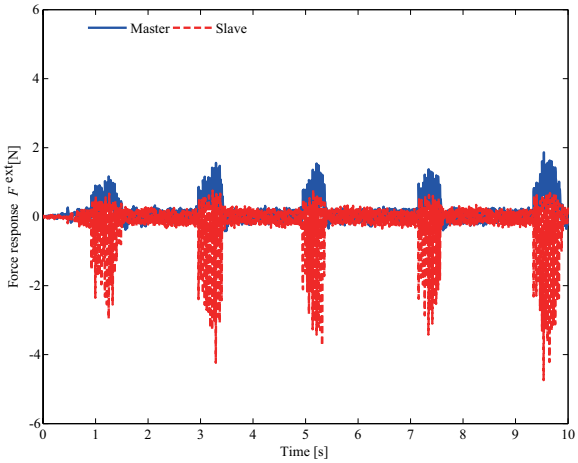

Fig. 4.10. Force response without time delay compensation (Communication delay time $T_d = 3$ ms).

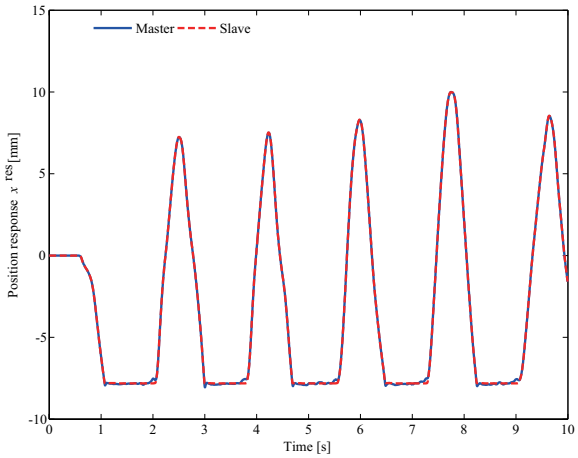

Fig. 4.11. Position response using motion-copying system (Communication delay time $T_d = 3$ ms).

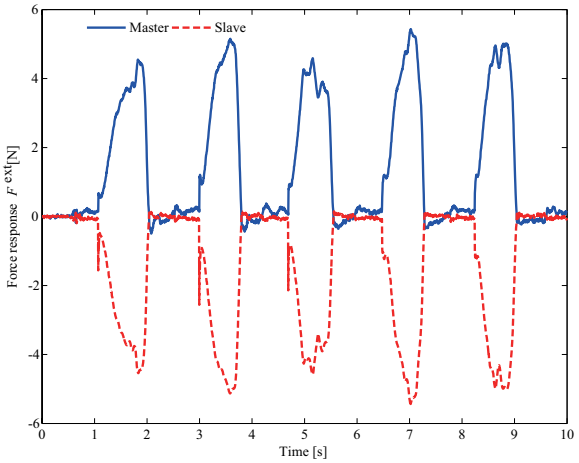

Fig. 4.12. Force response using motion-copying system (Communication delay time $T_d = 3$ ms).

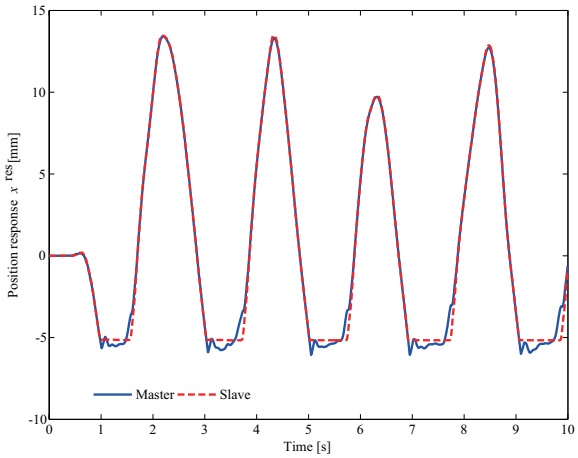

Fig. 4.13. Force response using motion-copying system (Communication delay time $T_d = 30$ ms).

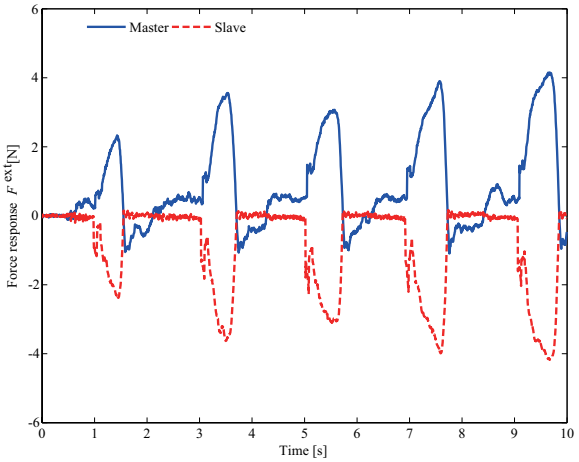

Fig. 4.14. Force response using motion-copying system (Communication delay time $T_d = 30$ ms).

The explained motion data memory in the previous section does not exist in the block diagram. Because the time delay of the communication network is used instead of the motion data memory. In short, the master side and the slave side are mutually coupled by the motion-copying system. More specifically, the bilateral controller using the motion-copying system is able to operate without influence of communication time delay as previously noted.

4.1.1.5 Experiment

Experimental Setup Fig. 4.8 shows the experimental device. The human operator touches a movable shaft of the master motor and actuate from side to side. On the contrary, the tip of the movable shaft in the slave side contacts to the environment. In the experiment, the environment is used as iron block. The each linear motor is controlled by RT-Linux 3.2, which realizes the bilateral control system. The experiment intentionally prepares time delay in between the master system and slave system to test proposed method. The setup parameters in the experiment is shown in Table 4.1.

Table 4.1. Setup Parameters

T_s	Period of control system	100	μs
K_{tn}	Force constant	3.33	N/A
M_n	Mass of nominal	0.18	kg
C_f	Assist gain	15	
K_p	Proportional gain of the PD controller	10000	
K_d	Differential gain of PD controller	200	
g_{pd}	Pole of pseudo derivative for the PD controller	10000	rad/s
g_{dis}	Pole of the disturbance observer	1000	rad/s
g_{reac}	Pole of the reaction force observer	1000	rad/s

Experimental Results The experimental results of the bilateral controller without compensation for communication time delay are shown in Figs. 4.9 and 4.10. The communication delay time is set to 3 ms. In this experiment, the delay time is set as constant value, because the thesis assumes that the jitter of the network is compensated by the jitter buffer [100]. The

vibration occurs in a part of contact to the environment in Fig. 4.9. Also, force response in Fig. 4.10 includes vibration. These vibrations occur on account of time delay of between the master system and the slave system. In this situation, the human operator cannot grasp the environment of the slave system.

On the contrary, Figs. 4.11 and 4.12 show the experimental results of the bilateral controller using the motion-copying system. Both force response and position response does not include vibration compared with the results without compensation. Additionally, the experimental results show that the bilateral controller is able to mutually convey the reaction force. Also, the law of action and reaction is reproduced. Therefore, the human operator obviously grasps the remote environment.

In case that communication delay time is increased, the experiment is carried out. Figs. 4.13 and 4.14 show the experimental results when the communication delay time is set to 30 ms. These experimental results clarifies that the bilateral controller including delay time normally operates in terms of the motion-copying system.

4.1.1.6 Conclusion

The thesis proposes a novel compensation of communication time delay for the bilateral control. In this thesis, the motion-copying system is used to compensate communication delay between the master system and the slave system. The motion-copying system is capable of saving and reproducing the human operated motion. Actually, the motion data memory which stores the motion does not employ for compensation of delay. The communication time delay is utilize in stead of the motion data memory in the proposed system. In other words, respective sides of the bilateral controller are mutually coupled by the motion-copying system. The motion-copying system reproduces both force and position in other side. Finally, problems of communication time delay in the bilateral control system are solved using the motion-copying system. The thesis confirms availability of the proposed method by the experiments. It will be useful for industrial applications, medical and welfare human assistance.

4.1.2 Bilateral Teleoperation over Network Based on Environmental Data Memory

4.1.2.1 Introduction

Information and communication technology which treats variety of information has been rapidly grown. The current communication networks provide text data, acoustic data, image and movie data in entire world. For example, Internet users get html text documents, mp3 sound files, JPEG image files and avi movie files. There has acoustic information and visual information. Therefore, the practical communication technology provides acoustic information and visual information to users. However, the human has five organs. Thus, the current communication technology is not enough to convey realistic environment, which exists in the distant place. In order to transmit the realistic remote environment in the real-world, the information and communication technology should treat olfactory, gustatory and haptic information. The thesis considers transmission of the haptic information.

Fig. 4.15 shows transmission of the acoustic information, the visual information and the haptic information. To transmit the information to the distant place, communication network which may cause the time delay has to be used. Since the acoustic information and the visual information are unilateral information, the time delay does not induce the problems. On the other hand, the haptic information is bilateral information. Therefore, the time delay between local side and remote side induces the problems. In concrete terms, vibration and/or overdrive are caused when bilateral control system provides the haptic information. To reduce the problems of the time delay, the scattering theory has been proposed [89, 90]. Moreover, experiment of bilateral control under the time delay by using experimental satellite which is called ETS-VII was carried out [101]. The method using smith compensator and neural network has been also proposed [91]. In addition, communication disturbance observer for the time delay has been proposed [94]. However, the control system should consider not only the time delay but also very long time delay.

The thesis proposes a novel bilateral control to eliminate the effect of the time delay, which

induces vibration and/or overdrive. The proposed bilateral control system consists of master system, slave system simulator and slave system. In order to imitate the real slave system, the slave system simulator utilizes environmental data memory. The environmental data memory is able to store and reproduce the environmental information of the real slave system. In the proposed system, the force information from the environmental data memory is provided instead of the force from the real slave system. Therefore, the human operator grasps the environmental haptic sense through the bilateral controller, which operates under the time delay. Moreover, the bilateral controller proposed in this thesis is able to operate under the very long time delay. In addition, unknown environment and non-linear environment can be treated, since the environmental data memory does not use environmental mathematical model at all.

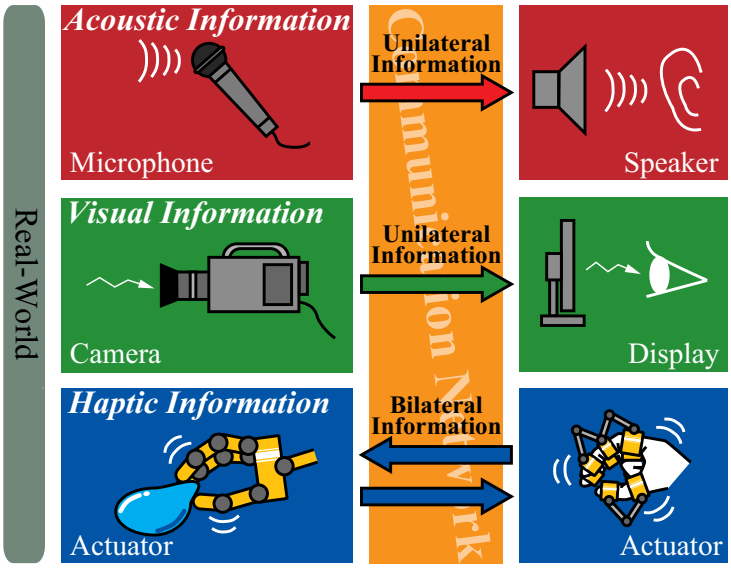

Fig. 4.15. Transmission of acoustic, visual and haptic information.

This research is organized as follows. In 4.1.2.2, concept of the proposed bilateral control system is explained. Subsection 4.1.2.3 mentions control method of the bilateral controller. Moreover, control method for the slave system in the real-world is also described. The environmental data memory is explained in 4.1.2.4. The experiment is shown in 4.1.2.5. In the experiment, the time delay of the communication network is set to 0, 1, 3, 5 and 10s. Finally,

the last subsection concludes this study.

4.1.2.2 Concept of Bilateral Control using Environmental Data Memory

Fig. 4.16 shows conceptual diagram of the proposed bilateral controller. The bilateral controller consists of master system, slave system, slave system simulator and environmental data memory. In the master side, the bilateral control system controls the master system and the slave system simulator using the environmental data memory. The acceleration response of the bilateral controller is fed to the slave system through the communication line, when the human operator drives the master system. The acceleration responses of the real slave system are stored to the environmental data memory in the master side. In short, the environmental data memory stores the environmental information in the slave side, so that the environmental data memory imitates the environment. Moreover, the responses of the slave system are not returned directly to the master side. Therefore, the bilateral controller is able to operate normally, even if the time delay of the communication network occurs. By this means, the proposed method is able to reduce the liabilities of the communication networks.

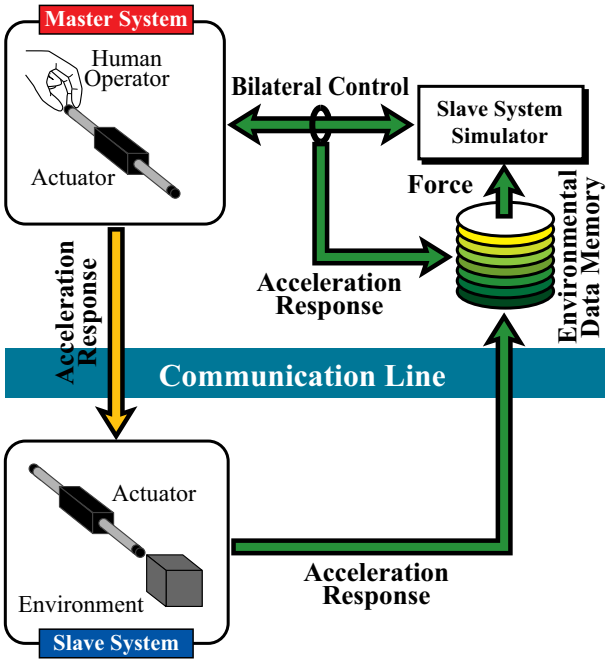

Fig. 4.16. Conceptual diagram of the proposed method.

4.1.2.3 Motion Control

In this section, control method of the proposed system is described.

Master System and Slave System Simulator Fig. 4.17 shows block diagram of the master system and the slave system simulator. i^{ref}, $\ddot{X}^{res}$, K_f, K_{fn} and M are current reference, actual acceleration response, force constant, nominal force constant and mass of the actuator. A disturbance observer [66] estimates disturbance force $\hat{F}^{dis}$ and cancels the disturbance, so that robust acceleration control is realized. The acceleration control which is operated by acceleration reference $\ddot{X}^{ref}$ drives the actuator. Meanwhile, a reaction force observer [64] estimates external force F^{ext} impressed by the human operator and/or the environment. The equivalent acceleration $\ddot{X}^{equ}$ is obtained using the estimated external force $\hat{F}^{ext}$ as

$$\ddot{X}^{equ} = \frac{\hat{F}^{ext}}{M_n}. \tag{4.13}$$

where M_n denotes nominal mass of the actuator. In the slave system simulator, a virtual actuator which is realized by the control computer generates the equivalent acceleration and the actual acceleration reference instead of the real-world actuator. The acceleration control shown in Fig. 4.17 is utilized in the proposed bilateral control system.

Fig. 4.18 shows block diagram of the bilateral control system proposed in this thesis. $\ddot{X}$ and F shown in Fig. 4.18 are acceleration and force. The subscript M, sim, S, C and D mean master, simulator, slave, common mode and differential mode. The superscript ref, equ, res and ext denote reference, equivalent, actual response and external. In the proposed system, modal decomposition is used in order to realize the bilateral control. The modal decomposition of two actuators is realized by a second-order quarry matrix $\boldsymbol{Q}_2$ defined as [63]

$$\boldsymbol{Q}_2 = \frac{1}{2}\begin{bmatrix} 1 & 1 \\ 1 & -1 \end{bmatrix}. \tag{4.14}$$

The first row expresses common mode; the other row expresses differential mode. The equivalent accelerations of common mode and differential mode are calculated by

$$\begin{bmatrix} \ddot{X}_C^{equ} \\ \ddot{X}_D^{equ} \end{bmatrix} = \boldsymbol{Q}_2 \begin{bmatrix} \ddot{X}_M^{equ} \\ \ddot{X}_{sim}^{equ} \end{bmatrix}. \tag{4.15}$$

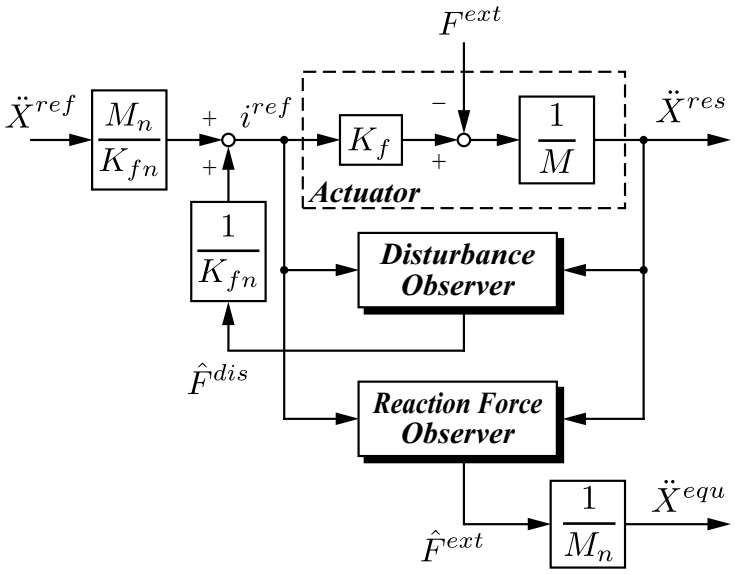

Fig. 4.17. Block diagram of master system, slave system simulator and slave system.

On the other hand, the quarry matrix transforms also actual acceleration responses of the master system and the slave system simulator into the modal space.

$$\begin{bmatrix} \ddot{X}_M^{res} \\ \ddot{X}_{sim}^{res} \end{bmatrix} = \boldsymbol{Q}_2 \begin{bmatrix} \ddot{X}_C^{res} \\ \ddot{X}_D^{res} \end{bmatrix} \tag{4.16}$$

A force controller C_f and a position regulator $C_p(s)$ calculate acceleration references using the equivalent acceleration and the actual acceleration as follows:

$$\ddot{X}_C^{ref} = -C_f\ \ddot{X}_C^{equ} \tag{4.17}$$

$$\ddot{X}_D^{ref} = -C_p(s)\ \ddot{X}_D^{res} \tag{4.18}$$

In this thesis, the force controller and the position regulator are represented as

$$C_f = K_{fp} \tag{4.19}$$

$$C_p(s) = \frac{1}{s^2}K_{pp} + \frac{1}{s}\ K_{pd}. \tag{4.20}$$

In other words, the bilateral controller controls independently the force of common mode and the position of differential mode in the modal space. These acceleration references calculated

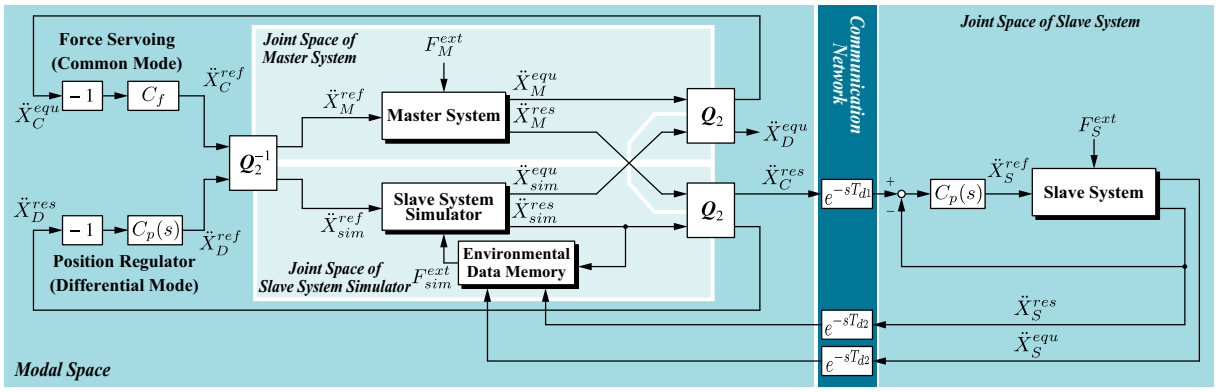

Fig. 4.18. Block diagram of bilateral control system over network based on environmental data memory.

by the respective controllers in the modal space are transformed into the joint space.

$$\begin{bmatrix} \ddot{X}_M^{ref} \\ \ddot{X}_{sim}^{ref} \end{bmatrix} = \boldsymbol{Q}_2^{-1} \begin{bmatrix} \ddot{X}_C^{ref} \\ \ddot{X}_D^{ref} \end{bmatrix} \tag{4.21}$$

where $\boldsymbol{Q}_2^{-1}$ means second-order inverse quarry matrix. Finally, the master system and the slave system simulator are operated by the acceleration references, which is obtained by (4.21).

By this means, the following equations are achieved:

$$F_M^{ext} + F_{sim}^{ext} = 0 \tag{4.22}$$

$$X_M^{res} - X_{sim}^{res} = 0. \tag{4.23}$$

where X_M^{res} and X_{sim}^{res} denote position response of the master system and the slave system simulator. Therefore, the bilateral control system is able to generate artificially the law of action and reaction.

Slave System in the real-world The acceleration reference which drives the slave system in the real-world is represented as

$$\ddot{X}_S^{ref} = C_p(s)\left(e^{-sT_{d1}}\ddot{X}_C^{res} - \ddot{X}_S^{res}\right) \tag{4.24}$$

where T_{d1} is communication time delay between the master side and the slave side. Since the actual acceleration response of common mode is obtained through the communication network,

the communication time delay occurs. Therefore, the slave system is operated by the delayed acceleration response.

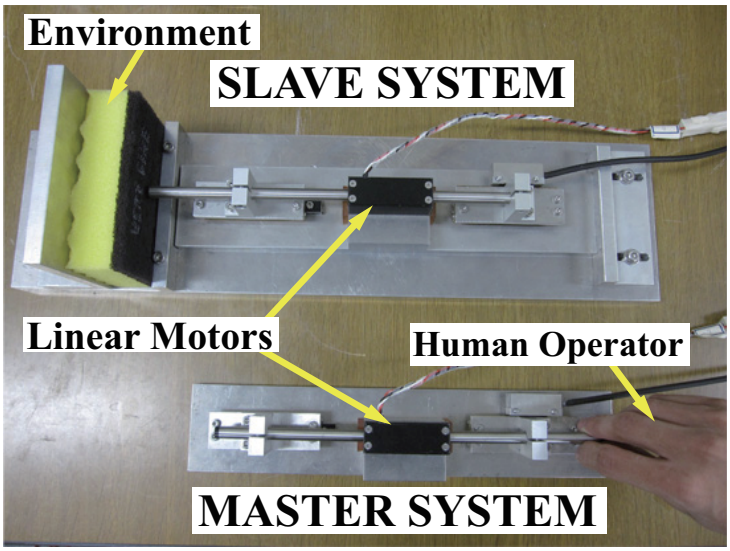

Fig. 4.19. Experimental setup

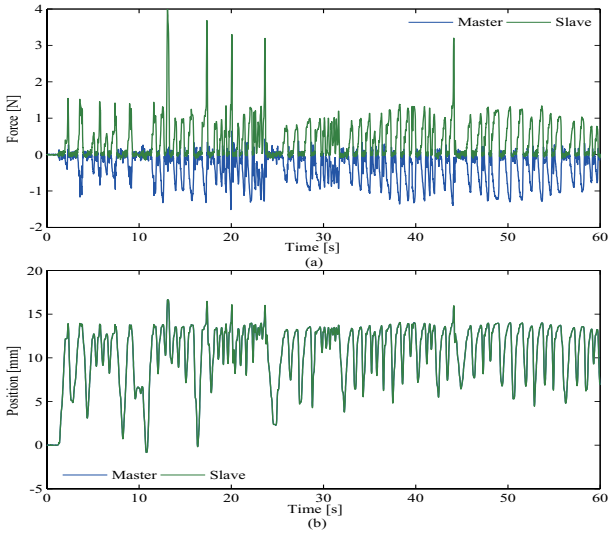

Fig. 4.20. Experimental results (**Time delay = 0 s**). (a) Force. (b) Position.

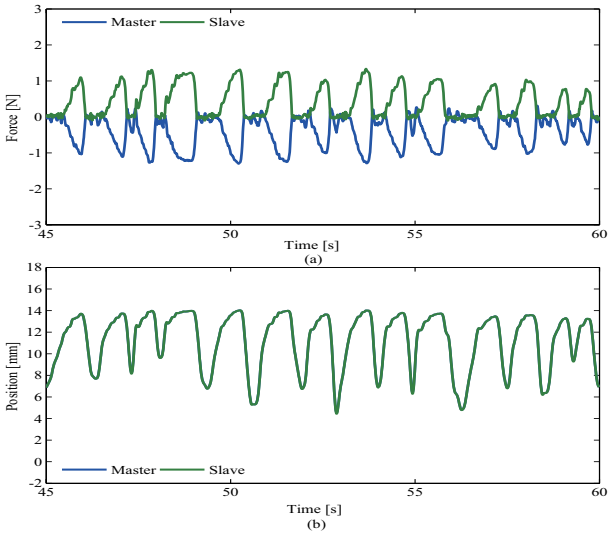

Fig. 4.21. Magnified figure of Fig. 4.20. (a) Shifted force. (b) Shifted position.

4.1.2.4 Environmental Data Memory

In this thesis, the environmental data memory is utilized in order to eliminate the effect of the communication time delay. This section explains about the environmental data memory.

Storage of Environmental Information To achieve the objective of this thesis, the proposed method carries out storage of the environmental information in the slave side. The environmental data memory stores the equivalent acceleration of the real slave system according to

$$F_{mem}\left(e^{-sT_{d2}}\frac{\ddot{X}_S^{res}}{s}\ ,\ e^{-sT_{d2}}\frac{\ddot{X}_S^{res}}{s^2}\right) = e^{-sT_{d2}}\frac{\ddot{X}_S^{equ}}{M_n} \tag{4.25}$$

where F_{mem} is the environmental data memory, which stores the force information in the slave side. T_{d2} denotes communication time delay between the slave side and the master side. The stiffness K and damper D of the environment which was stored to the environmental data memory are expressed as

$$K = \frac{\partial F_{mem}}{\partial X}\quad ,\quad D = \frac{\partial F_{mem}}{\partial \dot{X}}. \tag{4.26}$$

where X and $\dot{X}$ are position and velocity.

In this manner, the environmental data memory stores the environmental information without environmental mathematical model. Therefore, the proposed bilateral controller is able to operate under unknown environments.

Reproduction of Environmental Information The environmental information in the slave side which is stored to the environmental data memory is utilized in order to operate the slave system simulator. To imitate the slave system in the bilateral controller of the master side, the reaction force from the environment is required. The environmental data memory provides the reaction force of the slave system simulator as follows:

$$F_{sim}^{ext} = F_{mem}\left(\frac{\ddot{X}_{sim}^{res}}{s}\ ,\ \frac{\ddot{X}_{sim}^{res}}{s^2}\right) \tag{4.27}$$

Therefore, the human operator in the master side is able to grasp the environmental sense sored to the environmental data memory.

The proposed bilateral controller drives the master system and the slave system simulator, which has the environmental data memory. The environmental data memory imitates the environment in the slave side without environmental model. Since the environmental information in the memory is updated sequentially, the proposed system treats environmental change. Moreover, the slave system in the real-world is not controlled directly by the bilateral control system. Consequently, the proposed system is able to eliminate the effect of the time delay, which induces the vibration and/or overdrive.

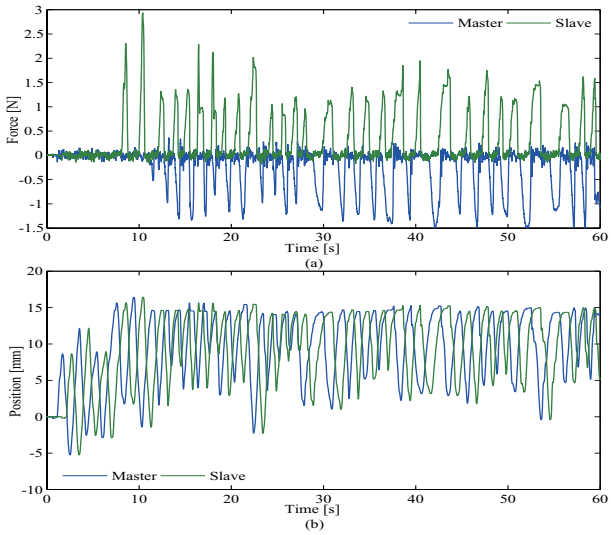

Fig. 4.22. Experimental results (**Time delay = 1 s**). (a) Force. (b) Position.

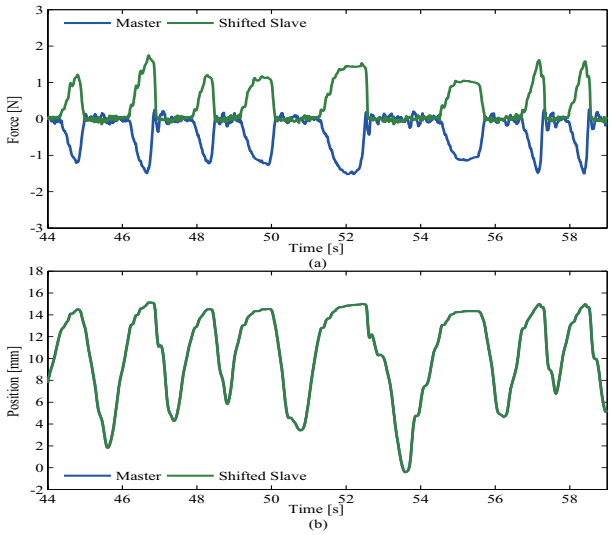

Fig. 4.23. Magnified figure of Fig. 4.22. (a) Shifted force. (b) Shifted position.

4.1.2.5 Experiment

In this thesis, the experiments are carried out to evaluate validity of the proposed method for the time delay. This section mentions about the experiment.

Experimental Setup Fig. 4.19 shows experimental devices used in the experiment. This experiment utilizes two linear motors, which are controlled by RTAI-3.7. The RTAI-3.7 realizes the proposed control system shown in Fig. 4.18. The human operator can touch the master system, and feels the environmental sense in the slave system through the proposed bilateral

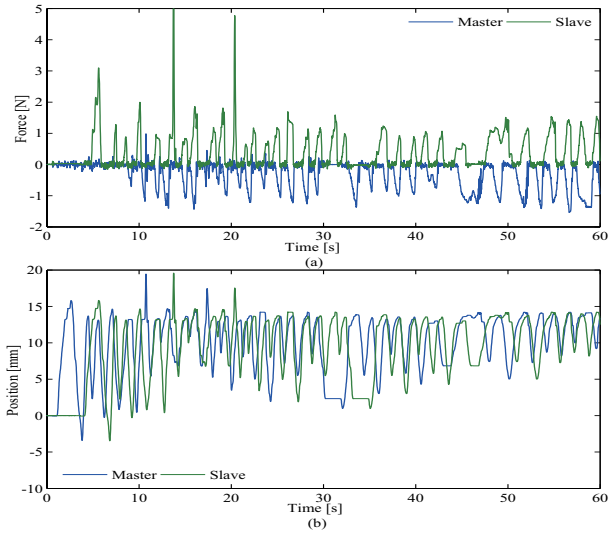

Fig. 4.24. Experimental results (**Time delay = 3 s**). (a) Force. (b) Position.

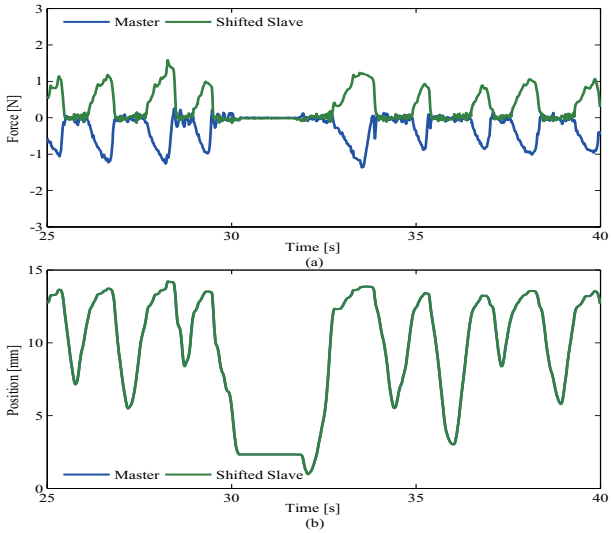

Fig. 4.25. Magnified figure of Fig. 4.24. (a) Shifted force. (b) Shifted position.

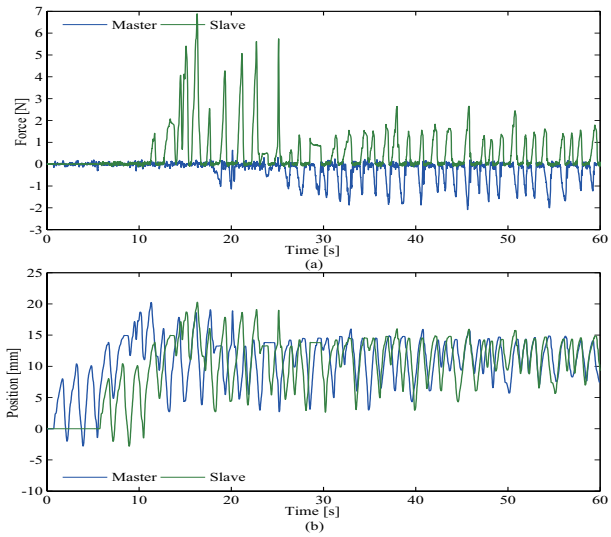

Fig. 4.26. Experimental results (**Time delay = 5 s**). (a) Force. (b) Position.

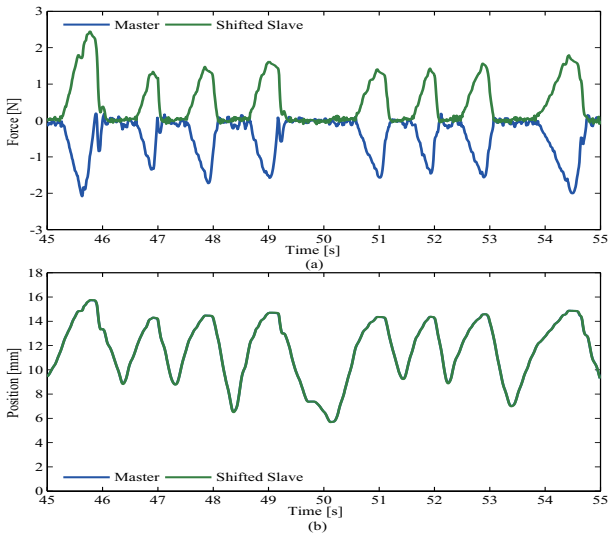

Fig. 4.27. Magnified figure of Fig. 4.26. (a) Shifted force. (b) Shifted position.

controller. The thesis utilizes sponge for the environment. The tip of the slave system contacts to the sponge. In order to emulate the communication network which induces the time delay, the control system generates intentionally the time delay between the master system and the slave system. Table 4.2 shows the setup parameters of the experiment.

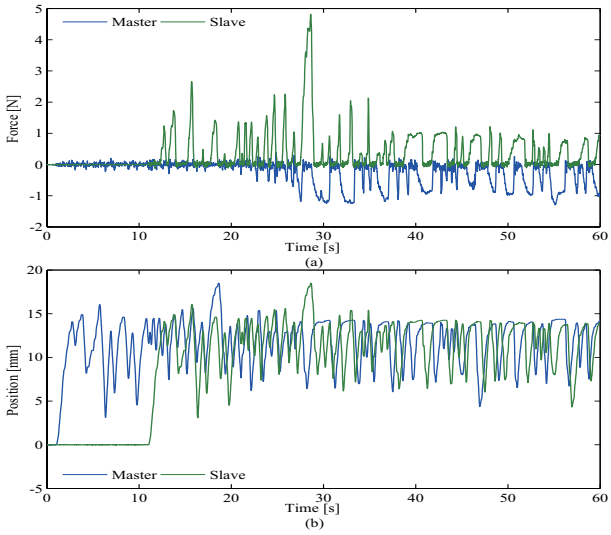

Fig. 4.28. Experimental results (**Time delay = 10 s**). (a) Force. (b) Position.

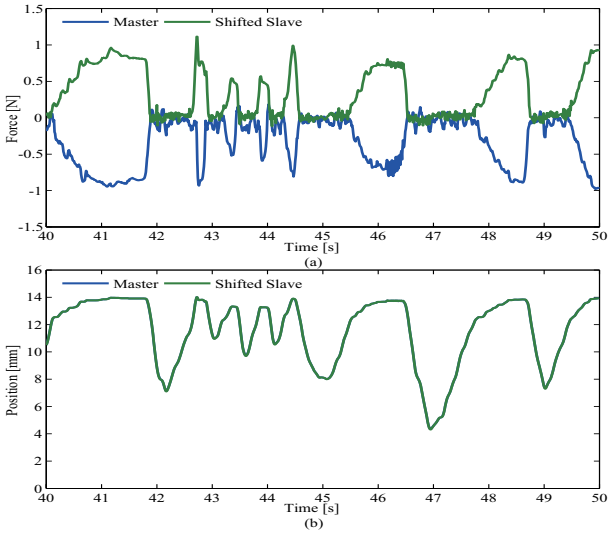

Fig. 4.29. Magnified figure of Fig. 4.28. (a) Shifted force. (b) Shifted position.

Table 4.2. Setup Parameters

T_s	Period of control system	100	μs
K_{fn}	Force constant	3.33	N/A
M_n	Mass of nominal	0.245	kg
K_{fp}	Gain of force controller	5	
K_{pp}	Proportional gain of position controller	10000	
K_{pd}	Velocity gain of position controller	200	
g_{dis}	Pole of the disturbance observer	500	rad/s
g_{reac}	Pole of the reaction force observer	500	rad/s

Experimental Results Figs. 4.20–4.29 show experimental results of the proposed bilateral control system. In this experiment, the time delay of the communication network T_{d1}, T_{d2} is set to 0s, 1s , 3s, 5s and 10s. Since the thesis assumes that the jitter of the network is compensated by the jitter buffer [100], the delay time is set as constant value. Figs. 4.21, 4.23, 4.25, 4.27 and 4.29 show magnified figures of the respective results. The force and position responses of the slave system in these figures are shifted intentionally in the time axis direction to evaluate easily. At first, the proposed bilateral controller cannot generate normally the force information. On the contrary, the proposed bilateral controller provides the environmental force after about

25s. In addition, the proposed system is able to operate even if the time delay is set to 10s. Moreover, the vibration from the time delay in the force and position responses is not induced. These experimental results confirm the validity of the proposed method for the time delay.

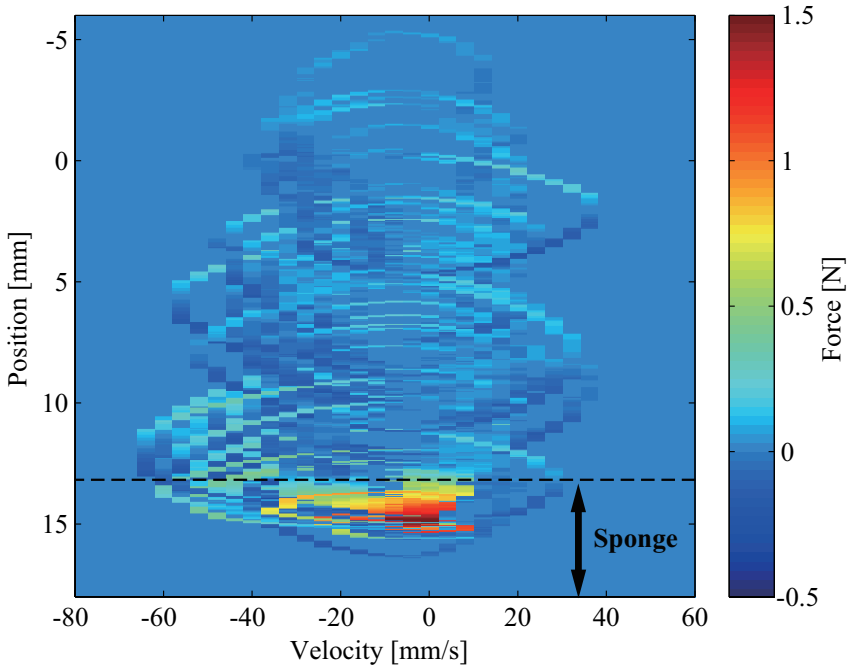

Fig. 4.30. Force information in the environmental data memory.

Fig. 4.30 shows the experimental result of Fig. 4.26. The environmental data shown in Fig. 4.30 expresses the environmental information in the real slave system without environmental mathematical model.

In order to evaluate the validity of the proposed method, correlation coefficients are calculated in this thesis. Table 4.3 shows the correlation coefficients between the master system and the slave system. In the correlation of the force, these values indicate approximately -0.9.

Table 4.3. Correlation coefficients

Delay Time [s]	Correlation of Force	Correlation of Position
0	-0.968	1.00
1	-0.917	1.00
3	-0.897	1.00
5	-0.882	1.00
10	-0.939	1.00

Moreover, the correlation coefficients of the position are 1.00. Therefore, the proposed bilateral controller provides the environmental sense in the slave side to the human operator.

The experiment shown in Figs. 4.20–4.29 confirms that the control law of the bilateral controller is able to be realized as follows:

$$F_M^{ext}(t) + F_S^{ext}(t + T_d) = 0 \tag{4.28}$$

$$X_M^{res}(t) - X_S^{res}(t + T_d) = 0 \tag{4.29}$$

where T_d denotes time delay of the communication network. In other words, the law of action and reaction is generated artificially through the communication network. Therefore, the human operator in the master side is able to grasp the environmental senses by the proposed method, even if the time delay between the master system and the slave system occurs. The experiment confirms that the proposed bilateral controller over the communication network operates normally.

4.1.2.6 Conclusions

This thesis proposes a novel bilateral control system using the environmental data memory. The environmental data memory stores the environmental information in the slave system. The slave system simulator which realizes the proposed bilateral controller utilizes the environmental data memory, so that the slave system simulator imitates the real slave system. The environmental data memory is able to reproduce without environmental mathematical model. Moreover, the slave system in the real-world is not controlled directly by the bilateral control system. Therefore, the proposed system is able to eliminate the effect of the time delay. By the proposed method, the bilateral controller operates normally even if the time delay between the master system and the slave system occurs. It will be useful for industrial applications, medical and welfare human support.

4.1.3 Bilateral Control using Compressor/Decompressor under Low-Rate Communication Network

4.1.3.1 Introduction

The information technology has been evolved by effort and knowledge of the human during the past several decades. The current information technology is directed to the text data, acoustic data, image data and video data. The communication network provides these data in entire world. However, since the human has five organs, the conventional communication technology is not enough. The residual information is olfactory, gustatory and tactile information. The thesis enhances the information technology with respect to the haptic information. Fig. 4.31 shows transfer of the visual, acoustic and haptic information. The acoustic and visual information are unilateral information, however, the haptic information is bilateral information. Therefore, the treatment of the haptic information is difficult. The transfer techniques of haptic information using the network systems are important element in order to extend application of the haptic information technologies. The bilateral control is one of the techniques, which shares the haptic information. The advanced repair in hazard area and the practical remote surgery is available, if the haptic sharing technology is more evolved. The sense of rocks on the moon can be grasped from the earth using the technology.

The general bilateral controller considering the effect of the network has been supposed in regard to the communication time delay [89]–[91]. However, the actual network systems include not only the communication time delay but also the influence of a data transfer period. The problems arise on condition that the data transfer rate is low. Consequently, the thesis utilizes the data compressors and decompressors in the bilateral controller based on a motion-copying system[38] to solve the problems. The motion-copying system based bilateral controller has been created to eliminate induced vibration by the communication time delay [102]. The thesis proposes the motion-copying system based novel bilateral controller, which considers the low-rate communication network. The data compressors and the decompressors are installed between a master system and a slave system in the bilateral controller. The respective systems output

the data of reaction force and position to generate a law of action and reaction. At the same time, the compressors compress previously the each data, so that an amount of the data can be reduced. The decompressors expand the compressed data and provide the data of reaction force and the data of position to the each system. The problem from the low-rate communication network is solved by this method.

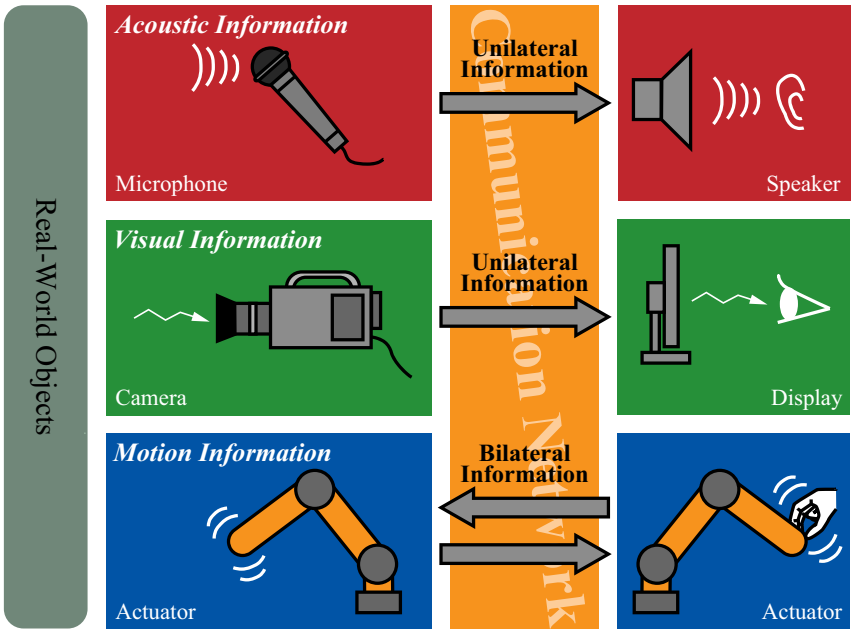

Fig. 4.31. Transfer of the visual, acoustic and haptic information.

This research is organized as follows. Subsection 4.1.3.2 describes concept of the motion-copying system. Subsection 4.1.3.3 explains motion control of the bilateral controller based on the motion-copying system. In 4.1.3.4, the data compressors and the data decompressors in the bilateral controller are presented. The method of the compression and the decompression is denoted in the subsection. The experimental results in 4.1.3.5 confirm the viability of the proposed method. The last section concludes this study.

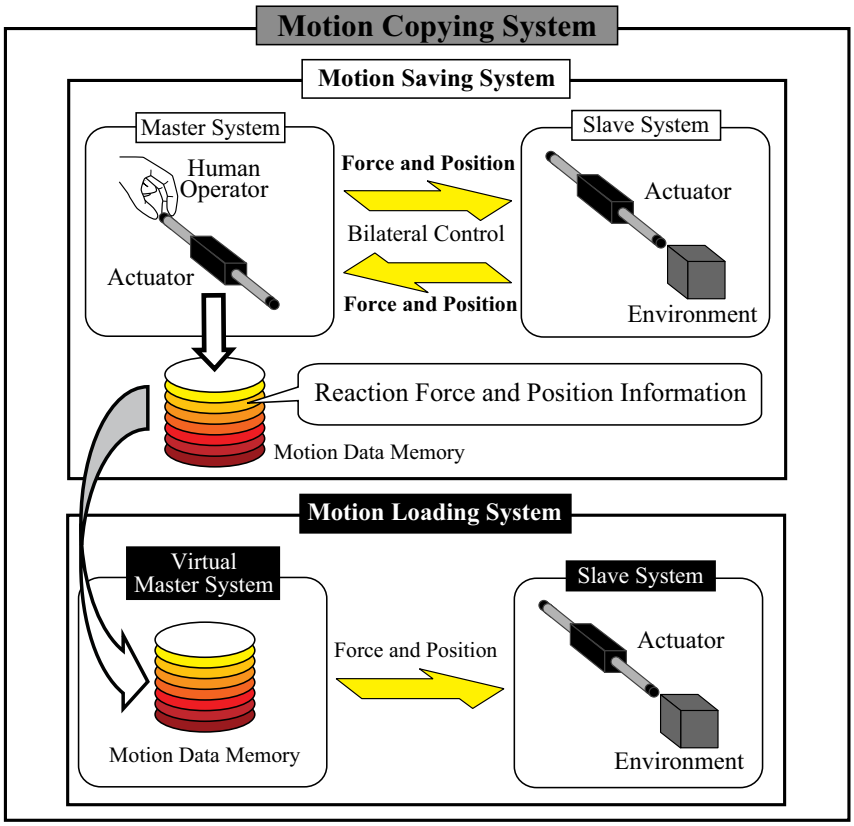

Fig. 4.32. Conceptual diagram of motion-copying system.

4.1.3.2 Motion-Copying System

This section explains concept of the motion-copying system [38]. In this thesis, the motion-copying system realizes the bilateral controller even if communication time delay occurs. Fig. 4.32 shows conceptual diagram of the motion-copying system. The motion-copying system consists of both the motion-saving system and the motion-loading system.

The motion-saving system is constructed by general bilateral controller. The human operator grasps the environment of other side using the control system. At the same time, impressed force by the human operator and position of the master motor is stored to motion data memory. The saved force and position information is used when the motion-loading system reproduces saved motion of the human operator. More specifically, the motion-saving system realizes save

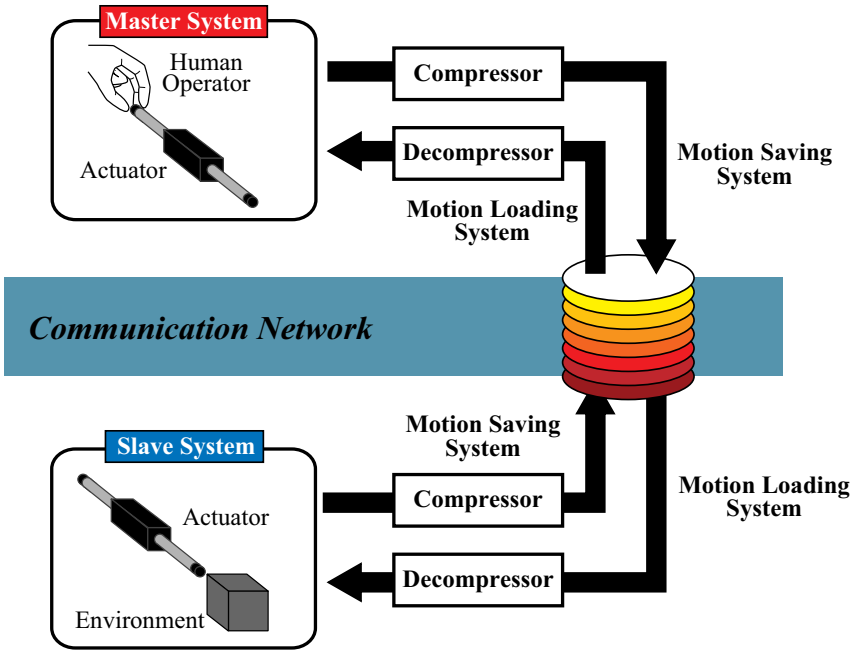

Fig. 4.33. Conceptual diagram of bilateral controller based on motion-copying system.

of the human operator motion.

The motion-loading system is operated by master-slave controller. A calculation method of controller value for realization of the motion-loading system is similar to the case of the motion-saving system. Though, the motion-loading system does not have a motor in the master-system side, because the motion data memory is used instead of the master system. The motion data memory holds the impressed force by the human operator and the position information of the master motor. In the motion-loading system, a motor of the slave system is operated by the motion data memory. The reproduced position and force by the motion-loading system corresponds to the saved ones.

4.1.3.3 Motion-Copying System based Bilateral Control

The construction method of the bilateral control based on the motion-copying system is described in this section.

Concept The motion-copying system is able to preserve and reproduce both force and position as previously noted. This function stabilizes the bilateral controller, which includes communication time delay [102]. Fig. 4.33 shows conceptual diagram of the motion-copying system based bilateral controller. The general motion-saving system preserves the force and position information to the memory. Also, the general motion-loading system reproduces the force and position using the memory. However, the motion-copying system based bilateral control preserves and reproduces using communication network. In short, the motion-copying system utilizes communication time delay instead of the motion data memory. The motion-copying system copies the motion in local system to remote system.

Motion Control The modal decomposition is applied to construct the bilateral controller. This thesis uses quarry matrix, which realizes modal decomposition. The second order quarry matrix $\boldsymbol{Q}_2$ is defined as [63]

$$\boldsymbol{Q}_2 = \frac{1}{2}\begin{bmatrix} 1 & 1 \\ 1 & -1 \end{bmatrix}. \tag{4.30}$$

This matrix $\boldsymbol{Q}_2$ decomposes to common mode and differential mode [65]. Fig. 4.34 shows block diagram of the bilateral controller based on motion-copying system. The system consists of two sections. The first section is master system; the other system is slave system. The communication network exists between the master system and the slave systems. The quarry matrix $\boldsymbol{Q}_2$ transforms from reaction force of the master and slave in the master side $\hat{F}^{ext}_{Mm}$, $\hat{F}^{ext}_{Sm}$ to reaction force of common mode and differential mode $\hat{F}^{ext}_{Cm}$, $\hat{F}^{ext}_{Dm}$.

$$\begin{bmatrix} F^{res}_{Cm} \\ F^{res}_{Dm} \end{bmatrix} = \boldsymbol{Q}_2 \begin{bmatrix} \hat{F}^{ext}_{Mm} \\ \hat{F}^{ext}_{Sm} \end{bmatrix} \tag{4.31}$$

In the slave side, the reaction force of the master and slave $\hat{F}^{ext}_{Ms}$, $\hat{F}^{ext}_{Ss}$ is transformed to F^{res}_{Cs}, F^{res}_{Cs}.

$$\begin{bmatrix} F^{res}_{Cs} \\ F^{res}_{Ds} \end{bmatrix} = \boldsymbol{Q}_2 \begin{bmatrix} \hat{F}^{ext}_{Ms} \\ \hat{F}^{ext}_{Ss} \end{bmatrix} \tag{4.32}$$

The position response of the common and differential mode x^{res}_{Cm}, x^{res}_{Dm} in the master side is calculated by

$$\begin{bmatrix} x^{res}_{Cm} \\ x^{res}_{Dm} \end{bmatrix} = \boldsymbol{Q}_2 \begin{bmatrix} x^{res}_{Mm} \\ x^{res}_{Sm} \end{bmatrix}. \tag{4.33}$$

where, x^{res}_{Mm} and x^{res}_{Sm} are position response of the master and slave in the master side. Correspondingly, the position responses in the slave side are calculated by

$$\begin{bmatrix} x^{res}_{Cs} \\ x^{res}_{Ds} \end{bmatrix} = \boldsymbol{Q}_2 \begin{bmatrix} x^{res}_{Ms} \\ x^{res}_{Ss} \end{bmatrix} \tag{4.34}$$

where, x^{res}_{Ms}, x^{res}_{Ss}, x^{res}_{Cs} and x^{res}_{Ds} are position response of the master, position response of the slave, position of the common mode and position of the differential mode, respectively.

The purpose of the bilateral controller is generation of the law of action and reaction. Thus, the reaction force of the common mode and the position of the differential mode in each side are controlled by

$$\ddot{x}^{ref}_{Cm} = -\ C_f\ F^{res}_{Cm} \quad , \quad \ddot{x}^{ref}_{Dm} = -\ C_p\ x^{res}_{Dm} \tag{4.35}$$

$$\ddot{x}^{ref}_{Cs} = -\ C_f\ F^{res}_{Cs} \quad , \quad \ddot{x}^{ref}_{Ds} = -\ C_p\ x^{res}_{Ds} \tag{4.36}$$

where, $\ddot{x}^{ref}_{Cm}$ and $\ddot{x}^{ref}_{Dm}$ denote acceleration reference of the common and differential mode in the master side. $\ddot{x}^{ref}_{Cs}$ and $\ddot{x}^{ref}_{Ds}$ are acceleration reference of the common mode and differential mode in the slave side. C_f and C_p are force controller and position controller, which are shown by

$$C_f = K_{fp} \tag{4.37}$$

$$C_p = K_{pp} + \frac{s\ g_{pd}}{s + g_{pd}}\ K_{pd} \tag{4.38}$$

where, K_{fp}, K_{pp}, K_{pd} and g_{pd} denote the proportional gain of the force controller, the proportional gain of the position controller, the differential gain of the position controller and the pole of the pseudo derivative. The controllers in equation (4.37),(4.38) derive respective acceleration references. These acceleration references are transformed by

$$\begin{bmatrix} \ddot{x}^{ref}_{Mm} \\ \ddot{x}^{ref}_{Sm} \end{bmatrix} = \boldsymbol{Q}_2^{-1} \begin{bmatrix} \ddot{x}^{ref}_{Cm} \\ \ddot{x}^{ref}_{Dm} \end{bmatrix} \tag{4.39}$$

$$\begin{bmatrix} \ddot{x}^{ref}_{Ms} \\ \ddot{x}^{ref}_{Ss} \end{bmatrix} = \boldsymbol{Q}_2^{-1} \begin{bmatrix} \ddot{x}^{ref}_{Cs} \\ \ddot{x}^{ref}_{Ds} \end{bmatrix} \tag{4.40}$$

where, $\ddot{x}_{Mm}^{ref}$ and $\ddot{x}_{Sm}^{ref}$ are acceleration references of the master and slave in the master side. $\ddot{x}_{Ms}^{ref}$ and $\ddot{x}_{Ss}^{ref}$ denote acceleration references in the slave side. The acceleration references control the actuators in each side.

Fig. 4.35 shows detailed block diagram of the master and slave system. $\ddot{x}^{ref}$, M_n, F^{ext}, $\dot{x}^{res}$ and x^{res} denote acceleration reference of a motor, mass of actuator, reaction force, velocity and position of a motor, respectively. i^{ref} and K_{fn} are current reference and nominal force constant. The disturbance observer [66] estimates and compensates disturbance force $\hat{F}^{dis}$ to realize robust acceleration control. The reaction force observer estimates the reaction force $\hat{F}^{ext}$, which is impressed by the environment [64].

Since the communication network is utilized instead of the motion data memory, the motion data memory does not exist in actual block diagram of the control system. In this wise, the bilateral controller based on the motion-copying system is constructed, so that affect of the communication time delay can be eliminated [102].

4.1.3.4 Bilateral Control using Compressor/Decompressor

This section explains motion-copying system based bilateral controller, which implemented data compressors and the decompressors.

Concept The general bilateral controller based on the motion-copying system conveys simply the force and position data [102]. These data should be compressed and decompressed using technologies of computer science in order to communicate efficiently. This thesis proposes that the method of compression and decompression is applied to the bilateral controller. The method compresses the force and position data, so that the amount of the data which flows in the network can be reduced. The conventional bilateral controller considers only the communication time delay. However, the actual communication network includes not only the communication time delay but also the effect of the data transfer rate. Therefore, the bilateral controller has to prepare for the low data transfer rate. The thesis confirms effectivity of the proposed method with respect to the low data transfer rate.

Compression/Decompression Fig. 4.36 shows block diagram of the bilateral controller, which implements compressor and decompressor. When the data transfer is repeated every the control period of N times, the period of the data transfer T_t is denoted by

$$T_t = NT_s \tag{4.41}$$

where, T_s is period of the control system. A counting value of the data transfer period j is defined using floor function as

$$j = \left\lfloor \frac{i}{N} \right\rfloor \quad (i = 0, 1, 2, \cdots) \tag{4.42}$$

where, i denotes a counting value of the control period. The reaction force data in the master system F_{Mm}^{ext} is compressed using a delta compression. The delta compression calculates the difference value of input signals, so that the data bits can be reduced. The difference compression is used in compression method of MPEG, which is utilized for video file format. The compressed reaction force F_M^{comp} is calculated by

$$F_M^{comp}(j) = F_{Mm}^{ext}(Nj) - F_{Mm}^{ext}(N(j-1)) \ . \tag{4.43}$$

Additionally, the compressor transmits the reaction force data F_M^{comp} to the slave side on condition that

$$i \bmod N = 0 \ . \tag{4.44}$$

Though this compression method is non-invertible, an amount of the force data is reduced to $1/N$.

On the other hand, the decompression of the compressed data F_M^{comp} is carried out by

$$F_{Ms}^{ext}(i) = \frac{F_M^{comp}(j)}{N} \times (i - Nj) + F_{Ms}^{ext}(Nj) \ . \tag{4.45}$$

Finally, the reaction force of the master F_{Ms}^{ext} is received in the slave side. In case of another parameters (F_{Ss}^{ext}, x_{Mm}^{res} and x_{Ss}^{res}), the calculation method of compression and decompression is same as above method. Since the above method immediately executes operations of compression/decompression, processing time is short.

Motion Control Fundamentally, the control method is same as the general bilateral controller based on the motion-copying system. However, the existence of the compressor and decompressor is the critical difference between the bilateral controller in Fig. 4.34 and the proposed method in Fig. 4.36.

4.1.3.5 Experiment

Experimental Setup Fig. 4.37 shows the experimental devices. The experimental devices consist of the actuator in each side and the actuator of a force control system. A block diagram of the force control system is shown in Fig. 4.38. The force control system provides the force, which impresses to the master system in the bilateral controller. The force command F^{cmd} is denoted by

$$F^{cmd} = \cos(2\pi ft + \pi) + 1 \tag{4.46}$$

where, f and t are frequency and time, respectively. The frequency f is set to 1.5 Hz in the experiment. Table 4.4 shows the setup parameters.

Table 4.4. Setup Parameters

T_s	Period of control system	100	μs
K_{fn}	Force constant	3.33	N/A
M_n	Mass of nominal	0.245	kg
C_f	Assist gain	10	
K_p	Proportional gain of the PD controller	10000	
K_d	Differential gain of PD controller	200	
g_{pd}	Pole of pseudo derivative for the PD controller	10000	rad/s
g_{dis}	Pole of the disturbance observer	1000	rad/s
g_{reac}	Pole of the reaction force observer	1000	rad/s

In the experiment, a control-system computer artificially generates the narrow-capacity communication line.

Experimental Results Figs. 4.39 to 4.44 show experimental results of the general bilateral controller based on motion-copying system and the proposed method. The vibration of the

reaction force occurs in case without the compressor and decompressor. On the contrary, the experimental results confirm that the bilateral controller normally operates in case of using the proposed method. The rate of compression in Fig. 4.40, Fig. 4.42 and Fig. 4.44 are 0 %, 90 % and 95 %. This section calculates a signal to noise ratio in order to confirm validity of the proposed method. The signal to noise ratio S_{NR} is given by

$$S_{NR} = 10 \log_{10} \frac{\sum {F_M^{ext}}^2}{\sum (F_M^{ext} - F^{cmd})^2} \ . \tag{4.47}$$

Fig. 4.45 shows the relation of the data transfer period and the signal to noise ratio. Though the non-invertible compression method adversely affects at 2.5ms, the validity of the proposed method is confirmed by the experimental results.

4.1.3.6 Conclusion

The thesis proposes novel bilateral controller based on motion-copying system considering the network of low-rate data transfer. Since the proposed system utilizes the non-invertible compressors and decompressors, the amount of data which flows in the network can be reduced. Therefore, the bilateral controller normally operates even if the data transfer rate of the network is low. By the experiment, the thesis confirms the validity of the proposed method. The problems arise in case without the compressors and the decompressors, however, the proposed method reduces the vibration of the reaction force. It will be useful for industrial applications, medical and welfare human assistance.

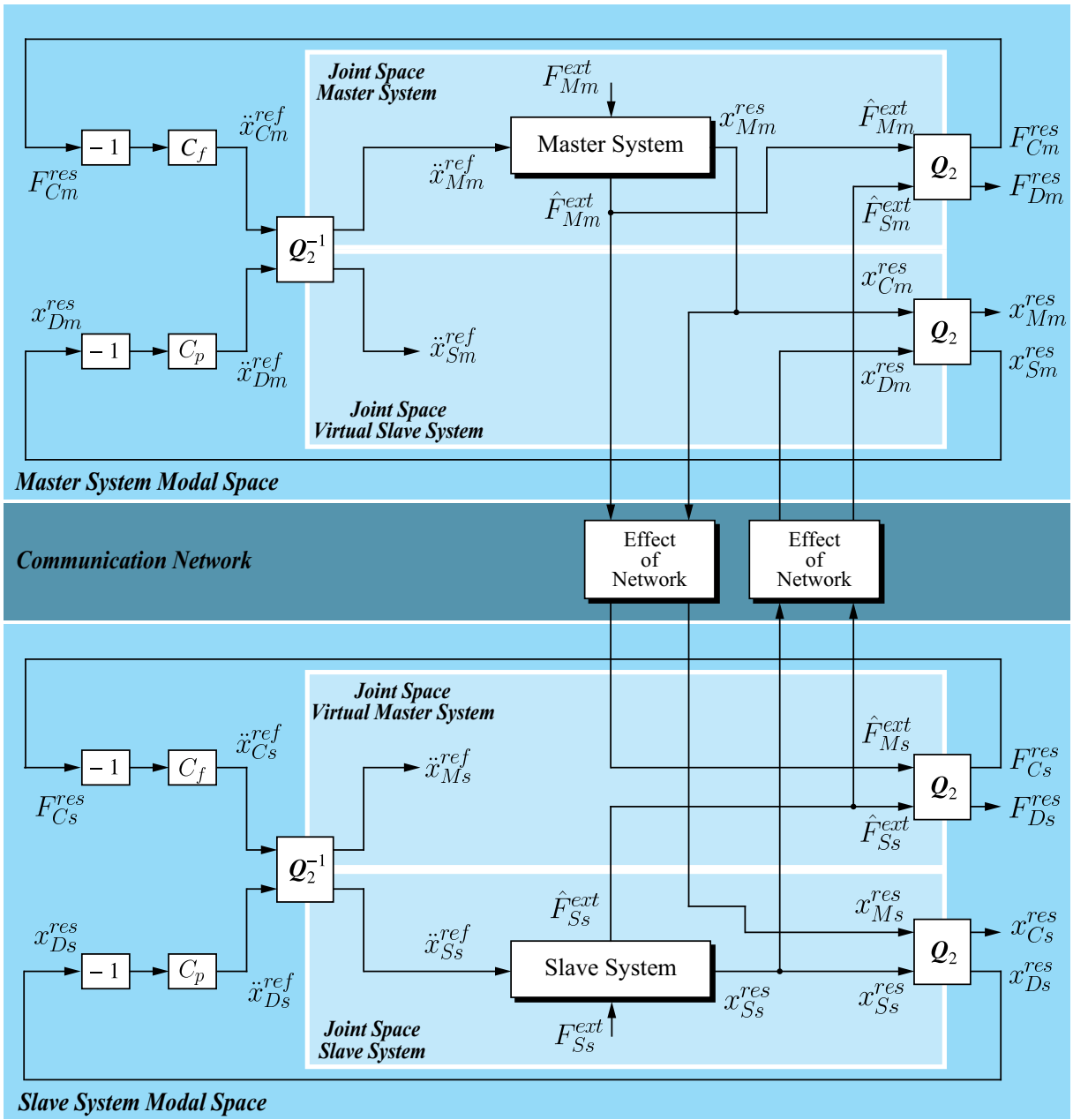

Fig. 4.34. Block diagram of bilateral controller based on motion-copying system considering effect of communication network.

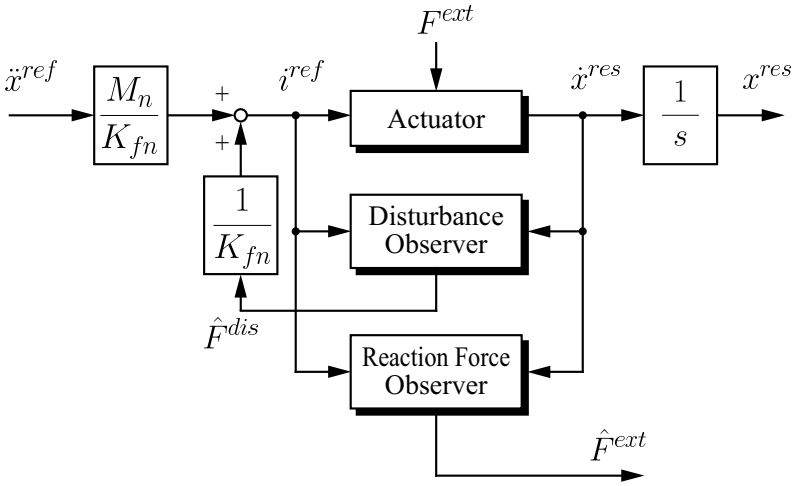

Fig. 4.35. Detailed block diagram of master and slave system.

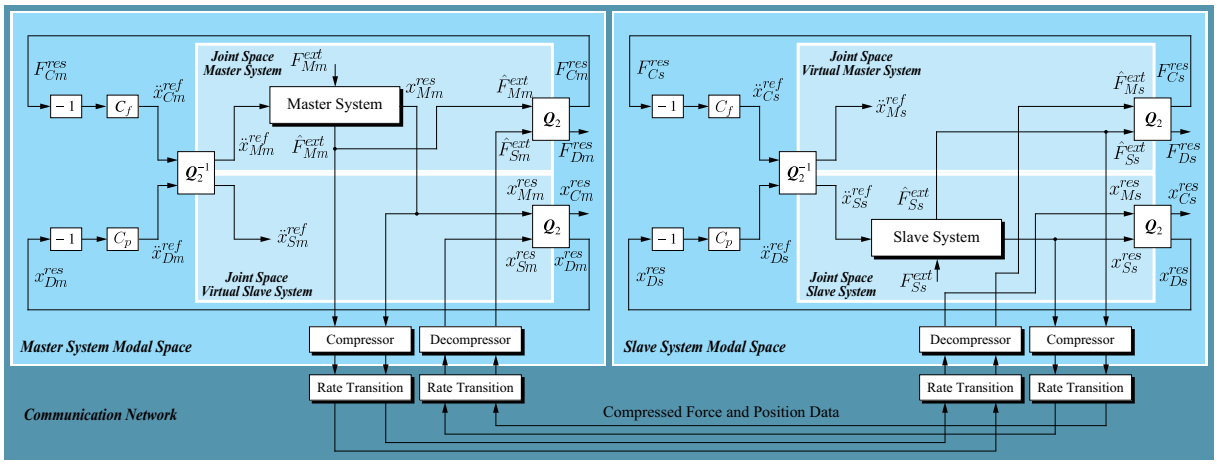

Fig. 4.36. Block diagram of bilateral control based on motion-copying system using compressors and decompressors.

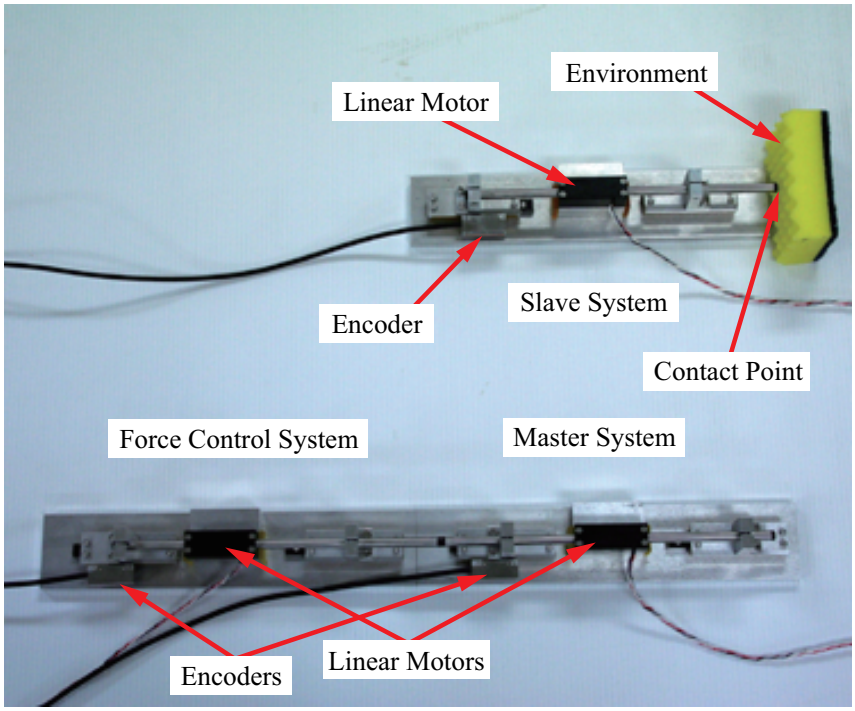

Fig. 4.37. Experimental devices.

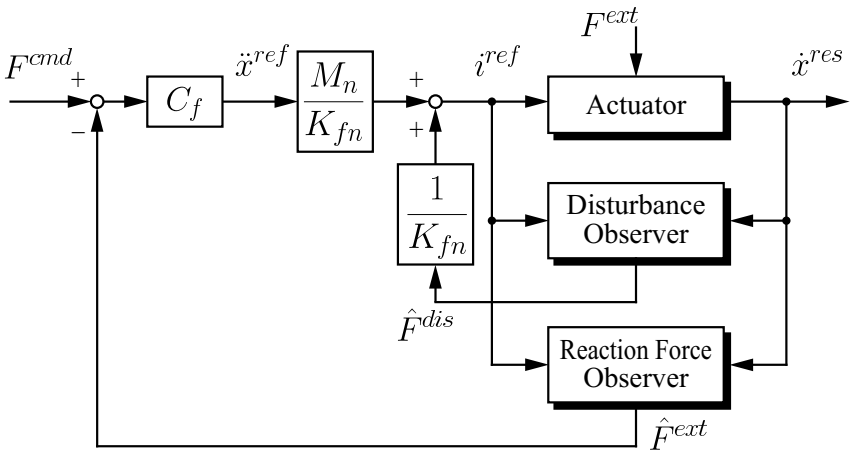

Fig. 4.38. Block diagram of force control system.

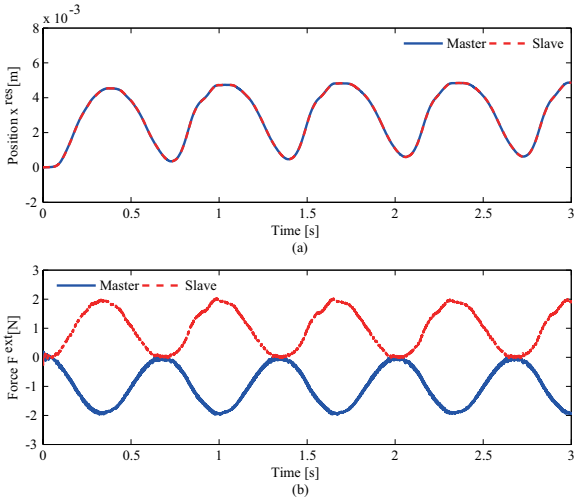

Fig. 4.39. Experimental results without proposed method. ($T_t = 100\mu$s)

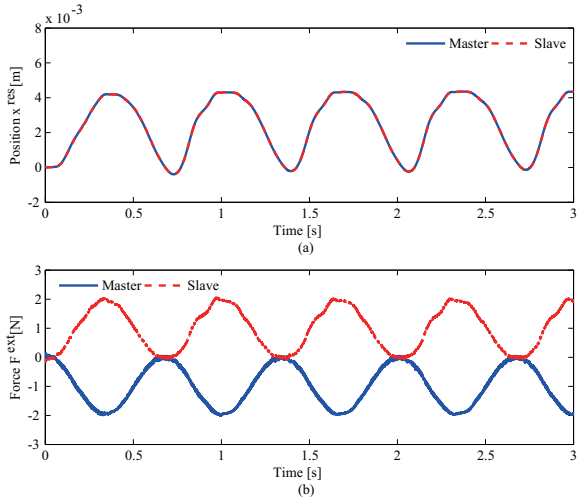

Fig. 4.40. Experimental results using proposed method. ($T_t = 100\mu$s)

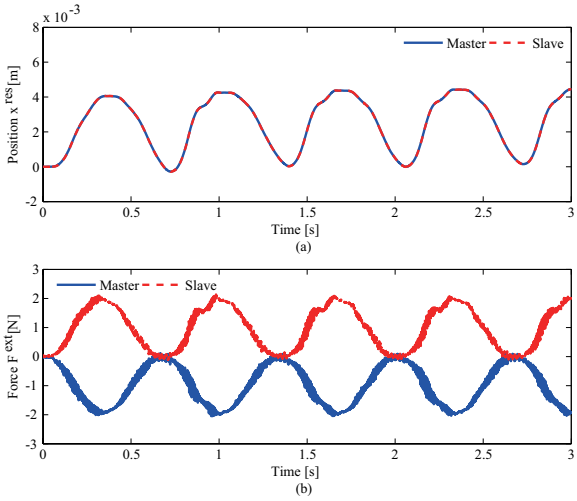

Fig. 4.41. Experimental results without proposed method. ($T_t = 1$ms)

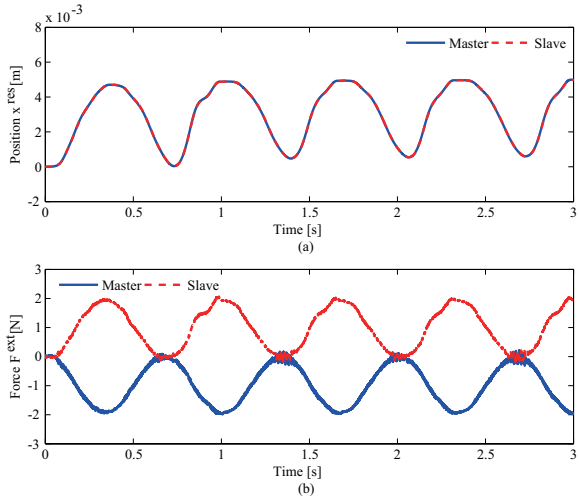

Fig. 4.42. Experimental results using proposed method. ($T_t = 1$ms)

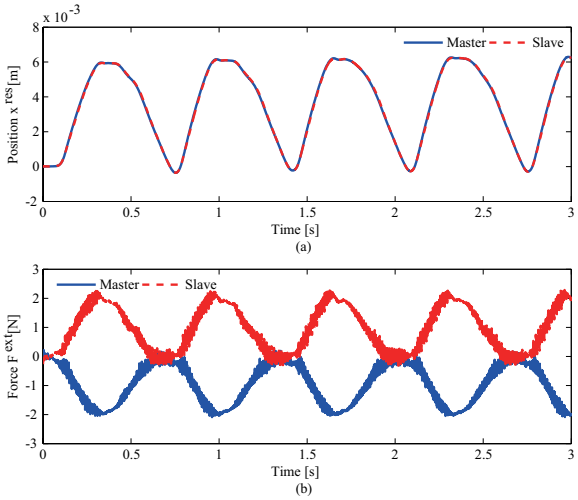

Fig. 4.43. Experimental results without proposed method. ($T_t = 2$ms)

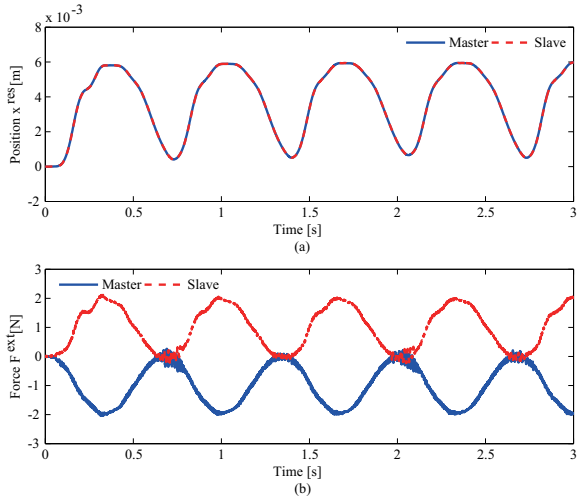

Fig. 4.44. Experimental results using proposed method. ($T_t = 2$ms)

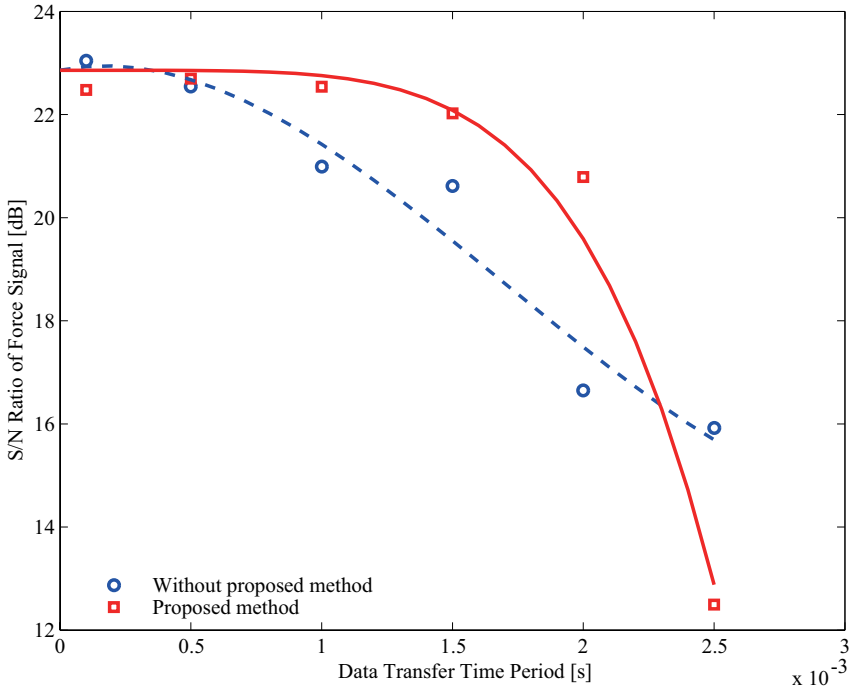

Fig. 4.45. Data transfer period T_t vs. S/N ratio of force signal.

4.1.4 Bilateral Control Using Master/Slave Simulator for Haptic Communication

4.1.4.1 Introduction

The bilateral controller is used to transmit and share haptic information between a master system and a slave system. In a transmission system, the bilateral controller encounters problems in the event of packet loss and/or disconnections. Fig. 4.46 shows a conceptual diagram of

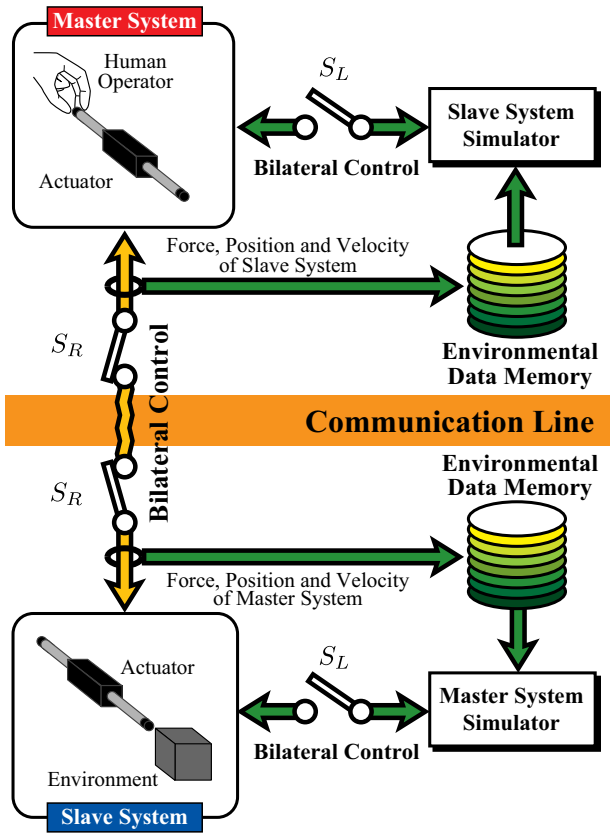

Fig. 4.46. Conceptual diagram of the proposed method

the proposed system. The proposed system consists of a master system, a slave system, and master/slave simulators. In this study, master/slave simulators and environmental data memory are used to reduce the above-mentioned problems. In the case of normal operation, the system is operated by the conventional bilateral control system. During th operation of the bilateral controller, the respective environmental data memories store force responses of the actuators in

the remote side; the environmental data memories also store the environmental characteristics. The control system is operated by the environmental data memory and master/slave simulator when the communication lines are disconnected. The stored force values are outputted as the reaction force of the simulators according to velocity and position responses By the proposed method, a human operator grasps the environmental sense even if the communication line is disconnected. The validity of the above method is confirmed by the experiment. The proposed method is expected to be useful in industrial applications and for providing medical and human support to patients.

4.1.4.2 Concept of Proposed Method

As mentioned above, the time delay and the packet loss of the communication network are problem in the practical use. This thesis focuses on the packet loss and disconnection of the network. In Fig. 4.47, if the packet loss and/or the disconnection occur, switches between

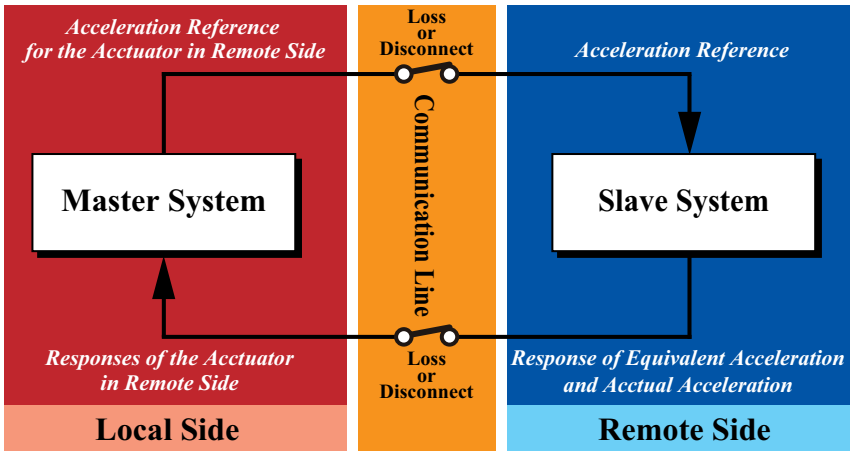

Fig. 4.47. Bilateral control through communication network.

the master system and the slave system is turned off. Therefore, response value of the systems cannot be transmitted and received in the each systems. Thus, the actuators are locked, and the bilateral controller does not operate normally. In short, the haptic transmission is not achieved.

Consequently, this thesis proposes solution which is capable of reducing the packet loss and the disconnection. To solve the problem, the proposed system uses master/slave simulators

and environmental data memory, when the loss and the disconnection occur. Fig. 4.46 shows conceptual diagram of the proposed method. When condition of the communication is normal, the switch S_R is set to on-state and the switch S_L is set to off-state. In this case, the normal bilateral control system is activated. At the same time, the environmental data memory stores the force according to velocity and position responses.

In the case of disconnection, the switch S_R is turned off, and the switch S_L is turned on. Additionally, the storage phase of the force is stopped, and the environmental data memory reproduces the force depending on the velocity and the position. In other words, the actuators in the local side is controlled by the master/slave simulator located in the local side. The switch S_R is set to ON-state and the switch S_L is set to OFF-state, when condition of the communication back to the normal state.

By this means, the transmission of the haptic sensation can be realized, even if the network failure occurs.

4.1.4.3 Motion Control

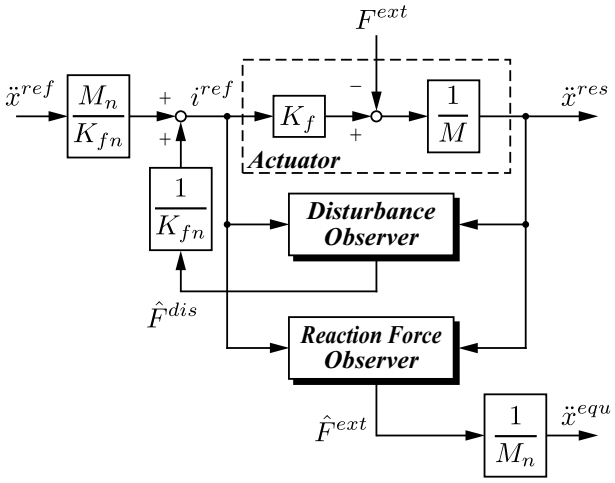

Fig. 4.48. Block diagram of master and slave systems.

Fig. 4.48 shows block diagram of the master/slave simulator. In Fig. 4.48, $\ddot{x}^{equ}$ represents

equivalent acceleration, which is derived as

$$\ddot{x}^{equ} = \frac{1}{M_n}\hat{F}^{ext} \tag{4.48}$$

where M_n means nominal mass of the actuators. The master/slave simulator shown in Fig. 4.48 is implemented in the control computer with real time operating system such as RTAI-3.7. Fig. 4.49 shows block diagram of the bilateral control system by using master/slave simulator. The proposed system consists of the master and slave side, which have modal space and joint space. In Fig. 4.49, subscripts M, S, C, and D denote master, slave, common mode, and differential mode, respectively. Moreover, super scripts m and s represent the master side and the slave side. In fact, the control method of the proposed system is same as the basic bilateral control.

4.1.4.4 Bilateral Control using Environmental Data Memory

Switching Method for Network Failure The switching method for network failure is described. In the case of network failure, the each systems are switched from the actuator in the remote side to the simulator in the local side.

In Fig. 4.49, coefficients of the switches is defined as $S_R,\ S_L$. The equivalent acceleration and the acceleraion response are determined as

$$^{m}\ddot{x}_S^{equ} = S_R{}^{s}\ddot{x}_S^{equ} + S_L{}^{m}\ddot{x}_S^{equ*} \tag{4.49}$$

$$^{m}\ddot{x}_S^{res} = S_R{}^{s}\ddot{x}_S^{res} + S_L{}^{m}\ddot{x}_S^{res*} \tag{4.50}$$

$$^{s}\ddot{x}_M^{equ} = S_R{}^{m}\ddot{x}_M^{equ} + S_L{}^{s}\ddot{x}_M^{equ*} \tag{4.51}$$

$$^{s}\ddot{x}_M^{res} = S_R{}^{m}\ddot{x}_M^{res} + S_L{}^{s}\ddot{x}_M^{res*}. \tag{4.52}$$

where $^{m}\ddot{x}_S^{equ*}$ and $^{m}\ddot{x}_S^{res*}$, $^{s}\ddot{x}_M^{equ*}$ and $^{s}\ddot{x}_M^{equ*}$ denote equivalent acceleration and acceleration response of the salve simulator, equivalent acceleration and acceleration response of the master simulator, This thesis defines that S_{comm} is set to 1 in the case of on-state and S_{comm} is set to 0 in the case of off-state. When the communication is established, the switch coefficients $S_R,\ S_L$

are set to

$$S_R = \begin{cases} 1 & (S_{comm} = 1) \\ 0 & (S_{comm} = 0) \end{cases} \tag{4.53}$$

$$S_L = \begin{cases} 0 & (S_{comm} = 1) \\ 1 & (S_{comm} = 0) \end{cases} . \tag{4.54}$$

In short, the basic bilateral controller is activated when the condition is normal. In case where the packet loss and/or the disconnection, the responses of the master/slave simulator is used.

Storage of Haptic Environment The environmental data memories store the force responses of the remote side, when the communication is established. The force response of the slave side ${}^{m}F_{S}^{env}$ is stored to the environmental data memory as follows:

$${}^{m}F_{S}^{env}({}^{m}\dot{x}_{S}^{res}, {}^{m}x_{S}^{res}) = M_n \, {}^{m}\ddot{x}_{S}^{equ} \tag{4.55}$$

where ${}^{m}\dot{x}_{S}^{res}$ and ${}^{m}x_{S}^{res}$ are position and velocity responses of the slave system in the master side. These responses are given by

$${}^{m}\dot{x}_{S}^{res} = \frac{1}{s} \, {}^{m}\ddot{x}_{S}^{res} \tag{4.56}$$

$${}^{m}x_{S}^{res} = \frac{1}{s^2} \, {}^{m}\ddot{x}_{S}^{res}. \tag{4.57}$$

As with the slave side, the force of the master system ${}^{s}F_{M}^{env}$ is stored according to

$${}^{s}F_{M}^{env}({}^{s}\dot{x}_{M}^{res}, {}^{s}x_{M}^{res}) = M_n \, {}^{s}\ddot{x}_{M}^{equ} \tag{4.58}$$

$${}^{s}\dot{x}_{M}^{res} = \frac{1}{s} \, {}^{s}\ddot{x}_{M}^{res} \tag{4.59}$$

$${}^{s}x_{M}^{res} = \frac{1}{s^2} \, {}^{s}\ddot{x}_{M}^{res} \tag{4.60}$$

where ${}^{s}\dot{x}_{M}^{res}$ and ${}^{s}x_{M}^{res}$ represent velocity and position responses of the master. Actually, 2-dimensional lookup tables are generated in the control computer. Since the environmental data memories stores the raw force data, the haptic sensation of target object is able to be stored without modeling the environment.

Reproduction of Haptic Environment The environmental data memories reproduce and output the environmental force to the master/slave simulator, when the disconnection is detected. In this case, the force of the slave simulator ${}^{m}F_{S}^{ext}$ and the force of the master simulator ${}^{s}F_{M}^{ext}$ are given by

$$
\begin{aligned}
{}^{m}F_{S}^{ext} &= {}^{m}F_{S}^{env}\left({}^{m}\dot{x}_{S}^{res}\ ,\ {}^{m}x_{S}^{res}\right) && (4.61)\\
{}^{s}F_{M}^{ext} &= {}^{s}F_{M}^{env}\left({}^{s}\dot{x}_{M}^{res}\ ,\ {}^{s}x_{M}^{res}\right). && (4.62)
\end{aligned}
$$

By this means, the proposed system is capable of providing the haptic sensation of the target environment, even if the network failure occurs.

4.1.4.5 Experiment

Experimental Setup Fig. 4.50 shows experimental setup. These actuators are controlled by the bilateral control system proposed in this thesis. In order to evaluate the proposed method, the position controller is implemented independently to one of actuator. The position command x^{cmd} is set as sinusoidal wave form given by

$$x^{cmd} = A\cos(2\pi \times 0.65t + \pi) + A. \tag{4.63}$$

Moreover, command modulated by frequency is also used as follows:

$$
\begin{aligned}
x^{cmd} &= -A\cos(2\pi \times 1.5t + f + \pi) + A && (4.64)\\
f &= -3\cos(2\pi \times 0.2t + \pi) && (4.65)
\end{aligned}
$$

where t is time, and amplitude of sinusoidal wave is set as $A = 2.0 \times 10^{-3}$ m. The target environment in the slave side is sponge. In addition, condition of the communication network is artificially set as

$$S_{comm} = \begin{cases} 1 & (0 \le t < 10\ ,\ 15 \le t) \\ 0 & (10 \le t < 15) \end{cases} \tag{4.66}$$

Table 4.5 shows setup parameters.

Table 4.5. Setup parameters.

T_s	Period of control system	100	μs
K_{fn}	Force constant	3.33	N/A
M_n	Mass of nominal	0.245	kg
K_{fp}	Force controller gain	5	
K_{pp}	Position controller gain	10000	
K_{pd}	Position controller gain	200	
g_{pd}	Pole of pseudo derivative	1000	rad/s
g_{dis}	Pole of the disturbance observer	1000	rad/s
g_{reac}	Pole of the reaction force observer	1000	rad/s

Experimental Results Figs. 4.51 and Fig. 4.52 show experimental results. In respective figures, (a) shows the force responses $\hat{F}_M^{ext}$, $\hat{F}_S^{ext}$, and (b) indicates the position responses of the master and slave systems x_M^{res}, x_S^{res}. Additionally, Fig. 4.53 shows the force response ${}^mF_S^{env}$, which stored to the environmental data memory.

The network failure occurs at 10 to 15 s, and the switch coefficients S_R and S_L are changed according to the detection. To evaluate performance of the proposed method, correlation coefficients between normal condition and failure condition are calculated. The correlation coefficients

Table 4.6. Correlation coefficient.

Experiment	Correlation coefficient of force responses	Correlation coefficient of position responses
Sine wave	0.9964	1.0000
FM wave	0.9776	1.0000

shown in Table 4.6 are almost equal to 1. Therefore, validity of the proposed method is verified.

4.1.4.6 Conclusion

The bilateral controller can be used for transmission and share of the haptic sensation between the master system and the slave system. In the transmission system, the bilateral controller encounters problems in the event of data packet loss and/or disconnections. In order to solve this problem, the master/slave simulator and the environmental data memory are utilized in this study. In the case of normal operation, the environmental data memory stores force data in the remote side. The control system is operated by the environmental data memory and master/slave simulator when the communication lines are disconnected. By the experiment, validity

of the proposed method is confirmed by the experiment. The proposed method is expected to be useful in industrial applications and for providing medical and human support to patients.

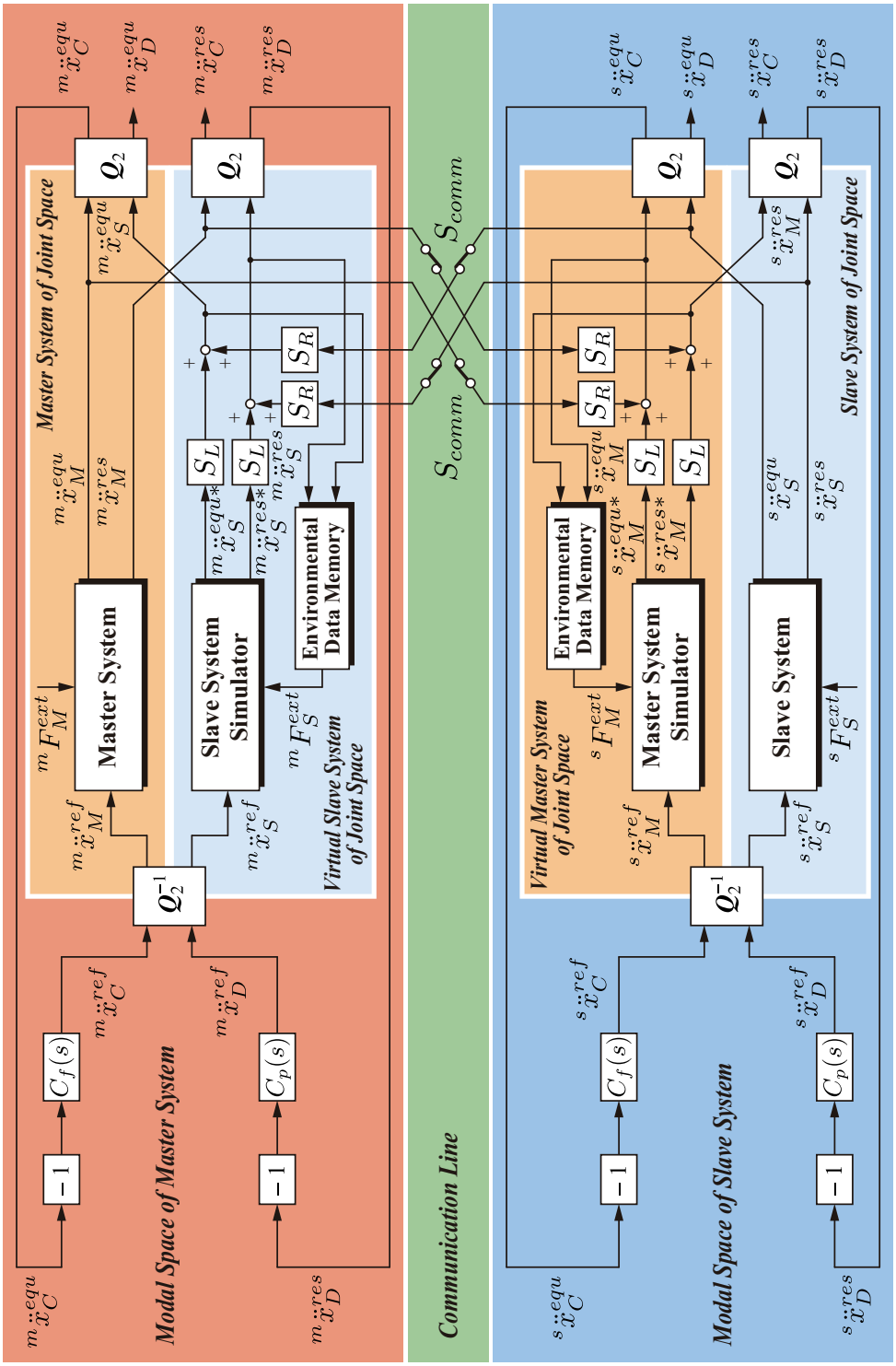

Fig. 4.49. Block diagram of bilateral control system by using master/slave simulator.

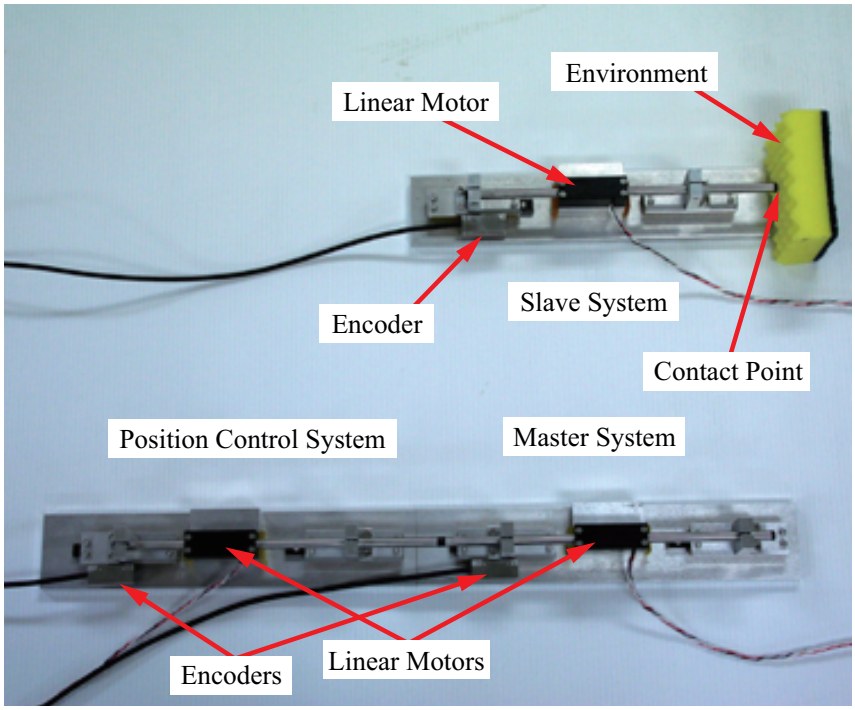

Fig. 4.50. Experimental setup.

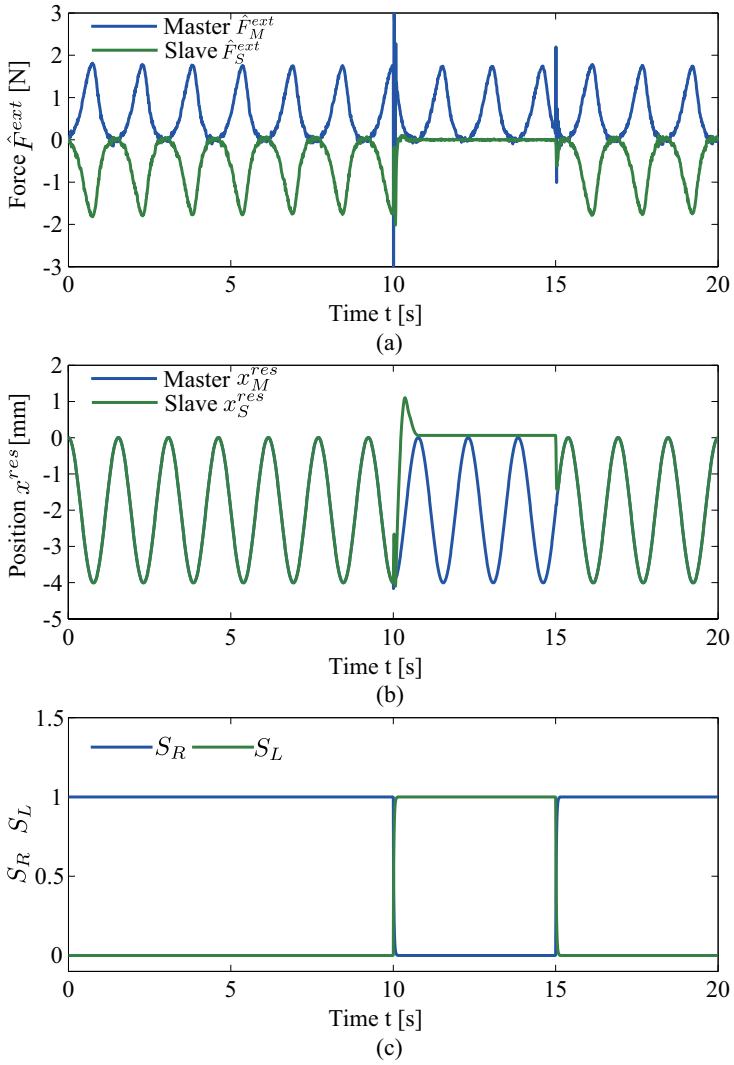

Fig. 4.51. Experimental results of sinusoidal waveform inputs. (a) Force responses $\hat{F}_M^{ext}$, $\hat{F}_S^{ext}$. (b) Position responses x_M^{res}, x_S^{res}. (c) Switching coefficients S_R, S_L.

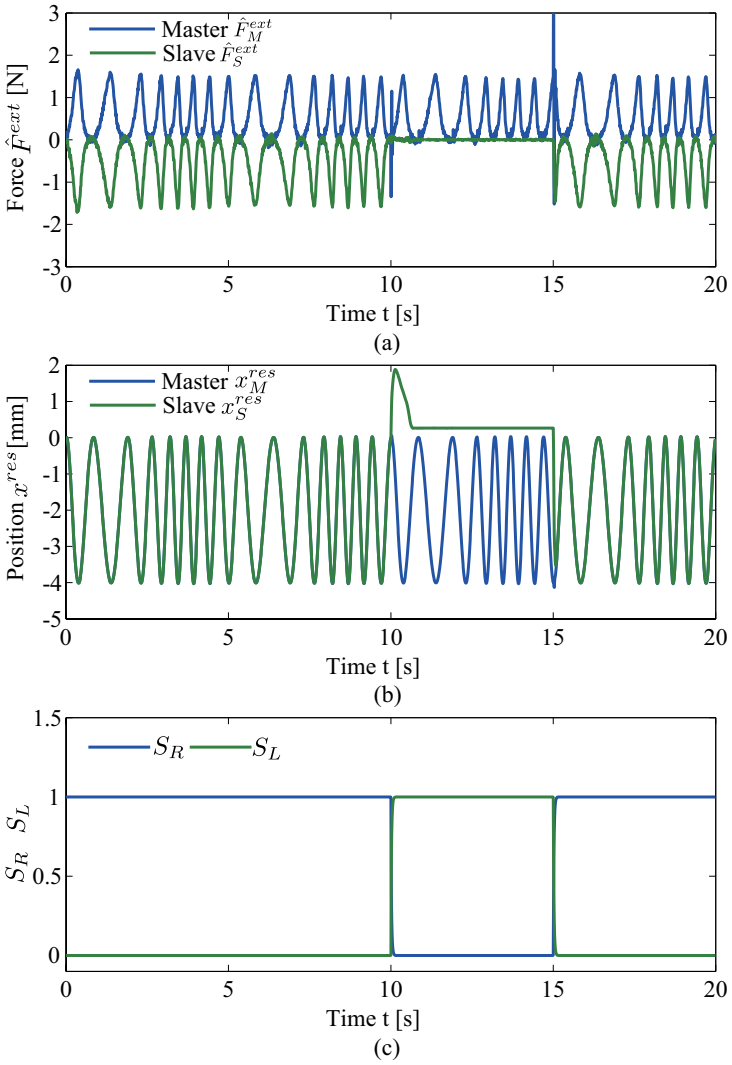

Fig. 4.52. Experimental results of frequency modulated signal inputs. (a) Force responses $\hat{F}_M^{ext}$, $\hat{F}_S^{ext}$. (b) Position responses x_M^{res}, x_S^{res}. (c) Switching coefficients S_R, S_L.

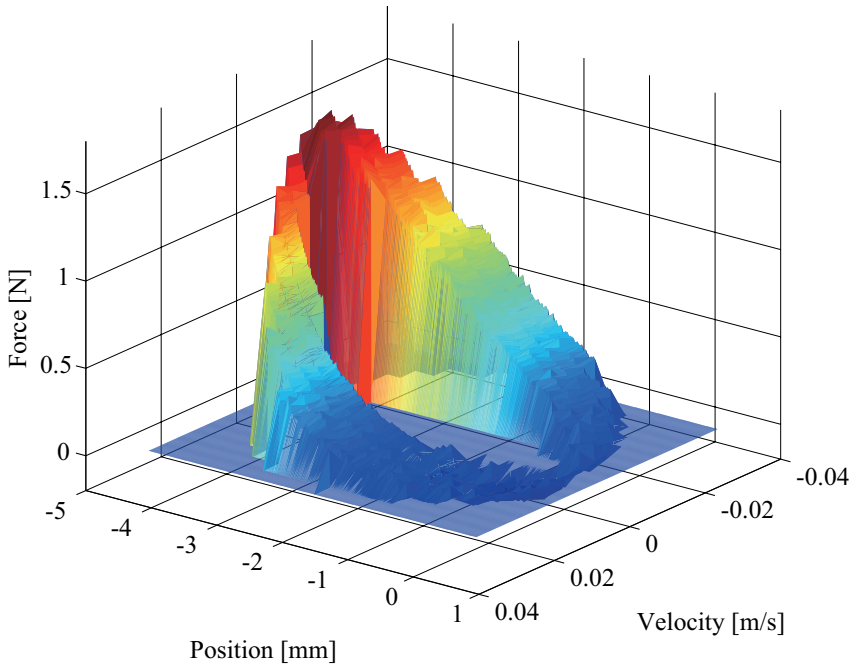

Fig. 4.53. Force information preserved in the environmental data memory.

4.2 Multilateral Control over Network

4.2.1 Introduction

The most important point is communication time delay, when the communication system and broadcasting system of haptic information are constructed. The communication time delay induces vibration and/or overdrive in the case of using a bilateral/multilateral control system with communication network. The thesis proposes a novel construction method for the multilateral control system including the communication time delay. In order to solve the problem of the communication time delay, the proposed method applies motion-copying system to the multilateral control. Fig.4.54 shows the concept of the multilateral control system with the

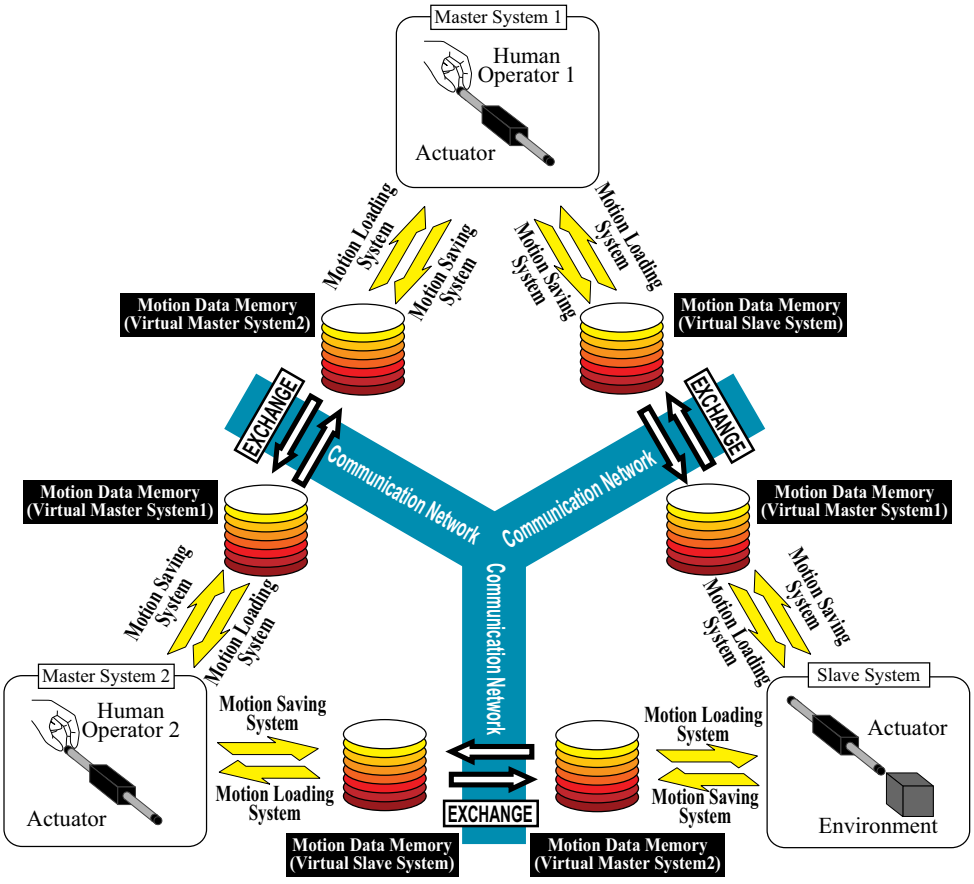

Fig. 4.54. Conceptual diagram of multilateral control with communication time delay by using motion-copying system

communication time delay using the motion-copying system. The motion-copying system copies local motion to other side to reduce the induced vibration and/or overdrive by the communication time delay. The proposed method utilizes the communication delay between respective systems instead of the motion data memory of a conventional motion-copying system. The force response of the proposed system does not include vibration by the communication time delay. This result exhibits that the multilateral control generates law of action and reaction. Therefore, the viability of the proposed method is confirmed by the experiments. The multilateral control system by using the motion-copying system has been normally operated even if the communication time delay exists between the several master side and the slave side. The proposed method will be useful for industrial applications, haptic communication and broadcasting.

4.2.2 Multilateral Control with Time Delay

Fig. 4.55 shows block diagram of the multilateral control over network. The multilateral control system is able to share haptic sensation between systems. In this thesis, the systems are connected with each other by using communication network. The equivalent acceleration of master systems $\ddot{x}_{M1}^{Fres}$ to $\ddot{x}_{MN-1}^{Fres}$, and equivalent acceleration of a slave system $\ddot{x}_{S}^{Fres}$ is calculated by N-order quarry matrix $\boldsymbol{Q}_N$ [65] as follows:

$$\begin{bmatrix} \ddot{x}_{C}^{Fres} \\ \ddot{x}_{D1}^{Fres} \\ \vdots \\ \ddot{x}_{DN-1}^{Fres} \end{bmatrix} = \boldsymbol{Q}_N \begin{bmatrix} e^{-sT_d}\ddot{x}_{M1}^{Fres} \\ \vdots \\ e^{-sT_d}\ddot{x}_{MN-1}^{Fres} \\ \ddot{x}_{S}^{Fres} \end{bmatrix} \tag{4.67}$$

where $\ddot{x}_{C}^{Fres}$, and $\ddot{x}_{D1}^{Fres}$ to $\ddot{x}_{DN-1}^{Fres}$ are equivalent acceleration in common mode and differential mode. T_d denote time delay of the communication network. Acceleration responses of the master systems $\ddot{x}_{M1}^{Pres}$ to $\ddot{x}_{MN-1}^{Pres}$, and acceleration response of the slave system $\ddot{x}_{S}^{Pres}$ are given by

$$\begin{bmatrix} \ddot{x}_{C}^{Pres} \\ \ddot{x}_{D1}^{Pres} \\ \vdots \\ \ddot{x}_{DN-1}^{Pres} \end{bmatrix} = \boldsymbol{Q}_N \begin{bmatrix} e^{-sT_d}\ddot{x}_{M1}^{Pres} \\ \vdots \\ e^{-sT_d}\ddot{x}_{MN-1}^{Pres} \\ \ddot{x}_{S}^{Pres} \end{bmatrix} \tag{4.68}$$

where $\ddot{x}_{C}^{Pres}$ represents acceleration of common mode, $\ddot{x}_{D1}^{Pres}$ to $\ddot{x}_{DN-1}^{Pres}$ are acceleration responses of differential mode. Force controller C_f calculates acceleration reference of the common mode

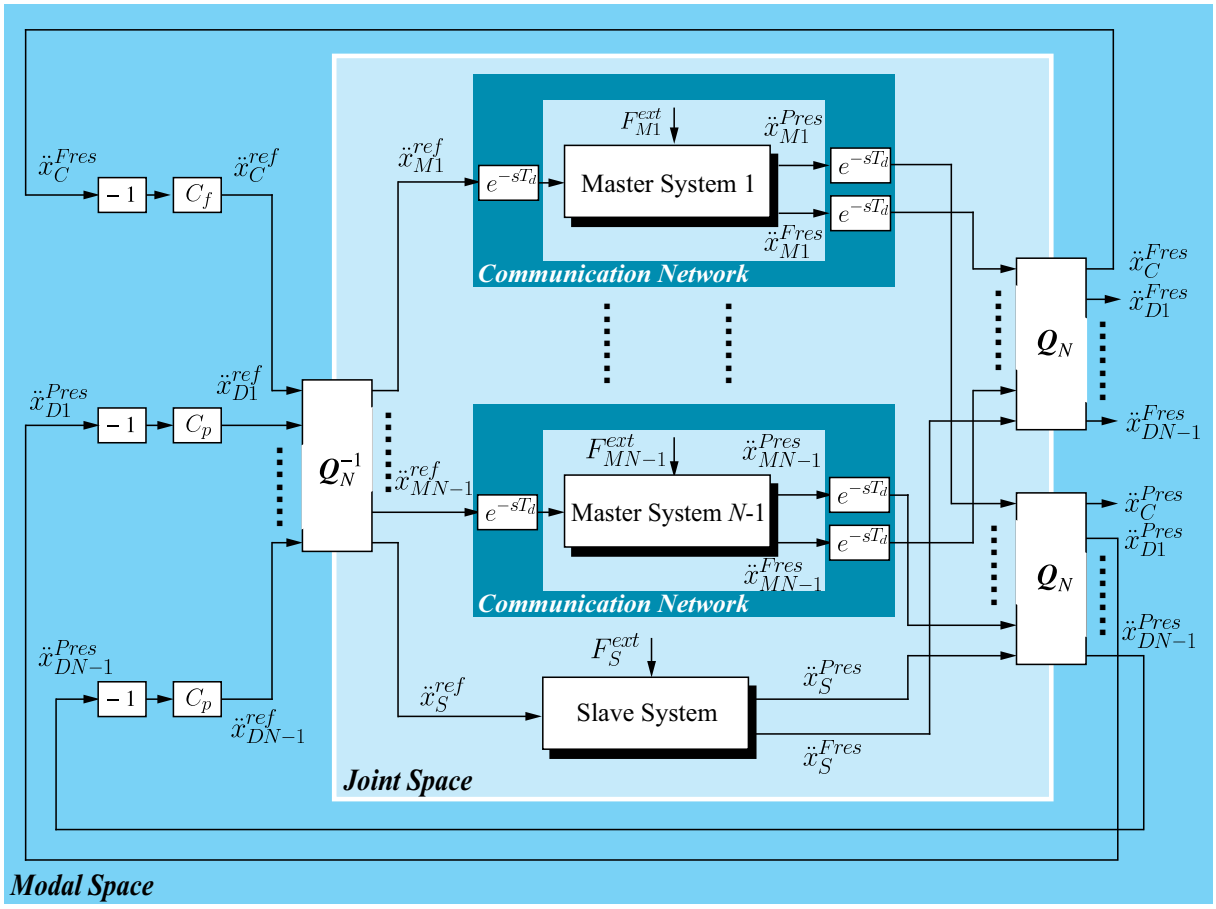

Fig. 4.55. Block diagram of multilateral control with communication time delay

$\ddot{x}_C^{ref}$ as follows:

$$\ddot{x}_C^{ref} = - C_f \ddot{x}_C^{Fres}. \tag{4.69}$$

On the other hand, position controllers C_p calculates acceleration references of differential mode $\ddot{x}_{D1}^{ref}$ to $\ddot{x}_{DN-1}^{ref}$ as follows:

$$\begin{bmatrix} \ddot{x}_{D1}^{ref} \\ \ddot{x}_{D2}^{ref} \\ \vdots \\ \ddot{x}_{DN-1}^{ref} \end{bmatrix} = -C_p \boldsymbol{I} \begin{bmatrix} \ddot{x}_{D1}^{Pres} \\ \ddot{x}_{D2}^{Pres} \\ \vdots \\ \ddot{x}_{DN-1}^{Pres} \end{bmatrix} \tag{4.70}$$

where $\boldsymbol{I}$ means unit matrix. By using $\boldsymbol{Q}_N^{-1}$, the acceleration references of the master systems $\ddot{x}_{M1}^{ref}$ to $\ddot{x}_{MN-1}^{ref}$ and the slave system $\ddot{x}_S^{ref}$ are transformed into modal space.

$$\begin{bmatrix} \ddot{x}_{M1}^{ref} \\ \vdots \\ \ddot{x}_{MN-1}^{ref} \\ \ddot{x}_S^{ref} \end{bmatrix} = \boldsymbol{Q}_N^{-1} \begin{bmatrix} \ddot{x}_C^{ref} \\ \ddot{x}_{D1}^{ref} \\ \vdots \\ \ddot{x}_{DN-1}^{ref} \end{bmatrix} \tag{4.71}$$

In fact, the time delay of the communication network T_d occurs between the systems. The time delay induces vibration of the actuators and/or running out of control.

4.2.3 Multilateral Control using Motion-Copying System

Fig. 4.56 shows block diagram of the multilateral control with communication time delay by using the motion-copying system. The main concept of the proposed method in this research is equal to the bilateral control described in the previous section. In this thesis, two master systems and one slave system are used. However, amount of the systems is unlimited.

In the case of three systems, adjacency matrix $\boldsymbol{A}$ is derived as

$$\boldsymbol{A} = \begin{bmatrix} 0 & 1 & 1 \\ 1 & 0 & 1 \\ 1 & 1 & 0 \end{bmatrix}. \tag{4.72}$$

The equivalent acceleration in the master system 1 are ${}^{m_1}\ddot{x}_{M1}^{Fres}$, ${}^{m_1}\ddot{x}_{M2}^{Fres}$, ${}^{m_1}\ddot{x}_S^{Fres}$. Moreover, in the case of the master system 2, ${}^{m_2}\ddot{x}_{M1}^{Fres}$, ${}^{m_2}\ddot{x}_{M2}^{Fres}$, ${}^{m_2}\ddot{x}_S^{Fres}$ represent the equivalent acceleration. ${}^{s}\ddot{x}_{M1}^{Fres}$, ${}^{s}\ddot{x}_{M2}^{Fres}$, ${}^{s}\ddot{x}_S^{Fres}$ denote the acceleration in the slave system. In this situation, the time delay of the equivalent acceleration is expressed as

$$\begin{aligned} &\begin{bmatrix} 0 & {}^{m_1}\ddot{x}_{M2}^{Fres} & {}^{m_1}\ddot{x}_S^{Fres} \\ {}^{m_2}\ddot{x}_{M1}^{Fres} & 0 & {}^{m_2}\ddot{x}_S^{Fres} \\ {}^{s}\ddot{x}_{M1}^{Fres} & {}^{s}\ddot{x}_{M2}^{Fres} & 0 \end{bmatrix} \\ &= e^{-sT_d}\boldsymbol{A} \begin{bmatrix} {}^{m_1}\ddot{x}_{M1}^{Fres} & 0 & 0 \\ 0 & {}^{m_2}\ddot{x}_{M2}^{Fres} & 0 \\ 0 & 0 & {}^{s}\ddot{x}_S^{Fres} \end{bmatrix}. \end{aligned} \tag{4.73}$$

In addition, the time delay of the acceleration responses is expressed as

$$\begin{bmatrix} 0 & {}^{m_1}\ddot{x}_{M2}^{Pres} & {}^{m_1}\ddot{x}_S^{Pres} \\ {}^{m_2}\ddot{x}_{M1}^{Pres} & 0 & {}^{m_2}\ddot{x}_S^{Pres} \\ {}^{s}\ddot{x}_{M1}^{Pres} & {}^{s}\ddot{x}_{M2}^{Pres} & 0 \end{bmatrix}$$

$$= e^{-sT_d}\boldsymbol{A}\begin{bmatrix} {}^{m_1}\ddot{x}_{M1}^{Pres} & 0 & 0 \\ 0 & {}^{m_2}\ddot{x}_{M2}^{Pres} & 0 \\ 0 & 0 & {}^{s}\ddot{x}_{S}^{Pres} \end{bmatrix} \tag{4.74}$$

where ${}^{m_1}\ddot{x}_{M1}^{Pres}$, ${}^{m_1}\ddot{x}_{M2}^{Pres}$, ${}^{m_1}\ddot{x}_{S}^{Pres}$ mean the acceleration responses in the master system 1, ${}^{m_2}\ddot{x}_{M1}^{Pres}$, ${}^{m_2}\ddot{x}_{M2}^{Pres}$, ${}^{m_2}\ddot{x}_{S}^{Pres}$ represent the acceleration responses in the master system 2, ${}^{s}\ddot{x}_{M1}^{Pres}$, ${}^{s}\ddot{x}_{M2}^{Pres}$, ${}^{s}\ddot{x}_{S}^{Pres}$ are the acceleration responses in the slave system, respectively.

The third order quarry matrix $\boldsymbol{Q}_3$ is defined as

$$\boldsymbol{Q}_3 = \frac{1}{3}\begin{bmatrix} 1 & 1 & 1 \\ 0 & 1 & -1 \\ 2 & -1 & -1 \end{bmatrix}. \tag{4.75}$$

By using the quarry matrix, the equivalent acceleration of common mode ${}^{m_1}\ddot{x}_{C}^{Fres}$, differential mode ${}^{m_1}\ddot{x}_{D1}^{Fres}$ and ${}^{m_1}\ddot{x}_{D2}^{Fres}$ are transformed into modal space as follows:

$$\begin{bmatrix} {}^{m_1}\ddot{x}_{C}^{Fres} \\ {}^{m_1}\ddot{x}_{D1}^{Fres} \\ {}^{m_1}\ddot{x}_{D2}^{Fres} \end{bmatrix} = \boldsymbol{Q}_3 \begin{bmatrix} {}^{m_1}\ddot{x}_{M1}^{Fres} \\ {}^{m_1}\ddot{x}_{M2}^{Fres} \\ {}^{m_1}\ddot{x}_{S}^{Fres} \end{bmatrix}. \tag{4.76}$$

The acceleration responses are calculated as with the equivalent acceleration.

$$\begin{bmatrix} {}^{m_1}\ddot{x}_{C}^{Pres} \\ {}^{m_1}\ddot{x}_{D1}^{Pres} \\ {}^{m_1}\ddot{x}_{D2}^{Pres} \end{bmatrix} = \boldsymbol{Q}_3 \begin{bmatrix} {}^{m_1}\ddot{x}_{M1}^{Pres} \\ {}^{m_1}\ddot{x}_{M2}^{Pres} \\ {}^{m_1}\ddot{x}_{S}^{Pres} \end{bmatrix} \tag{4.77}$$

where ${}^{m_1}\ddot{x}_{C}^{Pres}$ is acceleration response of common mode, ${}^{m_1}\ddot{x}_{D1}^{Pres}$ and ${}^{m_1}\ddot{x}_{D2}^{Pres}$ acceleration responses of differential mode. The each acceleration references are given by

$${}^{m_1}\ddot{x}_{C}^{ref} = -\, C_f\ {}^{m_1}\ddot{x}_{C}^{Fres} \tag{4.78}$$

$$\begin{bmatrix} {}^{m_1}\ddot{x}_{D1}^{ref} \\ {}^{m_1}\ddot{x}_{D2}^{ref} \end{bmatrix} = -C_p\boldsymbol{I}\begin{bmatrix} {}^{m_1}\ddot{x}_{D1}^{Pres} \\ {}^{m_1}\ddot{x}_{D2}^{Pres} \end{bmatrix}. \tag{4.79}$$

In the next step, the acceleration references of the respective systems are calculated by inverse quarry matrix $\boldsymbol{Q}_3^{-1}$ as follows:

$$\begin{bmatrix} {}^{m_1}\ddot{x}_{M1}^{ref} \\ {}^{m_1}\ddot{x}_{M2}^{ref} \\ {}^{m_1}\ddot{x}_{S}^{ref} \end{bmatrix} = \boldsymbol{Q}_3^{-1} \begin{bmatrix} {}^{m_1}\ddot{x}_{C}^{ref} \\ {}^{m_1}\ddot{x}_{D1}^{ref} \\ {}^{m_1}\ddot{x}_{D2}^{ref} \end{bmatrix}. \tag{4.80}$$

In the case of the master system 1, the master system 1 is controlled by the acceleration reference of the master system 1 ${}^{m_1}\ddot{x}_{M1}^{ref}$. In the master system 2 and the slave system, the control method described in (4.76) to (4.80) is same.

In fact, the motion data memories are unused in the proposed system. The time delay is used instead of the motion data memories, so that effect of the time delay can be reduced.

4.2.4 Experiment

4.2.4.1 Experimental Setup

Fig. 4.57 shows experimental setup. In this experiment, the aluminum block for environment in the slave side is used. In order to evaluate validity of the proposed method, the time delay of the communication network T_d is set as constant. Table 4.7 shows setup parameters.

Table 4.7. Setup parameters

T_s	Period of control system	100	μs
K_{fn}	Force constant	3.33	N/A
M_n	Mass of nominal	0.18	kg
K_f	Gain of force controller	30	
K_p	Proportional gain of position regulator	10000	
K_v	Differential gain of position regulator	1000	
g_{pd}	Pole of pseudo derivative for the PD controller	25000	rad/s
g_{dis}	Pole of the disturbance observer	300	rad/s
g_{reac}	Pole of the reaction force observer	300	rad/s

4.2.4.2 Experimental Results

The experimental result of the multilateral control without the proposed method is shown in Fig.4.58. The force response of the system includes vibration, which is induced by the communication time delay. Additionally, when the time delay T_d is set to more than 800 μs, the system runs out of control. On the other hand, Figs.4.59 to 4.61 show the experimental result using the motion-copying system. In this experiment, the time delay is set to 800 μs, 50 ms, and 100 ms. These experimental results exhibit that respective position responses and force

responses become possible same. Therefore, the multilateral control system normally operates without running out of control.

4.2.5 Conclusion

In the multilateral control system over network, the time delay of the communication network is one of the problem. In concrete terms, the time delay induces vibration and running out of control system. To solve this problem, this thesis proposed the multilateral control with the motion-copying system. Using the proposed method, effect of the time delay can be reduced, and share of the haptic sensation is realized. By the experiment, validity of the proposed system is verified.

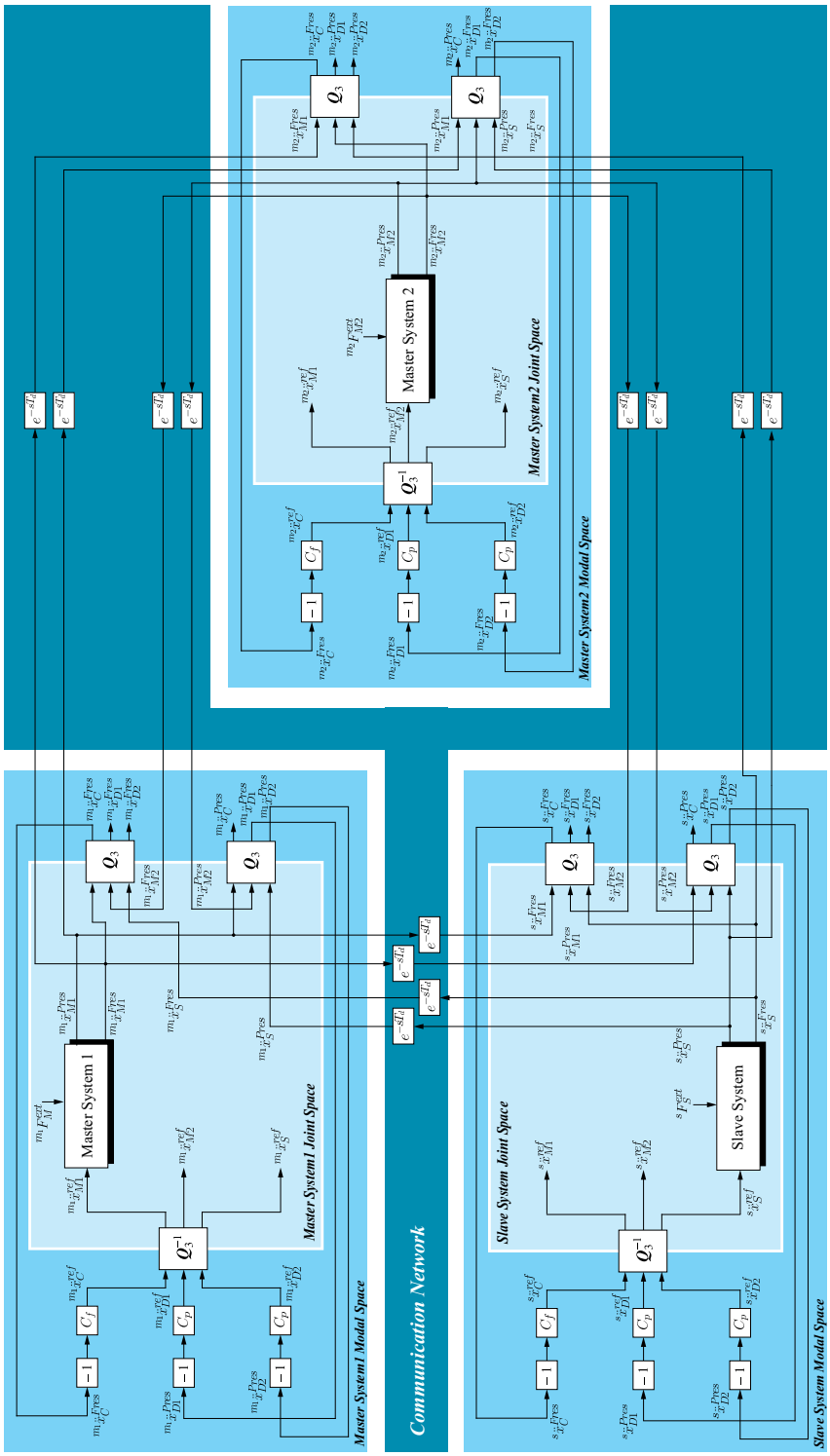

Fig. 4.56. Block diagram of multilateral control with communication time delay by using motion-copying system

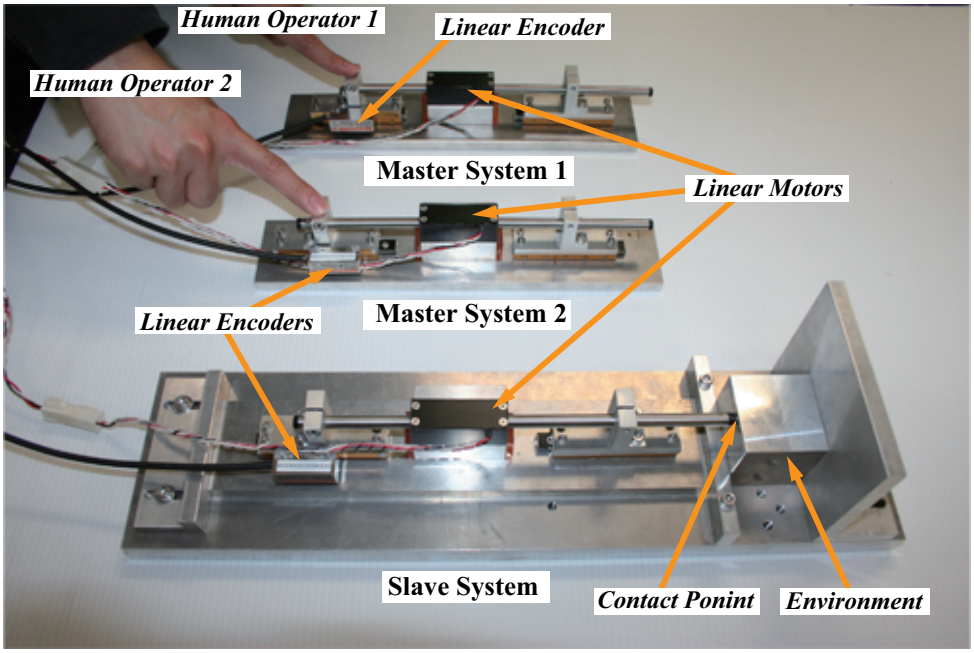

Fig. 4.57. Experimental setup.

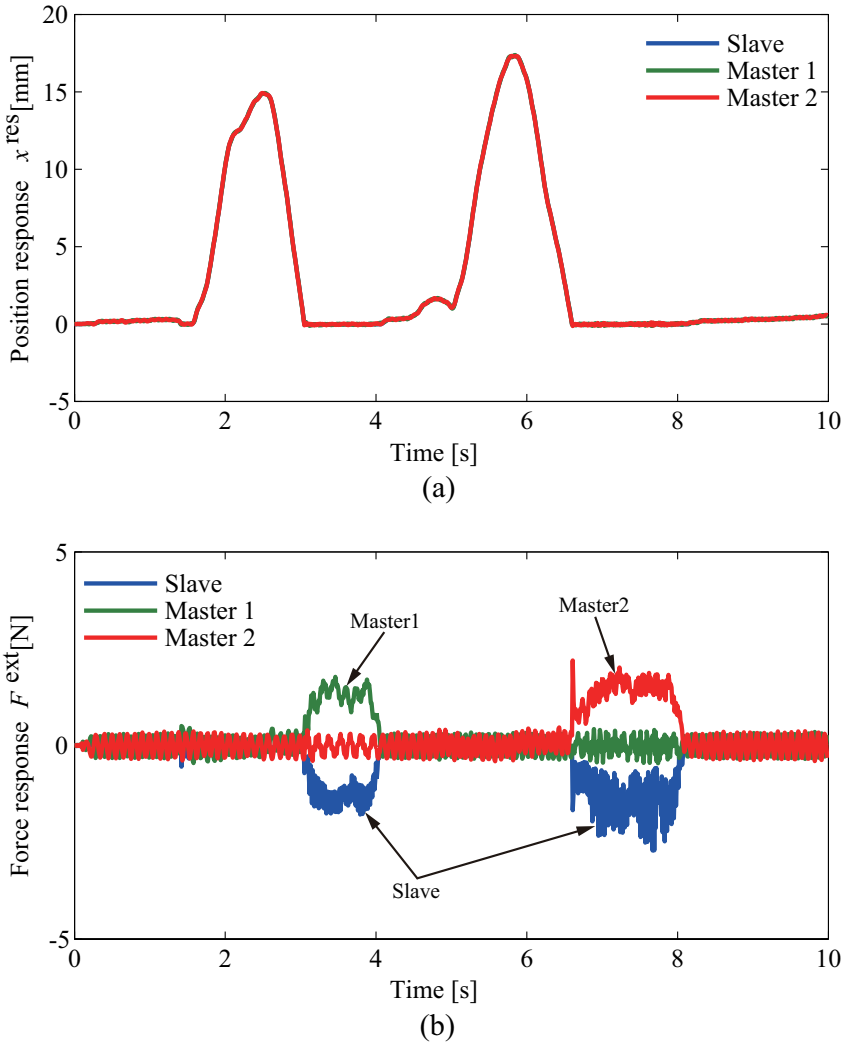

Fig. 4.58. Experimental results without proposed method (a) Position response (b) Force response ($T_d = 800$ μs)

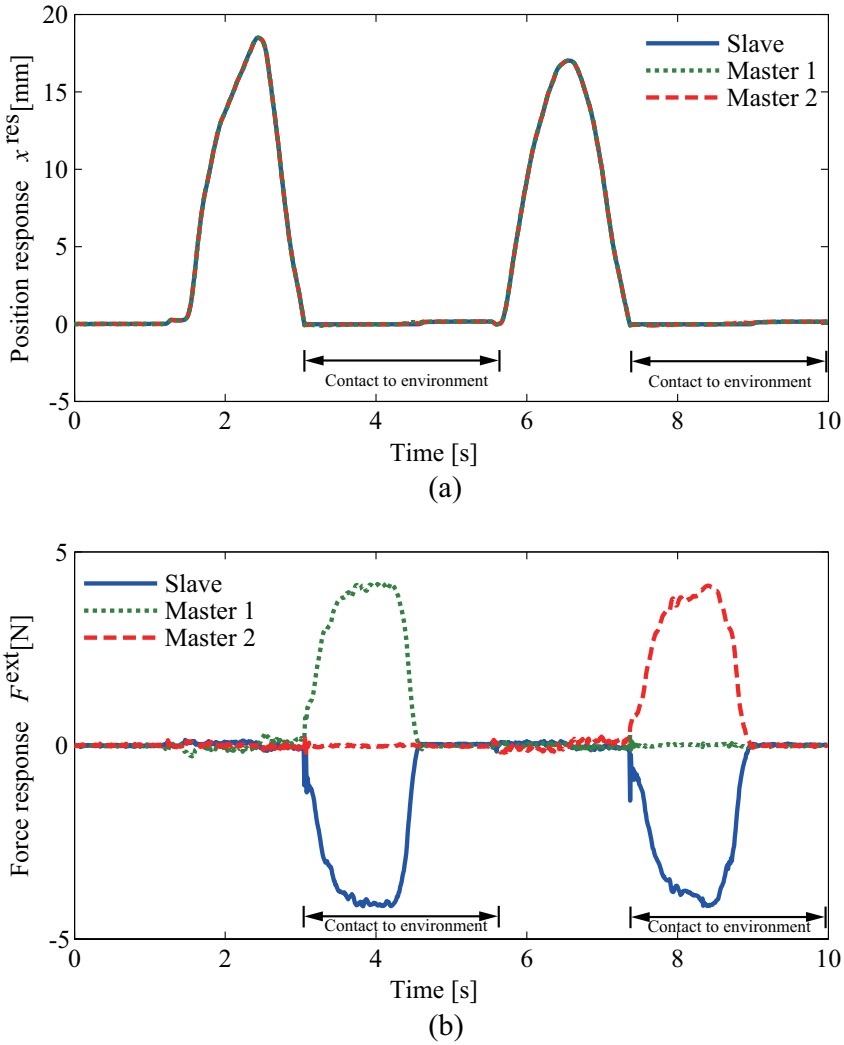

Fig. 4.59. Experimental results using motion-copying system (a) Position response (b) Force response ($T_d = 800$ μs)

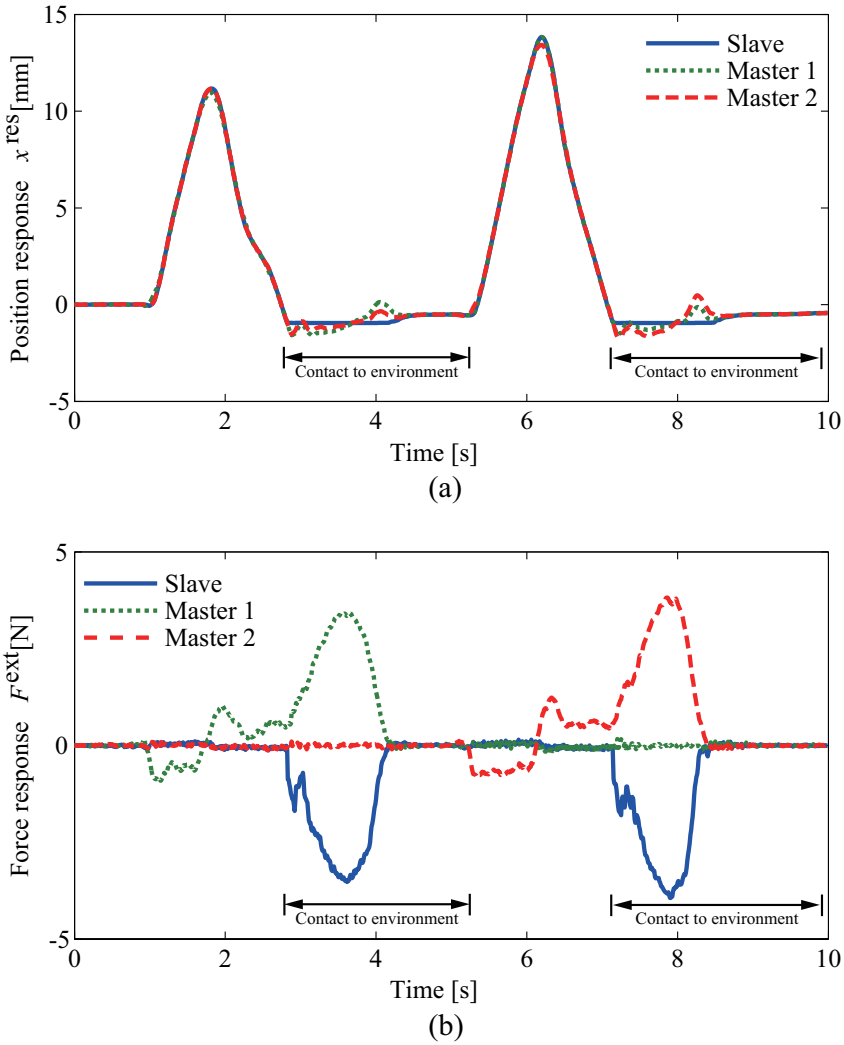

Fig. 4.60. Experimental results using motion-copying system (a) Position response (b) Force response ($T_d = 50$ ms)

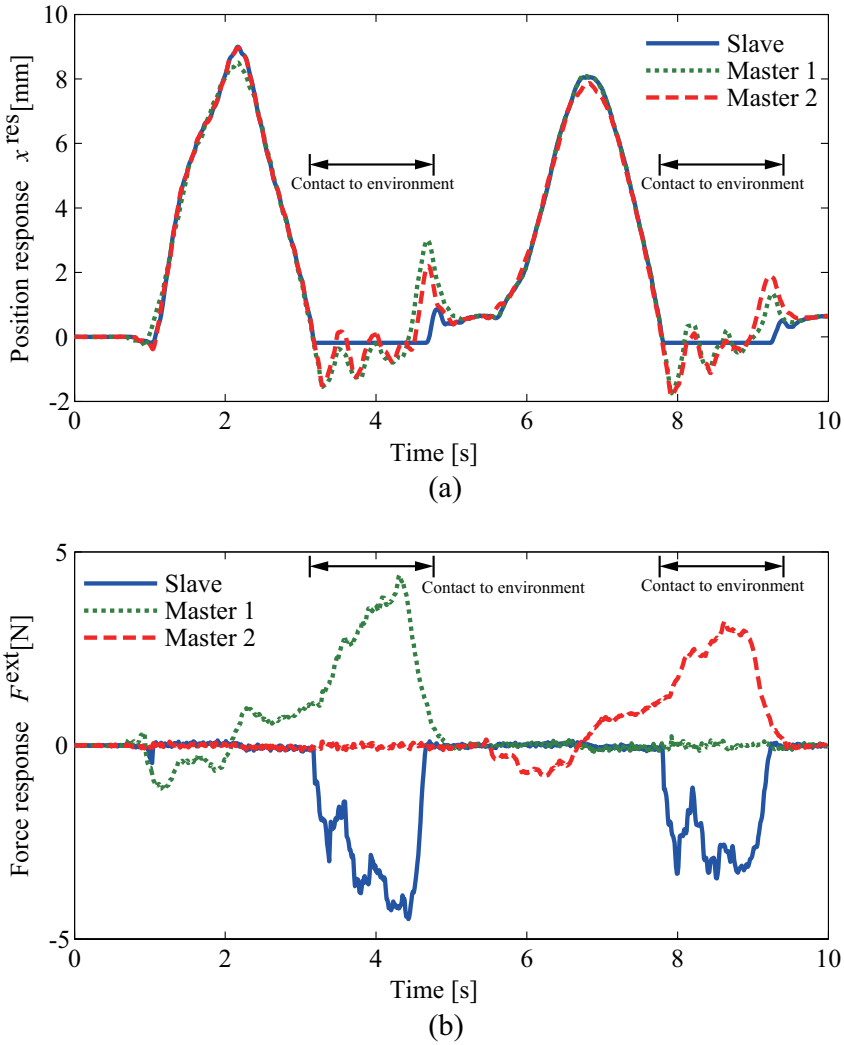

Fig. 4.61. Experimental results using motion-copying system (a) Position response (b) Force response ($T_d = 100$ ms)

Chapter 5

Reproduction of Human Motion

Abstract

The thesis proposes the motion index/search system based on real-world haptics. The motion index system indexes the human motion using the force and position stored by the motion-saving system. The motion index system is able to create the motion dictionary, which includes the desired indexed motions. In addition, the motion search system searches the motion of human operator by using moving covariance according to the indexed motions The motion search system proposed in this thesis is utilized to recognize the human motion. By the experimental results, the validity and the possibility of the motion index/search system are confirmed.

Additionally, this thesis also proposes searching system for haptic sensation of target object. As with text, auditory, and visual information, the search system of haptic information is realized. The searching system proposed in this thesis consists of the environment-copying system and the search algorithm. Firstly, environmental data memory in the environment-copying system stores force responses in order to reproduce the environmental haptic sensation. After that, search algorithm calculates similarity between force response of bilateral controller and force from the environmental data memory. Thus, the proposed system is capable of calculating the search results relevant to the haptic environment.

Besides, in the case of the haptic recognition if the size of the target object is different, the search result obtained by the search system becomes different environment even if the material of the object is same. Consequently, this thesis identifies the element stiffness, which does not

depend on the size of the target object. By the experiment, the value of the stiffness can be calculated by the force responses between nodes of environmental surface. This method can be utilized for recognition method of the haptic sensation.

In the last section, this thesis proposes selective motion-copying system, which is capable of storing and reproducing the human motion. In the normal motion-copying system, force and position are not reproduced accurately, when the environment in the reproduction phase is different from the environment in the storage phase. To solve this problem, the proposed method reproduces the human motion according to search results provided by environmental search algorithm. Therefore, the force and position corresponding to the stored motion is able to be reproduced even if the environment is changed. By the experiment, validity of the proposed method is verified.

5.1 Search of Haptic Sensation

5.1.1 Motion Index/Search System Based on Real-World Haptics

5.1.1.1 Introduction

In recent years, the information and communication technology has been rapidly grown. The communication network provides various information, which exists in the entire world. For example, we can get html documents, mp3 files and avi files which include the text data, the acoustic data and the visual data by using Internet. These acoustic information and visual information can be preserved and reproduced at any time and any place. In addition, sound and image library are available. The practical search engine is able to treat such information. The recognition and analysis of these information is realized.

However, the human has five organs including haptic organs as well as acoustic organs and visual organs. Fig. 5.1 shows the recognition, analysis and database of information which stimulates these organs. Compared with the acoustic information and the visual information, the haptic recognition and haptic analysis are not sufficiently realized. Therefore, the technology of haptic information should be more researched. The acquisition systems of human motion are

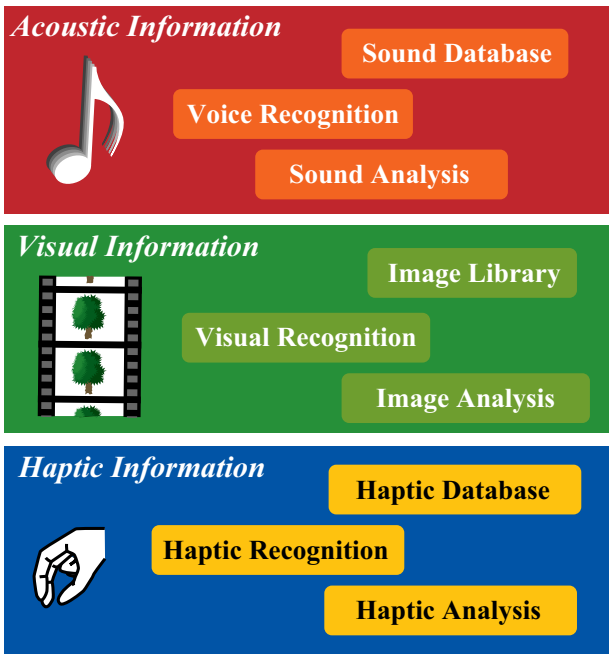

Fig. 5.1. Recognition, analysis and database of information.

developed [29]–[32]. However, the conventional method based on visual image cannot treat force information which is important element to acquire the motion. Moreover, some methods in terms of motion analysis have been proposed [103]–[105]. However, motion indexing system and motion searching system based on bilateral controller considering both position information and force information is not proposed.

The thesis proposes the motion index/search system, which treats the haptic information in the real-world. The motion index/search system consists of the motion index system and the motion search system. The motion index system indexes the desired motion by using the motion-saving system [38], and create the motion dictionary. Moreover, the motion search system compares the motions of human operator with the indexed motions stored in the motion dictionary. The motion search system calculates similarity of these motions according to moving covariance. In the case of conformity, the value calculated by the proposed method is increased. Thus, the proposed system is useful for recognition of the human motion.

This research is organized as follows. Subsection 5.1.1.2 mentions the bilateral control system

which realizes the proposed method. In 5.1.1.3, concept and algorithm of the motion index system is described. The motion searching system is explained in 5.1.1.4. Subsection 5.1.1.5 explains about experimental setup and several experimental results. Finally, this research is concluded in the last subsection.

5.1.1.2 Bilateral Control System

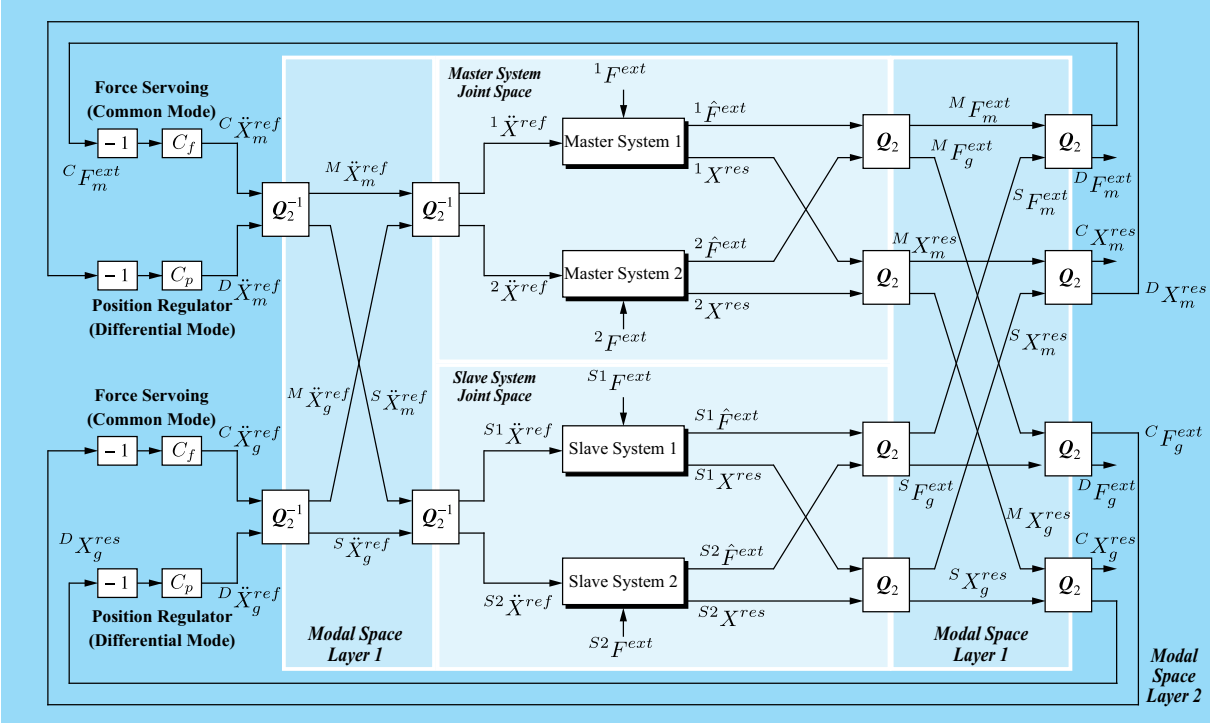

Fig. 5.2. Block diagram of bilateral control system.

Fig. 5.2 shows block diagram of the bilateral control system, which realizes the motion index/search system. The superscripts of left side ^{M}, ^{S}, ^{C}, ^{D} of parameters in Fig. 5.2 denote master, slave, common mode, differential mode, respectively. The superscripts of right side ^{ext}, ^{res} and ^{ref} denote external, response and reference. The subscripts $_{m}$, $_{g}$ are manipulating mode and grasping mode. F, X and $\ddot{X}$ are force, position and acceleration.

In this thesis, the bilateral control based on modal decomposition is constructed by quarry

matrix [65, 63]. The second-order quarry matrix is defined as

$$\boldsymbol{Q}_2 = \frac{1}{2}\begin{bmatrix} 1 & 1 \\ 1 & -1 \end{bmatrix}. \tag{5.1}$$

The force responses of the master system 1 ${}^1\hat{F}^{ext}$ and of master system 2 ${}^2\hat{F}^{ext}$ are transformed into the modal space by using the second-order quarry matrix.

$$\begin{bmatrix} {}^M F_m^{ext} \\ {}^M F_g^{ext} \end{bmatrix} = \boldsymbol{Q}_2 \begin{bmatrix} {}^1\hat{F}^{ext} \\ {}^2\hat{F}^{ext} \end{bmatrix} \tag{5.2}$$

Moreover, the quarry matrix transforms also from the position responses ${}^1\hat{X}^{res}$, ${}^2\hat{X}^{res}$ in the joint space into the position responses in the modal space.

$$\begin{bmatrix} {}^M X_m^{res} \\ {}^M X_g^{res} \end{bmatrix} = \boldsymbol{Q}_2 \begin{bmatrix} {}^1X^{res} \\ {}^2X^{res} \end{bmatrix} \tag{5.3}$$

In the manipulating mode, the force responses in the modal space of layer 1 are transformed into the modal space of layer 2.

$$\begin{bmatrix} {}^C F_m^{ext} \\ {}^D F_m^{ext} \end{bmatrix} = \boldsymbol{Q}_2 \begin{bmatrix} {}^M F_m^{ext} \\ {}^S F_m^{ext} \end{bmatrix} \tag{5.4}$$

The position responses in the modal space of layer 2 are obtained by

$$\begin{bmatrix} {}^C X_m^{res} \\ {}^D X_m^{res} \end{bmatrix} = \boldsymbol{Q}_2 \begin{bmatrix} {}^M X_m^{res} \\ {}^S X_m^{res} \end{bmatrix} \tag{5.5}$$

In addition, the quarry matrix transforms the position responses from the modal space of layer 1 into the modal space of layer 2.

A force controller C_f and a position regulator $C_p(s)$ calculate acceleration references in the modal space of layer 2.

$${}^C\ddot{x}_m^{ref} = -\,C_f\ {}^C F_m^{ext} \tag{5.6}$$

$${}^D\ddot{x}_g^{ref} = -\,C_p(s)\ {}^D X_m^{res} \tag{5.7}$$

In other words, the bilateral control system is able to control independently the force in the common mode and the position in the differential mode. In this thesis, C_f and $C_p(s)$ are defined

as

$$C_f = K_{fp} \tag{5.8}$$

$$C_p(s) = K_{pp} + \frac{s\ g_{pd}}{s + g_{pd}}\ K_{pd} \tag{5.9}$$

where, K_{fp}, K_{pp}, K_{pd} and g_{pd} are gain of the force controller, proportional gain, differential gain and pole of the position regulator. The calculated acceleration references are transformed into the modal space of layer 1 as

$$\begin{bmatrix} {}^{M}\ddot{X}_m^{ref} \\ {}^{S}\ddot{X}_m^{ref} \end{bmatrix} = \boldsymbol{Q}_2^{-1} \begin{bmatrix} {}^{C}\ddot{X}_m^{ref} \\ {}^{D}\ddot{X}_m^{ref} \end{bmatrix} \tag{5.10}$$

where, Q_2^{-1} is inverse quarry matrix. Moreover, the inverse quarry matrix transforms the acceleration references in the layer 1 into the joint space.

The calculation methods in the slave system and grasping mode are same as above methods. Finally, the actuators of the master system and of slave system are controlled by the acceleration references $\ddot{X}^{ref}$.

By this means, the bilateral control for real-world haptics is realized. In this thesis, the bilateral control system mentioned in this section is utilized, in order to realize the motion index/search system.

5.1.1.3 Motion Index System

This section describes the motion index system, which generates the motion dictionary.

Concept Fig. 5.3 shows conceptual diagram of the motion index system. The motion index system consists of the motion-saving system, the motion data memory and the indexing algorithm. The motion-saving systems which are utilized in the motion-copying system [38] preserve desired several motions to the motion data memories 1–P. P denotes a number of the desired motions.

The motion indexing algorithm indexes the motions, and generates the motion dictionary by using the motions stored in the motion data memories. The dictionary generated by this

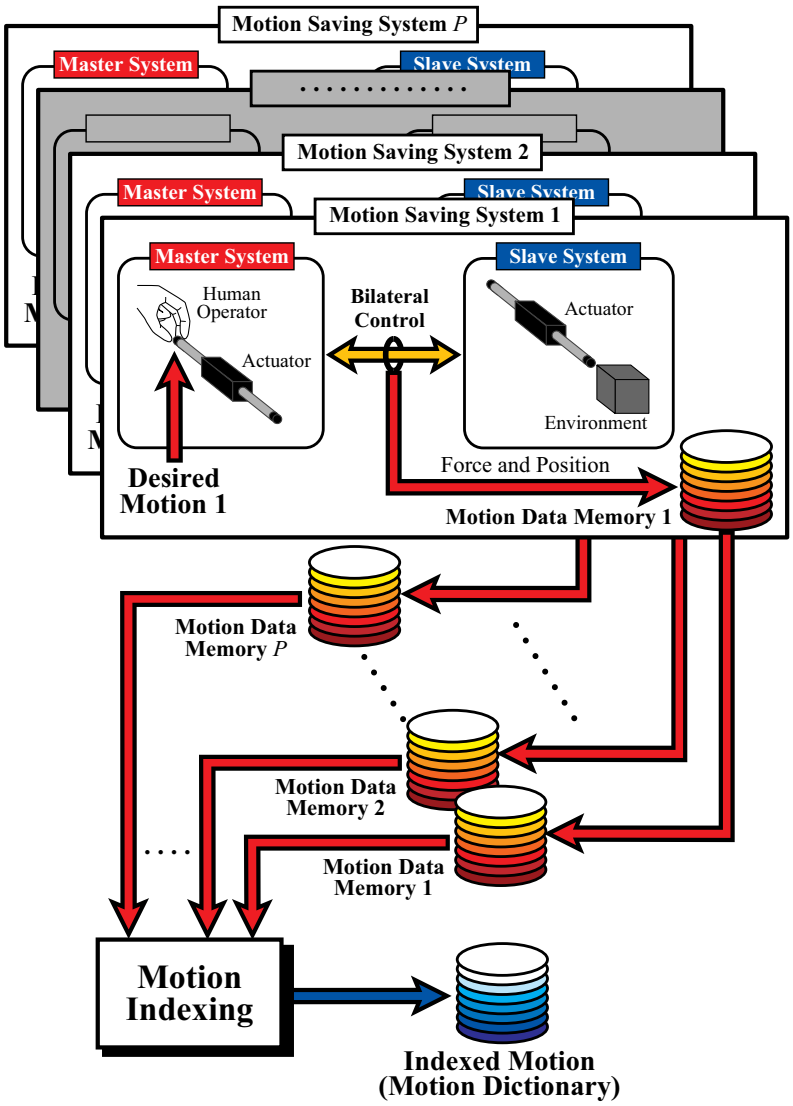

Fig. 5.3. Conceptual diagram of motion indexing system.

system has the indexed motions. The indexed motions are utilized to process a motion data in the motion search system.

Algorithm The motion index system uses the bilateral control system in order to measure the force information between the human operator and the environment. The motion index system adds the data of the desired motion to the motion dictionary based on the force information

and the position information. The force responses and the position responses are indexed as

$$ {}^{n}_{p}\Phi_{\ell} = {}^{n}_{p}F^{ext}_{\ell} \tag{5.11} $$

$$ {}^{n}_{p}\Xi_{\ell} = {}^{n}_{p}X^{res}_{\ell} \tag{5.12} $$

where, Φ, Ξ and ℓ ($\ell = 0, 1, 2, \cdots, N_1$) denote indexed forces, indexed positions and discrete time. N_1 is a number of the force data and the position data in the motion dictionary. n and p are actuator number and motion number. The motion number p means kind of motion. The motion dictionary consists of indexed forces Φ and indexed positions Ξ. By this means, the motion index system generates the motion dictionary.

5.1.1.4 Motion search system

In this section, the motion search system is explained.

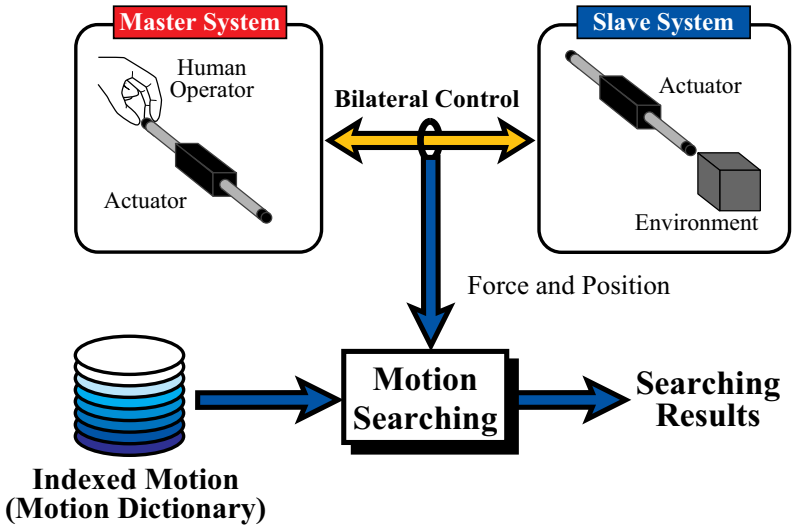

Fig. 5.4. Conceptual diagram of motion search system.

Concept Fig. 5.4 shows conceptual diagram of the motion search system. The motion search system consists of the bilateral control system, the motion dictionary and motion searching algorithm. The bilateral control system mentioned in section II is utilized in order to estimate the force impressed by the human operator. The motion searching algorithm calculates the searching

results using the force response and the position response in regard to indexed motions in the motion dictionary. The calculated searching results provide the motion information, which is given by the human operator. By the proposed method, the control system is able to understand what the human operator is doing.

Algorithm In order to search the motions, the motion search system calculates similarity. In this thesis, value of moving covariance which provides the similarity is utilized. Firstly, average values of the indexed motions are calculated by

$$ {}^{n}_{p}\overline{\Phi}_{j} = \frac{1}{N_j}\sum_{k=1}^{N_j} {}^{n}_{p}\tilde{\Phi}_{k,j} \tag{5.13} $$

$$ {}^{n}_{p}\overline{\Xi}_{j} = \frac{1}{N_j}\sum_{k=1}^{N_j} {}^{n}_{p}\tilde{\Xi}_{k,j} \tag{5.14} $$

where, $\tilde{\Phi}$, $\tilde{\Xi}$ and k are scaled indexed force, scaled indexed position and time in the moving window. j denotes scaling factor respect to time. If j is increased, the indexed force and the indexed position are contracted. Meanwhile, if j is decreased, the data are extended. At the same time, width of the moving window is changed. The scaling operation does not execute on condition that $j = 1$. N_j denotes a number of the data in the moving window.

The average values of force response $\overline{F}^{ext}$ and position response $\overline{X}^{res}$ are calculated by

$$ {}^{n}\overline{F}^{ext}_{j} = \frac{1}{N_j}\sum_{k=i-N_j}^{i} {}^{n}\tilde{F}^{ext}_{k,j} \tag{5.15} $$

$$ {}^{n}\overline{X}^{res}_{j} = \frac{1}{N_j}\sum_{k=i-N_j}^{i} {}^{n}\tilde{X}^{res}_{k,j} \tag{5.16} $$

where, $\tilde{F}$, $\tilde{X}$ and i are scaled force response, scaled position response and time.

Secondly, the motion search system calculates the moving covariance of the force information ${}^{n}_{p}\phi_{i,j}$ as

$$ {}^{n}_{p}\phi_{i,j} = \sum_{k=1}^{N_j}\left({}^{n}_{p}\tilde{\Phi}_{k,j} - {}^{n}_{p}\overline{\Phi}_{j}\right)\left({}^{n}\tilde{F}^{ext}_{i-N_j+k,j} - {}^{n}\overline{F}^{ext}_{j}\right). \tag{5.17} $$

where, i is time. In addition, the moving covariance of the position information ${}^{n}_{p}\xi_{i,j}$ is given by

$$ {}^{n}_{p}\xi_{i,j} = \sum_{k=1}^{N_j} \left({}^{n}_{p}\tilde{\Xi}_{k,j} - {}^{n}_{p}\overline{\Xi}_{j} \right) \left({}^{n}\tilde{X}^{res}_{i-N_j+k,j} - {}^{n}\overline{X}^{res}_{j} \right). \tag{5.18} $$

Finally, the searching results R are calculated by

$$ {}_{p}R_{i,j} = \sum_{n=1}^{n_{act}} {}^{n}_{p}\phi_{i,j} + \sum_{n=1}^{n_{act}} {}^{n}_{p}\xi_{i,j} \tag{5.19} $$

where, n_{act} is a number of the actuator in the master side. The results are plotted by using the time i, the scaling factor j and searching results ${}_{p}R$. In fact, the search algorithm proposed in the thesis is similar to wavelet transform, which generates the haptograph mentioned in Chapter 2.

5.1.1.5 Experiment

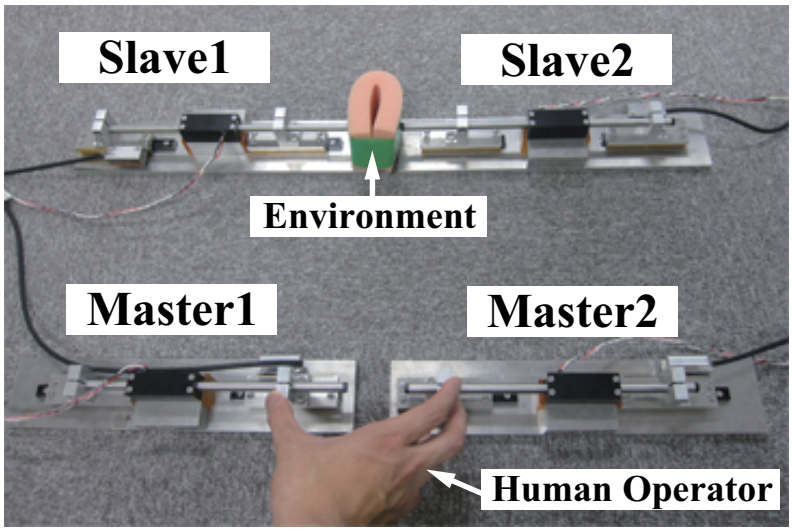

Fig. 5.5. Experimental Setup

Experimental Setup Fig. 5.5 shows experimental devices, which is used in this experiment. The experimental devices consist of four linear actuators and position sensors. These linear actuators move from side to side, and are controlled by the control system shown in Fig. 5.2. The human operator grasps the environment sense through the bilateral control system. The environment is a sponge. The RTAI-3.7 realizes the proposed system.

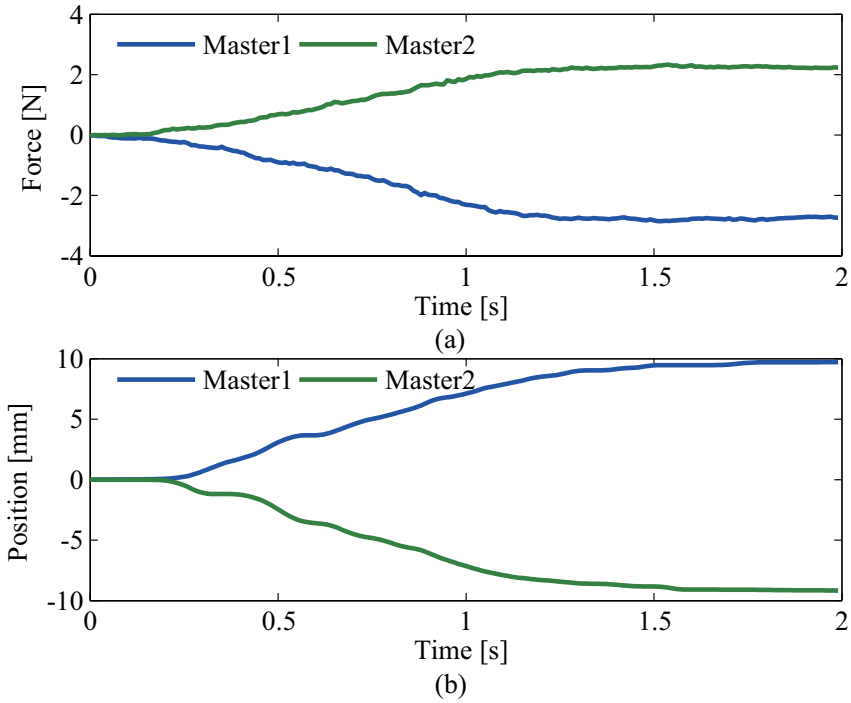

Fig. 5.6. Indexed Motion (Grasping Motion). (a) Forces ${}^{1}_{1}\Phi$ and ${}^{2}_{1}\Phi$. (b) Positions ${}^{1}_{1}\Xi$ and ${}^{2}_{1}\Xi$.

Experimental Results of Motion Index System Figs. 5.6 and 5.7 show the experimental results of motion indexing. The grasping motion and the release motion are indexed by the motion index system in this thesis. The motion number p of the grasping motion is 1. Meanwhile, the motion number p of the release motion is 2.

Experimental Results of Motion search system In this thesis, the searching results are provided by offline calculation. However, calculated amount of the proposed method is not huge. Moreover, the calculated amount can be reduced in the case where calculation period is decreased. Thus, the proposed method can also search in online mode.

Figs. 5.8 and 5.9 show the experimental results of grasping motion. The searching results of grasping motion shown in the each figure (c) have red area. On the other hand, the results of release motion shown in (d) are almost blue.

Moreover, Figs. 5.10 and 5.11 show the experimental results of kneading motion. In these

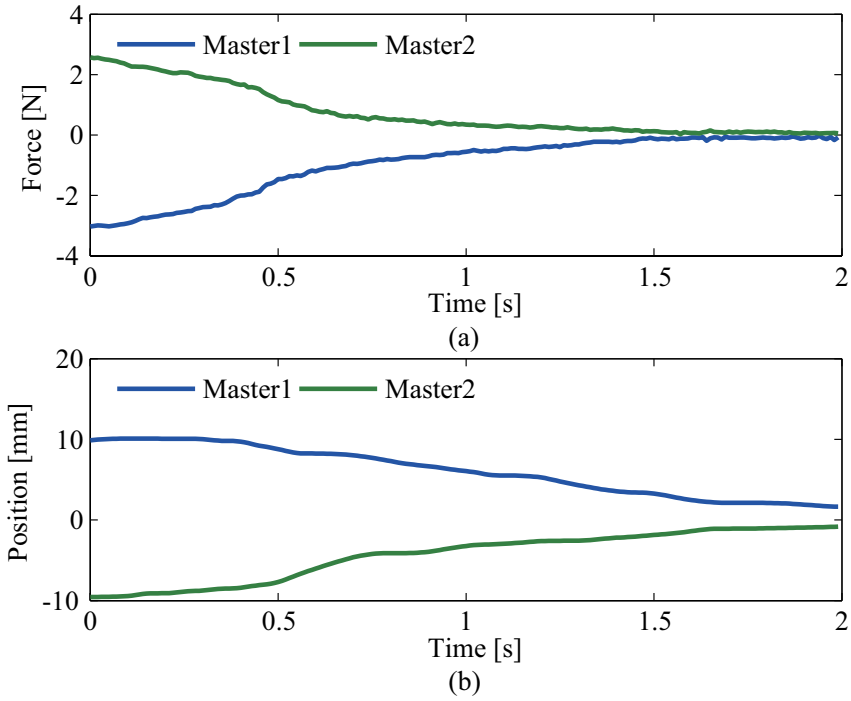

Fig. 5.7. Indexed Motion (Release Motion). (a) Forces ${}^1_2\Phi$ and ${}^2_2\Phi$. (b) Positions ${}^1_2\Xi$ and ${}^2_2\Xi$.

figures, the grasping results show red when the human operator executes the grasping motion. In the case of release motion, the release results is red. Therefore, the motion search system is able to search the motion of human operator by using the indexed motion.

By the experiments, the validity of the motion search system is confirmed.

5.1.1.6 Conclusion

The thesis proposes the motion index/search system based on real-world haptics. The motion index system indexes the human motion using the force and position stored by the motion-saving system. This system is able to create the motion dictionary, which includes the desired indexed motions. Meanwhile, the motion search system searches the motion of human operator according to the indexed motions. The proposed system is utilized to recognize the human motion. By the experimental results, the validity and possibility of the proposed method were confirmed.

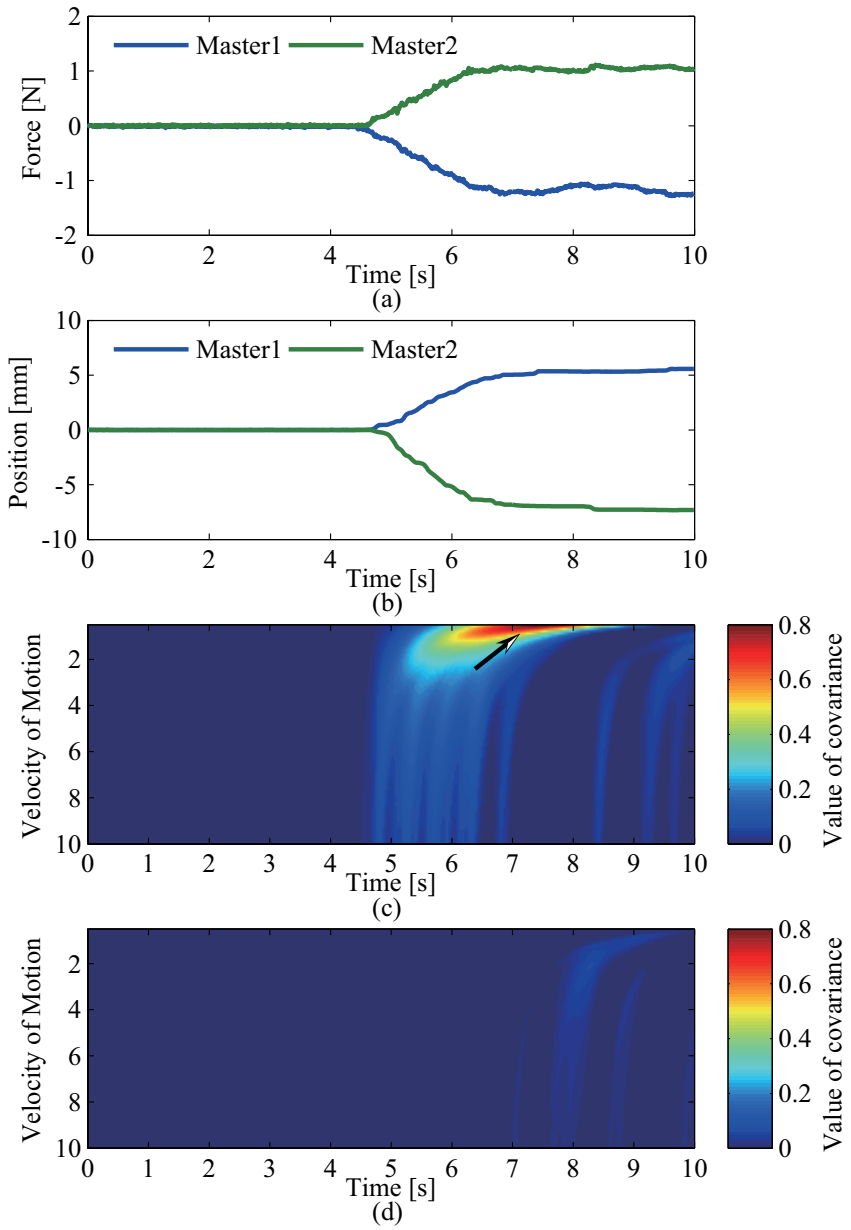

Fig. 5.8. Grasping motion. (a) Force ${}^{M1}F^{ext}$ and ${}^{M2}F^{ext}$. (b) Position ${}^{M1}X^{res}$ and ${}^{M2}X^{res}$. (c) searching result of grasping motion ${}_1R$. (d) searching result of release motion ${}_2R$.

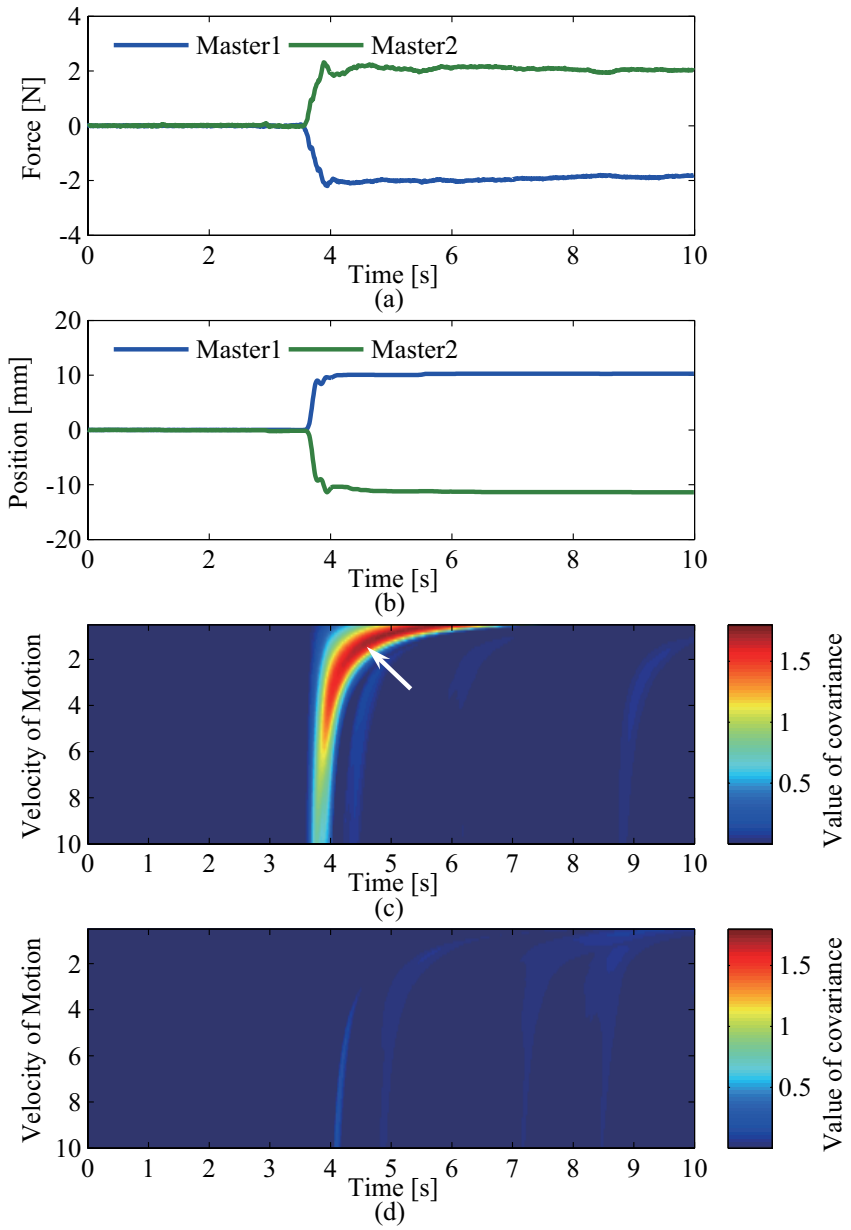

Fig. 5.9. Fast grasping motion. (a) Force ${}^{M1}F^{ext}$ and ${}^{M2}F^{ext}$. (b) Position ${}^{M1}X^{res}$ and ${}^{M2}X^{res}$. (c) searching result of grasping motion ${}_1R$. (d) searching result of release motion ${}_2R$.

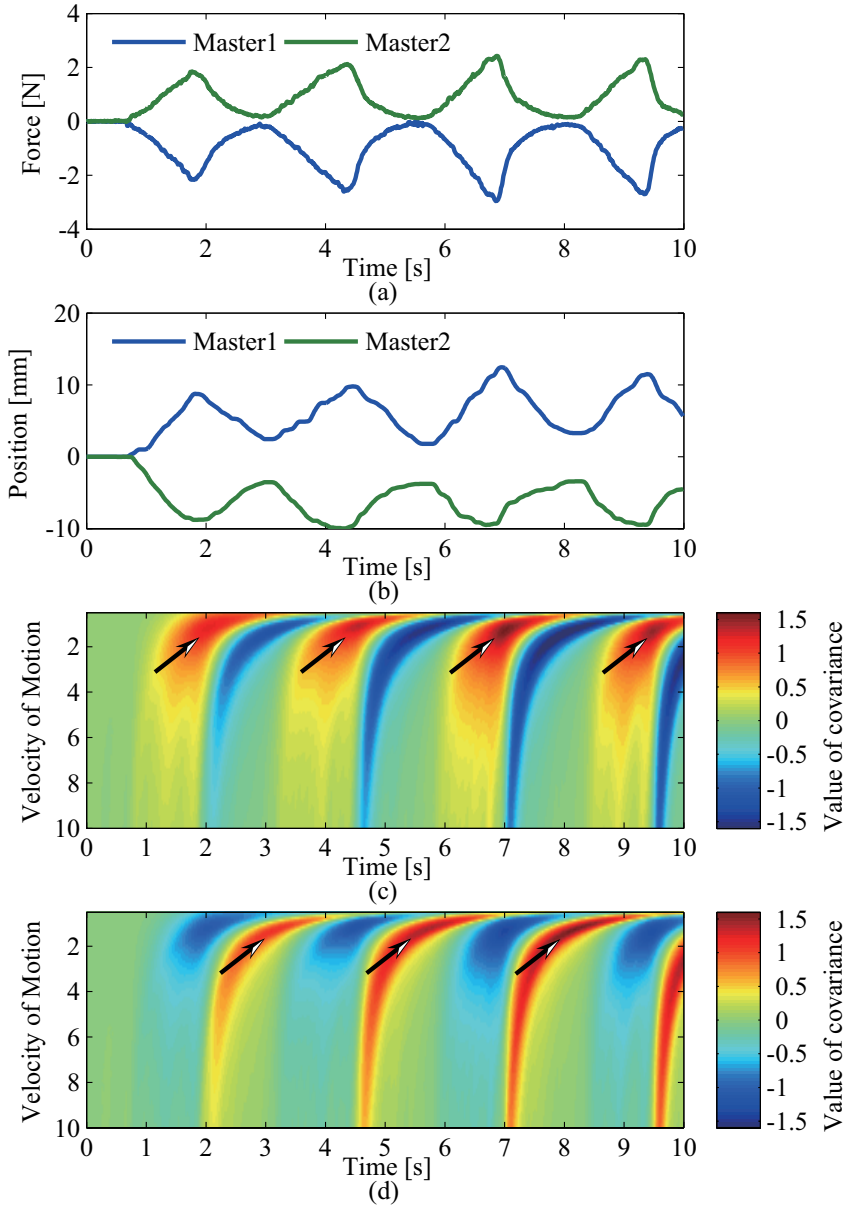

Fig. 5.10. Kneading motion. (a) Force ${}^{M1}F^{ext}$ and ${}^{M2}F^{ext}$. (b) Position ${}^{M1}X^{res}$ and ${}^{M2}X^{res}$. (c) searching result of grasping motion ${}_1R$. (d) searching result of release motion ${}_2R$.

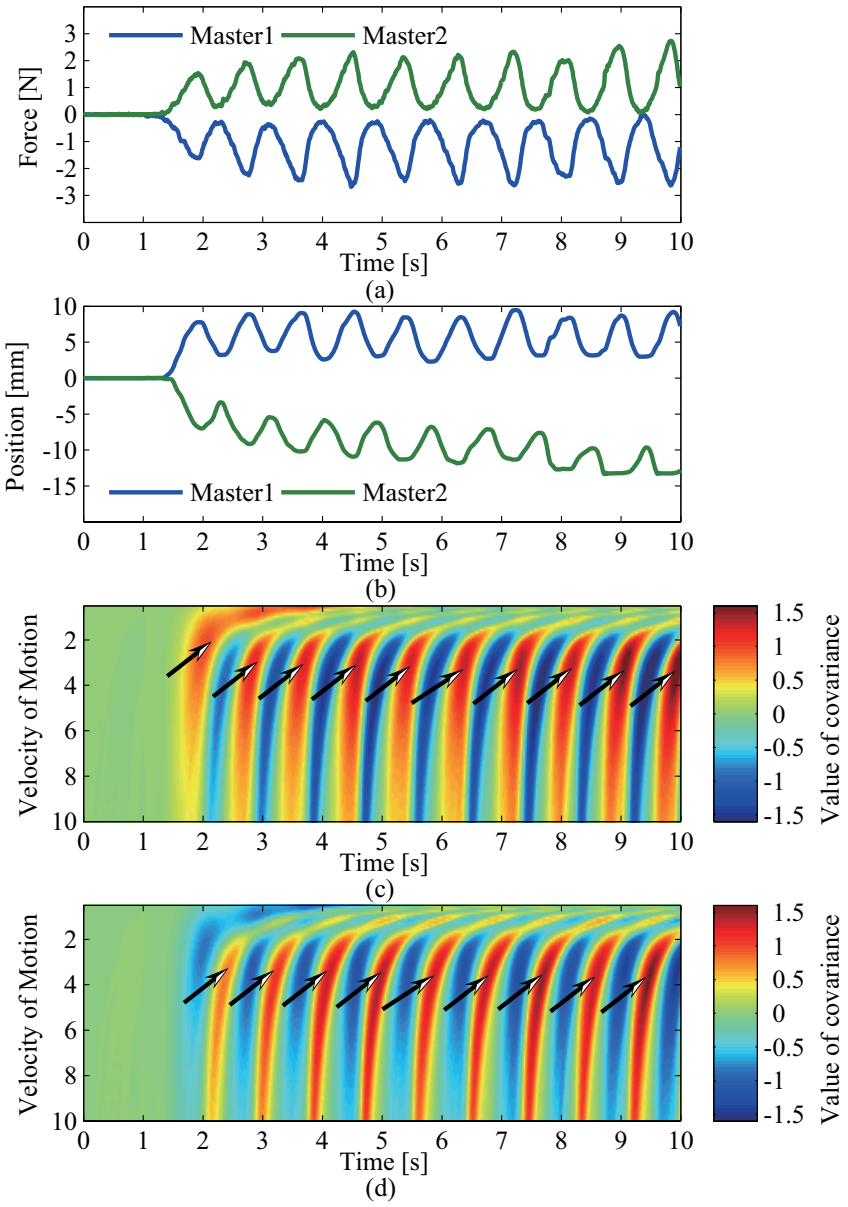

Fig. 5.11. Fast kneading motion. (a) Force ${}^{M1}F^{ext}$ and ${}^{M2}F^{ext}$. (b) Position ${}^{M1}X^{res}$ and ${}^{M2}X^{res}$. (c) searching result of grasping motion ${}_1R$. (d) searching result of release motion ${}_2R$.

5.1.2 Searching System of Haptic Environment

5.1.2.1 Introduction

Power electronics is contributing to our society. For example, inverter and converter which are capable of converting power are necessary for driving a motor mounted on electric train. In recent years, research and development relevant to techniques for electric vehicle has been also conducted. To operate efficiently the inverter and the converter, various techniques researched in field of power electronics is needed. Power electronics bring benefits to green technology. Besides, since performance of local controller such as current control is important element, power electronics is necessary to stable control of electric actuators in field of motion control. As with power electronics, motion control is also contributing to our life. Actuators of industrial machine tools which manufacture various products are controlled based on motion control. Using techniques of power electronics and motion control, industrial robot and medical robot accomplish very complicated task. Furthermore, power electronics and motion control are useful for treatment of haptic information as well as control of the actuators. In the real-world haptics, transmission [44, 45], storage, and reproduction [106] of haptic sensation are realized by using the electric actuators. Therefore, the real-world haptics is in interdisciplinary field of power electronics and motion control as shown in Fig 5.12.

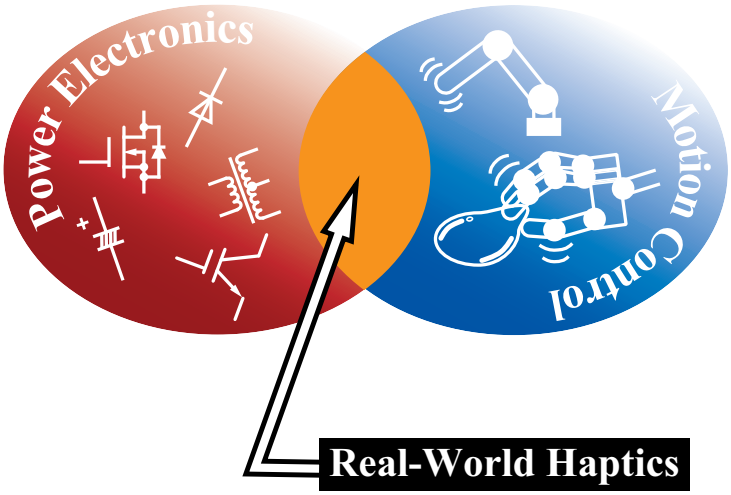

Fig. 5.12. Relation of power electronics, motion control, and real-world haptics.

This thesis focuses on the haptic information in the real-world. In the practical use, techniques relevant to the haptic information have not established yet though human has not only auditory organs and visual organs but also haptic organs. As with acoustic information and visual information, the real-world haptics should be much researched to treat freely the haptic information. In fact, method of storage and of reproduction for the haptic information has been proposed in the laboratory as mentioned above. Moreover, the haptic camera which is capable of estimating mechanical impedance of haptic environment was proposed [92]. However, compared with text documents, search method for the haptic information in the real-world has not been realized apparently yet. On the other hand, method of similarity search for the acoustic information was researched [107]. In the visual information, database systems and retrieval techniques have been proposed [108]–[111].

Hence, this thesis proposes search system based on the real-world haptics. The proposed method utilizes environment-copying system [112], which is capable of storing and reproducing the haptic sensation. The environment-copying system consists of two systems. The one of the system is environment-saving system; the other system is environment-loading system. At first, environmental data memory in the environment-saving system stores the haptic characteristics. After that, search algorithm proposed in this thesis is able to calculate similarity between the force data stored to the environmental data memory and the force response of the bilateral control [44, 45]. By using proposed method, once the environmental haptic information is stored, search result relevant to the haptic environment is obtained.

This research is organized as follows. Subsection 5.1.2.2 explains concept of the environment-copying system. In 5.1.2.3, concept and realization method of the searching system is presented. The experimental result of the proposed method is shown in 5.1.2.4. The last subsection concludes this research.

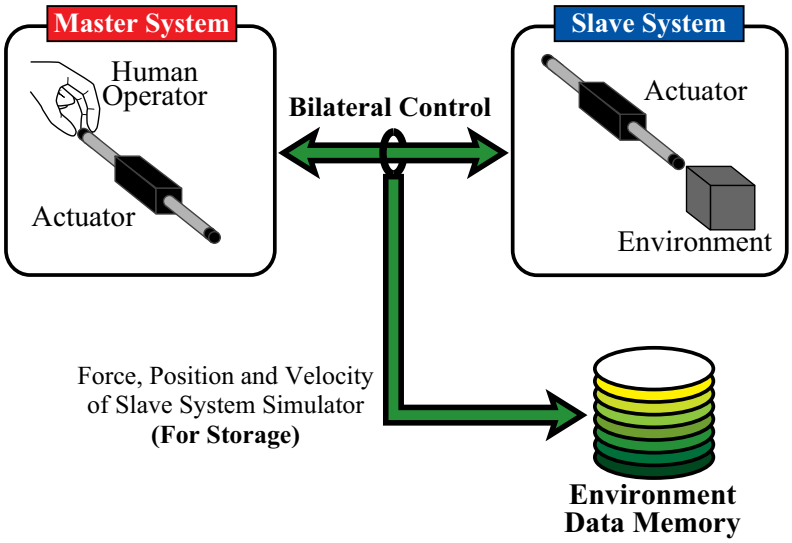

Fig. 5.13. Conceptual diagram of the environment-saving system.

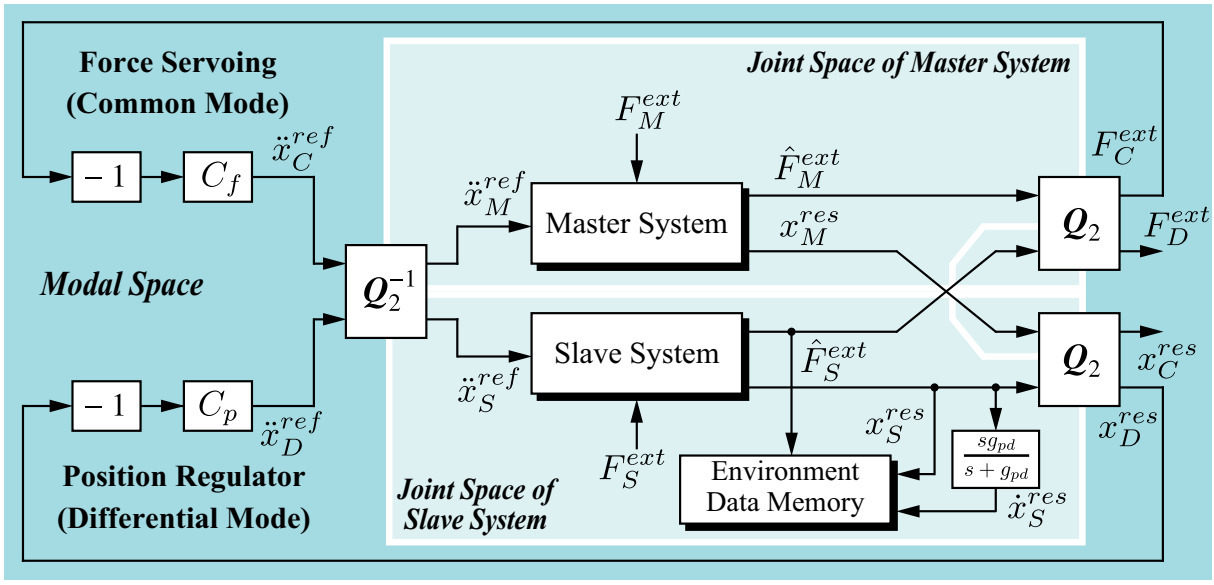

Fig. 5.14. Block diagram of the environment-saving system.

5.1.2.2 Environment-Copying System

Concept In order to realize the search system for haptic information, the environment-copying system which stores and reproduces the haptic sensation is needed. In this section, fundamental concept of the environment-copying system [112] is explained.

The environment-copying system consists of two systems. The first system is environment-saving system; the other system is environment-loading system. In the environment-saving system, actuators are operated by bilateral controller [44, 45] to measure force between master system and slave system. The force which occurs between operator in the master side and haptic environment in the slave side expresses haptic sensation. The environment-saving system is capable of storing the force response to the environmental data memory depending on position response and velocity response of actuators. Accordingly, storage of the haptic sensation is realized.

In addition, the environment-loading system reproduces the force according to the environment data memory, which was generated by the environment-saving system, in order to provide the environmental haptic sensation to the human operator in the master side.

By this method, the human operator is able to feel the environmental haptic sensation beyond time and space without the real environment.

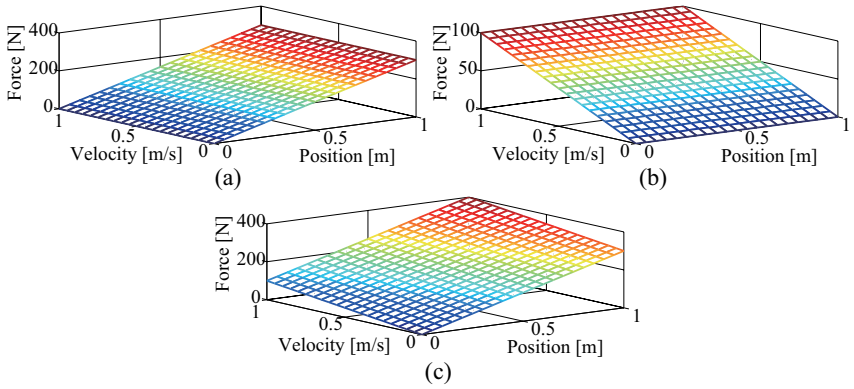

Fig. 5.15. Force information in the environment data memory. (a) In case of stiffness. (b) In case of damper. (c) In case of stiffness and damper.

Environment-Saving System Fig. 5.13 shows conceptual diagram of the environment-saving system. The environment-saving system consists of a master system and a slave system, which are operated by a bilateral control. The local controller in each system is acceleration control using disturbance observer [66].

In this thesis, the bilateral control [44, 45] based on modal decomposition using quarry matrix [65, 63] is utilized. The second-order quarry matrix is defined as

$$\boldsymbol{Q}_2 = \frac{1}{2}\begin{bmatrix} 1 & 1 \\ 1 & -1 \end{bmatrix}. \tag{5.20}$$

Fig. 5.14 shows block diagram of the environment-saving system by using the bilateral controller. In Fig. 5.14, superscript ref, ext, and res represent reference, external, and response. Moreover, subscript M, S, C, and D are master, slave, common mode, and differential mode. F, x, $\dot{x}$, and $\ddot{x}$ denote force, position, velocity, and acceleration. $\hat{F}$ represents estimated force by the reaction force observer [64]. The force controller C_f and the position regulator C_p in Fig. 5.14 are described as

$$C_f = K_{fp} \tag{5.21}$$

$$C_p(s) = K_{pp} + \frac{s\ g_{pd}}{s + g_{pd}}\ K_{pd} \tag{5.22}$$

where K_{fp}, K_{pp}, K_{pd} and g_{pd} denote gain of the force controller, proportional gain, differential gain and pole of the position regulator, respectively.

The environment-saving system stores the force information of the actuator in the slave side to the environmental data memory F^{mem}

$$F^{mem}\left(\dot{\chi}, \chi\right) = \hat{F}_S^{ext} \tag{5.23}$$

where $\hat{F}_S^{ext}$ is force estimated by the reaction force observer [64] in slave side. χ denotes quantized position calculated as

$$\chi = \left\lfloor \frac{x_S^{res} - X_{min}}{\Delta X} + 0.5 \right\rfloor \tag{5.24}$$

$$\Delta X = \frac{X_{max} - X_{min}}{N_x} \tag{5.25}$$

where X_{max}, X_{min}, and N_x represent maximum value of position, minimum value of position, and number of division with respect to position, respectively. Moreover, quantized velocity $\dot{\chi}$ is given by

$$\dot{\chi} = \left\lfloor \frac{\dot{x}_S^{res} - \dot{X}_{min}}{\Delta \dot{X}} + 0.5 \right\rfloor \tag{5.26}$$

$$\Delta\dot{X} = \frac{\dot{X}_{max} - \dot{X}_{min}}{N_{\dot{x}}} \tag{5.27}$$

where $\dot{x}_S^{res}$ is velocity response of the actuator in the slave side. The velocity response is obtained by pseudo derivative. $\dot{X}_{max}$, $\dot{X}_{min}$, and $N_{\dot{x}}$ are maximum velocity, minimum velocity, and number of division with respect to velocity, respectively. In other words, the environment-saving system fills in 2-dimensional lookup table of the force depending on the position responses and the velocity responses.

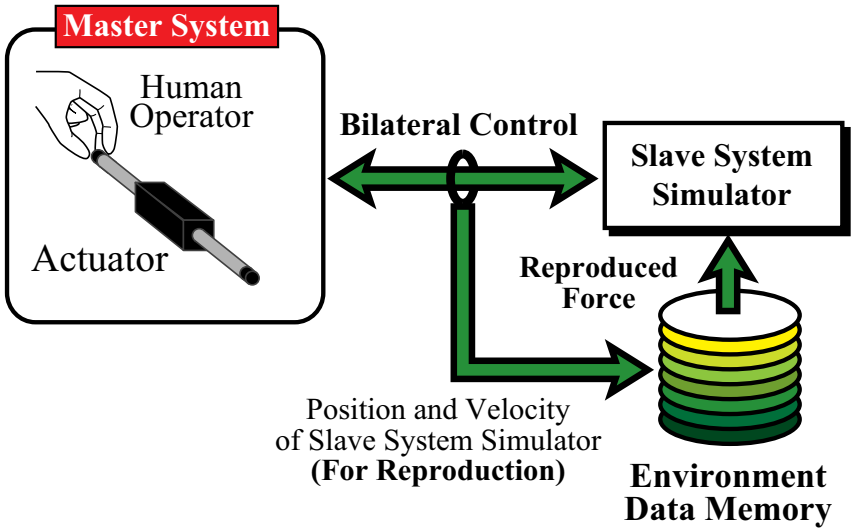

Fig. 5.16. Conceptual diagram of the environment-loading system.

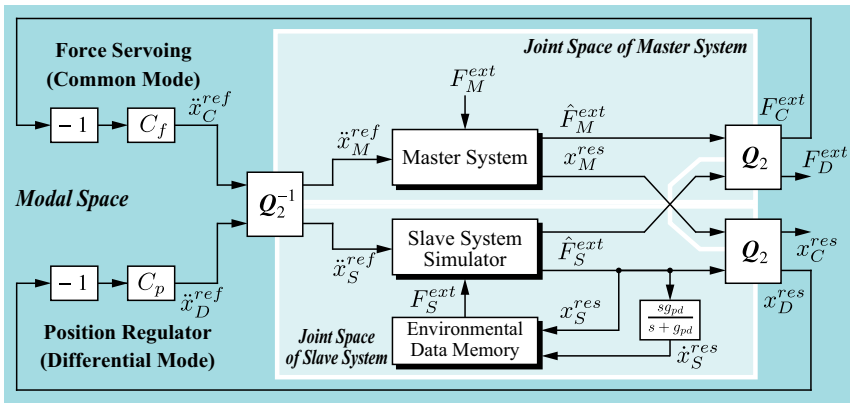

Fig. 5.17. Block diagram of the environment-loading system.

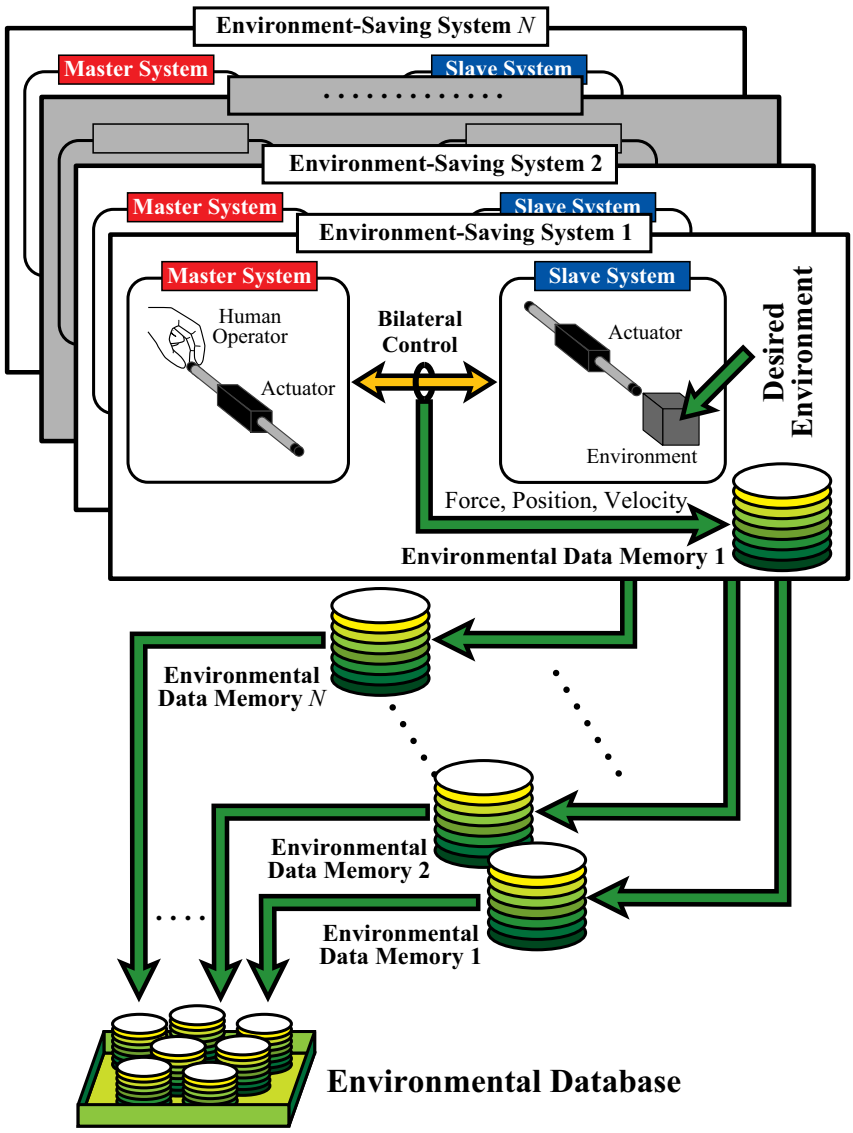

Fig. 5.18. Storage of environmental haptic information.

Environmental Data Memory As mentioned above, the environmental data memory is utilized to treat the haptic sensation. In general, environmental haptic sensation is represented as mechanical impedance including stiffness and damper. The force f generated by the stiffness K_e and the damper D_e is represented as

$$f = D_e \dot{x}^{res} + K_e x^{res}. \tag{5.28}$$

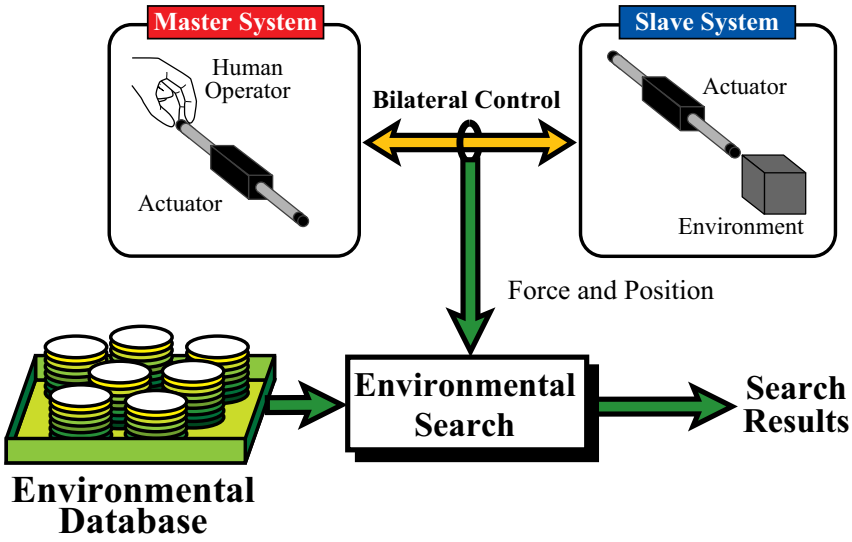

Fig. 5.19. Conceptual diagram of environmental search system.

In the case of simple environment, the stiffness and the damper are useful for representation of haptic environment. However, complicate environment in the real-world cannot be represented by using the simple impedance. In the real-world haptics, since K_e and D_e are complicated function, modeling for haptic environment is difficult.

Consequently, this research utilizes the environmental data memory, which is able to treat directly raw force data from the environment without the model. In the environment data memory, the environmental stiffness K_e and the environmental damper D_e are expressed as

$$K_e = \frac{\partial F^{mem}}{\partial x^{res}} \tag{5.29}$$

$$D_e = \frac{\partial F^{mem}}{\partial \dot{x}^{res}}. \tag{5.30}$$

Fig. 5.15 shows force information in the environment data memory in case where the environment consists of pure stiffness and/or damper. The conventional expression method using the simple stiffness and the damper considers only the plane in Fig. 5.15. On the other hand, the environmental data memory which treats the raw force data is capable of treating unmodeled environment. In other words, haptic sensation of unknown environment such as nonlinear environment is able to be stored and reproduced. In this point, the environment-copying system

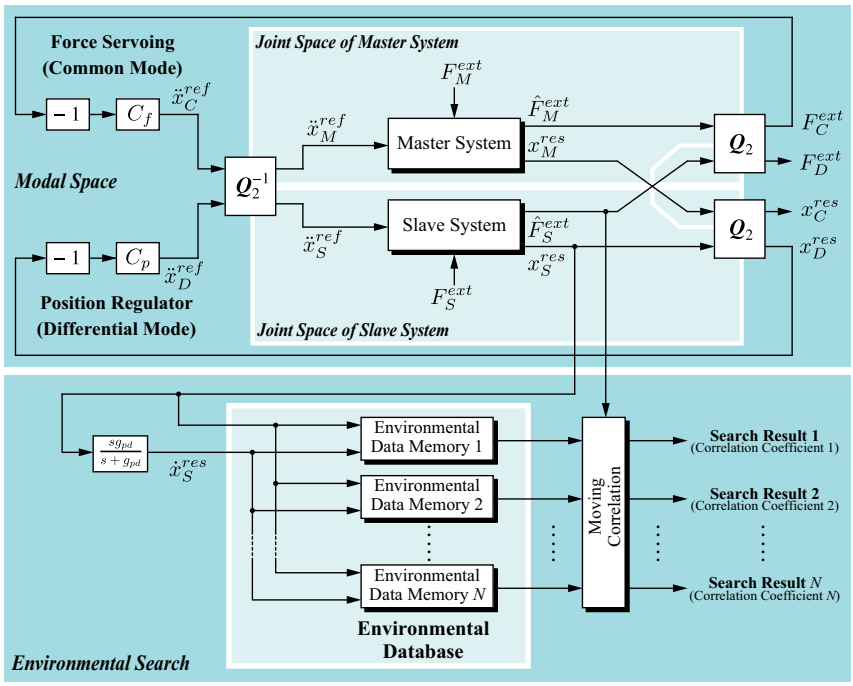

Fig. 5.20. Block diagram of search system for haptic environment.

has large advantage.

Environment-Loading System Figs. 5.16 and 5.17 show conceptual diagram of the environment-loading system and block diagram. The actuators in the environment-loading system are also operated by the bilateral controller as with the environment-saving system. However, the slave system is unused in the real-world. In the environment-loading system, slave system simulator is used instead of the real slave system. In order to reproduce the haptic sensation, the environmental data memory which has haptic characteristics reconstructs force signal depending on the position and velocity responses of the slave system simulator. The force given to the slave system simulator F_S^{ext} is calculated as

$$F_S^{ext} = F^{mem}\left(\dot{\chi}, \chi\right). \tag{5.31}$$

In fact, the environmental data memory consists of 2-dimensional lookup table constructed by the environment-saving system. In short, the slave system simulator is operated according to the

environment characteristics. The environmental data memory and the slave simulator imitate the real-world environment in the slave side, so that the actuator in the master side is able to stimulate hand of the human operator.

5.1.2.3 Searching System

In this section, search method proposed in this thesis is described. The search method utilizes the environmental data memory mentioned in previous section.

Storage of Environmental Characteristics Fig. 5.18 shows generation method of the environmental haptic information. To obtain the environmental characteristics in the real-world, several environment-saving systems are utilized. The environment-saving systems store the force response of respective environments. By this method, the environmental data is able to be generated.

Concept Figs. 5.19 and 5.20 show conceptual diagram and block diagram of environmental search system. The actuators in the master side and the slave side are controlled by the bilateral controller [44, 45], so that the haptic transmission is achieved. In this situation, force occurs due to the law of action and reaction. At the same time, the reaction force observer provides the force from environment, which is in the slave side. Additionally, reaction force stored in the environmental data memories is reproduced simultaneously. After that, search algorithm calculates similarity between the force response in the bilateral controller and the force reproduced by the memories. The similarity is provided by moving correlation coefficient. Accordingly, search result for haptic environment is calculated. The detailed explanation of the search algorithm is mentioned in next subsection.

Search Algorithm Firstly, mean values of the force response and the reproduced force information are calculated in the window in order to obtain search results.

$$\overline{F}^{ext}_{S,i} = \frac{1}{W} \sum_{k=i-W}^{i} F^{ext}_{S,k} \tag{5.32}$$

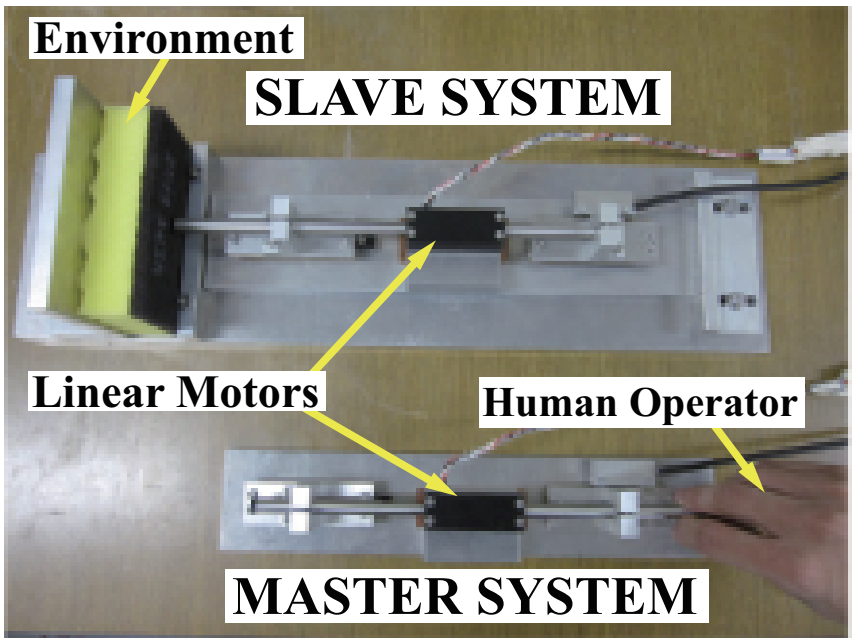

Fig. 5.21. Experimental setup.

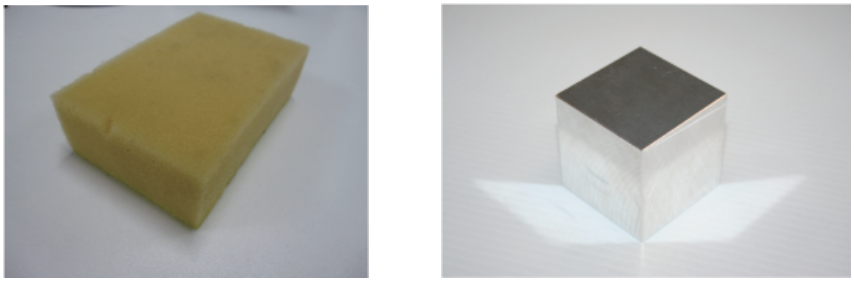

(a) (b)

Fig. 5.22. Environments used in the experiment. (a) Sponge. (N=1) (b) Aluminum block. (N=2)

$$ {}^{N}\overline{F}_{i}^{mem} = \frac{1}{W} \sum_{k=i-W}^{i} {}^{N}F_{k}^{mem} \tag{5.33} $$

where i, k and W denote time, time in the window and width of the window, respectively. N is number of environmental data memory, and denotes kind of environment stored to the environmental data memories. Secondly, the environmental search system calculates the moving correlations between the force response and the force information reproduced from the environ-

mental data memories as follows:

$$ {}^{N}R_i = \frac{\sum_{k=1}^{W} \left({}^{N}F^{mem}_{i-W+k} - {}^{N}\overline{F}^{mem}_{i} \right) \left(F^{ext}_{S,i-W+k} - \overline{F}^{ext}_{S,i} \right)}{S^{mem} S^{ext}} \tag{5.34} $$

where S^{mem} and S^{ext} are defined as

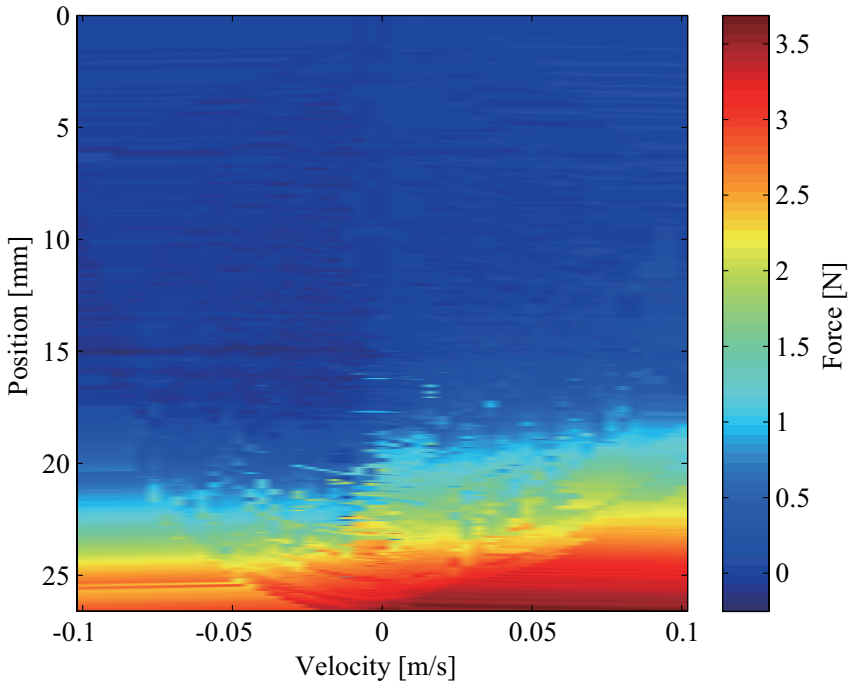

Fig. 5.23. Stored force information to environmental data memory. (Environment is sponge. N=1)

$$ S^{mem} = \sqrt{\sum_{k=1}^{W} \left({}^{N}F^{mem}_{i-W+k} - {}^{N}\overline{F}^{mem}_{i} \right)^2} \tag{5.35} $$

$$ S^{ext} = \sqrt{\sum_{k=1}^{W} \left(F^{ext}_{S,i-W+k} - \overline{F}^{ext}_{S,i} \right)^2}. \tag{5.36} $$

In (5.34), ${}^{N}R_i$ is search result of time i and of environment N. The search results provide similarity between environment stored to the environmental data memories and the current environment. In other words, the control system is able to know the environment, which contacts with the end effector.

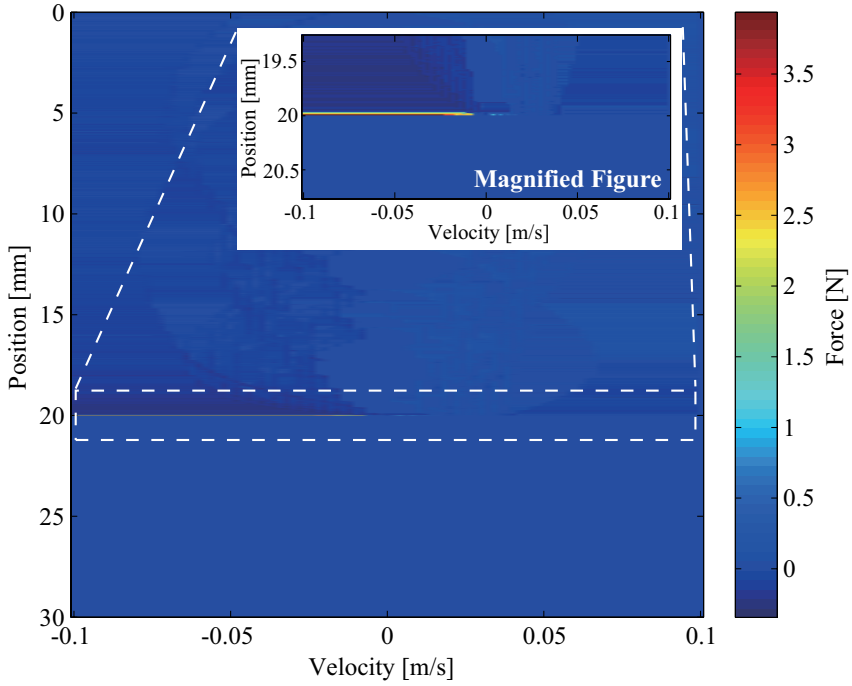

Fig. 5.24. Stored force information to environmental data memory. (Environment is aluminum block. N=2)

5.1.2.4 Experiment

Fig. 5.21 shows experimental setup. In the experiment, sponge and aluminum alloy shown in Fig. 5.22 are prepared. To verify validity of the search result, the experiments are conducted.

Storage Phase The environment-saving system for the sponge stores the force information to the environmental data memory 1. On the other hand, force response of the aluminum alloy is also stored to the environmental data memory 2. Figs. 5.23 and 5.24 show force information stored to the environmental data memory 1 and 2, respectively.

Search Phase Fig. 5.25 shows experimental results in the case where the sponge is put on the slave system. The search results is shown in Fig. 5.25(d). In Fig. 5.25(d), search result of the sponge is larger than search result of the aluminum alloy. Therefore, the proposed system is able to estimate haptic sensation of the sponge.

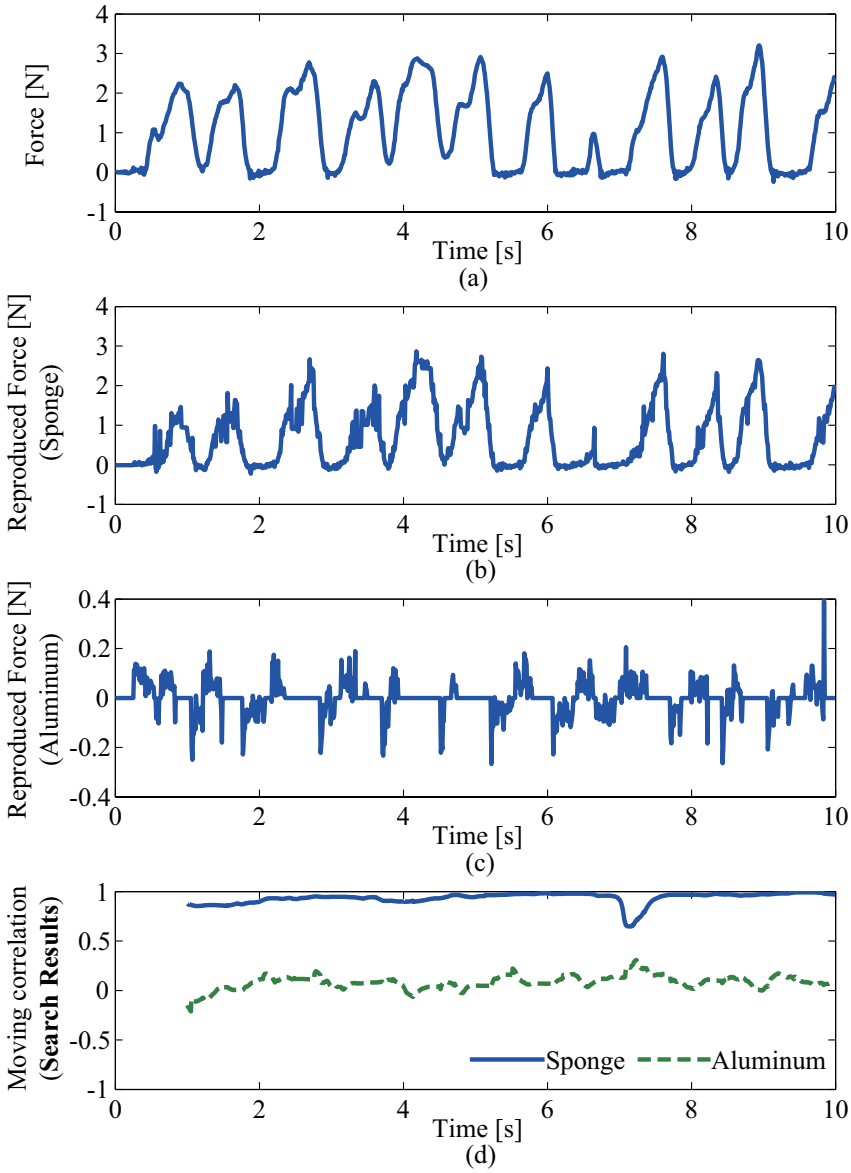

Fig. 5.25. Experimental results. (a) Force response F^{ext}. (b) Reproduced Force in the case of sponge ${}^{1}F^{mem}$. (c) Reproduced force in the case of aluminum alloy ${}^{2}F^{mem}$. (d) Search results ${}^{1}R$, ${}^{2}R$.

5.1.2.5 Conclusion

This thesis proposes searching system for haptic information. The proposed system consists of the environment-copying system and the search algorithm. In the storage phase, environmen-

tal data memory in the environment-copying system stores force responses in order to reproduce the environmental haptic sensation. After that, search algorithm calculates similarity between force response of bilateral controller and force from the environmental data memory. Thus, the searching system proposed in this thesis is able to calculate search results relevant to haptic environment. By the experiments, validity of the proposed method was verified. The searching system will be useful for industrial applications, medical and welfare human support.

5.1.3 Identification of Stiffness in Differential Mode

5.1.3.1 Introduction

In the previous subsection, the haptic sensation of the target object is stored by using the environmental force at one-point. However, if the size of the target object is different, the search result obtained by the search algorithm becomes different environment even if the material of the object is same. Consequently, this thesis identifies the element stiffness, which does not depend on the size of the target object. In the experiment, the value of the stiffness in the differential mode is calculated by the environmental force responses and the position responses between the 2 points. The validity of the method is verified by the experimental results.

5.1.3.2 Identification Method

As mentioned in introduction, the detection algorithm of a target environment described in the previous subsection cannot provide accurate search results, if the size of the target object is changed. Because the entire stiffness of an object is estimated by the algorithm. Consequently, the element stiffness between 2 nodes is identified.

Fig. 5.26 shows model of the target object. In the surface of the target object, 2 nodes are

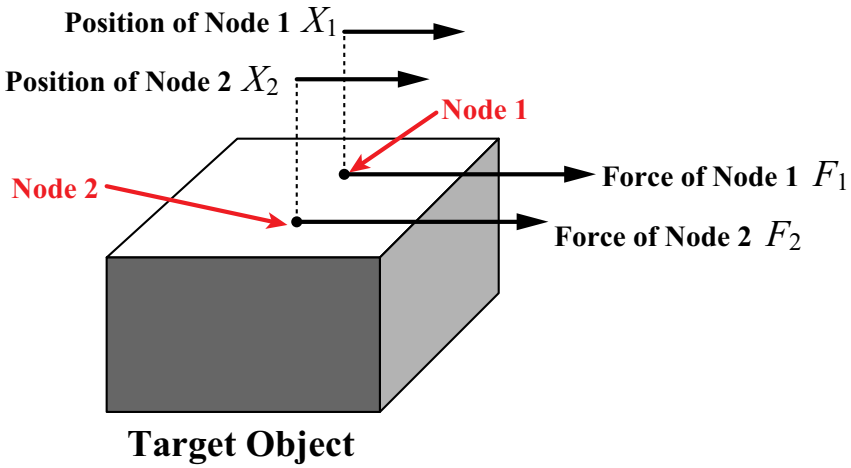

Fig. 5.26. Model of target object.

assigned. F_1 and F_2 mean the force at the node 1 and the node 2, respectively. The position of

the node 1 and the node 2 is represented as X_1 and X_2. Moreover, the stiffness between node 1 and node 2 is denoted as K_{12}. Using 2 linear actuators which are controlled by the position regulators shown in Fig. 5.27, the thesis assumes that the force and position at each node can be obtained.

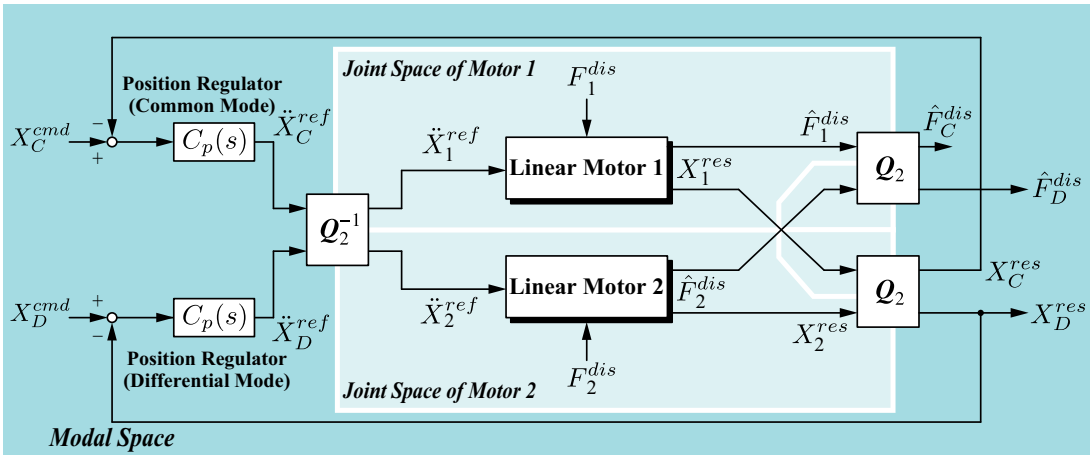

Fig. 5.27. Position control system in modal space.

In the position control system, the position responses X_1^{res} and X_2^{res} are transformed into modal space as follows:

$$\begin{bmatrix} X_C^{res} \\ X_D^{res} \end{bmatrix} = \boldsymbol{Q}_2 \begin{bmatrix} X_1^{res} \\ X_2^{res} \end{bmatrix} \tag{5.37}$$

where $\boldsymbol{Q}_2$ represents quarry matrix. Additionally, the position regulators $C_p(s)$ in the modal space calculate acceleration references of each mode $\ddot{X}_C^{ref}$ and $\ddot{X}_D^{ref}$ depending on the position command. The position command of common mode is set as $X_C^{cmd} = 0$. In the next step, the acceleration references in modal space are transformed into the acceleration references in joint space $\ddot{X}_1^{ref}$ and $\ddot{X}_2^{ref}$. By this method, the position controller is constructed. As with the position, the force responses in the joint space $\hat{F}_1^{dis}$ and $\hat{F}_2^{dis}$ is also transformed into the joint space as follows:

$$\begin{bmatrix} \hat{F}_C^{dis} \\ \hat{F}_D^{dis} \end{bmatrix} = \boldsymbol{Q}_2 \begin{bmatrix} \hat{F}_1^{dis} \\ \hat{F}_2^{dis} \end{bmatrix} \tag{5.38}$$

where $\hat{F}_C^{dis}$ and $\hat{F}_D^{dis}$ denote the force responses in the modal space.

In the thesis, F_1 and F_2 shown in Fig. 5.26 are corresponding to $\hat{F}_1^{dis}$ and $\hat{F}_2^{dis}$, respectively. Moreover, X_1 and X_2 are X_1^{res} and X_2^{res}. Therefore, the element stiffness K_{12} between node 1 and node 2 can be calculated as

$$K_{12} = \frac{F_D^{dis}}{X_D^{res}}. \tag{5.39}$$

In other words, K_{12} represents stiffness in the differential mode. To reduce noise of the calculated stiffness, low pass filter is utilized as follows:

$$\hat{K}_{12} = \frac{g_{lpf}}{s + g_{lpf}} K_{12} \tag{5.40}$$

where g_{lpf} denotes cutoff frequency of the low pass filter. By this means, the stiffness $\hat{K}_{12}$ in the differential mode can be experimentally identified in order to represent the haptic sensation of the target object.

5.1.3.3 Experiment

Experimental Setup Figs. 5.28 and 5.29 show model of an experimental device and experimental setup. In the experiment, the target object is rubber block. The position command

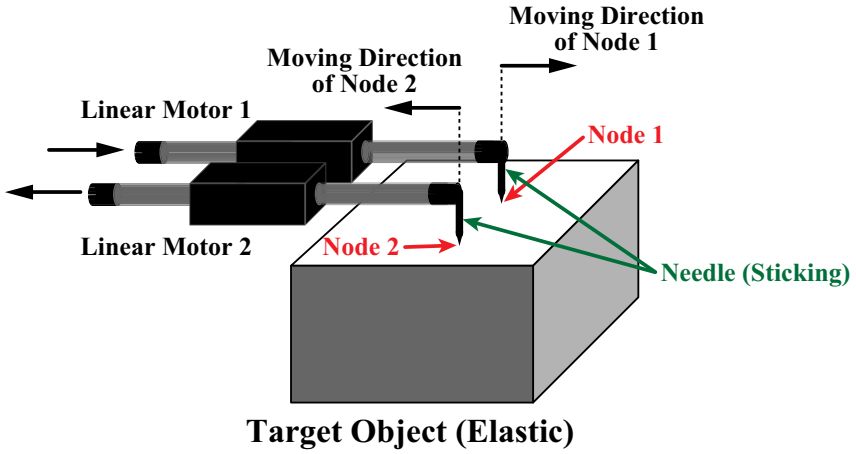

Fig. 5.28. Model of experimental devices.

in the differential mode is set as lamp signal $X_D^{cmd} = 0.25t \ \ mm.$ t represents time. Therefore, x-axis distance of the respective actuators is 0.5 mm at 10 s, and the actuators move to opposite

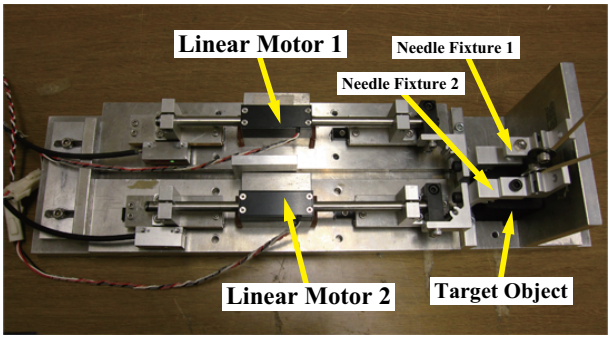

(a) Full view.

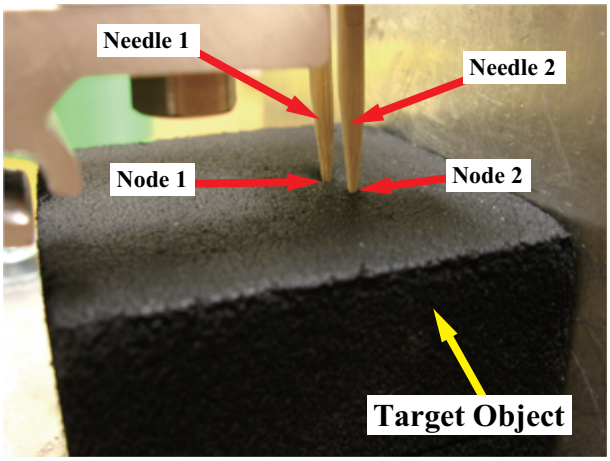

(b) Magnified figure.

Fig. 5.29. Experimental setup.

direction. Besides, the position command X_C^{cmd} in the common mode is set to 0 mm. The bandwidth of the low pass filter for the calculation of the stiffness g_{lpf} is set to 30 rad/s.

Experimental Results Figs. 5.30 and 5.31 show the experimental results. The experimental results confirms that the force and position responses at respective nodes are obtained. Moreover, the force and position responses in the modal space are also calculated. In Fig. 5.31(c), the stiffness between node 1 and node 2 can be identified. The value of the stiffness K_{12} is approximately 560 N/m. Since distance between node 1 and node 2 is very close, the stiffness

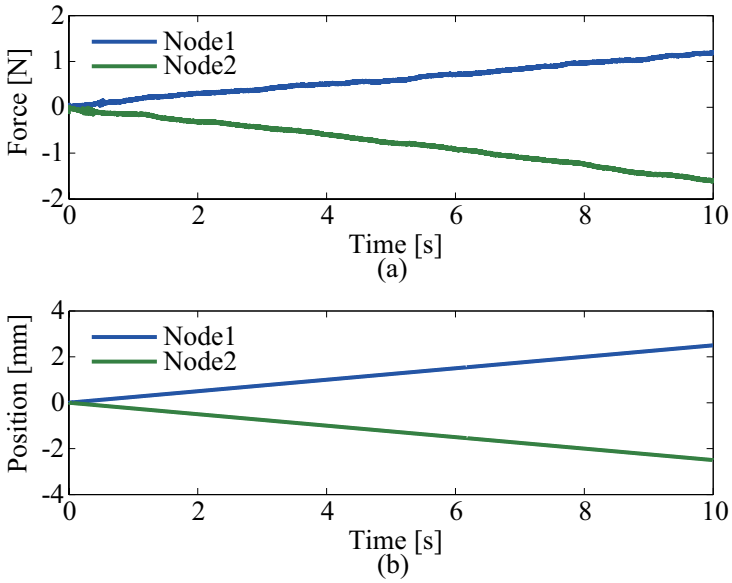

Fig. 5.30. Experimental results. (a) Force responses $\hat{F}_1^{dis}$, $\hat{F}_2^{dis}$. (b) Position responses X_1^{res}, X_2^{res}.

estimated by this method represents element of the materials, and is not depending on the size of the target object.

5.1.3.4 Conclusion

In the case of the haptic recognition method mentioned in the previous subsection, if the size of the target object is different, the search result obtained by the search system becomes different environment even if the material of the object is same. Consequently, this thesis identifies the element stiffness, which does not depend on the size of the target object. By the experiment, the value of the stiffness could be calculated by the force responses and the position responses between respective nodes. This method can be utilized for recognition method of the haptic sensation.

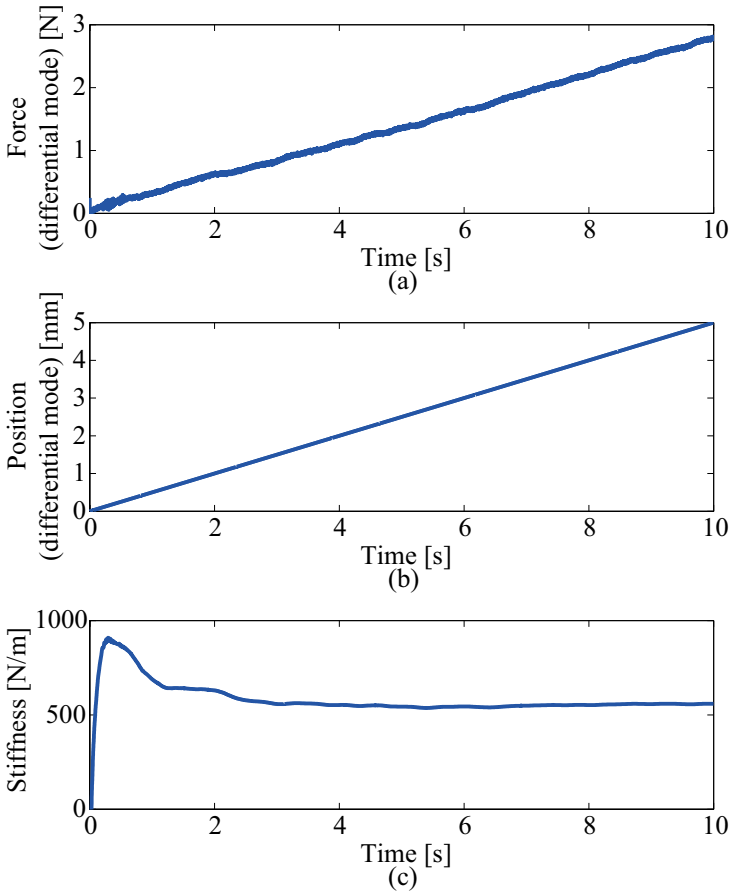

Fig. 5.31. Experimental results. (a) Force responses in the differential mode $\hat{F}_D^{dis}$. (b) Position responses in the differential mode X_D^{res}. (c) Identified stiffness between node 1 and node 2 $\hat{K}_{12}$.

5.2 Selective Motion-Copying System

5.2.1 Introduction

In recent years, information and communication technology has been continuously grown. The current information technology treats acoustic information and visual information such as JPEG documents, mp3 files and video files and so on. The acoustic and visual information are considered in the practical techniques. However, the human has five organs, which recognize acoustic, visual, olfactory, gustatory and haptic information. Therefore, the information technology should treat residual information in order to provide realistic environment in the distant place.

In this thesis, the haptic information is considered. The acquisition method of the human motion based on visual information has been proposed [29]–[32]. However, these methods are not able to obtain the force information between the human and the environment. In addition, the abstraction method of human motion using the force information is proposed [33]. The hybrid control which treats both the force information and the position information has been proposed [34]–[35]. However, treatment of the haptic information in the real-world is not considered in the research. Though the method using virtual environment was proposed [72], the error of environmental model might be induced.

In addition, motion-copying system has been proposed [38]. The motion-copying system stores the motion of the human operator. Moreover, the motion-copying system is able to reproduce not only position but also force without mathematical model of the environment. Therefore, the motion-copying system is capable of imitating the human motion. However, the normal motion-copying system cannot reproduce the force and the position, when the environment is changed.

In this thesis, selective motion-copying system is proposed. In order to reproduce the force and the position accurately, the environmental search algorithm detects the environment and provides the environmental information to the motion-copying system. By the proposed method, the human motion is able to be reproduced even if the environment in the reproduction phase

is changed.

This research is organized as follows. In 5.2.2, concept of the normal motion-copying system is explained. In 5.2.3, storage method of environmental haptic information is described. The selective motion-copying system is explained in 5.2.4. The detailed control method is also described. In 5.2.5, the experimental results are shown. Finally, the last subsection concludes this study.

5.2.2 Motion-Copying System

In this section, fundamental concept of the motion-copying system is explained. Fig. 5.32

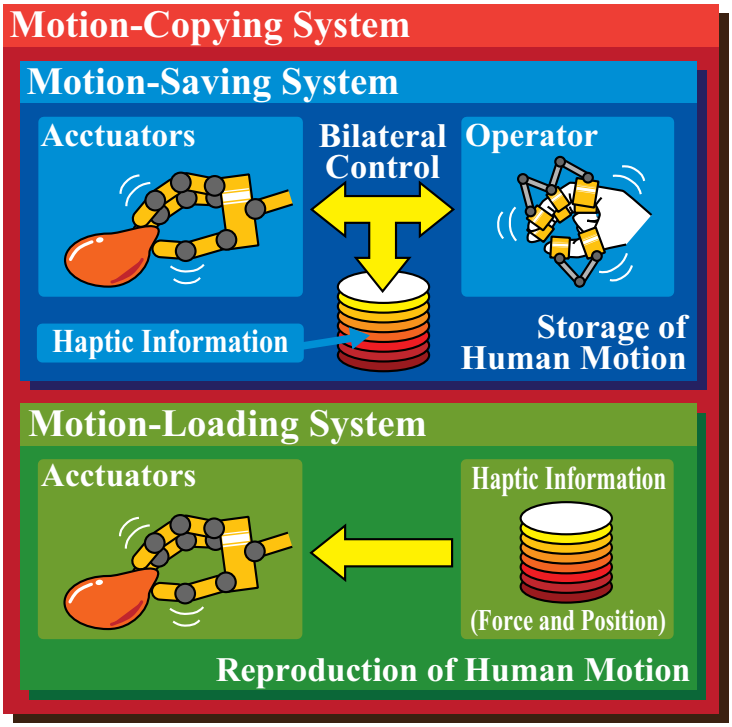

Fig. 5.32. Conceptual diagram of motion-copying system.

shows conceptual diagram of the motion-copying system, which consists of motion-saving system and motion-loading system. The motion-saving system stores force and position responses of actuators to motion data memories, in order to achieve storage of the human motion. On the other hand, the motion-loading system is able to reproduce the force information and the

position information, which were stored by the motion-saving system.

However, the normal motion-copying system cannot accurately reproduce the force and the position, when the environment in the reproduction phase is different from the environment in the storage phase. In this thesis, the selective motion-copying system is proposed to solve this problem.

5.2.3 Storage of Environmental Haptic Information

Before the motion-saving system stores motion of the human operator, the proposed method obtains the target environmental haptic information in the slave side in order to realize the selective motion-loading system.

5.2.3.1 Concept

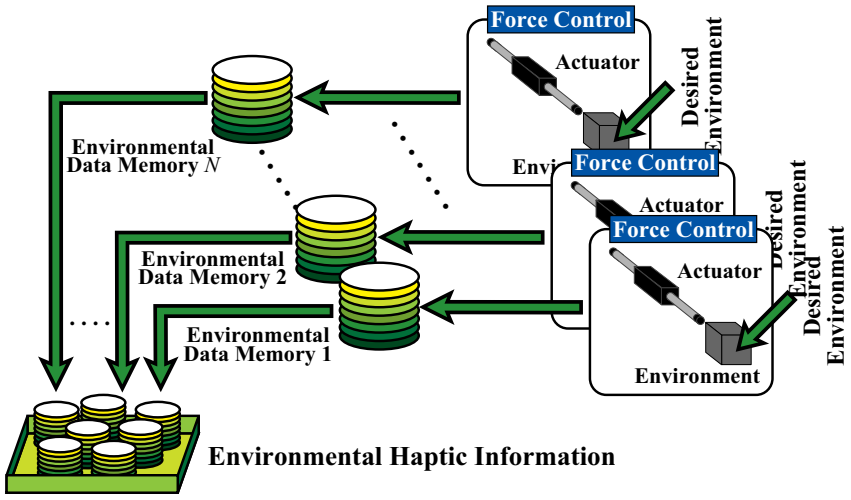

Fig. 5.33. Storage of environmental haptic information.

Fig. 5.33 shows how to store environmental haptic information. To obtain environmental characteristics, force responses and position responses are stored to environmental data memories 1 to N by using actuators which are controlled by force controllers. N represents kind of the environment. In this system, reaction force information according to the position responses are able to be stored.

5.2.3.2 Motion Control

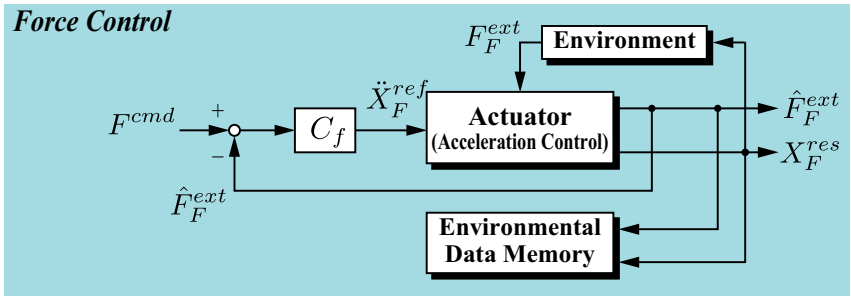

Fig. 5.34. Storage of environmental haptic information.

Fig. 5.34 shows block diagram of force controller, which realizes storage of environmental haptic information. F^{cmd} and C_f represent force command and force controller. An actuator is controlled by acceleration control, which is realized by disturbance observer [66]. The estimated reaction force $\hat{F}_F^{ext}$ and the position response X_F^{res} are used to storage of the haptic information.

5.2.3.3 Storage Method

In general, the reaction force f from haptic environment which consists of stiffness and friction components is generated as

$$f(\dot{x}(t), x(t)) = D(x(t))\frac{dx(t)}{dt} + K(x(t))x(t) \tag{5.41}$$

where x, t, D ,and K are position, time, viscous friction, and stiffness, respectively. This thesis assumed that reaction force from stiffness f_K is changed according to the position as follows:

$$f_K(x(t)) = K(x(t))x(t). \tag{5.42}$$

Moreover, reaction force from friction f_D is calculated as

$$f_D(\dot{x}(t), x(t)) = D(x(t))\frac{dx(t)}{dt}. \tag{5.43}$$

In (5.43), since force response is expressed as a function of velocity and position, 2-dimensional lookup table is required in order to realize storage of reaction force from the environment. In

the above method, size of memories become large and the storage time become long, due to using 2-dimensional lookup table.

Consequently, momentum from friction p_D is calculated in this thesis as

$$\begin{aligned} p_D(x(t)) &= \int D(x(t))\frac{dx(t)}{dt}dt + p_0 \\ &= \int D(x(t))dx(t) + p_0 \end{aligned} \tag{5.44}$$

where p_0 denotes initial momentum. Since the momentum is expressed as a function of only the position, 1-dimensional lookup tables are enough to store the environmental haptic information.

Finally, the reaction force from stiffness and the momentum are stored to the environmental data memory depending on the position.

$$F_{mem}[i_x] = f_K \tag{5.45}$$

$$P_{mem}[i_x] = p_D - p_0. \tag{5.46}$$

where F_{mem} and P_{mem} represent force memory and momentum memory. i_x denotes quantized position calculated as

$$i_x = \left\lfloor \frac{x(t) - X_{min}}{\Delta X} + 0.5 \right\rfloor \tag{5.47}$$

$$\Delta X = \frac{X_{max} - X_{min}}{N_x} \tag{5.48}$$

where X_{max}, X_{min}, and N_x are maximum value of position, minimum value of position, and number of division. However, decomposition to the force from stiffness f_K and the force from friction f_D is needed before calculating the momentum.

5.2.3.4 Decomposition Method of Reaction Force

In the normal method [112], the force from stiffness and the force from friction are decomposed as

$$f(t) = \begin{cases} f_K(x(t)) & (\ -\varepsilon < \dot{x}(t) < \varepsilon \ ) \\ f_D(x(t)) & (\text{ otherwise }) \end{cases} \tag{5.49}$$

where ε is threshold in terms of velocity. In short, the force from stiffness can be calculated when the velocity is nearly equal to 0. However, this method cannot capably decompose to the force from stiffness and the force from friction.

Consequently, the decomposition is realized by using FFT in this thesis. Firstly, estimated force and position response are transformed into frequency domain

$$\Phi[k] = \sum_{n=1}^{N_n} \hat{F}_F^{ext}[n] \exp\left\{\frac{-j2\pi(k-1)(n-1)}{N_n}\right\} \tag{5.50}$$

$$\Xi[k] = \sum_{n=1}^{N_n} X_F^{res}[n] \exp\left\{\frac{-j2\pi(k-1)(n-1)}{Nn}\right\} \tag{5.51}$$

where Φ, Ξ, n, k, and N_n are force in the frequency domain, position in the frequency domain, discrete time, discrete frequency, and number of data. Φ and Ξ are expressed as following complex number

$$\Phi[k] = \alpha[k] + j\beta[k] \tag{5.52}$$

$$\Xi[k] = \gamma[k] + j\delta[k] \tag{5.53}$$

where α and γ, β and δ represent real part, imaginary part, respectively. The phase of force θ_F and the phase of position θ_X are calculated as

$$\theta_F[k] = \tan^{-1}\frac{\beta[k]}{\alpha[k]} \tag{5.54}$$

$$\theta_X[k] = \tan^{-1}\frac{\delta[k]}{\gamma[k]}. \tag{5.55}$$

In the next step, maximum values of force from stiffness F_{Kmax} and damper F_{Dmax} are calculated as

$$F_{Kmax}[k] = \sqrt{\alpha[k]^2 + \beta[k]^2}\ \cos(\theta_X[k] - \theta_F[k]) \tag{5.56}$$

$$F_{Dmax}[k] = \sqrt{\alpha[k]^2 + \beta[k]^2}\ \sin(\theta_X[k] - \theta_F[k]). \tag{5.57}$$

The force from stiffness in the frequency domain Φ_K and the force from damper in the frequency domain Φ_D are calculated as

$$\Phi_K[k] = F_{Kmax}[k] \exp(j\theta_X[k]) \tag{5.58}$$

$$\Phi_D[k] = F_{Dmax}[k] \exp\left\{ j \left(\theta_X[k] - \frac{\pi}{2} \right) \right\}. \tag{5.59}$$

In other words, the force decomposition is realized because phase of the force from stiffness is equal to phase of the position. Finally, force from stiffness and force from friction are able to be calculated by following equations by using IFFT

$$f_K[n] = \frac{1}{N_n} \sum_{k=1}^{N_n} \Phi_K[k] \exp\left\{ \frac{j2\pi(k-1)(n-1)}{N_n} \right\} \tag{5.60}$$

$$f_D[n] = \frac{1}{N_n} \sum_{k=1}^{N_n} \Phi_D[k] \exp\left\{ \frac{j2\pi(k-1)(n-1)}{N_n} \right\}. \tag{5.61}$$

By this means, this method decomposes to the force from stiffness f_K and the force from friction f_D.

5.2.4 Selective Motion-Copying System

The proposed motion-copying system utilizes the environmental data memories described in the previous section to adapt to change of the target environment. In this section, the proposed method in this thesis is mentioned.

5.2.4.1 Concept

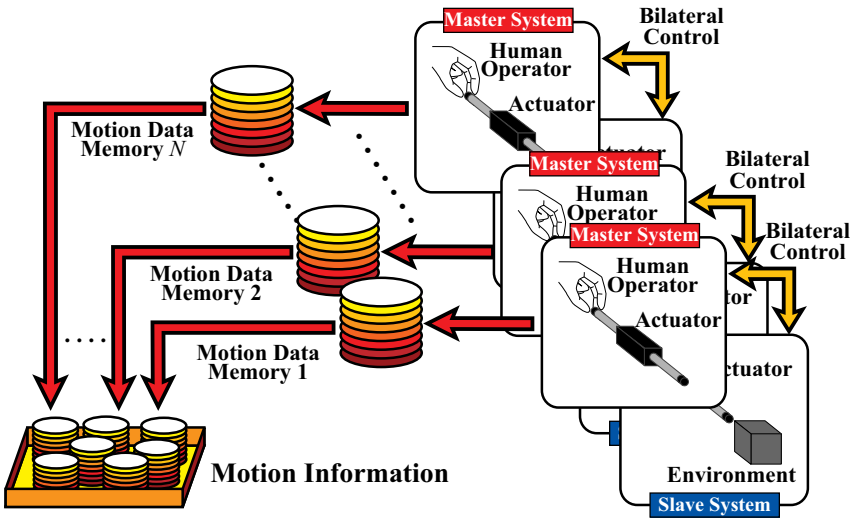

Fig. 5.35. Conceptual diagram of motion-saving systems.

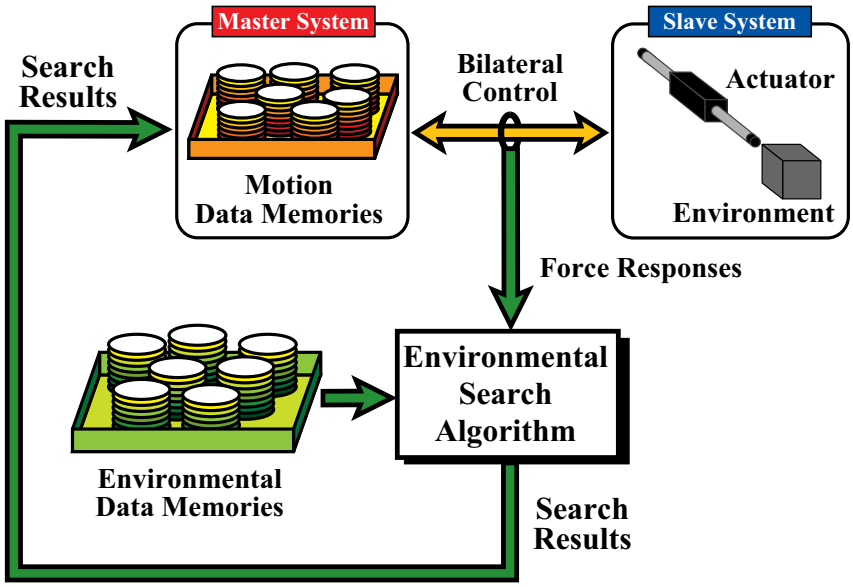

Fig. 5.36. Conceptual diagram of selective motion-loading system. (Proposed method)

Figs. 5.35 and 5.36 show conceptual diagrams of the motion-saving system and the selective motion-loading system. Basically, the motion-saving system used in this research is same as the normal motion-loading system. Therefore, the motion data memories simply store the human motion with the respective target environments.

On the other hand, compared with the normal motion-loading system, the proposed motion-loading system is improved in terms of adaptation to haptic environment. In the reproduction phase, environmental search algorithm calculates search results when the motion-loading system reproduces the human motion, which was stored by the motion-saving system. The search results provide similarity between the target environment and the environmental data memories. At the same time, the motion data memories in the virtual master side reproduces the motion of human operator according to the environmental search results. The motion reproduced by the motion-loading system is also changed when kind of the environment is changed. In short, the proposed system is able to reproduce suitable motion for the target environment. Therefore, the selective motion-loading system is capable of reproducing the force and the position corresponding with the stored ones, even if the environment is changed.

5.2.4.2 Motion-Saving System

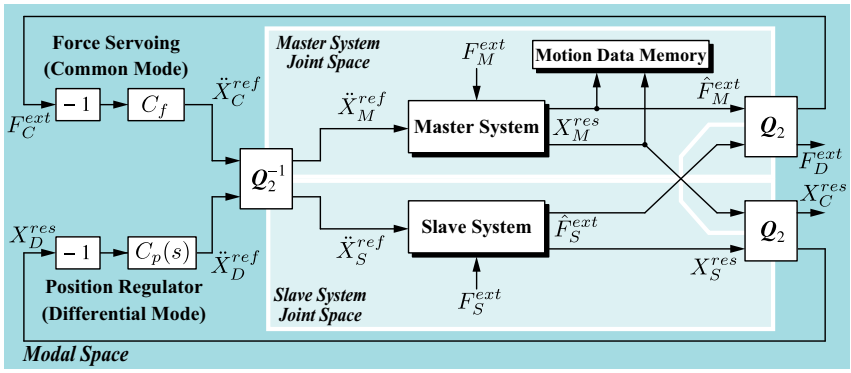

Fig. 5.37. Block diagram of motion-saving system.

Fig. 5.37 shows block diagram of the motion-saving system. In order to store the human motion, estimation of the force between the operator and the target environment is required. Therefore, the motion-saving system is controlled by the bilateral controller using modal decomposition [65]. The modal decomposition utilizes second-order quarry matrix [63] defined as

$$\boldsymbol{Q}_2 = \frac{1}{2}\begin{bmatrix} 1 & 1 \\ 1 & -1 \end{bmatrix}. \tag{5.62}$$

C_f and $C_p(s)$ are force controller and position regulator, respectively.

$$C_f = K_{pf} \tag{5.63}$$

$$C_p(s) = K_{pp} + sK_{dp} \tag{5.64}$$

where K_{pf} is control gain of the force controller, K_{pp} and K_{pd} are control gain of the position regulator. In other words, the each controller achieves force control of common mode and position control of differential mode, simultaneously. Moreover, the motion-saving system stores the force response $\hat{F}_M^{ext}$ and the position response X_M^{res} to the motion data memory.

5.2.4.3 Selective Motion-Loading System

Fig. 5.38 shows block diagram of the selective motion-loading system proposed in this thesis. Fundamentally, control method of the actuator in the slave side is almost same as the control

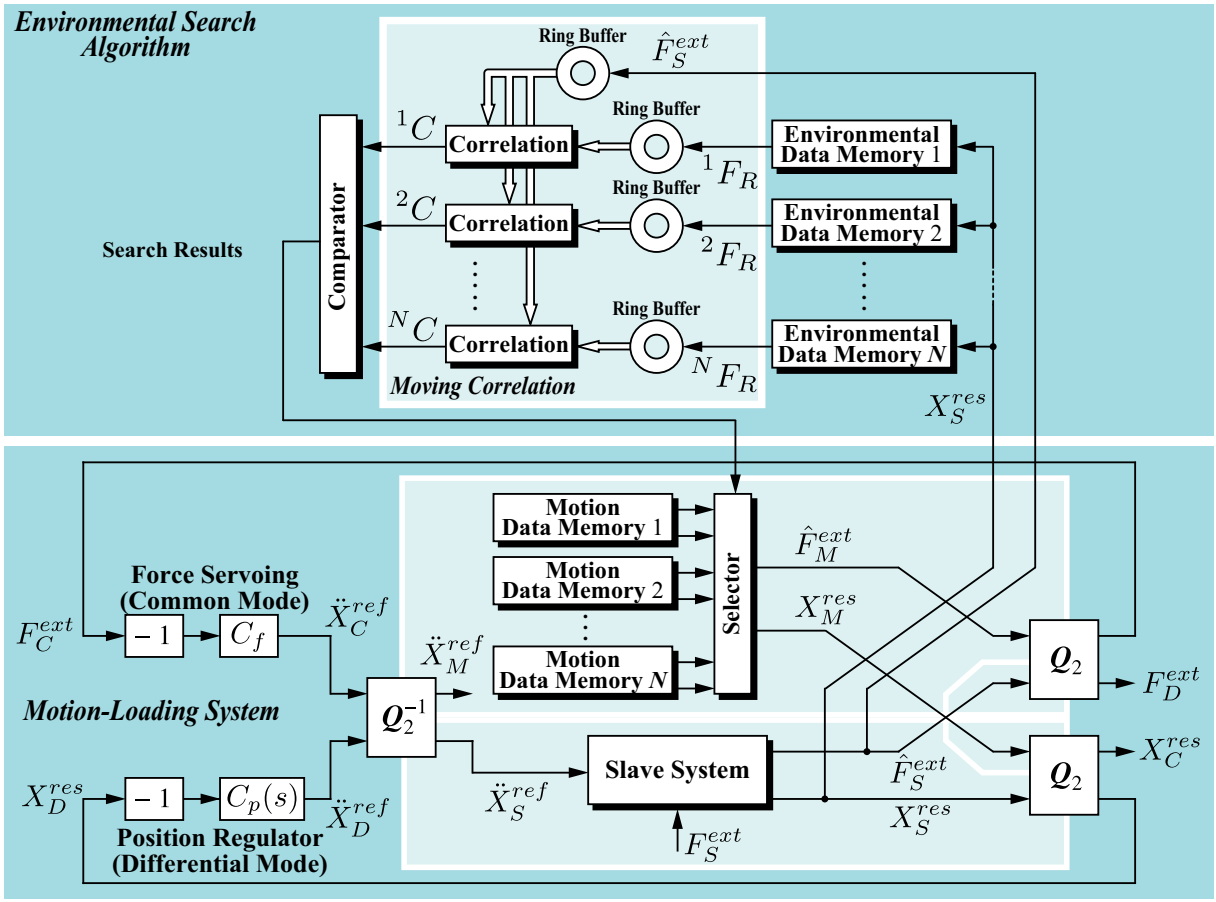

Fig. 5.38. Block diagram of selective motion-loading system. (Proposed method)

method of the motion-saving system. However, the motion data memories are utilized instead of the real actuator in the master side. In other words, the motion data memories imitate the human operator. In addition, compared with the normal method, environmental search algorithm is newly implemented. According to the search results from the algorithm, the motion information is appropriately selected by the selector.

5.2.4.4 Environmental Search Algorithm

The search results provided by the environmental search algorithm are indicators of similarity between the target environment in the slave side and the environmental data memories. At first, the force from stiffness and the momentum are reproduced by the environmental data memories

depending on the position response of the slave system X_S^{res}.

$$f_K[n] = F_{mem}[i_x] \tag{5.65}$$

$$p_D[n] = P_{mem}[i_x] \tag{5.66}$$

Moreover, environmental force ${}^N F_R$ is reproduced by

$${}^N F_R[n] = f_D[n] + f_K[n] \tag{5.67}$$

where n represents discrete time. f_D is calculated as

$$f_D[n] = \frac{2g_{pd}(p_D[n] - p_D[n-1]) + (2 - T_s g_{pd}) f_D[n-1]}{2 + T_s g_{pd}} \tag{5.68}$$

where g_{pd} and T_s represent bandwidth of pseudo derivative and sampling time. N is number of environmental data memory, and denotes kind of environment. In the next step, average values are calculated to obtain moving correlation coefficients

$$\overline{F}_S^{ext}[n] = \frac{1}{W} \sum_{\ell=n-W}^{n} F_S^{ext}[\ell] \tag{5.69}$$

$${}^N\overline{F}_R[n] = \frac{1}{W} \sum_{\ell=n-W}^{n} {}^N F_R[\ell] \tag{5.70}$$

where ℓ and W denote time in the window function and width of the window, respectively. The moving correlation C is determined by

$${}^N C[n] = \frac{\sum_{\ell=n-W}^{n} \left({}^N F_R[\ell] - {}^N\overline{F}_R[\ell] \right) \left(F_S^{ext}[\ell] - \overline{F}_S^{ext}[\ell] \right)}{S_R[n] S^{ext}[n]} \tag{5.71}$$

where $S_R[n]$ and $S^{ext}[n]$ are calculated as

$$S_R[n] = \sqrt{\sum_{\ell=n-W}^{n} \left({}^N F_R[\ell] - {}^N\overline{F}_R[\ell] \right)^2} \tag{5.72}$$

$$S^{ext}[n] = \sqrt{\sum_{\ell=n-W}^{n} \left(F_S^{ext}[\ell] - \overline{F}_S^{ext}[\ell] \right)^2}. \tag{5.73}$$

In short, the search algorithm calculates moving correlation between the force information from the environmental data memories 1 to N and the force response of the actuator. In this research, the window function is square form realized by ring buffer. Finally, search results are determined by comparison of each value of moving correlation coefficients ${}^N C[n]$.

5.2.5 Experiment

5.2.5.1 Normal Motion-Copying System

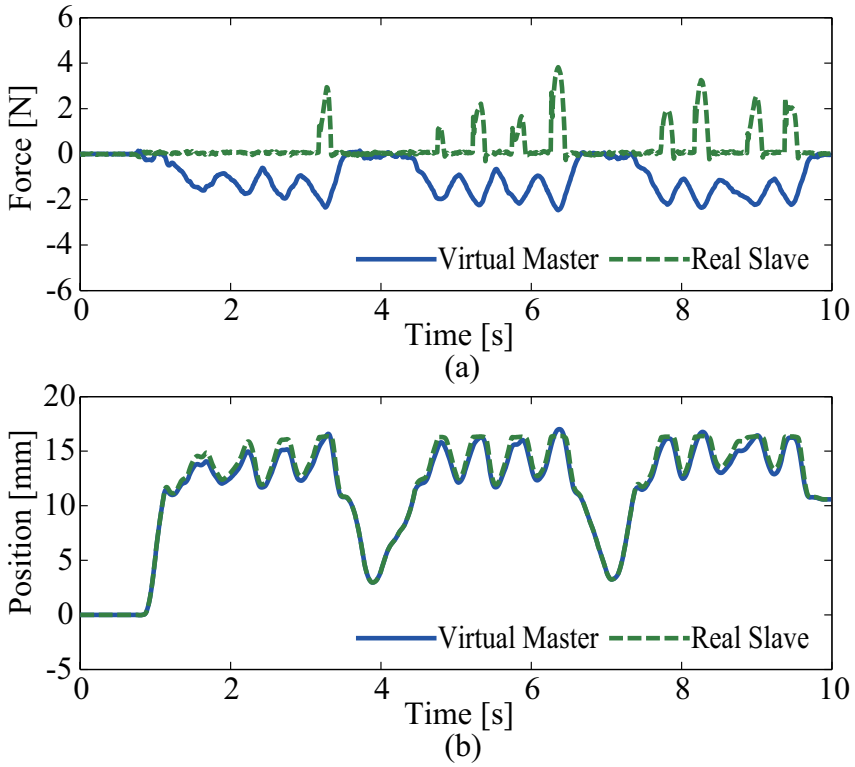

Fig. 5.39. Experimental results of normal motion-loading system. (Rubber block) (a) Force $\hat{F}_M^{ext}$, $\hat{F}_S^{ext}$. (b) Position X_M^{res}, X_S^{res}.

Figs. 5.39 and 5.40 shows experimental results of the normal motion-loading system. Since environment in the reproduction phase is different from environment in the storage phase, the normal motion-loading system is not able to reproduce the stored force and the stored position.

5.2.5.2 Storage of Environmental Haptic Information

In this experiment, environmental characteristics of two environments are stored. The one of environment is a rubber ball; other is a rubber block. These environments of pictures are shown in Fig. 5.41. In addition, the experimental setup is shown in Fig. 5.42.

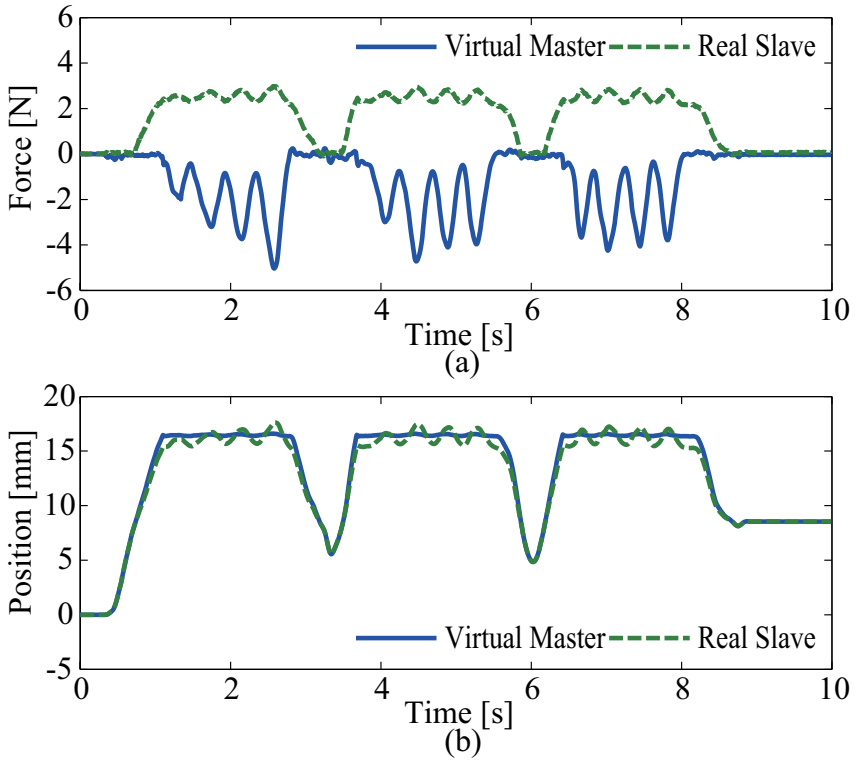

Fig. 5.40. Experimental results of normal motion-loading system. (Rubber ball) (a) Force $\hat{F}_M^{ext}$, $\hat{F}_S^{ext}$. (b) Position X_M^{res}, X_S^{res}.

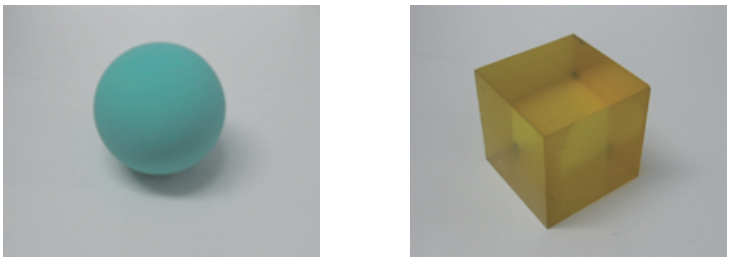

Fig. 5.41. Environments used in the experiment. (a) Rubber ball. (b) Rubber block.

In the storage phase of environmental information, force command F^{cmd} is given by

$$F^{cmd} = -\frac{F_{max}}{2}\cos(2\pi f t) + \frac{F_{max}}{2} \tag{5.74}$$

where F_{max} is maximum value of force, and is set to 3 N. f represents sinusoidal frequency. In this experiment, f is set to 0.25 Hz. Figs. 5.43 and 5.44 show the experimental results of

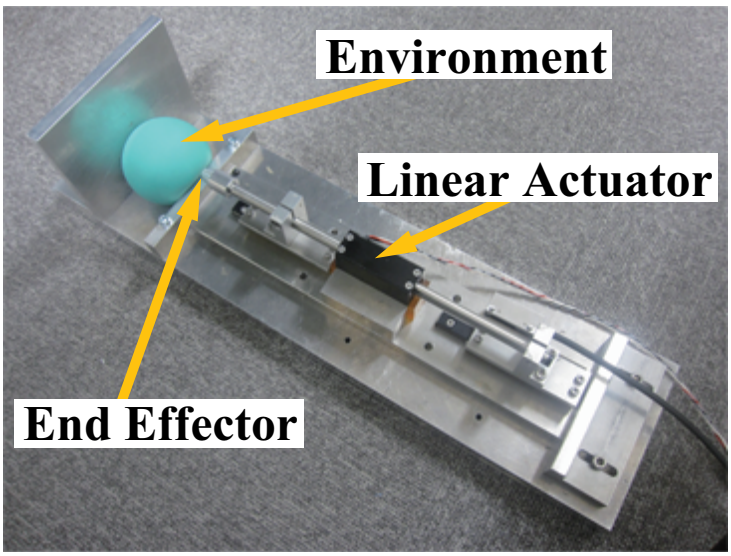

Fig. 5.42. Experimental setup of selective motion-loading system.

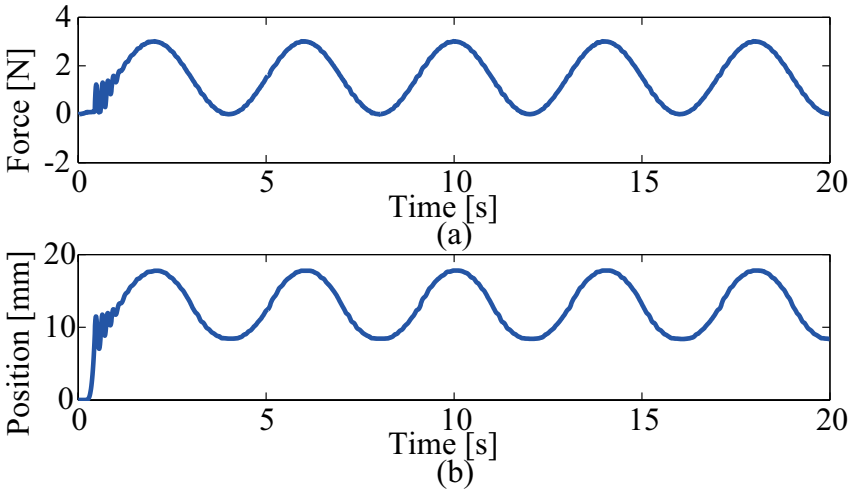

Fig. 5.43. Experimental results of haptic storage. (Rubber ball) (a) Force $\hat{F}_F^{ext}$. (b) Position X_F^{res}.

storage and decomposition results. The environmental data memories are shown in Figs. 5.45 and 5.46. The environmental characteristics are represented by these figures.

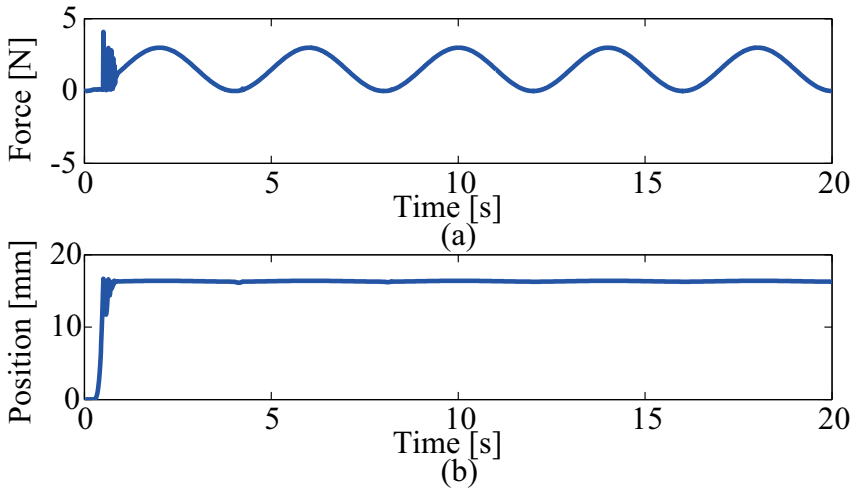

Fig. 5.44. Experimental results of haptic storage. (Rubber block) (a) Force $\hat{F}_F^{ext}$. (b) Position X_F^{res}.

5.2.5.3 Proposed Method

Fig. 5.47 shows the experimental results of the selective motion-loading system proposed in this thesis. In this experiment, target environment in the slave side is changed from the rubber ball to the rubber block at 4 s. The search results is appropriately calculated. In addition, the proposed system is able to appropriately reproduce the force and the position according to the search results, even if the target environment is changed.

5.2.6 Conclusion

This thesis proposed the selective motion-copying system which realizes storage and reproduction of human motion. The environmental search algorithm was applied for the motion-copying system. The normal motion-copying system cannot reproduce force and position, when the environment is changed. Hence, the environmental search algorithm detects the environment and provides the environment information to the motion-copying system, in order to reproduce the force and the position accurately. By the experiment, validity of the proposed method was verified. It will be useful for industrial applications, medical and welfare human support.

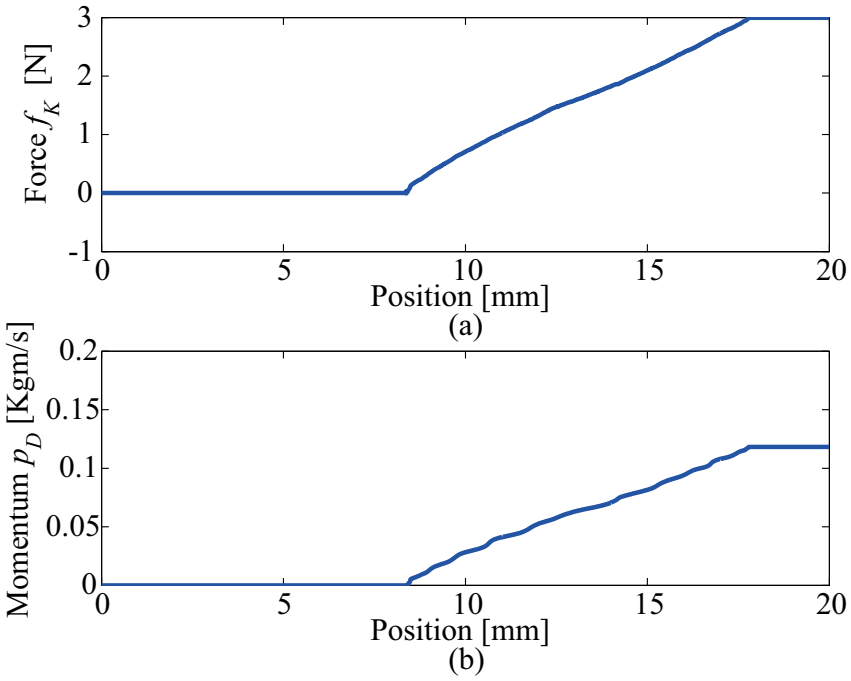

Fig. 5.45. Environmental data memory. (Rubber Ball) (a) Force f_K. (b) Momentum p_D.

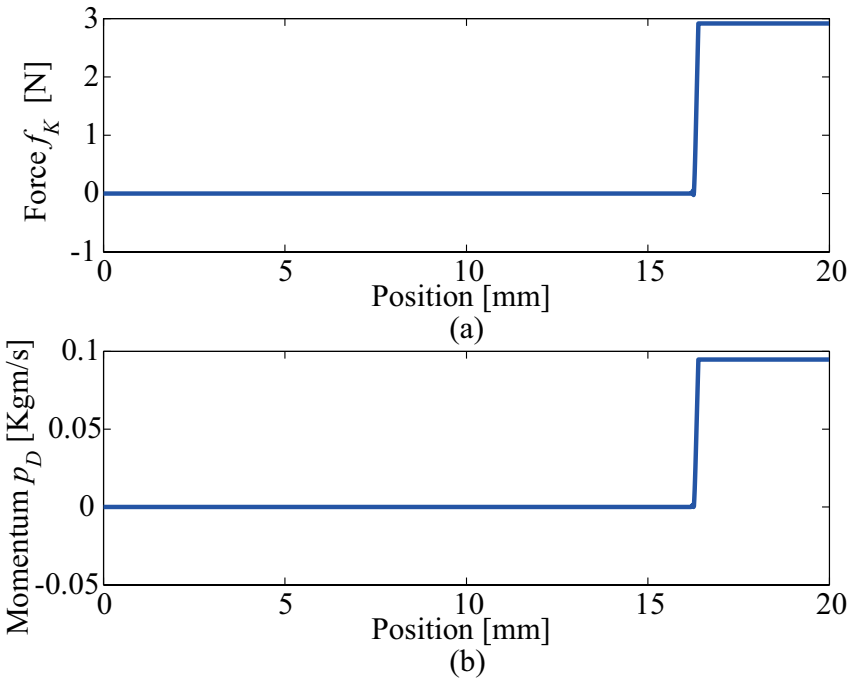

Fig. 5.46. Environmental data memory. (Rubber Block) (a) Force f_K. (b) Momentum p_D.

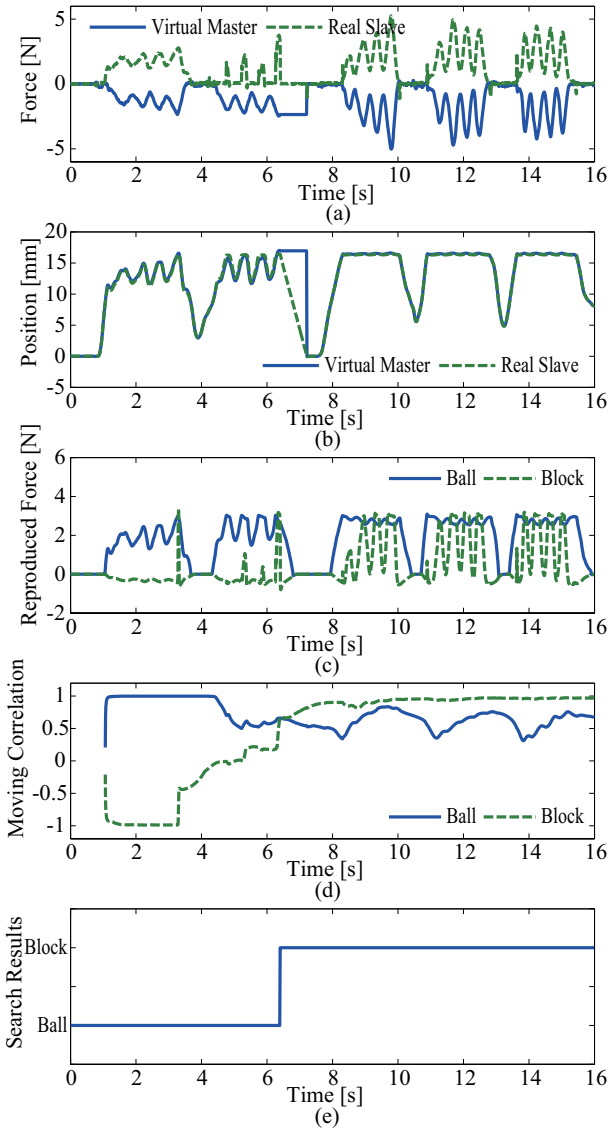

Fig. 5.47. Experimental results of selective motion-loading system. (a) Force $\hat{F}_M^{ext}$, $\hat{F}_S^{ext}$. (b) Position X_M^{res}, X_S^{res}. (c) Reproduced force by environmental data memory F_R. (d) Moving correlation C. (e) Search results.

Chapter 6

Conclusions

As mentioned in introduction, great many researchers are conducting research and development regarding acoustic information and visual information. On the other hand, the technique for haptic information has not adequately researched yet. In concrete terms, storage, reproduction, recognition, and transmission method for the haptic information is not in practical use. Consequently, this thesis studied the haptic recognition for reproduction of human motion.

In Chapter 2, the mobile robot obtains the haptic information of the road surface from the haptograph that is generated by the haptic recognition algorithm. Gabor continuance wavelet transform realizes the haptic recognition algorithm. The calculated haptograph images vary according to material and/or condition of the road surface. It is possible to make haptic map that visualizes the driving road environment. This thesis exhibited enhancing tactile recognition ability of the mobile robot respect to the driving road environment. By using this method, the mobile robot is able to avoid rough road taking ride ability into account.

The thesis proposed the motion-copying system considering single and/or multi degree-of-freedom human motion in Chapter 3. The motion-copying system consists of the motion-saving system and the motion-loading system. The motion-saving system stores the human motion of the human operator to the motion data memories by using the bilateral controller. The motion-loading system reproduces the force and position information, which is stored in the motion data memories. In this thesis, the motion-copying system stores and reproduces the force responses as well as the position responses, so that the motion-copying system is able to

treat single and/or multi degree-of-freedom motion of the human operators. In other words, the motion-loading system is able to reproduce the complex motion beyond time and space.

In addition, the thesis proposed the novel motion-copying system considering variable reproduction velocity. The motion-loading system is operated by the virtual master-slave controller according to the stored motion data. In this system, the reproduction velocity can be freely changed when the motion-loading system reproduces the force and the position. Thus, the motion-copying system considering variable reproduction velocity is realized.

In this study, the thesis also examined the stability of the motion-copying system, which preserves and reproduces the motion of the human operator. The motion-copying system is able to reproduce the force and the position according to the stored force and position in the motion data memory. By using the transfer function between the stored force and the reproduced force, the stability of the motion-loading system was theoretically confirmed by displacement of the poles with transition of the stiffness and of the damper. By the experiments, the thesis confirmed that the motion-copying system does not run out of the control even if the environmental mechanical impedance is changed.

In order to improve the force reproducibility in the reproduction phase, the motion-copying system proposed in this thesis used the acceleration response provided by the acceleration observer. By the experiment, validity of the proposed method was verified. Additionally, the force reproducibility was evaluated by using three evaluation methods.

In Chapter 4, the motion-copying system was used to compensate communication delay between the master system and the slave system. The motion-copying system is capable of saving and reproducing the human operated motion. Actually, the motion data memory which stores the motion, does not employ for compensation of delay. The communication time delay is utilize in stead of the motion data memory in the proposed system. In other words, respective sides of the bilateral controller are mutually coupled by the motion-copying system. The motion-copying system reproduces both the force and the position in other side. By this method, the effect of the time delay on the communication network was reduced.

Besides, this thesis proposed the novel bilateral control system using the environmental data memory. The environmental data memory stores the environmental information in the slave system. The slave system simulator which realizes the proposed bilateral controller, utilizes the environmental data memory, so that the slave system simulator imitates the real slave system. The environmental data memory is able to reproduce without environmental mathematical model. Moreover, the slave system in the real-world is not controlled directly by the bilateral control system. Therefore, the proposed system is able to eliminate the effect of the time delay.

The thesis proposed the novel bilateral controller based on the motion-copying system considering the network of low-rate data transfer. Since the proposed system utilizes the lossy compressors and decompressors, an amount of the data which flows in the network can be reduced. Therefore, the bilateral controller normally operates even if the data transfer rate of the network is low. By the experiment, the thesis confirmed the validity of the proposed method.

In Chapter 5, the thesis proposed the selective motion-copying system which realizes storage and reproduction of the human motion. The normal motion-copying system cannot reproduce force and position, when the environment is changed. Hence, the environmental search algorithm was applied for the motion-copying system. The environmental search algorithm detects the environment and provides the environment information to the motion-copying system, in order to reproduce accurately the force and the position. In other words, the appropriate stored motion is selected depending on the target objects. By the experiment, validity of the proposed method was verified.

The proposed method in this thesis will be useful for industrial applications, medical, welfare human support. The motion-copying system stores and reproduces specific special human motion, which are provided by expert engineers, skilled workers or medical operators in industrial or medical fields. More specifically, the numerical controlled machine tools which imitate the motion of skilled operators can be realized assuming that the proposed method is applied to industrial applications.

As mentioned above, in order to treat haptic information as with auditory and visual image,

the thesis proposed the haptic recognition methods for reproduction of human motion, and realized the motion reproduction based on real-world haptics.

References

[1] R.S. Culley : "Automatic telegraphs," *Journal of the Society of Telegraph Engineers*, Vol. 1, No. 1, pp. 39, 1872.

[2] J. Aylmer : "Underground telegraphs in France," *Journal of the Society of Telegraph Engineers*, Vol. 6, No. 17, pp. 170, 1877.

[3] Jno. Gott. : "Bell's telephone," *Journal of the Society of Telegraph Engineers*, Vol. 5, No. 15, pp. 500–502, 1876.

[4] W.H. Preece : "The telephone," *Journal of the Society of Telegraph Engineers*, Vol. 5, No. 15, pp. 525–530, 1876.

[5] S. Bidwell : "Telegraphic photography," *Journal of the Society of Telegraph Engineers and of Electricians*, Vol. 10, No. 38, pp. 354–360, 1881.

[6] N. Ashbridge : "Television in Great Britain," *The Institute of Radio Engineers*, Vol. 25, No. 6, pp. 697, Jun. 1937.

[7] W.O. Swinyard : "Industrial and professional applications of television technique," *The IEE - Part IIIA: Television*, Vol. 99, No. 20, pp. 651, 1952.

[8] R.C.G. Williams : "VHF and UHF Television Receiving Equipment," *The Institute of Radio Engineers*, Vol. 48, No. 6, pp. 1066, Jun. 1960.

[9] G. Hicks and B. Wessler : "Measurement of HOST costs for transmitting network data," ARPA Network Information Center, Stanford Research Institute, pp. 392, Sep. 1972.

[10] R. Kanodia : "Performance improvements in ARPANET teletransfer from multics," ARPA Network Information Center, Stanford Research Institute, pp. 662, Nov. 1974.

[11] L. Kleinrock, H. Opderbeck : "Throughput in the ARPANET–Protocols and Measurement," *IEEE Transactions on Communications*, Vol. 25, No. 1, pp. 95–104, Jan. 1977.

[12] Q. Zhou, K. Yuan, H. Wang, H. Hu : "FPGA-based colour image classification for mobile robot navigation," *IEEE International Conference on Industrial Technology, ICIT 2005*, pp.921–925, Dec. 2005.

[13] H. Malm, A. Heyden : "Extensions of Plane-Based Calibration to the Case of Translational Motion in a Robot Vision Setting," *IEEE Transactions on Robotics and Automation*, Vol. 22, No. 2, pp. 322–333, Apr. 2006.

[14] Y. Yabuta, H. Mizumoto, S. Arii : "Binocular Robot Vision System with Shape Recognition," *International Joint Conference, SICE-ICASE 2006*, pp. 5002–5005, Oct. 2006.

[15] A. Inoue, S. Katsura, T. Murakami : "Autonomous Mobile Robot Control for Ride Quality Improvement by Estimated Human Parameter and Road Condition," *The 6th Japan-France Congress on Mechatronics & 4th Asia-Europe Congress on Mechatronics Mechatronics-SAITAMA*, pp. 459–464, Sep. 9-12, 2003.

[16] H. Seki, T. Sugimoto, S. Tadakuma : "Novel Straight Road Driving Control of Power Assisted Wheelchair Based on Disturbance Estimation of Right and Left Wheels," *IEEJ Transactions on IA*, Vol. 126-D, No. 6, pp. 764–770, Jun. 2006.

[17] T. Mukai, M. Onishi, S. Hirano, L. Zhiwei : "Development of Soft Areal Tactile Sensors for Human-Interactive Robots," *IEEE Conference on Sensors*, pp. 831–834, Oct. 2007.

[18] A. J. Lynette, K. Jacquelyn, T. Edgar : "Tactile Vocabulary for Tactile Displays," *Symposium on Haptic Interfaces for Virtual Environment and Teleoperator Systems, EuroHaptics Conference 2007*, pp. 574–575, Mar. 2007.

[19] K. Sreenath, F. L. Lewis, D.O. Popa : "Localization of a Wireless Sensor Network with Unattended Ground Sensors and Some Mobile Robots," *IEEE Conference on Robotics, Automation and Mechatronics*, pp. 1–8, Dec. 2006.

[20] K. Seung-Hun, R. Chi-Won, K. Sung-Chul, P. Min-Yong : "Outdoor Navigation of a Mobile Robot Using Differential GPS and Curb Detection," *IEEE International Conference on Robotics and Automation*, pp. 3414–3419, Apr. 2007.

[21] J.-S. Choi, B. K. Kim : "Near-time-optimal trajectory planning for wheeled mobile robots with translational and rotational sections," *IEEE Transactions on Robotics and Automation*, Vol. 17, No. 1, pp. 85–90, Feb. 2001.

[22] K. Huebner, J. Zhang : "Stable Symmetry Feature Detection and Classification in Panoramic Robot Vision Systems," *IEEE/RSJ International Conference on Intelligent Robots and Systems*, pp. 3429–3434, Oct. 2006.

[23] G. Peng, X. Huang, J. Gao, Y. Wu : "Vision Based Intelligent Control for Mobile Robot," *The Sixth World Congress on Intelligent Control and Automation, WCICA 2006*, Vol. 2 pp. 9124–9128, Jun. 2006.

[24] K. Irie, S. Katsura, K. Ohishi : "Haptograph Representation of Tactile Information by Wide Bandwidth Force Control," *The IEEJ Technical Meeting on Industrial Instrumentation and Control, IIC'07*, Vol. 3, pp. 57–63, Mar. 2007.

[25] S. Katsura, K. Irie, K. Ohishi : "Visualization of Environmental Information by Haptograph Based on Wideband Force Control," *The 33rd Annual Conference of the IEEE Industrial Electronics Society, IECON 2007*, pp. 368–373, 2007.

[26] S. Katsura, Y. Yokokura, K. Ohishi : "Acquisition and visualization of personal characteristics by haptograph," *The 10th IEEE International Workshop on Advanced Motion Control, AMC'08*, pp. 434–439, 2008.

[27] Y. Yokokura, S. Katsura, K. Ohishi : "Haptic recognition and mapping of driving road environment by haptograph," *SICE 2007 Annual Conference*, pp. 2296–2301.

[28] X. Yun, Y. Yamamoto : "Internal Dynamics of a Wheeled Mobile Robot," *The IEEE/RSJ International Conference on Intelligent Robots and Systems, IROS'93*, pp. 1288–1294, Jul. 1993.

[29] Y. Kuniyoshi, M. Inaba, H. Inoue : "Learning by Watching: Extracting Reusable Task Knowledge from Visual Observation of Human Performance," *IEEE Transactions on Robotics and Automation*, Vol. 10, No. 6, pp. 799–822, Dec. 1994.

[30] K. Ikeuchi, T. Suehiro : "Toward an Assembly Plan from Observation Part I: Task Recognition with Polyhedral Objects," *IEEE Transactions on Robotics and Automation*, Vol. 10, No. 3, pp. 368–385, Jun. 1994.

[31] K. Ogawara, J. Takamatsu, H. Kimura, K. Ikeuchi : "Extraction of Essential Interactions Through Multiple Observations of Human Demonstrations," *IEEE Transactions on Industrial Electronics*, Vol. 50, No. 4, pp. 667–675, Aug. 2003.

[32] C. Chang, R. Ansari, A. Khokhar : "Density propagation for tracking initialization with multiple cues [human motion visual tracking]," *IEEE International Conference, ICASSP '04*, Vol. 3, pp. 629, May. 2004.

[33] T. Shimono, S. Katsura, K. Ohnishi : "Bilateral Motion Control for Reproduction of Real World Force Sensation based on the Environmental Model," *IEEJ Transactions on Industry Applications*, Vol. 126, No. 8, pp. 1059–1068, Aug. 2006.

[34] K. Ohishi, M. Miyazaki, M. Fujita : "Hybrid Control of Force and Position without Force Sensor," *The International Conference of the IEEE Industrial Electronics Society, IECON'92*, Vol. 2, pp. 670–675, Nov. 1992.

[35] T. Yoshikawa, K. Harada, A. Matsumoto : "Hybrid Position/Force Control of Flexible-Macro/Rigid-Micro Manipulator Systems," *IEEE Transactions on Robotics and Automation*, Vol. 12, No. 4, pp. 663–640, Aug. 1996.

[36] K. Khayati, P. Bigras, L.-A. Dessaint : "A Multistage Position/Force Control for Constrained Robotic Systems With Friction: Joint-Space Decomposition, Linearization, and Multiobjective Observer/Controller Synthesis Using LMI Formalism," *IEEE Transactions on Industrial Electronics*, Vol. 53, No. 5, Oct. 2006.

[37] F. Jatta, G. Legnani, A. Visioli : "Friction compensation in hybrid force/velocity control of industrial manipulators," *IEEE Transactions on Industrial Electronics*, Vol. 53, No. 2, Apr. 2006.

[38] Y. Yokokura, S. Katsura, K. Ohishi : "Motion Copying System Based on Real-World Haptics," *The 10th IEEE International Workshop on Advanced Motion Control, AMC'08-TRENTO*, pp. 613–618, Mar. 2008.

[39] S. Katsura, N. Tsunashima, W. Yamanouchi, Y. Yokokura : "Preservation and reproduction of real-world haptic information,", *International Power Electronics Conference, IPEC 2010*, pp. 2216–2221, 2010.

[40] N. Tsunashima, S. Katsura : "Continuous integration of motion components using motion copying system," *ICCAS-SICE 2009*, pp. 1569–1574, 2009.

[41] H. Tanaka, K. Ohnishi : "Haptic data compression/decompression using DCT for motion copy system," *IEEE International Conference on Mechatronics, ICM 2009*, pp. 1–6, 2009.

[42] H. Kuwahara, K. Ohnishi, N. Tsunashima, S. Katsura : "Design method for motion reproduction system including time scaling based on robot dynamics," *IEEE International Conference on Industrial Technology, ICIT 2010*, pp. 483–488, 2010.

[43] K. Nagase, S. Katsura, Y. Kasahara, K. Ohnishi : "Advanced motion copying system of multi degree-of-freedom human motion Nagase," *International Conference on Electrical Machines and Systems, ICEMS 2009*, pp. 1–6, 2009.

[44] B. Hannaford : "A Design Framework for Teleoperators with Kinesthetic Feedback," *IEEE Transactions on Robotics and Automation*, Vol. 9, No. 5, pp. 426–434, 1989.

[45] D.A. Lawrence : "Stability and Transparency in Birateral Teleoperation," *IEEE Transactions on Robotics and Automation*, Vol. 9, No. 5, pp. 624–637, Oct. 1993.

[46] K. Hashtrudi Zaad, S.E. Salcudean : "On the Use of Local Force Feedback for Transparent Teleoperation," *IEEE International Conference on Robotics and Automation, ICRA 1999*, pp. 1863–1869, May, 1999.

[47] Y. Yokokohji, T.Yoshikawa : "Bilateral Control of Master-slave Manipulators for Ideal Kinesthetic Coupling – Formulation and Experiment", *IEEE Transactions on Robotics and Automation*, Vol. 10, No. 5, pp. 605–620, 1994.

[48] K. Hashtrudi Zaad, S. E. Salcudean : "Bilateral Parallel Force / Position Teleoperation Control," *Journal of Robotic Systems*, Vol. 19, No. 4, pp. 155–167, 2002.

[49] S. Tachi, T. Sakaki : "Impedance Controlled Master Slave Manipulation System Part 1:Basic Concept and Application to the System with Time Delay," *Journal of the Robotics Society of Japan*, Vol. 8, No. 3, pp. 241–252, 1990.

[50] W. Iida, K. Ohnishi : "Reproducibility and Operationality in Bilateral Teleoperation," *The 8th IEEE International Workshop on Advanced Motion Control, AMC'04*, pp. 217–222, 2004.

[51] G. M. H. Leung, B. A. Francis, J. Apkarian : "Bilateral Controller for Teleoperators with Time Delay Via 1-Synthesis," *IEEE Transactions on Robotics and Automation*, Vol. 11, No. 1, pp. 105–116, 1995.

[52] S. Katsura, K. Ohnishi : "Transmission and Reproduction of Force Sensation by Bilateral Control," *IEEJ Transactions on Industry Applications*, Vol. 123-D, No. 11, pp. 1371–1376, 2003.

[53] Y. Matsumoto, S. Katsura, K. Ohnishi : "An Analysis and Design of Bilateral Control Based on Disturbance Observer," *The 10th IEEE International Conference on Industrial Technology, ICIT'03-MARIBOR*, pp. 802–807, Dec. 2003.

[54] N. Hayashida, T. Yakoh, T. Murakami, K. Ohnishi : "The Sensorless Bilateral Robot Manipulator Using the Twin Drive System," *Journal of the Japan Society for Precision Engineering*, Vol. 67, No. 11, pp. 1834–1838, 2001.

[55] J. Yan, S. E. Salcudean : "Teleoperation Controller Design Using H1-Optimization with Application to Motionscaling," *IEEE Transactions on Control Systems Technology*, Vol. 4, No. 3, pp. 244–258, 1993.

[56] Joonyoung Park : "Real time bilateral control for Internet based telerobotic system Jahng-Hyon Park," *IEEE/RSJ International Conference on Intelligent Robots and Systems, IROS 2003*, Vol. 2, pp. 1106–1110, 2003.

[57] P. Huynh, Y. Nakamura, T. Arai, T. Tanikawa, N. Koyachi : "Symmetric damping bilateral control for parallel manipulators," *The 8th International Conference on Advanced Robotics, ICAR'97*, pp. 401–406, 1997.

[58] Y. Kakizoe, H. Nakamura, H. Nishitani : "Remote bilateral control of master-slave manipulators with an environment observer," *SICE 2007 Annual Conference*, pp. 95–99, 2007.

[59] A. Caiti, G. Cannata, G. Casalino, S. Reto : "The local force control loop approach in bilateral control of master-slave systems," *The 35th IEEE Decision and Control 1996*, Vol. 1, pp. 747–752, 1996.

[60] T. Chen, D. Zhao, Z. Zhang : "Research on Master-Slave Robots Bilateral Control Strategy with Force Tele-Presence," *IEEE International Conference on Automation and Logistics 2007*, pp. 2301–2305, 2007.

[61] W. Yamanouchi, Y. Yokokura, S. Katsura, K. Ohishi : "Bilateral teleoperation with dimensional scaling for realization of mobile-hapto," *The 34th Annual Conference of Industrial Electronics, IECON 2008*, pp. 1590–1595, 2008.

[62] S. Sakaino, T. Sato, K. Ohnishi : "Modal transformation for bilateral control and cooperational robot motion - Kinematics and dynamics," *IEEE International Conference on Industrial Technology, ICIT 2009*, pp. 1–6, 2009.

[63] S. Katsura, K. Ohnishi : "Advanced Motion Control for Wheelchair in Unknown Environment" *IEEE International Conference on Systems, Man, and Cybernetics 2006, SMC '06-TAIPEI*, pp. 4926–4931, Oct. 2006.

[64] T. Murakami, F. Yu, K. Ohnishi : "Torque Sensorless Control in Multidegree-of-freedom Manipulator," *IEEE Transactions on Industrial Electronics*, Vol. 40, No. 2, pp. 259–265, Apr. 1993.

[65] S. Katsura, K. Ohishi : "Modal System Design of Multi-Robot Systems by Interaction Mode Control," *IEEE Transactions on Industrial Electronics*, Vol. 54, No. 3, pp. 1537–1546, Jun. 2007.

[66] K. Ohnishi, M. Shibata, T. Murakami : "Motion Control for Advanced Mechatronics," *IEEE/ASME Transactions on Mechatronics*, Vol. 1, No. 1, pp. 56–67, Mar. 1996.

[67] K. Ohishi, K. Ohnishi, K. Miyachi : "Torque-Speed Regulation of DC Motor Based on Load Torque Estimation Method," *The IEEJ International Power Electronics Conference, IPEC'83-TOKYO*, pp. 1209–1218, 1983.

[68] Y. Han; Y. Kim, J. Choi, H. Woo : "The position control of induction motors using the binary disturbance observer," *The 24th Annual Conference of the IEEE Industrial Electronics Society, IECON'98*, Vol. 3, pp. 1457–1463, 1998.

[69] K. Ohishi : "Realization of fine motion control based on disturbance observer," *The 10th IEEE International Workshop on Advanced Motion Control, AMC'08*, pp. 1–8, 2008.

[70] Y. Kim, J. Seok, I. Noh, S. Won : "An adaptive disturbance observer for a two-link robot manipulator," *International Conference on Control, Automation and Systems, ICCAS 2008*, pp. 141–145, 2008.

[71] K. Kim, K. Rew, S. Kim : "Disturbance Observer for Estimating Higher Order Disturbances in Time Series Expansion," *IEEE Transactions on Automatic Control*, Vol. 55, No. 8, pp. 1905–1911, 2010.

[72] J. Lloyd, J. Beis, D. Pai, D. Dowe : "Programming Contact Tasks using a Reality-based Virtual Environment Integrated with Vision," *IEEE Transactions on Robotics and Automation*, Vol. 15, No. 3, pp. 423–434, Jun. 1999.

[73] S. Katsura , Y. Matsumoto and K. Ohnishi : "Realization of "Law of action and reaction" by multilateral control," *IEEE Transactions on Industrial Electronics*, Vol. 52, pp. 1196–2005.

[74] S. Katsura and K. Ohnishi : "A realization of haptic training system by multilateral control," *IEEE Transactions on Industrial Electronics*, Vol. 53, pp. 1935–2006.

[75] S. Katsura and K. Ohishi : "Modal system design of multi-robot systems by interaction mode control," *The 9th IEEE International Workshop Advanced Motion Control*, Vol. 1, pp. 84-89, 2006.

[76] S. Katsura , K. Ohnishi and K. Ohishi : "Transmission of force sensation by environment quarrier based on multilateral control," *IEEE Transactions on Industrial Electronics*, Vol. 54, pp. 898-906, 2007.

[77] R. Kubo, T. Shimono, K. Ohnishi : "Flexible Controller Design of Bilateral Grasping Systems Based on a Multilateral Control Scheme," *IEEE Transactions on Industrial Electronics*, Vol. 56, No. 1, pp. 62–68, Jan. 2009.

[78] T. Suzuyama, S. Katsura and K. Ohishi : "Decoupled haptic transmission by multilateral control" *The 9th IEEE International Workshop Advanced Motion Control*, Vol. 1, pp. 334-339, 2006.

[79] T. Shimono, S. Katsura, R. Kubo and K. Ohnishi : "Multilateral control for skill education based on haptic data storage," *IEEE International Conference on Industrial Technology, ICIT 2006*, pp. 334–339, Dec. 2006.

[80] T. Suzuyama, S. Katsura, K. Ohishi : "A Representation of Information Connection in Multilateral System," *The Papers of Technical Meeting on Industrial Instrumentation and Control, IEE Japan IIC-07-60*, Vol. 3, pp. 45–50, 2007.

[81] T. Asai, S. Katsura, K. Ohishi : "Multilateral Control Considering Condition of System Connection," *The 34th Annual Conference of IEEE Industrial Electronics, IECON 2008*, pp. 1644–1649, Nov. 2008.

[82] S. Katsura, K. Ohnishi : "Multilateral Servo Control for Haptic Communication," *IEEE International Conference on Industrial Technology, ICIT 2008*, pp. 1–6, Apr. 2008.

[83] T. Okura, S. Katsura : "System connection in multilateral control system considering number of subsystems," *International Conference on Electrical Machines and Systems, ICEMS 2009*, pp. 1–6, 2009.

[84] T. Suzuyama, S. Katsura, K. Ohishi : "Decoupling Type Multilateral Control by Using Identity Ratio," *IEEJ Transactions on Industry Applications*, Vol. 127-D, No. 6, pp. 571-578, Jun. 2007.

[85] K. Irie, S. Katsura, K. Ohishi : "Wideband Motion Control by Acceleration Disturbance Observer," *The 12th International Power Electronics and Motion Control Conference, EPE-PEMC 2006*, pp. 361–366.

[86] S. Katsura, K. Irie, T. Suzuyama, K. Ohishi : "Bilateral Force Feedback Control Based on Wideband Acceleration Control," *The 4th IEEE International Conference on Mechatronics, ICM 2007*, pp. 1-6, 2007.

[87] S. Katsura, M. Kondo, K. Ohishi : "Wideband force sensing for haptic energy transmission utilizing FPGA," *The 13th International Power Electronics and Motion Control Conference, EPE-PEMC 2008*, pp. 1614–1619, 2008.

[88] Seiichiro Katsura, Kouhei Irie, Kiyoshi Ohishi : "Wideband Force Control by Position-Acceleration Integrated Disturbance Observer," *IEEE Transactions on Industrial Electronics*, Vol. 55, No. 4, pp. 1699-1706, Apr., 2008.

[89] R.J. Anderson, M.W. Spong : "Bilateral Control of Teleoperation with Time Delay," *IEEE Transactions on Automatic Control*, Vol. 34, No.5, pp. 494–501, 1989.

[90] G. Niemeyer, J.J.E. Slotine : "Stable Adaptive Teleoperation," *IEEE Journal of Oceanic Engineering*, Vol. 16, No. 1, pp. 152–162, 1989.

[91] A.C. Smith, K. Van Hashtrudi-Zaad : "Neural network-based teleoperation using Smith predictors," *IEEE International Conference Mechatronics and Automation, ICMA 2005*, Vol. 3, pp. 1654–1659, Jul. 2005.

[92] J. E. Lloyd, D. K. Pai : "Robotic Mapping of Friction and Roughness for Reality-Based Modeling," *Proceedings of the IEEE International Conference on Robotics and Automation, ICRA'01*, Vol. 2, pp. 1884–1890, May. 2001.

[93] S. Katsura, Y. Matsumoto, K. Ohnishi: "Realization of "Law of Action and Reaction" by Multilateral Control," *IEEE Transactions on Industrial Electronics*, Vol. 52, No. 5, pp. 1196–1205, Oct. 2005.

[94] K. Natori, R. Oboe, K. Ohnishi : "Robust Time Delayed Control Systems with Communication Disturbance Observer," *The 33rd Annual Conference of the IEEE Industrial Electronics Society, IECON 2007*, pp. 316–321, Nov. 2007.

[95] K. Natori, T. Tsuji, K. Ohnishi : "Time delay compensation by communication disturbance observer in bilateral teleoperation systems," *The 9th IEEE International Workshop on Advanced Motion Control, AMC'06*, pp. 218–223, 2006.

[96] K. Natori, K. Ohnishi : "A Design Method of Communication Disturbance Observer for Time Delay Compensation," *The 32nd Annual Conference on IEEE Industrial Electronics, IECON 2006*, pp. 730–735, 2006.

[97] K. Natori, R. Kubo, K. Ohnishi : "Effects of controller parameters on transparency of time delayed bilateral teleoperation systems with communication disturbance observer," *IEEE International Symposium on Industrial Electronics, ISIE 2008*, pp. 1287–1292, 2008.

[98] K. Natori, R. Oboe, K. Ohnishi : "A novel structure of time delayed control systems with communication disturbance observer," *The 10th IEEE International Workshop on Advanced Motion Control, AMC'08*, pp. 330–335, 2008.

[99] D. Yashiro, K. Ohnishi : "A communication disturbance observer with a band-pass filter for delay time compensation," *IEEE International Symposium on Industrial Electronics, ISIE 2010*, pp. 3585–3589, 2010.

[100] A. Kato, H. Nishi, K. Ohnishi : "Network Bilateral Control System with Jitter Buffer," *IEEJ Transactions on Industry Applications*, Vol. 126-D, No. 12, pp. 1737–1738, 2006.

[101] T. Imaida, Y. Yokokohji, T. Doi, M. Oda, T. Yoshikawa "Ground-Space Teleoperation of a Robot Arm Mounted on Engineering Test Satellite No. VII by Direct Bilateral Coupling under a Long Time Delay Condition ," *Journal of the Robotics Society of Japan*, Vol. 21, No. 3, pp. 85–96, 2003.

[102] Y. Yokokura, S. Katsura, K. Ohishi : "Multilateral Control with Communication Time Delay by Using Motion Copying System," *The Annual Conference of IEEJ Industry Applications Society, JIASC '08-KOCHI*, pp. 425–430 Aug. 2008.

[103] S. Yonemoto, D. Arita, R. Taniguchi : "Real-time human motion analysis and IK-based human figure control," *IEEE Workshop on Human Motion*, pp. 149–154, Dec. 2000.

[104] Y. Shinoda, S. Murakami, Y. Mito, R. Watanuma, M. Marumo : "Motion analysis of Nihon Buyo using motion capture system," *ICROS-SICE International Joint Conference, ICCAS-SICE 2009-FUKUOKA*, pp. 5417 - 5420, Aug. 2009.

[105] L. Tao Liu, Y. Inoue, K. Shibata : "A Wearable Sensor System for Human Motion Analysis and Humanoid Robot Control," *IEEE International Conference on Robotics and Biomimetics, ROBIO '06-KUNMING*, pp. 43–48 , Dec. 2006.

[106] Y. Yokokura, S. Katsura, K. Ohishi : "Stability Analysis and Experimental Validation of a Motion-Copying System," *IEEE Transactions on Industrial Electronics*, Vol. 56, No. 10, pp. 3906–3913, Oct. 2009.

[107] R. Bardeli : "Similarity Search in Animal Sound Databases," *IEEE Transactions on Multimedia*, Vol. 11, No. 1, pp. 68–76, Jan. 2009.

[108] P. Huang and C. Lee : "Image database design based on 9D-SPA representation for spatial relations," *IEEE Transactions on Knowledge and Data Engineering*, Vol. 16, No. 12, pp. 1486–1496, Nov. 2004.

[109] B. E. Prasad, A. Gupta, H.-M. D. Toong, S. E. Madnick : "A Microcomputer-Based Image Database Management System," *IEEE Transactions on Industrial Electronics*, Vol. 34, No. 1, pp. 83–88, Mar. 1987.

[110] S.-C. Pei, C. Cheng : "Extracting color features and dynamic matching for image database retrieval," *IEEE Transactions on Circuits and Systems for Video Technology*, Vol. 9, No. 3, pp. 501–512, Apr. 1999.

[111] G. Petraglia, M. Sebillo, M. Tucci, G. Tortora : "Virtual images for similarity retrieval in image databases,' *IEEE Transactions on Knowledge and Data Engineering*, Vol. 13, No. 6, pp. 951–967, Nov. 2001.

[112] Y. Yokokura, S. Katsura : "Environment Copying System Based on Real-World Haptics," *The 35th Annual Conference of the IEEE Industrial Electronics Society, IECON'09-PORTO*, pp.1879–1884, Nov. 2009.

List of Achievements

Journals

[1] Y. Yokokura, S. Katsura, K. Ohishi : "A Realization of Motion Copying System Based on Multilateral Control," IEEJ Transactions on Industry Applications, Vol. 128-D, No. 9, pp. 1140–1146, Sep. 2008.

[2] Y. Yokokura, S. Katsura, K. Ohishi : "Functionalization of Tactile Sensation for Mobile Robot Based on Haptograph and Modal Decomposition," IEEJ Transactions on Industry Applications, Vol. 129-D, No. 2, pp. 136–143, Feb. 2009.

[3] Y. Yokokura, S. Katsura, K. Ohishi : "Stability Analysis and Experimental Validation of a Motion-Copying System," IEEE Transactions on Industrial Electronics, Vol. 56, No. 10, pp. 3906–3913, Oct. 2009.

[4] Y. Yokokura, S. Katsura, K. Ohishi : "Bilateral Control Using Master/Slave Simulator for Haptic Communication," IEEJ Transactions on Industry Applications, Vol. 130-D, No. 4, pp. 485–491, Apr. 2010.

[5] N. Tsunashima, Y. Yokokura, S. Katsura : "Saving and Reproduction of Human Motion Data by Using Haptic Devices with Different Configurations," IEEJ Transactions on Industry Applications, Vol. 131-D, No. 3, Mar. 2011. [Accepted]

[6] Y. Yokokura, S. Katsura : "Construction of Motion Database Based on Real-World Haptics," IEEJ Transactions on Industry Applications, Vol. 131-D, No. 3, Mar. 2011. [Accepted]

International Conferences (oral presentation)

[1] Y. Yokokura, S. Katsura, K. Ohishi : "Haptic Recognition and Mapping of Driving Road Environment by Haptograph," *SICE Annual Conference 2007-TAKAMATSU*, pp. 2296–2301, Sep. 2007.

[2] Y. Yokokura, S. Katsura, K. Ohishi : "Motion Copying System Based on Real-World Haptics," *The 10th IEEE International Workshop on Advanced Motion Control AMC'08-TRENTO*, pp. 613–618, Mar. 2008.

[3] S. Katsura, Y. Yokokura, K. Ohishi : "Acquisition and visualization of personal characteristics by haptograph," *The 10th IEEE International Workshop on Advanced Motion Control AMC'08-TRENTO*, pp. 434–439, Mar. 2008.

[4] Y. Yokokura, S. Katsura, K. Ohishi : "Motion Copying System Based on Real-World Haptics in Variable Speed," *The 13th International Power Electronics and Motion Control Conference EPE-PEMC 2008-POZNAN*, pp. 1604–1609, Sep. 2008.

[5] W. Yamanouchi, Y. Yokokura, S. Katsura, K. Ohishi : "Bilateral Teleoperation with Dimensional Scaling for Realization of Mobile-Hapto," *The 34th Annual Conference of the IEEE Industrial Electronics Society IECON'08-ORLANDO*, pp. 1590–1595, Nov. 2008.

[6] Y. Yokokura, S. Katsura, K. Ohishi : "Bilateral Control with Communication Time Delay by Using Motion Copying System," *The 34th Annual Conference of the IEEE Industrial Electronics Society IECON'08-ORLANDO*, pp. 1718–1723, Nov. 2008.

[7] Y. Yokokura, S. Katsura, K. Ohishi : "Bilateral Control using Compressor/Decompressor under the Low-Rate Communication Network," *The 5th IEEE International Conference on Mechatronics ICM 2009-MALAGA*, pp. 1–6, Apr. 2009.

[8] Y. Yokokura, S. Katsura : "Reproduction of Multi Degree-of-Freedom Haptic Motion by Motion Copying System," *International Workshop on Vision and Control for Access Space*

2009 VCAS09-XIAN, Sep. 2009.

[9] Y. Yokokura, S. Katsura : "Environment Copying System Based on Real-World Haptics," *The 35th Annual Conference of the IEEE Industrial Electronics Society IECON'09-PORTO*, pp. 1879–1884, Nov. 2009.

[10] Y. Yokokura, S. Katsura : "Bilateral Teleoperation over Network Based on Environmental Data Memory," *The 12th International Conference on Electrical Machines and Systems ICEMS 2009-TOKYO*, pp. 1–6, Nov. 2009.

[11] Y. Yokokura, S. Katsura : "Motion Index/Search System Based on Real-World Haptics," *The 11th International Workshop on Advanced Motion Control AMC 2010-NAGAOKA*, pp. 436–441, Mar. 2010.

[12] Y. Yokokura and S. Katsura : "Reproduction of Real-World Haptic Information," *IEEE International Symposium on Industrial Electronics ISIE 2010-BARI*, pp. 3601–3606, Jul. 2010.

[13] Y. Yokokura and S. Katsura : "Searching System of Haptic Environment," *The 14th International Power Electronics and Motion Control Conference EPE-PEMC 2010-OHRID*, pp. 1–6, Sep. 2010.

[14] Y. Yokokura, S. Katsura : "Adaptive Motion-Copying System Based on Real-World Haptics," *The 36th Annual Conference of the IEEE Industrial Electronics Society IECON'10-GLENDALE*, pp. 1228–1233, Nov. 2010.

[15] Y. Yokokura, S. Katsura : "Representation of Haptic Environment by Using Spatial Laplace Operator," *The 8th France-Japan and 6th Europe-Asia Congress on Mechatronics, MECATRONICS'10-YOKOHAMA*, pp. 355–360, Nov. 2010.

International Conferences (poster presentation)

[1] W. Yamanouchi, Y. Yokokura, S. Katsura, K. Ohishi : "Real-world force feedback control for

mobile-hapto," *The 13th International Power Electronics and Motion Control Conference EPE-PEMC 2008-POZNAN*, pp. 1187-1192, Sep. 2008.

[2] Y. Yokokura and S. Katsura : "Realization of Motion Distributor Based on Real-World Haptics," *The International Symposium on Application of Biomechanical Control Systems to Precision Engineering ISAB 2010-IWAKI*, p. 235, Jul. 2010.

Domestic Conferences

[1] Y. Yokokura, S. Katsura, K. Ohishi : "Functionalization of Tactile Sensation for Mobile Robot Based on Haptograph and Modal Decomposition," *The Annual Conference of the IEEJ Industry Applications Society JIASC'07-OSAKA*, Vol. II, pp. 199-204, Aug. 2007.

[2] Y. Yokokura, S. Katsura, K. Ohishi : "Navigation of a Mobile Robot by Haptic Map," *The 50th Japan Joint Automatic Control Conference JACC*, pp. 188-193, Nov. 2007.

[3] Y. Yokokura, S. Katsura, K. Ohishi : "Visualization of Environmental Impedance Based on Haptograph," *IEEJ Industry Applications Society Technical Meeting on Niigata office, Tokyo section*, Vol. IEEE-12, p. 115, Nov. 2007.

[4] S. Katsura, Y. Yokokura, K. Ohishi : "Personal Verification by Haptic Signature," *IEEJ Industry Applications Society Technical Meeting on Niigata office, Tokyo section*, Vol. IEEE-11, p. 114, Nov. 2007.

[5] Y. Yokokura, S. Katsura, K. Ohishi : "A Realization of Motion Copying System Based on Multilateral Control," *IEEJ Technical Meeting on Industrial Instrumentation and Control*, IIC-08-118, Vol. 7, pp. 7-12, Mar. 2008.

[6] W. Yamanouchi, Y. Yokokura, S. Katsura, K. Ohishi : "Bilateral Force Feedback Control in Different Configuration for Mobile-Hapto,' *IEEJ Technical Meeting on Industrial Instrumentation and Control*, IIC-08-123, Vol. 7, pp. 37-43, Mar. 2008.

[7] S. Katsura, Y. Yokokura, K. Ohishi : "Reproduction of Real-World Haptic Information Using Haptograph," *IEEJ Technical Meeting on Industrial Instrumentation and Control*, IIC-08-128, Vol. 7, pp. 69-75, Mar. 2008.

[8] Y. Yokokura, S. Katsura, K. Ohishi : "A Realization of Real-World Haptic Feedback by Mobile-Hapto," *IEEJ Annual Meeting*, Vol. 4, pp. 304-305, Mar. 2008.

[9] W. Yamanouchi, Y. Yokokura, S. Katsura, K. Ohishi : "Bilateral Control in Different Configuration for Mobile-Hapto," *IEEJ Annual Meeting*, Vol. 4, pp. 302-303, Mar. 2008.

[10] Y. Yokokura, S. Katsura, K. Ohishi : "Multilateral Control with Communication Time Delay by Using Motion Copying System," *The Annual Conference of the IEEJ Industry Applications Society JIASC'08-KOUCHI*, Vol. II, pp. 425-430, Aug. 2008.

[11] W. Yamanouchi, Y. Yokokura, S. Katsura, K. Ohishi : "Dimension scaring bilateral control for different motion area system," *IEEJ Technical Meeting on Industrial Instrumentation and Control*, IIC-09-52, Vol. 2, pp. 47-52, Mar. 2009.

[12] Y. Yokokura, S. Katsura, K. Ohishi : "Bilateral Control Using Master/Slave Simulator for Haptic Communication," *IEEJ Technical Meeting on Industrial Instrumentation and Control*, IIC-09-51, Vol. 2, pp. 41-46, Mar. 2009.

[13] W. Yamanouchi, Y. Yokokura, S. Katsura, K. Ohishi : "Haptic Acceleration System Based on Dimension Scaling Bilateral Control," *IEEJ Annual Meeting*, Vol. 4, pp. 382-383, Mar. 2009.

[14] Y. Yokokura, S. Katsura, K. Ohishi : "Motion Copying System by Using Data Compression/Decompression," *IEEJ Annual Meeting*, Vol. 4, pp. 384-385, Mar. 2009.

[15] Y. Yokokura, S. Katsura, K. Ohishi : "A Realization of Environment Quarrier for Multilateral Control by Using Environmental Data Memory," *The 27th Annual Conference of the Robotics Society of Japan*, pp. 1-4, Sep. 2009.

[16] Y. Yokokura, S. Katsura, K. Ohishi : "Dynamic Force Compensation for Bilateral Control by Using Environmental Data Memory," *The 52th Japan Joint Automatic Control Conference JACC*, pp. 1-6, Nov. 2009.

[17] Y. Yokokura, S. Katsura, K. Ohishi : "Construction of Motion Database Based on Real-World Haptics," *IEEJ Technical Meeting on Industrial Instrumentation and Control*, IIC-10-78, Vol. 8, pp. 31-36, Mar. 2010.

[18] N. Tsunashima, Y. Yokokura, S. Katsura : "Saving and Reproduction of Human Motion Using Haptic Devices with Different Configurations," *IEEJ Technical Meeting on Industrial Instrumentation and Control*, IIC-10-158, Vol. 18, pp. 33-38, Mar. 2010.

[19] Y. Yokokura, S. Katsura, K. Ohishi : "Haptic Motion Control for Improvement of Operationality," *The 28th Annual Conference of the Robotics Society of Japan*, pp. 1-4, Sep. 2010.

Award

[1] SICE 2007 Annual Conference International Award Finalists

Career

[1] April, 2009〜

GCOE RA

Keio University Graduate School

The Global COE Program

[2] April, 2010〜

Research Fellow (DC2)

The Japan Society for the Promotion of Science